A molecular understanding of the Na^+–Ca^{2+} exchanger NCX3

Lauriane Y.M. Michel

A molecular understanding of the Na^{+}-Ca^{2+} exchanger NCX3

Lauriane Y.M. Michel

Department of Physiology – Radboud Institute for Molecular Life Sciences
Radboud University Medical Center

The research presented in this thesis was performed at the Department of Physiology and within the Center for System Biology and Bioenergetics (CSBB), Radboud university medical center and financed by the CSBR (Centre for Systems Biology Research) initiative from the Netherlands Organization for Scientific Research (NWO; No: CSBR09/013V). Printing of this thesis was financially supported by the department of Physiology.

ISBN 978-90-9029885-6

Print: Ipskamp Drukkers, Nijmegen, The Netherlands
Layout: J Ontwerp
Cover design: Studio Hoek

A molecular understanding of the Na^{+}-Ca^{2+} exchanger NCX3

Proefschrift

ter verkrijging van de graad van doctor
aan de Radboud Universiteit Nijmegen
op gezag van de Rector Magnificus prof. dr. J.H.J.M. van Krieken,
volgens besluit van het college van decanen
in het openbaar te verdedigen op dinsdag 18 oktober 2016
om 14.30 uur precies

door

Lauriane Yvette Marie Michel
geboren op 28 december 1987
te Laval, Frankrijk

Promotoren
Prof. dr. R.J.M. Bindels
Prof. dr. J.G.J. Hoenderop

Copromotor
Dr. P.H.G.M. Willems

Manuscriptcommissie
Prof. dr. B.G.M. van Engelen
Prof. dr. B. Wieringa
Prof. dr. R. Masereeuw (Universiteit Utrecht)

A molecular understanding of the Na^{+}-Ca^{2+} exchanger NCX3

Doctoral thesis

to obtain the degree of doctor
from Radboud University Nijmegen
on the authority of the Rector Magnificus prof. dr. J.H.J.M. van Krieken,
according to the decision of the Council of Deans
to be defended in public on Tuesday, October 18, 2016
at 14.30 hours

by

Lauriane Yvette Marie Michel
born in Laval, France
on December 28, 1987

Supervisors
Prof. dr. R.J.M. Bindels
Prof. dr. J.G.J. Hoenderop

Co-supervisor
Dr. P.H.G.M. Willems

Doctoral Thesis Committee
Prof. dr. B.G.M. van Engelen
Prof. dr. B. Wieringa
Prof. dr. R. Masereeuw (Utrecht University)

"In order to seek truth, it is necessary once in the course of our life, to doubt, as far as possible, of all things."

"Que pour examiner la vérité il est besoin, une fois dans sa vie, de mettre toutes choses en doute autant qu'il se peut."

René Descartes (1596-1650)

Table of contents

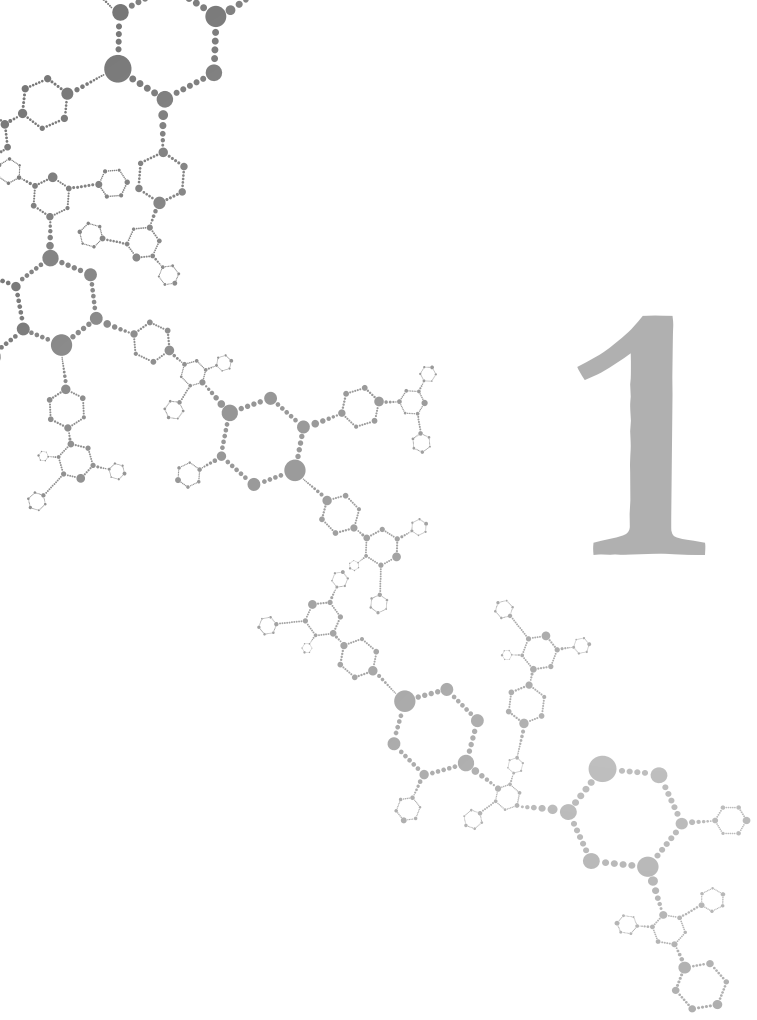

1

General Introduction

Adapted from:
Towards understanding the role of the Na^+-Ca^{2+} exchanger isoform 3

Lauriane Y.M. Michel[1,2], Joost G.J. Hoenderop[1], René J.M. Bindels[1,2]

[1] Department of Physiology, Radboud University Medical Center, The Netherlands
[2] Centre for System Biology and Bioenergetics, Radboud University Medical Center, The Netherlands

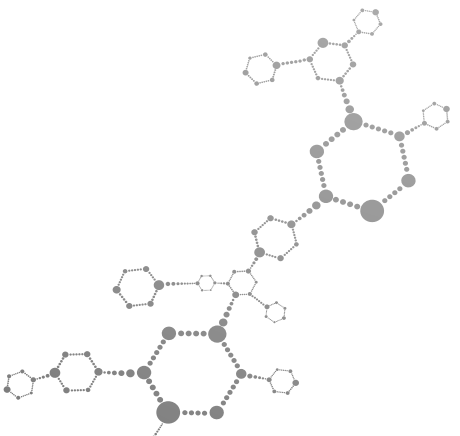

Rev Physiol Biochem Pharmacol 168, 31-57 (2015)

Calcium: properties and physiology

Calcium basics

Calcium (Ca) is an essential element for human health. Among the five stable isotopes found in nature (^{40}Ca, ^{42}Ca, ^{43}Ca, ^{44}Ca, ^{46}Ca), ^{40}Ca is the most abundant, representing 97% of the naturally occurring Ca. Within the periodic table of elements, Ca of atomic number 20 belongs to the alkaline earth metals group due to its oxidative capacity of +2 that derives from the distribution of its electrons around the nucleus (1). For every element, negatively charged electrons are distributed among the multiple orbitals, following an organized pattern. In the case of alkaline earth metals, two electrons located in the outermost orbital, can be easily lost and participate in chemical bond formation with additional elements. Upon loss of its outermost electrons, the element is in its ionized form. In the same manner, Ca as a pure metal is extremely reactive and occurs exclusively in its divalent cation form in nature. This cationic form is referred to as Ca^{2+} (1). in its divalent cation form in nature. This cationic form is referred to as Ca^{2+} (1).

Biological functions

Because of its numerous physiological functions, Ca^{2+} is implicated at every level of human physiology, from whole-body to cellular level. Ca^{2+}, in the human body, is either: i) ionized, also called free Ca^{2+}; *ii*) complexed to organic compounds; *iii*) precipitated in inorganic salts. The latter constitutes a major storage of Ca^{2+} and phosphate precipitated in calciumhydroxyapatite ($Ca_{10}(PO_4)_6(OH)_2$) and provides rigidity to the bones and teeth (2). On average, 1 kg of Ca^{2+} is stored in the skeleton of a human body. Ca^{2+} originates from dietary intake absorbed in the intestine depending on requirements (3). Subsequently, Ca^{2+} circulates in the bloodstream and other body fluids either as ionized Ca^{2+} or complexed to proteins. Their relative amounts vary widely; while both forms are equally present in the bloodstream, free Ca^{2+} constitutes more than 80% of the Ca^{2+} in cerebro-spinal fluid (4).

The concentration of ionized Ca^{2+} ($[Ca^{2+}]$) in the circulation is maintained within a narrow range (1.05 – 1.30 mM) by the concerted action of the parathyroid hormone (PTH), vitamin D ($1,25\text{-}(OH)_2D_3$) and calcitonin to enable proper functioning of the cardiovascular system, the neuronal circuitry, the blood clotting cascade and the inflammatory response (5-7). In the event of a low dietary supply, Ca^{2+} homeostasis is maintained in the circulation by bone resorption at the detriment of bone mass. Intracellularly, Ca^{2+} concentration ($[Ca^{2+}]_i$) is tightly maintained in resting cells, at a lower level (~ 20-100 nM) (8,9) thus spatio-temporal rises in $[Ca^{2+}]_i$ play a major role in membrane potential depolarization and receptor–mediated processes such as contraction, secretion and mitochondrial energy production (10). Furthermore, acting as a second messenger in numerous signaling pathways, intracellular Ca^{2+} is also implicated in cell proliferation, migration, differentiation and apoptosis. Because of its numerous

physiological functions, impairments of the [Ca^{2+}] in the blood or the cytoplasm may have serious clinical implications such as hypertension, muscle weakness, seizures, tetany and cardiac arrhythmias (11-13). Therefore, a tight control of [Ca^{2+}] in resting conditions and during physiological events is essential to maintain the integrity of the human body.

Regulation of intracellular Ca^{2+}

Ca^{2+} in organelles

Ca^{2+} concentration and its dynamic changes such as during Ca^{2+} transient are essential to most physiological functions and imply an absolute requirement for a tight regulation of the $[Ca^{2+}]_i$. In this regard, a large percentage of cellular Ca^{2+} is not available in the cytosplasm but sequestered in organelles, for which [Ca^{2+}] vary widely depending on cell types and physiological status. The endo(sarco)plasmic reticulum (ER/SR) is the most substantial intracellular Ca^{2+} store with concentration ($[Ca^{2+}]_{ER}$) fluctuating from 0.05 to 1 mM (14,15). Lower but significant levels of Ca^{2+} are also sequestered in mitochondria where a concentration ($[Ca^{2+}]_{mito}$) from 0.2 to 26 µM is measured in the matrix (16). Ca^{2+} sequestration and maintenance of $[Ca^{2+}]_i$ are prerequisite for Ca^{2+} to function as an intracellular messenger and implicate numerous players: *i*) plasma and intracellular membranes are virtually impermeable to Ca^{2+}; *ii*) Ca^{2+}-binding proteins buffer Ca^{2+} in the cytosol and enable the storage of large amounts of Ca^{2+} in the lumen of the ER/SR; *iii*) mitochondrias can temporarily sequester large amounts of Ca^{2+} during a cytosolic Ca^{2+} rise and, thus, participate with the ER/SR in controlling the spatio-temporal dynamics of the cytosolic Ca^{2+} signals; *iv*) pores and channels allow for passive diffusion and Ca^{2+} entry according to the electrochemical gradient; *v*) Ca^{2+}-ATPases actively pump Ca^{2+} out of the cytosolic compartment; and finally *vi*) secondary active Ca^{2+} transporters use the electrochemical gradient of a particular solute to transport Ca^{2+} out of the cytosol (17).

Ca^{2+}-binding proteins

Within the cell, numerous proteins have the ability to bind and release Ca^{2+} in a $[Ca^{2+}]_i$-dependent manner and are divided between the proteins implicated in Ca^{2+} transport and the Ca^{2+}-binding proteins (CBPs), solely involved in sensing and buffering Ca^{2+} (18). Among the most described CBPs, calbindin, annexins and calcineurin, located in the cytoplasm, bind ionized Ca^{2+} and therefore, contribute to the Ca^{2+} buffering capacity of the cytosol. CBPs present as well in all organelles are of tremendous importance in the sarcoplasmic (calsequestrin) and endoplasmic (calreticulin) reticulum, the intracellular Ca^{2+} store in muscle fiber and non-muscular cells, respectively (19). Following a decrease in $[Ca^{2+}]_{ER/SR}$ induced by the opening of the Ryanodine Receptor (RyR) in the muscle fibers or the Inositol 1,4,5-Triphosphate Receptor (IP_3R) in other cell types, CBPs located in the ER/SR are able to operate the rapid release of Ca^{2+} due to their high capacity and

low affinity. Among CBPs, Ca^{2+}-sensor proteins participate in the regulation of cellular processes through their capacity to transduce cytosolic Ca^{2+} signals to downstream proteins. Due to their high concentration and localization, some of them act also as Ca^{2+} buffer, it is the case for calmodulin (20). By their Ca^{2+}-binding kinetics, concentration and localization, CBPs play a crucial role in spatial and dynamic shaping of cytosolic Ca^{2+}.

Ca^{2+} transport

Ca^{2+} transport across the cell membrane is achieved by two major mechanisms: passive diffusion and active transport. While the former transfers Ca^{2+} along its electrochemical gradient, the latter enables Ca^{2+} transport against its gradient via its coupling to ATP hydrolysis, providing the energy required for this uphill transport. Among the most described transporters implicated exclusively in Ca^{2+} transport are the plasma membrane Ca^{2+}-ATPase (PMCA) and the sarco-endoplasmic reticulum Ca^{2+}-ATPase (SERCA). For its part, the passive diffusion across the plasma membrane depends on the permeability of the lipid bilayer as well as the size and hydrophobicity of the transported molecules (21). Due to the poor permeability of the bilayer for charged solutes, passive diffusion of ions such as Ca^{2+} does not naturally occur through the plasma membrane. Nevertheless, intrinsic proteins permeable to specific ions and molecules enable the passive diffusion of Ca^{2+} along its electrochemical gradient. This diffusion can be operated by pore that remains always open as it is the case for the mitochondrial permeability transition pore that, once formed, allows for Ca^{2+} release from the mitochondrial matrix into the cytosol. Passive diffusion occurs as well by gated channel that switches from a close state to an open or gated state, conformational changes being regulated by different signals, for instance the ryanodine and IP_3 receptor belongs to the ligand-gated channels while the gating of Ca_v family is voltage-dependent (17). Finally, the SLC family of solute carriers, referred as uniporters (symporters and antiporters), constitutes the third category of intrinsic proteins able to perform diffusion of multiple solutes across the lipid bilayer (22). In this case, uniporters contain intracellular and extracellular gates that alternatively open thus the downhill electrochemical gradient of the first solute drives the uphill transport of other molecules. This transport is therefore referred to as facilitated diffusion. Through this mechanism, the SLC8 family of Na^+-Ca^{2+} exchangers operates Ca^{2+} transport by exchanging Na^+ against Ca^{2+} across the plasma membrane.

The Sodium-Calcium exchanger family

Na^+-Ca^{2+} exchange

The NCX (SLC, Solute carrier 8) branch of Na^+-Ca^{2+} exchangers is found in all cell types and belongs to the Ca^{2+}:cation antiporter superfamily (CaCA). NCX catalyzes the exchange of Na^+ and Ca^{2+} across the plasma membrane by facilitated diffusion with a

stoichiometry of 3:1 respectively (23) following a ping-pong mechanism also called consecutive mechanism (24,25). NCX is able to facilitate both the extrusion and the influx of Ca^{2+} (26,27). These two modes of exchange are referred to as forward and reverse mode, respectively. The switch from one mode to the other is highly dependent on the electrochemical gradients of both Na^+ and Ca^{2+} across the plasma membrane (28).

The NCX family by its decisive role in Ca^{2+} and Na^+ homeostasis and its expression in all cell types is involved in many physiological events throughout the body. In this regard, NCX in muscle tissues is mostly known as being the predominant mechanism for Ca^{2+} extrusion during muscle relaxation. NCX is important in the cardiac development, and its loss of function causes heart defect and heart failure on the mid-term (29). NCX is required as well in skeletal and smooth muscle, where it could possibly act as a modulator of the sarcoplasmic reticulum (SR) content. NCX is also implicated during brain development and neurotransmitter release. In non-excitable tissues, NCX carries out very diverse roles such as the Ca^{2+} reabsorption in the distal convoluted tubules of the kidney and the Na^+ extrusion in erythrocytes, whereas in pancreatic β-cells it participates to the control of insulin release.

Structural features of the NCX family

In mammals three isoforms have been found: NCX1, NCX2 and NCX3 encoded by three distinct genes (30). The occurrence of two parallel genome duplications early in the vertebrate lineage gave rise to, most likely, four isoforms of NCX. However, the fourth isoform, NCX4, present in teleosts has been lost in birds and mammals during evolution (30). From this early duplication, NCX isoforms conserved a high degree of sequence homology of about 70% in mammals. Therefore, NCX isoforms share several structural properties.

Transmembrane domain

All members of the NCX family share a common architecture consisting of 10 transmembrane (TM) domains (31,32), arranged in two clusters separated by a large intracellular loop of 500 residues. The TM domains allow for the ion translocation across the plasma membrane. Recent progress in the obtainment of high–resolution crystal structures of NCX brought information on these domains of the exchanger. In its outward-facing conformation, the crystal structure of NCX_Mj, the prokaryotic NCX of *Methanococcus janaschii* (33) confirmed the presence of 10 TM segments arranged around a tightly packed core region (**Figure 1A**). This core region contains four cation-binding sites. However the different sites share several negatively charged ligands. Therefore Ca^{2+}- and Na^+-binding sites cannot be occupied simultaneously, which confirms a ping-pong mechanism of translocation. Extracellular Na^+ and Ca^{2+} reach these binding sites by two passages specific for each cation.

Less information is available on the inward-facing conformation of NCX. However, the crystal structures of other exchangers from the CaCA superfamily shed light on the

mechanisms of exchange. Among the CaCA family, two highly conserved α-repeats motifs are located at the TM segments 2-3 and the TM segments 7-8 (34-36). The crystal structures of two prokaryotic Ca^{2+}-H^{+} antiporter in their inward-facing conformation reported TMs 2 and 7 in an X-shaped conformation while TM segments 3 and 8 are tilted in parallel. Such conformation is also observed in NCX_Mj (37). Additionally, the rotation of the kink angle of TM segments 2 and 7 observed between the two CaCA members suggest that these two conserved TM segments are engaged in the transition between inward and outward conformation. Nishiwaza *et al*. proposed that the conformational changes of TM2 and TM7 induced by the binding of Ca^{2+} enable the sliding from one conformation to the other (38).

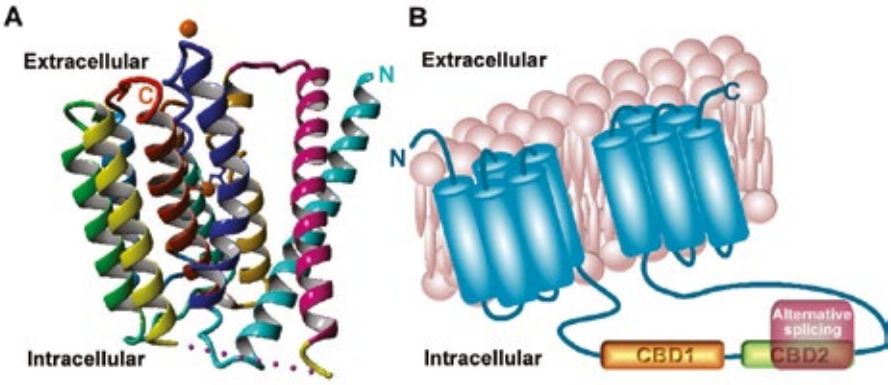

Figure 1 Structure of NCX.

First crystal structure of a Na^{+}-Ca^{2+} exchanger **A**, found in *Methanococcus jannaschii* (NCX_Mj) as reported by Liao *et al*. (33) (Protein Data Bank accession number: 3V5S). This bacterial exchanger contains a short intracellular loop of 6 residues while mammalian isoforms have a cytoplasmic loop of about 500 residues as depicted in the topology of NCX3 **B**, which here illustrates the two Ca^{2+}-binding domains CBD1 and CBD2, where the alternate splice site is located.

Intracellular loop of NCX

The large intracellular loop found in the mammalian NCX is not directly involved in the ion translocation across the membrane. Importantly, however, the binding of non-transported ions and molecules to this cytoplasmic region plays a crucial role in the allosteric regulation of the exchanger (**Figure 1B**). Thus, upon removal of this loop, allosteric regulation is lost, however, the exchanger remains fully active (39). Within this intracellular domain, two Ca^{2+}-binding domains 1 and 2 (CBD1 and CBD2) are found. The remaining residues of the intracellular loop belong to the Catenin Like Domain (CLD). Both CBDs share a similar structure that includes a β-sandwich and an unstructured F-G

loop that contains a α-helix. Within these CBDs Ca^{2+} is bound by several acidic residues such as aspartate and glutamate.

During a cytosolic Ca^{2+} transient, CBD1 is the primary sensor of the change in cytosolic Ca^{2+} concentration and the first activator of the exchanger (40). Despite the presence of four Ca^{2+}-binding sites (Ca1, Ca2, Ca3, Ca4) (35), only the Ca3 and Ca4 are directly implicated in this process. (41,42). On the other hand, the "steady-state" activation by Ca^{2+} and the Na^{+}-dependent inactivation of the exchanger are both attributed to the CBD2 domain (43). This secondary sensor has only two Ca^{2+}-binding sites (CaI and CaII) and here again only the first site CaI is directly involved in the regulation of the exchanger (35,44).

When characterized together, the CBD1 and CBD2, also called CBD12 adopt an antiparallel structure, the two domains being connected to each other by a small linker (45,46). The binding of Ca^{2+}, at the sites previously reported, rigidifies the CBD12 conformation and reduces the flexibility between the two domains (47-49). The interactions between domains are of tremendous importance, as the CBD2 will influence the affinity of Ca3 and Ca4 of CBD1 (42). Finally, Khananshvili's group has recently hypothesized that in physiological conditions Ca1, Ca2 and CaII of CBD1 and CBD2 are occupied by Mg^{2+} (43,50). This binding would modulate the affinity of the remaining Ca^{2+}-binding sites, decreasing the affinity at the Ca3 and Ca4 and increasing it at the CaII.

The Catenine Like domain (CLD), present in direct contact between the TM segments and the CBDs is suggested to be implicated in both the Na^{+}-dependent inactivation in interaction with the CBD2 and in the regulation by Ca^{2+} (51,52). The changes of conformation following the Ca^{2+}-binding at the CBDs are most likely reducing or increasing the tension between the CLD and the TM, a process that would relay the Ca^{2+}-binding events to the TM segments responsible for ion translocation (44).

Distinctive characteristics of NCX3

Homology

Since its cloning from rat brain by Philipson's group (53) in 1996, the sequence of NCX3 is known. NCX3 shares about 75% homology of sequence with NCX1 and NCX2 (**Table 1**). However, in line with the function they carry out, the different sections of the exchanger do not share the same homology within the NCX family. Thus, the residues of the 10 TM domains have higher homology to NCX1 and NCX2 (>75%) than the cytoplasmic loop that shares about 60% (**Table 1**). This conservation together with the similar stoichiometry of exchange (Na^{+}:Ca^{2+}) observed within the NCX family tend to prove that the translocation mechanism is similar within the NCX family. In this manner, the capacities exerted specifically by NCX3 would result from its cytoplasmic loop.

Table 1 Percentage of similarity in amino acid sequences between human isoforms of NCX in the different domains of the exchanger.

Domains of NCX3	Residues	Conservation human NCX1	Conservation human NCX2
Complete Exchanger	1-927	> 70%	> 70%
N-term- to TM5	1-251	> 70%	> 70%
Intracellular loop	252-727	> 60%	> 60%
CBD1	370-500	> 60%	> 60%
CBD2	501-650	> 55%	> 55%
TM6 to C-term	728-927	> 80%	> 80%

Residues (with 1 as the first methionine of the amino acid sequence of hNCX3); Conservation of sequence determined between hNCX3 (accession NP_892114) and either hNCX1 (accession NP_066920) or hNCX2 (accession NP_055878).

The structure of the CBD1 of NCX3 is not resolved yet. Nonetheless, the conservation of some key acidic and basic residues lead to the same Ca^{2+}-binding sites and a structure most likely similar to NCX1. Therefore, the regulation of NCX3 capacity of exchange by CBD1 is probably comparable to NCX1 (44). The comparison of the CBD2 has proven to be more difficult because of the alternative splicing of the NCX family causing various possibilities of sequence for the CBD2. In the case of NCX1, more than 15 splice variants have been identified (54,55) showing a tissue specific distribution and exchange properties that fulfill the tissue requirements (55,56) (**Figure 2**). NCX2 does not appear to undergo alternative splicing as only one variant has been found (55). In the case of NCX3, only a few splice variants have been found.

Alternative splicing

The NCX3 gene is composed of 9 exons (55) numbered 1 to 9 (**Figure 2**), of which exons 3 and 4, also named A and B respectively, are mutually exclusive (55). Exon 5, also called exon C, is optional. Thus, in the rat, three splice variants are detected; in mice only two splice variants have been originally described. The variant containing exon A and C is found in skeletal muscle (NCX3-AC), while variants expressing the exon B are expressed in the brain. Nevertheless, possible differences in function arising from this splicing have not yet been investigated. Additionally three truncated forms of NCX3 are found in humans. Two truncated variants are found in the fetal brain and appear to contain exons 4 to 9 and 6 to 9 (57). The third truncated variant is found in skeletal muscle and comprises the exons 1, 2 and 6 (58). Due to their expression restricted to fetal stage, these truncated forms are likely to be under the control of alternative promoters.

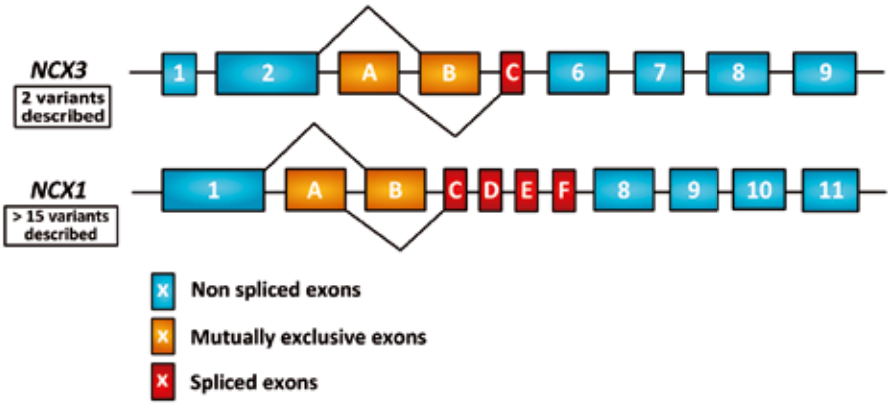

Figure 2 Alternative splicing of NCX1 and NCX3.

Schematic view of the exons constituting NCX3 (upper) and NCX1 (bottom) gene sequence and the alternatively spliced exons giving rise to multiple variants in mice (53,54).

The structure of the CBD2 of NCX3-B has been recently solved and compared to the CBD2 of NCX1-AD. A similar orientation is found between the β-sandwich and the unique α-helix of the F-G loop (59). In NCX1, the orientation of the α-helix differs among the splice variants and has been associated with the activation or inhibition during a rise in $[Ca^{2+}]_i$ (60). In NCX3 this helix is located after the alternatively splice region. Its orientation is therefore unchanged among the splice variants and correspond to an activation by elevation of $[Ca^{2+}]_i$.

With regard to the mutually exclusive exons, in NCX1, exon A and B have been hypothesized to be implicated in the signal transmission to the TM domains and in the capacity to alleviate the Na^+-dependent inactivation (44). The remaining exons spliced in NCX1, exon C, D, E and F would regulate the affinity at the Ca^{2+}-binding site of CBD1 (61). In the case of NCX3, the alternatively spliced exons A, B and C are conserved among species but they have a rather low homology with the corresponding exons of NCX1 and NCX2 (55-65%) (**Table 2**). It is therefore not possible to fully translate the observed effect of the alternative splicing of NCX1 to NCX3. Besides, it has been observed that the splice variants of NCX3 have different Ca^{2+}-binding sites in their CBD2 with different affinity for Ca^{2+} compared to NCX1 (50).

Table 2 Conservation of the amino-acids sequence coded by each exon of NCX3 in the NCX family.

Exon NCX3	Conservation Human/ Rodents	Number of Residues	Conservation human NCX1	Conservation human NCX2	Localization
Exon 1	Non translated	/	/	/	5' UTR
Exon 2	> 95%	594	68%	67%	TM segments Intracellular loop
Exon 3 (Exon A)	> 90%	36	64%	/	Intracellular loop
Exon 4 (Exon B)	100%	35	50%	66%	Intracellular loop
Exon 5 (Exon C)	100%	-ALLLSP-	-ALLLNEL-	-ALLLNQ-	Intracellular loop
Exon 6	> 95%	42	76%	85%	Intracellular loop
Exon 7	> 95%	33	88%	88%	Intracellular loop
Exon 8	> 95%	92	87%	86%	TM segments
Exon 9	> 95%	125	78%	82%	TM segments 3'UTR

Conservation of sequence determined between amino acid sequences of rodents NCX3 (accessions NP_001161392 and NP_536688), hNCX3 (accession NP_892114) and either hNCX1 (accession NP_066920) or hNCX2 (accession NP_055878). Exon 5, short exon coding for 6-7 amino acids for which sequence is provided between dashes.

Thus, the structural studies performed in the past few years brought crucial information on the mechanisms of translocation of NCX and the roles of the CBD1 and CBD2 in the regulation of the exchanger. Nonetheless, the exact mechanisms by which the intracellular loop influences the TM segments and the properties carried by each alternatively spliced exon of NCX3 are not yet fully understood.

Expression of NCX3 in tissues and organelles

Tissue expression

Another characteristic of NCX3 lies in its tissue-specific expression. NCX1 is highly expressed in heart, brain and kidney and is found at lower level in almost all cell types, while NCX2 expression is restricted to the brain. As for NCX3, initially detected in the brain and skeletal muscle (55), its distribution is actually much broader (**Table 3**).

Table 3 Specific tissue distribution of NCX3 and its roles in physiological conditions.

Organs	Regions/Cell types	Species investigated	Physiological Process involved	References
Central Nervous system	Cerebellum Trigeminal Ganglion Pons Thalamus Ventral striatum Hippocampus Amygdale	Rat Mice	Spatial learning Memory	(62-66)
Muscular system	Skeletal muscle	Rat Mice	Relaxation Long-term exercise	(67,68)
Osseous tissue	Osteoclast Osteoblast	Chicken Mouse	Bone formation/ resorption Osteoclastic pit formation Osteoblast differentiation	(69-71)
Dental tissue	Ameloblast Odontoblast	Rat	Dentinogenesis	(72,73)
Immune system	Dendritic cells Macrophages Monocytes Mast cells	Rat Mouse Human	TNFα production Respiratory burst during phagocytosis	(64,74-77)
Digestive system	Gastric myofibroblasts		Proliferation/migration	(78)
Urogenital system	Urethrae Bladder Oocytes	Rat Xenopus laevis	Activity of the Interstitial cells of Cajal Regulation Ca^{2+} signaling	(79,80)
Auditory system	Cochlea	Rat	Unknown	(81)
Others	Preadipocytes Trophoblasts Platelets	Human	Ca^{2+} oscillations Ca^{2+} efflux Collagen activation	(82,83)

Crosstalk with organelles

With regard to its localization within the cell, the first transmembrane segment of NCX3 presumably serves as a signal peptide routing this polytopic protein to the plasma membrane, similarly to NCX1. However, beyond its role at the plasma membrane, NCX3 is involved in Ca^{2+} handling throughout the entire cell.

Since the 2000's NCX isoforms have been hypothesized to participate and interfere with mitochondrial processes, in addition to the mitochondrial exchanger NCLX (84). Specifically, NCX3 is responsible for the conservation of the mitochondrial membrane potential. This capacity could contribute to the protective effect of NCX3 during hypoxia

(85,86). This crucial mechanism in stress conditions remains poorly understood but would, most likely, involve a relationship between the plasma membrane NCX and the mitochondria through a signaling pathway or a common interacting partner. A direct localization of NCX3 at the outer membrane of the mitochondria is less probable as the presence of multiple α-helical proteins is rather rare at the outer membrane of the mitochondria and requires a presequence recognized by the translocase of the outer membrane (87) that is absent in NCX3.

In numerous cell types, NCX is localized at the plasma membrane next to the junctional sarcoplasmic/endoplasmic reticulum (SR/ER) (88-92). Additionally, many experimental data support the assumption that the NCX family has a role in the regulation of the Ca^{2+} levels in the ER and SR potentially by working in its reverse mode of exchange (93-97). This latter point has been matter of debate in the past decades, as it was originally thought that the electrochemical gradient across the plasma membrane could not favor a reversal of NCX to allow a Ca^{2+} influx and therefore the reverse mode would be restricted to non-physiological conditions. However in the last ten years, the reversal of the NCX1 mode of exchange has been shown to occur in several physiological situations where membrane potential reach a value more positive than the reversal potential. This reversal can occur in excitable tissue during specific physiological events triggering a rise in intracellular Na^+ concentration ($[Na^+]_i$) as observed at the repolarization phase of the action potential in cardiomyocytes (98) and in early postnatal stages (99). Likewise, several pathological conditions allow the reversal of NCX activity as seen in hypoxic conditions and neuronal excitotoxicity or in failing human myocytes (100).

Regulations of NCX3 activity

Ionic regulation

NCX3 as all member of the NCX family can function in both forward and reverse mode. Nonetheless, according to the theoretical reversal potential (approximately -35mV), NCX3 in cells at resting conditions operates mostly in its forward mode (23). Among the NCX family, both modes of exchange are extremely dependent on $[Ca^{2+}]_i$. Thus, in a counterintuitive manner, the reverse mode has an absolute requirement for a rise in $[Ca^{2+}]_i$ in a physiological range from 0,1 to 1μM (26).The NCX family has a tremendous asymmetry in the affinity for Ca^{2+} on both side of the plasma membrane. The apparent affinity varies by a factor 10^3, Ca^{2+} having an affinity in the range of the mM (101) at the external side and μM at the internal side (26,59). On the Ca^{2+} efflux mode, the effect of extracellular Ca^{2+} remains controversial as it has been shown to inhibit the forward mode of NCX1 (102). However, Baker *et al*. did not find any effect of extracellular Ca^{2+} on the Ca^{2+} efflux process (103). These characteristics have been assumed to be similar in NCX3, though no study has investigated the exact activation constants.

Intracellular and extracellular Na^+ have also a crucial role in the NCX regulation. More precisely, a rise in intracellular Na^+ inhibits Ca^{2+} efflux through NCX with an inhibition constant of 30 mM (27). Moreover raising intracellular Na^+ has a similar effect as a rise in intracellular Ca^{2+}, in activating the Ca^{2+} influx with an affinity constant (Km) value of 50-80mM (27,104). Similar properties are observed for NCX3. Nonetheless, at high $[Na^+]_i$, NCX1 becomes inactive, a phenomenon also called Na^+-dependent inactivation and attributed to CBD2 (43,51). Such phenomenon could be of importance when facing high $[Na^+]_i$ such as during hypoxic conditions.

Intracellular pH has also a significant influence on NCX function. At an acidic pH, protons cause an inhibition of NCX activity, while a basic pH stimulates NCX. A small variation of pH has a great impact on NCX, even in conditions close to physiological pH (105). The increased intracellular concentration of proton ($[H^+]_i$) competes with Ca^{2+} for binding at the CBDs and reduces affinity for Ca^{2+}. On top of that, protons have a second inhibitory effect, requiring the presence of Na^+ (106). Thus, cellular acidification can lead to complete inhibition of NCX (107). Finally, it has to be noted that transport and/or inhibition/stimulation phenomenon caused by many divalent and monovalent cations have been found in the case of NCX1 and can presumably apply to NCX3 as well (108-110).

The alternative splicing of NCX1, similarly to NCX3, introduces variations in the CBD2 domain. This phenomenon affects greatly the ionic regulations of NCX1 by both Na^+ and Ca^{2+} (44,60), specifically the Na^+-dependent inactivation, the regulation of the latter by Ca^{2+}, and the Ca^{2+} activation (56). The influence of the alternative splicing on the capacities of exchange of NCX3 remains unknown. It most likely implicates as well variations in its ionic regulations although in a distinct manner from NCX1 due to the diversity of the spliced regions between the two isoforms.

Regulation by other molecules

Many molecules can regulate the Na^+-Ca^{2+} exchanger: phosphoarginine stimulates the forward mode of the exchanger directly at the transport sites, independently of the intracellular loop (111). The NADH/NAD^+ redox state of the cell also regulates NCX function; cytosolic NADH inhibits NCX (112), in a process involving reactive oxygen species (ROS) production in a manner independent of mitochondrial respiration. Although the activity of NCX1 and NCX2 are increased by nitric oxide, NCX3 is downregulated by such treatment (113). Finally, phosphatidylinositol-4,5-Phosphate (PIP_2) can bind NCX, a process dependent on both Ca^{2+} and ATP levels within a cell (114) providing the protection against proton regulation (115) and demonstrating how ATP can influence NCX exchange. ATP and its analogs containing a hydrolysable phosphate group have indeed been found to activate and promote Ca^{2+} efflux through the forward mode of NCX1 (26,28). This stimulation occurs mainly through the intracellular loop (26), through an increase in PIP_2 production and binding (115,116). However, upon a comparative study of the NCX isoforms, the Philipson's lab observed that NCX3 is

unaffected by ATP depletion. It remains unclear if this phenomenon is linked with PIP_2 production and physiological ATP stimulation (117).

Post-translational regulation

In 2008, pull down experiments confirmed the capacity of NCX1 to form dimers (118), a capacity assumed to be conserved among the NCX family. Further studies on the mechanisms underlying this phenomenon showed that the dimerization occurs in the plasma membrane and that Ca^{2+} plays an important role in this process together with residues coordinating the Ca^{2+}-binding site of CBD1 (119)

As for phosphorylation, its effects vary from tissue to tissue. Protein Kinase C (PKC) phosphorylation elevates the activity of NCX1 in cardiac and smooth muscle (52,120). However the opposite effect is observed in mesangial cells (121) and chromaffin cells (122). As for Protein Kinase A (PKA), the phosphorylation of NCX1 remains controversial (123). However, the exact mechanisms through which PKC and PKA regulate NCX1 function and presumably NCX3 remain unknown.

Finally, members of the NCX family can be cleaved by proteolytic enzymes, as first described in the case of NCX1 being cleaved by caspase-3 (124). It was originally thought that this cleavage could be part of the neuronal death program due to the loss of NCX activity. Nonetheless recent studies revealed that the cleaved NCX is hyperactive and most likely participates in a rescue mechanism by maintaining ER content (93). If the initial investigation of the complete NCX family revealed that ischemic conditions trigger cleavage of both NCX1 and NCX3 *in vivo* (125), during direct glutamate excitotoxicity, only NCX3 is cleaved in cerebellar granule neurons. This cleavage, confirmed in numerous studies since then, is attributed to calpain-1 and calpain-2 (93,126-128). Although predictions give rise to more than twenty different cleavage sites in the exchanger, investigations have centered upon four cleavage sites in the intracellular loop (125). The hyperfunctionality observed is in accordance with the implication of the cytoplasmic loop in the regulation by intracellular Ca^{2+} levels and the loss of regulation obtained by its deletion.

NCX3 in health and disease

Osseous tissue

NCX3 is the major isoform of NCX expressed in osseous tissue (69,71). More precisely, NCX3 plays an important role during osteoblast differentiation (71) through mechanisms implicating regulation of Ca^{2+} delivery to the osteoid, due to its localization close to the mineralizing bone surface (129). Additionally NCX3 is a major contributor of Ca^{2+} efflux from the osteoblasts in order to produce calcifying bone matrix (70). In osteoclasts, NCX3, along with NCX1, is involved in the Ca^{2+} transport allowing for the formation of the osteoclastic pit, necessary for the bone resorption process (69).

Immune system

The involvement of NCX in the immune system, controlling the Ca^{2+} influx in neutrophils, was first described 30 years ago (130). Since then, many observers have confirmed that the NCX family plays a crucial role in immune cells function (131). However, the first proof of the specific involvement of NCX3 appeared only recently, through its implication in the production of tumor necrosis factor-alpha (TNFα) in macrophages and monocytes (77). NCX1 and NCX3 are both involved in the Ca^{2+} uptake inducing TNFα production (77). In the microglia, where all isoforms of NCX are expressed, the reverse mode of NCX is responsible for the Ca^{2+} influx recorded during the respiratory burst accompanying phagocytosis processes (64).

In dendritic cells, immunosuppressive drugs such as dexamethasone lower the increase in $[Ca^{2+}]_i$ after exposure to lipopolysaccharides. This effect is attributed to an upregulation of NCX3, as increased expression and exchange capacity are detected after treatment (132). This correlates with the ability of the dendritic cells to mature and to perform their roles in the adaptive immune response. Studies on other immunosuppressive drugs showed very different effects on NCX isoforms and expression. This could be explained by the different cell types used in these studies and therefore the variability in the variants that are endogenously expressed (133,134).

NCX3 in the brain

Physiological conditions

In the brain, NCX3 is involved in numerous cellular processes. One of them is brain development, as NCX3 participates in the glial cells differentiation, driving the maturation of oligodendrocytes and myelin formation (135). The regulation of the NCX3 promoter through Ca^{2+} signals demonstrates that NCX3 might have a crucial role in neuronal differentiation and neuronal functions (136-138). Studies involving NCX3 Knock-out (KO) mice have unraveled the role of NCX3 in the modulation of the long-term potentiation (LTP) in the hippocampus, a region where NCX3 is typically highly expressed (65); the absence of NCX3 results in a significant loss of spatial learning and memory (139). However, it is not possible to conclude whether these deficits are due to developmental problems or adult dysfunctions. Finally, a recent study unraveled a possible coupling between NCX and the postsynaptic histamine receptors in the medial vestibular nucleus of the medulla that would mediate the post-synaptic actions of histamine (66).

Pathophysiological implications

In the 90's, a first investigation of the role of NCX in the brain during stress conditions led investigators to designate NCX as one the best candidates to perform the Ca^{2+} uptake observed during anoxia (140). Follow-up studies suggested a neuroprotective role for

NCX during hypoxia (141,142). Since 2000 and the description of the three main isoforms, many studies investigated these isoforms, pinpointing the importance of the third isoform of the NCX family during stress conditions.

The studies performed by the Annunziato's group (143) focused on ischemic conditions and showed the neuroprotective effect of both NCX1 and NCX3 during permanent artery occlusion. *In vitro* studies mimicking hypoxia in BHK cells depicted a neuroprotective effect exclusively for the third isoform of NCX (86), an effect confirmed by the increased brain damage observed in NCX3 KO mice in ischemic conditions (144). NCX3 is also involved in preconditioning mechanisms. After a short ischemia, NCX1 and NCX3 upregulation correlates with the regions depicting a protective effect to ischemia (145). Overexpression of both NCX2 and NCX3 in cortical neuronal cultures increases survival after ischemia from 20 to 80% (146). Finally, hyperoxic preconditioning leads to an upregulation of NCX3, which also has a similar protective effect (147).

The molecular mechanisms by which NCX is involved in pathophysiological conditions involve the cleavage of NCX1 and NCX3 by calpain 1 and 2 after ischemia. However, only NCX3 is cleaved by a direct excitotoxic exposure (125). Carafoli's and Nicotera's groups first hypothesized that the Ca^{2+} rise observed in excitotoxicity could be linked to the cleaved NCX and the ensuing loss of Ca^{2+} extrusion. Such loss of function would favor the accumulation of Ca^{2+} intracellulary therefore having a neurodegenerative impact. Recently, Annunziato's group concluded from their functional studies that the cleaved NCX3 is most likely hyperfunctional in its reverse mode, triggering a significant Ca^{2+} uptake (93), increasing the Ca^{2+} content of the ER and therefore delaying caspase-12 activation and neuronal cell death (**Figure 3**). The cleavage of NCX3 is also triggered by $A\beta_{1\text{-}42}$ peptide exposure, a peptide well known to accumulate in the brain of Alzheimer's disease (AD) patients, suggesting a cellular response, common to different stress types, and regulating the activity and expression of NCX3. Furthermore, level of cleaved NCX3 correlates perfectly with the level of $A\beta_{1\text{-}42}$ and calpain activity in AD patients post-mortem, further correlation between NCX3 and neuronal damage (127). Thus, NCX3 is well accepted as having a major role in the Ca^{2+} dysregulation deriving from excitotoxicity, and most likely acting in a neuroprotective manner in diverse pathologies. In this regard, the cleavage by calpain, rather than an aberrant proteolytic cleavage, constitutes a posttranslational regulation allowing for a tight regulation of the exchanger in correlation with the stress status of the cell.

Finally, NCX3 seems to be implicated not only in the excitotoxic conditions but also in the hyperexcitability state underlying the apparition of seizures, as an inhibition of NCX3 significantly reduces frequency and severity of seizures (148,149).

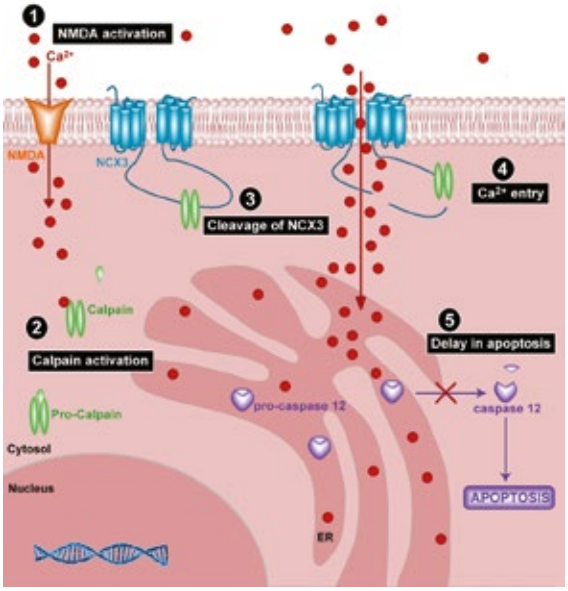

Figure 3 Calpain-mediated cleavage of NCX3 in neuronal excitotoxicity

Sequential events occurring during neuronal excitotoxicity and leading to the cleavage of NCX3 by calpain triggering Ca^{2+} entry and delaying neuronal cell death.1) the activation of the N-methyl-D-aspartate Receptor (NMDA) allowing for a mild Ca^{2+} entry causing 2) the autolysis of calpain. Thereafter, the cleavage by calpain of 3) NCX3 within the intracellular loop triggers 4) a strong influx of Ca^{2+} that increases ER content and 5) delays the activation of caspase-12 (125,150).

Skeletal muscle

Excitation-contraction coupling and neuromuscular transmission

In contrast to the development of the brain, NCX3 is only minutely involved in skeletal muscle development; thus in newborn rats its expression is barely detectable during the first weeks of life (67). During this period NCX1 might play a more important role as its expression is increased during differentiation and muscle development (67,151), before progressively decreasing in tandem with the maturation of the muscle fibers.

During the excitation-contraction (E-C) coupling, Ca^{2+} stored in the sarcoplasmic reticulum of the muscle fibers is release through the Ryanodine receptor (RyR) into the sarcoplasm. There, Ca^{2+} by binding to the troponin allows for the shortening of the sarcomere and the beginning of the contraction. Relaxation of the fiber is achieved by the re-uptake of Ca^{2+} into the SR by the SERCA and the Ca^{2+} extrusion extracellularly by NCX. In this regard, NCX3 plays an important role. The Na^{+}-Ca^{2+} exchange capacities in

both forward and reverse mode, assessed in skeletal muscle from NCX3 KO mice, exhibits a significant reduction in exchange capacity. In addition, skeletal muscle necrosis is found in the KO, confirmation of the crucial role of NCX3 in physiological conditions (68). However, it has to be noted that these recordings of NCX activity have been performed on flexor digitorum brevis (FDB), a fast-twitch muscle. Observations made in the last 20 years suggest that NCX is more important in slow-twitch muscle; as slow-twitch muscle contracts when external Na^+ is removed, an effect absent in fast-twitch muscle (152).

NCX3 is present at the neuromuscular junction (NMJ), and its absence results in dysfunctional stimulation of the muscle, and in particular a delayed neurotransmitter release during repetitive nerve stimulation (68). This effect suggests that NCX3, at the NMJ, has an important role in the nerve terminals in clearing Ca^{2+}, allowing the nerve terminal to release neurotransmitter at a full capacity (68).

Pathophysiological Implications

Little is known about the involvement of NCX3 in skeletal muscle pathologies. However in the pathogenesis of the Duchenne muscular dystrophy (DMD), dysregulation of the Ca^{2+} homeostasis is observed. This process has been attributed to an enhancement of the store-operated Ca^{2+} entry (SOCE) (153). However, both an upregulation of NCX3 and an increase in NCX capacity have been observed in DMD myotubes (153,154). Neither the effect of this upregulation during the pathogenesis of DMD nor the potential link of NCX3 with SOCE has yet been investigated. Additionally, the discovery of the cleavage of NCX3 by calpain 1 and 2 raises questions as to whether NCX3 is a substrate of calpain 3. Calpain 3 is predominant in the skeletal muscle and its loss of function is associated with the Limb-Girdle muscular dystrophy 2A (LGMD2A) (155), a so-called calpainopathy. In the absence of functional calpain-3, then, NCX3 might participate in the Ca^{2+} dysregulation associated with the pathogenesis of this muscular dystrophy.

Outline of this thesis

Na^+-Ca^{2+} exchange is critical for the maintenance of Ca^{2+} homeostasis. In human, three isoforms of the Na^+-Ca^{2+} exchanger are expressed. Of these, NCX1 has been extensively studied, providing a good basis for understanding the molecular aspects of the NCX family. However, the physiological role of NCX3 remains poorly understood. Its tissue expression together with its proposed involvement in the Ca^{2+} fluxes in relation with the ER and its cleavage by the Ca^{2+}-sensitive protease, calpain, suggest very distinctive functions and regulations for this isoform (150). Therefore, the aim of this thesis was to unravel the regulatory mechanisms of NCX3 such as ionic regulation, splicing and post-translational modifications in order to better comprehend its roles in brain and skeletal muscle.

By focusing on the alternative splicing of NCX3, **Chapter 2** elucidates the function of two different splice variants of NCX3 to understand their implications in muscle and neuronal physiology. Using fura-2 based Ca^{2+} imaging, this study provides a complete characterization of the two splice variants, NCX3-B and NCX3-AC, in both mode of exchange, pinpointing differences in their ionic regulation by intracellular Ca^{2+} and Na^{+} and further elucidating the underlying molecular mechanisms. In addition to the ionic regulation, numerous intracellular factors are involved in the modulation of the activity of NCX3, mostly by post-translational modification of its intracellular loop as addressed in **Chapters 3 and 4**. **Chapter 3** examines the influence of PKA and PKC phosphorylation on each variant of NCX3. Exchange activity is measured in both forward and reverse mode by means of Ca^{2+} imaging. Moreover, directed mutagenesis of putative phosphorylation sites located in the intracellular loop of the exchanger is used in order to dissect the molecular determinants of these regulations. **Chapter 4** investigates the influence of calpain on the function of NCX3 in skeletal muscle and discloses a distinct sensitivity of the two variants of NCX3. Using bioinformatics tools, a novel cleavage site is identified, and confirmed by site-directed mutagenesis. Primary interest is dedicated to the calpain-3, isoform specific of the skeletal muscle, and responsible for the limb-girdle muscular dystrophy 2A (LGMD2A) where Ca^{2+} disturbances are observed.

The past 10 years of research have implicated NCX in numerous pathological conditions (156). Among others roles, NCX and specifically NCX3 appeared to play a pivotal role during stress conditions such as neuronal excitotoxicity and has been linked to the aberrant Ca^{2+} influx seen in Alzheimer's disease and in diverse neuronal injuries (125,144,157). The study presented in **Chapter 5** provides an overview of the expression at the RNA level of the two isoforms of NCX, NCX1 and NCX3, in the healthy brain. By absolute quantification, these expressions are carefully compared in the diverse regions of the central nervous system with special attention devoted to the expression of NCX3 splice variants. The study identifies a third variant of NCX3 in mice and further examines NCX expression in hyper-glutamatergic conditions, using the glutamate dehydrogenase 1 (glud1) mice, and in excitotoxic conditions, using the alzheimer's disease mice model, AβPP-PS1.

Finally, the findings of this thesis are summarized in **Chapter 6**, and discussed by placing them in the context of the current knowledge regarding the physiological implications of NCX3.

References

1. **Campbell, A. K.** *Intracellular Calcium*, John Wiley & sons (2014)
2. **Greenberg, A. C. A.** *Primer on kidney diseases*, Elsevier Saunders (2005)
3. **McCormick, C. C.** Passive diffusion does not play a major role in the absorption of dietary calcium in normal adults. *The Journal of nutrition* 132, 3428-3430 (2002)
4. **Moe, S. M.** Disorders involving calcium, phosphorus, and magnesium. *Primary care* 35, 215-237, v-vi (2008)
5. **Sabanayagam, C., and Shankar, A.** Serum calcium levels and hypertension among U.S. adults. *Journal of clinical hypertension* 13, 716-721 (2011)
6. **Hoenderop, J. G., Muller, D., Van Der Kemp, A. W., Hartog, A., Suzuki, M., Ishibashi, K., Imai, M., Sweep, F., Willems, P. H., Van Os, C. H., and Bindels, R. J.** Calcitriol controls the epithelial calcium channel in kidney. *Journal of the American Society of Nephrology : JASN* 12, 1342-1349 (2001)
7. **Renkema, K. Y., Alexander, R. T., Bindels, R. J., and Hoenderop, J. G.** Calcium and phosphate homeostasis: concerted interplay of new regulators. *Annals of medicine* 40, 82-91 (2008)
8. **Schiaffino, S., and Reggiani, C.** Fiber types in mammalian skeletal muscles. *Physiological reviews* 91, 1447-1531 (2011)
9. **Favus MJ, G. D.** Regulation of Calcium and Magnesium. in *Primer on the metabolic bone diseases and disorders of mineral metabolism*, John wiley & Sons, Inc. pp pp 171-179 (2)
10. **van de Graaf, S. F., Bindels, R. J., and Hoenderop, J. G.** Physiology of epithelial Ca2+ and Mg2+ transport. *Reviews of physiology, biochemistry and pharmacology* 158, 77-160 (2007)
11. **Schafer, A. L., and Shoback, D. M.** Hypocalcemia: Diagnosis and Treatment. in *Endotext* (De Groot, L. J., Beck-Peccoz, P., Chrousos, G., Dungan, K., Grossman, A., Hershman, J. M., Koch, C., McLachlan, R., New, M., Rebar, R., Singer, F., Vinik, A., and Weickert, M. O. eds.), South Dartmouth (MA). pp (2000)
12. **Tan, H. L., Kupershmidt, S., Zhang, R., Stepanovic, S., Roden, D. M., Wilde, A. A., Anderson, M. E., and Balser, J. R.** A calcium sensor in the sodium channel modulates cardiac excitability. *Nature* 415, 442-447 (2002)
13. **Berl, T., Levi, M., Ellis, M., and Chaimovitz, C.** Mechanism of acute hypercalcemic hypertension in the conscious rat. *Hypertension* 7, 923-930 (1985)
14. **Lamboley, C. R., Murphy, R. M., McKenna, M. J., and Lamb, G. D.** Endogenous and maximal sarcoplasmic reticulum calcium content and calsequestrin expression in type I and type II human skeletal muscle fibres. *The Journal of physiology* 591, 6053-6068 (2013)
15. **Bygrave, F. L., and Benedetti, A.** What is the concentration of calcium ions in the endoplasmic reticulum? *Cell calcium* 19, 547-551 (1996)
16. **Ivannikov, M. V., and Macleod, G. T.** Mitochondrial free Ca(2)(+) levels and their effects on energy metabolism in Drosophila motor nerve terminals. *Biophysical journal* 104, 2353-2361 (2013)
17. **Boron WF, B. E.** *Medical physiology*, Saunders; 2 edition (2012)
18. **Yanez, M., Gil-Longo, J., and Campos-Toimil, M.** Calcium binding proteins. *Advances in experimental medicine and biology* 740, 461-482 (2012)
19. **Joachim K, M. M.** *Calcium: a matter of life or death*, Elsevier Science (2007)
20. **Schwaller, B.** Cytosolic Ca2+ buffers. *Cold Spring Harbor perspectives in biology* 2, a004051 (2010)
21. **Boron, W. F., and Boulpaep, E. L.** *Medical physiology : a cellular and molecular approach*, 2nd ed., Saunders/Elsevier, Philadelphia, PA (2009)

22. **He, L., Vasiliou, K., and Nebert, D. W.** Analysis and update of the human solute carrier (SLC) gene superfamily. *Human genomics* 3, 195-206 (2009)

23. **Eisner, D. A., and Lederer, W. J.** Na-Ca exchange: stoichiometry and electrogenicity. *The American journal of physiology* 248, C189-202 (1985)

24. **Hilgemann, D. W., Collins, A., Cash, D. P., and Nagel, G. A.** Cardiac Na(+)-Ca2+ exchange system in giant membrane patches. *Annals of the New York Academy of Sciences* 639, 126-139 (1991)

25. **Li, J. M., and Kimura, J.** Translocation mechanism of cardiac Na-Ca exchange. *Annals of the New York Academy of Sciences* 639, 48-60 (1991)

26. **DiPolo, R., and Beauge, L.** Characterization of the reverse Na/Ca exchange in squid axons and its modulation by Cai and ATP. Cai-dependent Nai/Cao and Nai/Nao exchange modes. *J Gen Physiol* 90, 505-525 (1987)

27. **DiPolo, R., and Beauge, L.** Ca2+ transport in nerve fibers. *Biochim Biophys Acta* 947, 549-569 (1988)

28. **Baker, P. F., and Glitsch, H. G.** Does metabolic energy participate directly in the Na+-dependent extrusion of Ca2+ -Ca2+ ions from squid giant axons? *The Journal of physiology* 233, 44P-46P (1973)

29. **Wakimoto, K., Kobayashi, K., Kuro, O. M., Yao, A., Iwamoto, T., Yanaka, N., Kita, S., Nishida, A., Azuma, S., Toyoda, Y., Omori, K., Imahie, H., Oka, T., Kudoh, S., Kohmoto, O., Yazaki, Y., Shigekawa, M., Imai, Y., Nabeshima, Y., and Komuro, I.** Targeted disruption of Na+/Ca2+ exchanger gene leads to cardiomyocyte apoptosis and defects in heartbeat. *The Journal of biological chemistry* 275, 36991-36998 (2000)

30. **On, C., Marshall, C. R., Chen, N., Moyes, C. D., and Tibbits, G. F.** Gene structure evolution of the Na+-Ca2+ exchanger (NCX) family. *BMC evolutionary biology* 8, 127 (2008)

31. **John, S. A., Liao, J., Jiang, Y., and Ottolia, M.** The cardiac Na+-Ca2+ exchanger has two cytoplasmic ion permeation pathways. *Proceedings of the National Academy of Sciences of the United States of America* 110, 7500-7505 (2013)

32. **Szerencsei, R. T., Kinjo, T. G., and Schnetkamp, P. P.** The topology of the C-terminal sections of the NCX1 Na (+) /Ca (2+) exchanger and the NCKX2 Na (+) /Ca (2+) -K (+) exchanger. *Channels (Austin)* 7, 109-114 (2013)

33. **Liao, J., Li, H., Zeng, W., Sauer, D. B., Belmares, R., and Jiang, Y.** Structural insight into the ion-exchange mechanism of the sodium/calcium exchanger. *Science* 335, 686-690 (2012)

34. **Kamiya, T., and Maeshima, M.** Residues in internal repeats of the rice cation/H+ exchanger are involved in the transport and selection of cations. *The Journal of biological chemistry* 279, 812-819 (2004)

35. **Nicoll, D. A., Sawaya, M. R., Kwon, S., Cascio, D., Philipson, K. D., and Abramson, J.** The crystal structure of the primary Ca2+ sensor of the Na+/Ca2+ exchanger reveals a novel Ca2+ binding motif. *The Journal of biological chemistry* 281, 21577-21581 (2006)

36. **Winkfein, R. J., Szerencsei, R. T., Kinjo, T. G., Kang, K., Perizzolo, M., Eisner, L., and Schnetkamp, P. P.** Scanning mutagenesis of the alpha repeats and of the transmembrane acidic residues of the human retinal cone Na/Ca-K exchanger. *Biochemistry* 42, 543-552 (2003)

37. **Wu, M., Tong, S., Waltersperger, S., Diederichs, K., Wang, M., and Zheng, L.** Crystal structure of Ca2+/H+ antiporter protein YfkE reveals the mechanisms of Ca2+ efflux and its pH regulation. *Proceedings of the National Academy of Sciences of the United States of America* 110, 11367-11372 (2013)

38. **Nishizawa, T., Kita, S., Maturana, A. D., Furuya, N., Hirata, K., Kasuya, G., Ogasawara, S., Dohmae, N., Iwamoto, T., Ishitani, R., and Nureki, O.** Structural basis for the counter-transport mechanism of a H+/Ca2+ exchanger. *Science* 341, 168-172 (2013)

39. **Matsuoka, S., Nicoll, D. A., Reilly, R. F., Hilgemann, D. W., and Philipson, K. D.** Initial localization of regulatory regions of the cardiac sarcolemmal Na(+)-Ca2+ exchanger. *Proceedings of the National Academy of Sciences of the United States of America* 90, 3870-3874 (1993)

40. **Hilge, M., Aelen, J., and Vuister, G.** W. Ca2+ regulation in the Na+/Ca2+ exchanger involves two markedly different Ca2+ sensors. *Mol Cell* 22, 15-25 (2006)

41. **Chaptal, V., Ottolia, M., Mercado-Besserer, G., Nicoll, D. A., Philipson, K. D., and Abramson, J.** Structure and functional analysis of a Ca2+ sensor mutant of the Na+/Ca2+ exchanger. *The Journal of biological chemistry* 284, 14688-14692 (2009)

42. **Giladi, M., Boyman, L., Mikhasenko, H., Hiller, R., and Khananshvili, D.** Essential role of the CBD1-CBD2 linker in slow dissociation of Ca2+ from the regulatory two-domain tandem of NCX1. *The Journal of biological chemistry* 285, 28117-28125 (2010)

43. **Giladi, M., and Khananshvili, D.** Molecular determinants of allosteric regulation in NCX proteins. *Adv Exp Med Biol* 961, 35-48 (2013)

44. **Hilge, M., Aelen, J., Foarce, A., Perrakis, A., and Vuister, G. W.** Ca2+ regulation in the Na+/Ca2+ exchanger features a dual electrostatic switch mechanism. P*roceedings of the National Academy of Sciences of the United States of America* 106, 14333-14338 (2009)

45. **Hilge, M., Aelen, J., Perrakis, A., and Vuister, G. W.** Structural basis for Ca2+ regulation in the Na+/Ca2+ exchanger. *Annals of the New York Academy of Sciences* 1099, 7-15 (2007)

46. **Ottolia, M., Nicoll, D. A., John, S., and Philipson, K. D.** Interactions between Ca2+ binding domains of the Na+-Ca2+ exchanger and secondary regulation. *Channels (Austin)* 4, 159-162 (2010)

47. **Johnson, E., Bruschweiler-Li, L., Showalter, S. A., Vuister, G. W., Zhang, F., and Bruschweiler, R.** Structure and dynamics of Ca2+-binding domain 1 of the Na+/Ca2+ exchanger in the presence and in the absence of Ca2+. *Journal of molecular biology* 377, 945-955 (2008)

48. **Wu, F., Wei, G. Z., Li, W. J., Liu, B., Zhou, J. J., Wang, H. C., and Gao, F.** Low extracellular K+ increases intracellular Ca2+ oscillation and injury by activating the reverse mode Na+-Ca2+ exchanger and inhibiting the Na+, K+ ATPase in rat cardiomyocytes. *International journal of cardiology* 140, 161-168 (2010)

49. **Wu, M., Tong, S., Gonzalez, J., Jayaraman, V., Spudich, J. L., and Zheng, L.** Structural basis of the Ca2+ inhibitory mechanism of Drosophila Na+/Ca2+ exchanger CALX and its modification by alternative splicing. *Structure* 19, 1509-1517 (2011)

50. **Breukels, V., Touw, W. G., and Vuister, G. W.** Structural and dynamic aspects of Ca2+ and Mg2+ binding of the regulatory domains of the Na+/Ca2+ exchanger. *Biochem Soc Trans* 40, 409-414 (2012)

51. **Hilgemann, D. W., Matsuoka, S., Nagel, G. A., and Collins, A.** Steady-state and dynamic properties of cardiac sodium-calcium exchange. Sodium-dependent inactivation. *J Gen Physiol* 100, 905-932 (1992)

52. **Iwamoto, T., Pan, Y., Wakabayashi, S., Imagawa, T., Yamanaka, H. I., and Shigekawa, M.** Phosphorylation-dependent regulation of cardiac Na+/Ca2+ exchanger via protein kinase C. *The Journal of biological chemistry* 271, 13609-13615 (1996)

53. **Nicoll, D. A., Quednau, B. D., Qui, Z., Xia, Y. R., Lusis, A. J., and Philipson, K. D.** Cloning of a third mammalian Na+-Ca2+ exchanger, NCX3. *J Biol Chem* 271, 24914-24921 (1996)

54. **Kofuji, P., Lederer, W. J., and Schulze, D. H.** Mutually exclusive and cassette exons underlie alternatively spliced isoforms of the Na/Ca exchanger. *J Biol Chem* 269, 5145-5149 (1994)

55. **Quednau, B. D., Nicoll, D. A., and Philipson, K. D.** Tissue specificity and alternative splicing of the Na+/Ca2+ exchanger isoforms NCX1, NCX2, and NCX3 in rat. *The American journal of physiology* 272, C1250-1261 (1997)

56. **Dyck, C., Omelchenko, A., Elias, C. L., Quednau, B. D., Philipson, K. D., Hnatowich, M., and Hryshko, L. V.** Ionic regulatory properties of brain and kidney splice variants of the NCX1 Na(+)-Ca(2+) exchanger. *J Gen Physiol* 114, 701-711 (1999)

57. **Lindgren, R. M., Zhao, J., Heller, S., Berglind, H., and Nister, M.** Molecular cloning and characterization of two novel truncated isoforms of human Na+/Ca2+ exchanger 3, expressed in fetal brain. *Gene* 348, 143-155 (2005)

58. **Gabellini, N., Bortoluzzi, S., Danieli, G. A., and Carafoli, E.** The human SLC8A3 gene and the tissue-specific Na+/Ca2+ exchanger 3 isoforms. *Gene* 298, 1-7 (2002)

59. **Breukels, V., Touw, W. G., and Vuister, G. W.** NMR structure note: solution structure of Ca(2)(+) binding domain 2B of the third isoform of the Na(+)/Ca(2)(+) exchanger. *J Biomol NMR* 54, 115-121 (2012)

60. **Giladi, M., Lee, S. Y., Hiller, R., Chung, K. Y., and Khananshvili, D.** Structure-dynamic determinants governing a mode of regulatory response and propagation of allosteric signal in splice variants of Na+/Ca2+ exchange (NCX) proteins. *The Biochemical journal* 465, 489-501 (2015)

61. **Giladi, M., Bohbot, H., Buki, T., Schulze, D. H., Hiller, R., and Khananshvili, D.** Dynamic features of allosteric Ca2+ sensor in tissue-specific NCX variants. *Cell calcium* 51, 478-485 (2012)

62. **Boscia, F., D'Avanzo, C., Pannaccione, A., Secondo, A., Casamassa, A., Formisano, L., Guida, N., Scorziello, A., Di Renzo, G., and Annunziato, L.** New roles of NCX in glial cells: activation of microglia in ischemia and differentiation of oligodendrocytes. *Advances in experimental medicine and biology* 961, 307-316 (2013)

63. **Kuroda, H., Sobhan, U., Sato, M., Tsumura, M., Ichinohe, T., Tazaki, M., and Shibukawa, Y.** Sodium-calcium exchangers in rat trigeminal ganglion neurons. *Mol Pain* 9, 22 (2013)

64. N**ewell, E. W., Stanley, E. F., and Schlichter, L. C.** Reversed Na+/Ca2+ exchange contributes to Ca2+ influx and respiratory burst in microglia. *Channels (Austin)* 1, 366-376 (2007)

65. **Papa, M., Canitano, A., Boscia, F., Castaldo, P., Sellitti, S., Porzig, H., Taglialatela, M., and Annunziato, L.** Differential expression of the Na+-Ca2+ exchanger transcripts and proteins in rat brain regions. *J Comp Neurol* 461, 31-48 (2003)

66. **Zhang, X. Y., Yu, L., Zhuang, Q. X., Peng, S. Y., Zhu, J. N., and Wang, J. J.** Postsynaptic mechanisms underlying the excitatory action of histamine on medial vestibular nucleus neurons in rats. *British journal of pharmacology* 170, 156-169 (2013)

67. **Fraysse, B., Rouaud, T., Millour, M., Fontaine-Perus, J., Gardahaut, M. F., and Levitsky, D. O.** Expression of the Na(+)/Ca(2+) exchanger in skeletal muscle. *American journal of physiology. Cell physiology* 280, C146-154 (2001)

68. **Sokolow, S., Manto, M., Gailly, P., Molgo, J., Vandebrouck, C., Vanderwinden, J. M., Herchuelz, A., and Schurmans, S.** Impaired neuromuscular transmission and skeletal muscle fiber necrosis in mice lacking Na/Ca exchanger 3. *J Clin Invest* 113, 265-273 (2004)

69. **Li, J. P., Kajiya, H., Okamoto, F., Nakao, A., Iwamoto, T., and Okabe, K.** Three Na+/Ca2+ exchanger (NCX) variants are expressed in mouse osteoclasts and mediate calcium transport during bone resorption. *Endocrinology* 148, 2116-2125 (2007)

70. **Sosnoski, D. M., and Gay, C. V.** NCX3 is a major functional isoform of the sodium-calcium exchanger in osteoblasts. *J Cell Biochem* 103, 1101-1110 (2008)

71. **Stains, J. P., Weber, J. A., and Gay, C. V.** Expression of Na(+)/Ca(2+) exchanger isoforms (NCX1 and NCX3) and plasma membrane Ca(2+) ATPase during osteoblast differentiation. *J Cell Biochem* 84, 625-635 (2002)

72. **Okumura, R., Shibukawa, Y., Muramatsu, T., Hashimoto, S., Nakagawa, K., Tazaki, M., and Shimono, M.** Sodium-calcium exchangers in rat ameloblasts. *Journal of pharmacological sciences* 112, 223-230 (2010)

73. **Tsumura, M., Okumura, R., Tatsuyama, S., Ichikawa, H., Muramatsu, T., Matsuda, T., Baba, A., Suzuki, K., Kajiya, H., Sahara, Y., Tokuda, M., Momose, Y., Tazaki, M., Shimono, M., and Shibukawa, Y.** Ca2+ extrusion via Na+-Ca2+ exchangers in rat odontoblasts. *J Endod* 36, 668-674 (2010)

74. **Aneiros, E., Philipp, S., Lis, A., Freichel, M., and Cavalie, A.** Modulation of Ca2+ signaling by Na+/Ca2+ exchangers in mast cells. *Journal of immunology* 174, 119-130 (2005)

75. **Donnadieu, E., and Trautmann, A.** Is there a Na+/Ca2+ exchanger in macrophages and in lymphocytes? *Pflugers Archiv : European journal of physiology* 424, 448-455 (1993)

76. **Nurbaeva, M. K., Schmid, E., Szteyn, K., Yang, W., Viollet, B., Shumilina, E., and Lang, F.** Enhanced Ca(2)(+) entry and Na+/Ca(2)(+) exchanger activity in dendritic cells from AMP-activated protein kinase-deficient mice. *FASEB J* 26, 3049-3058 (2012)

77. **Staiano, R. I., Granata, F., Secondo, A., Petraroli, A., Loffredo, S., Frattini, A., Annunziato, L., Marone, G., and Triggiani, M.** Expression and function of Na+/Ca2+ exchangers 1 and 3 in human macrophages and monocytes. *Eur J Immunol* 39, 1405-1418 (2009)

78. **Kemeny, L. V., Schnur, A., Czepan, M., Rakonczay, Z., Jr., Gal, E., Lonovics, J., Lazar, G., Simonka, Z., Venglovecz, V., Maleth, J., Judak, L., Nemeth, I. B., Szabo, K., Almassy, J., Virag, L., Geisz, A., Tiszlavicz, L., Yule, D. I., Wittmann, T., Varro, A., and Hegyi, P.** Na+/Ca2+ exchangers regulate the migration and proliferation of human gastric myofibroblasts. *American journal of physiology. Gastrointestinal and liver physiology* 305, G552-563 (2013)

79. **Solis-Garrido, L. M., Pintado, A. J., Andres-Mateos, E., Figueroa, M., Matute, C., and Montiel, C.** Cross-talk between native plasmalemmal Na+/Ca2+ exchanger and inositol 1,4,5-trisphosphate-sensitive Ca2+ internal store in Xenopus oocytes. *The Journal of biological chemistry* 279, 52414-52424 (2004)

80. **Zhong, X., Deng, J., He, P., You, N., Wang, Q., Song, B., and Li, L.** Reverse mode of the sodium/calcium exchanger subtype 3 in interstitial cells of Cajal from rat bladder. *Urology* 82, 254 e257-212 (2013)

81. **Yamauchi, D., Nakaya, K., Raveendran, N. N., Harbidge, D. G., Singh, R., Wangemann, P., and Marcus, D. C.** Expression of epithelial calcium transport system in rat cochlea and vestibular labyrinth. *BMC physiology* 10, 1 (2010)

82. **Hu, R., He, M. L., Hu, H., Yuan, B. X., Zang, W. J., Lau, C. P., Tse, H. F., and Li, G. R.** Characterization of calcium signaling pathways in human preadipocytes. *Journal of cellular physiology* 220, 765-770 (2009)

83. **Roberts, D. E., Matsuda, T., and Bose, R.** Molecular and functional characterization of the human platelet Na(+) /Ca(2+) exchangers. *British journal of pharmacology* 165, 922-936 (2012)

84. **Palty, R., Silverman, W. F., Hershfinkel, M., Caporale, T., Sensi, S. L., Parnis, J., Nolte, C., Fishman, D., Shoshan-Barmatz, V., Herrmann, S., Khananshvili, D., and Sekler, I.** NCLX is an essential component of mitochondrial Na+/Ca2+ exchange. *Proceedings of the National Academy of Sciences of the United States of America* 107, 436-441 (2010)

85. **Scorziello, A., Savoia, C., Sisalli, M. J., Adornetto, A., Secondo, A., Boscia, F., Esposito, A., Polishchuk, E. V., Polishchuk, R. S., Molinaro, P., Carlucci, A., Lignitto, L., Di Renzo, G., Feliciello, A., and Annunziato, L.** NCX3 regulates mitochondrial Ca(2+) handling through the AKAP121-anchored signaling complex and prevents hypoxia-induced neuronal death. *Journal of cell science* 126, 5566-5577 (2013)

86. **Secondo, A., Staiano, R. I., Scorziello, A., Sirabella, R., Boscia, F., Adornetto, A., Valsecchi, V., Molinaro, P., Canzoniero, L. M., Di Renzo, G., and Annunziato, L.** BHK cells transfected with NCX3 are more resistant to hypoxia followed by reoxygenation than those transfected with NCX1 and NCX2: Possible relationship with mitochondrial membrane potential. *Cell calcium* 42, 521-535 (2007)

87. **Wiedemann, N., Frazier, A. E., and Pfanner, N.** The protein import machinery of mitochondria. *The Journal of biological chemistry* 279, 14473-14476 (2004)

88. **Blaustein, M. P., Juhaszova, M., Golovina, V. A., Church, P. J., and Stanley, E. F.** Na/Ca exchanger and PMCA localization in neurons and astrocytes: functional implications. *Annals of the New York Academy of Sciences* 976, 356-366 (2002)

89. **Juhaszova, M., and Blaustein, M. P.** Na+ pump low and high ouabain affinity alpha subunit isoforms are differently distributed in cells. *Proceedings of the National Academy of Sciences of the United States of America* 94, 1800-1805 (1997)

90. **Lencesova, L., O'Neill, A., Resneck, W. G., Bloch, R. J., and Blaustein, M. P.** Plasma membrane-cytoskeleton-endoplasmic reticulum complexes in neurons and astrocytes. *The Journal of biological chemistry* 279, 2885-2893 (2004)

91. **Kuszczak, I., Kuner, R., Samson, S. E., and Grover, A. K.** Proximity of Na+ -Ca2+ -exchanger and sarco/endoplasmic reticulum Ca2+ pump in pig coronary artery smooth muscle: fluorescence microscopy. *Molecular and cellular biochemistry* 339, 293-300 (2010)

92. **Moore, E. D., Etter, E. F., Philipson, K. D., Carrington, W. A., Fogarty, K. E., Lifshitz, L. M., and Fay, F. S.** Coupling of the Na+/Ca2+ exchanger, Na+/K+ pump and sarcoplasmic reticulum in smooth muscle. *Nature* 365, 657-660 (1993)

93. **Pannaccione, A., Secondo, A., Molinaro, P., D'Avanzo, C., Cantile, M., Esposito, A., Boscia, F., Scorziello, A., Sirabella, R., Di Renzo, G., and Annunziato, L.** A New Concept: Abeta1-42 Generates a Hyperfunctional Proteolytic NCX3 Fragment That Delays Caspase-12 Activation and Neuronal Death. *J Neurosci* 32, 10609-10617 (2012)

94. **Hove-Madsen, L., and Tort, L.** Characterization of the relationship between Na+ -Ca2+ exchange rate and cytosolic calcium in trout cardiac myocytes. *Pflugers Archiv : European journal of physiology* 441, 701-708 (2001)

95. **Germinario, E., Esposito, A., Midrio, M., Peron, S., Palade, P. T., Betto, R., and Danieli-Betto, D.** High-frequency fatigue of skeletal muscle: role of extracellular Ca(2+). *European journal of applied physiology* 104, 445-453 (2008)

96. **Davis, K. A., Samson, S. E., Hammel, K. E., Kiss, L., Fulop, F., and Grover, A. K.** Functional linkage of Na+-Ca2+-exchanger to sarco/endoplasmic reticulum Ca2+ pump in coronary artery: comparison of smooth muscle and endothelial cells. *Journal of cellular and molecular medicine* 13, 1775-1783 (2009)

97. **Lemos, V. S., Poburko, D., Liao, C. H., Cole, W. C., and van Breemen, C.** Na+ entry via TRPC6 causes Ca2+ entry via NCX reversal in ATP stimulated smooth muscle cells. *Biochemical and biophysical research communications* 352, 130-134 (2007)

98. **Armoundas, A. A., Hobai, I. A., Tomaselli, G. F., Winslow, R. L., and O'Rourke, B.** Role of sodium-calcium exchanger in modulating the action potential of ventricular myocytes from normal and failing hearts. *Circulation research* 93, 46-53 (2003)

99. **Huang, J., Hove-Madsen, L., and Tibbits, G. F.** SR Ca2+ refilling upon depletion and SR Ca2+ uptake rates during development in rabbit ventricular myocytes. *American journal of physiology. Cell physiology* 293, C1906-1915 (2007)

100. **Piacentino, V., 3rd, Margulies, K. B., and Houser, S. R.** Ca influx via the Na/Ca exchanger maintains sarcoplasmic reticulum Ca content in failing human myocytes. *Annals of the New York Academy of Sciences* 976, 476-477 (2002)

101. **Blaustein, M. P., and Santiago, E. M.** Effects of internal and external cations and of ATP on sodium-calcium and calcium-calcium exchange in squid axons. *Biophysical journal* 20, 79-111 (1977)

102. **Ashley, C. C., Ellory, J. C., and Hainaut, K.** Calcium movements in single crustacean muscle fibres. *The Journal of physiology* 242, 255-272 (1974)

103. **Baker, P. F., and McNaughton, P. A.** Kinetics and energetics of calcium efflux from intact squid giant axons. *The Journal of physiology* 259, 103-144 (1976)

104. **Baker, P. F., Blaustein, M. P., Hodgkin, A. L., and Steinhardt, R. A.** The influence of calcium on sodium efflux in squid axons. *The Journal of physiology* 200, 431-458 (1969)

105. **Doering, A. E., and Lederer, W. J.** The action of Na+ as a cofactor in the inhibition by cytoplasmic protons of the cardiac Na(+)-Ca2+ exchanger in the guinea-pig. *The Journal of physiology* 480 (Pt 1), 9-20 (1994)

106. **Doering, A. E., and Lederer, W. J.** The mechanism by which cytoplasmic protons inhibit the sodium-calcium exchanger in guinea-pig heart cells. *The Journal of physiology* 466, 481-499 (1993)

107. **Boyman, L., Hagen, B. M., Giladi, M., Hiller, R., Lederer, W. J., and Khananshvili, D.** Proton-sensing Ca2+ binding domains regulate the cardiac Na+/Ca2+ exchanger. *The Journal of biological chemistry* 286, 28811-28820 (2011)

108. **Iwamoto, T., Uehara, A., Nakamura, T. Y., Imanaga, I., and Shigekawa, M.** Chimeric analysis of Na(+)/Ca(2+) exchangers NCX1 and NCX3 reveals structural domains important for differential sensitivity to external Ni(2+) or Li(+). *The Journal of biological chemistry* 274, 23094-23102 (1999)

109. **Russell, J. M., and Blaustein, M. P.** Calcium efflux from barnacle muscle fibers. Dependence on external cations. *J Gen Physiol* 63, 144-167 (1974)

110. **Trosper, T. L., and Philipson, K. D.** Effects of divalent and trivalent cations on Na+-Ca2+ exchange in cardiac sarcolemmal vesicles. *Biochimica et biophysica acta* 731, 63-68 (1983)

111. **DiPolo, R., Berberian, G., and Beauge, L.** Phosphoarginine regulation of the squid nerve Na+/Ca2+ exchanger: metabolic pathway and exchanger-ligand interactions different from those seen with ATP. *The Journal of physiology* 554, 387-401 (2004)

112. **Liu, T., and O'Rourke, B.** Regulation of the Na+/Ca2+ exchanger by pyridine nucleotide redox potential in ventricular myocytes. *The Journal of biological chemistry* 288, 31984-31992 (2013)

113. **Secondo, A., Molinaro, P., Pannaccione, A., Esposito, A., Cantile, M., Lippiello, P., Sirabella, R., Iwamoto, T., Di Renzo, G., and Annunziato, L.** Nitric oxide stimulates NCX1 and NCX2 but inhibits NCX3 isoform by three distinct molecular determinants. *Molecular pharmacology* 79, 558-568 (2011)

114. **Beauge, L., Asteggiano, C., and Berberian, G.** Regulation of phosphatidylinositol-4,5-biphosphate bound to the bovine cardiac Na+/Ca2+ exchanger. *Annals of the New York Academy of Sciences* 976, 288-299 (2002)

115. B**erberian, G., Forcato, D., and Beauge, L.** Key role of a PtdIns-4,5P2 micro domain in ionic regulation of the mammalian heart Na+/Ca2+ exchanger. *Cell calcium* 45, 546-553 (2009)

116. **Hilgemann, D. W., and Ball, R.** Regulation of cardiac Na+,Ca2+ exchange and KATP potassium channels by PIP2. *Science* 273, 956-959 (1996)

117. **Linck, B., Qiu, Z., He, Z., Tong, Q., Hilgemann, D. W., and Philipson, K. D.** Functional comparison of the three isoforms of the Na+/Ca2+ exchanger (NCX1, NCX2, NCX3). *The American journal of physiology* 274, C415-423 (1998)

118. **Ren, X., Nicoll, D. A., Galang, G., and Philipson, K. D.** Intermolecular cross-linking of Na+-Ca2+ exchanger proteins: evidence for dimer formation. *Biochemistry* 47, 6081-6087 (2008)

119. **John, S. A., Ribalet, B., Weiss, J. N., Philipson, K. D., and Ottolia, M.** Ca2+-dependent structural rearrangements within Na+-Ca2+ exchanger dimers. *Proceedings of the National Academy of Sciences of the United States of America* 108, 1699-1704 (2011)

120. **Iwamoto, T., Wakabayashi, S., and Shigekawa, M.** Growth factor-induced phosphorylation and activation of aortic smooth muscle Na+/Ca2+ exchanger. *The Journal of biological chemistry* 270, 8996-9001 (1995)

121. **Mene, P., Pugliese, F., and Cinotti, G. A.** Regulation of Na(+)-Ca2+ exchange in cultured human mesangial cells. *The American journal of physiology* 261, F466-473 (1991)

122. **Lin, L. F., Kao, L. S., and Westhead, E. W.** Agents that promote protein phosphorylation inhibit the activity of the Na+/Ca2+ exchanger and prolong Ca2+ transients in bovine chromaffin cells. *Journal of neurochemistry* 63, 1941-1947 (1994)

123. **Morad, M., Cleemann, L., and Menick, D. R.** NCX1 phosphorylation dilemma: a little closer to resolution. Focus on "Full-length cardiac Na+/Ca2+ exchanger 1 protein is not phosphorylated by protein kinase A". *American journal of physiology. Cell physiology* 300, C970-973 (2011)

124. **Schwab, B. L., Guerini, D., Didszun, C., Bano, D., Ferrando-May, E., Fava, E., Tam, J., Xu, D., Xanthoudakis, S., Nicholson, D. W., Carafoli, E., and Nicotera, P.** Cleavage of plasma membrane calcium pumps by caspases: a link between apoptosis and necrosis. *Cell death and differentiation* 9, 818-831 (2002)

125. **Bano, D., Young, K. W., Guerin, C. J., Lefeuvre, R., Rothwell, N. J., Naldini, L., Rizzuto, R., Carafoli, E., and Nicotera, P.** Cleavage of the plasma membrane Na+/Ca2+ exchanger in excitotoxicity. *Cell* 120, 275-285 (2005)

126. **Araujo, I. M., Carreira, B. P., Pereira, T., Santos, P. F., Soulet, D., Inacio, A., Bahr, B. A., Carvalho, A. P., Ambrosio, A. F., and Carvalho, C. M.** Changes in calcium dynamics following the reversal of the sodium-calcium exchanger have a key role in AMPA receptor-mediated neurodegeneration via calpain activation in hippocampal neurons. *Cell death and differentiation* 14, 1635-1646 (2007)

127. **Atherton, J., Kurbatskaya, K., Bondulich, M., Croft, C. L., Garwood, C. J., Chhabra, R., Wray, S., Jeromin, A., Hanger, D. P., and Noble, W.** Calpain cleavage and inactivation of the sodium calcium exchanger-3 occur downstream of Abeta in Alzheimer's disease. *Aging cell* 13, 49-59 (2014)

128. **Gerencser, A. A., Mark, K. A., Hubbard, A. E., Divakaruni, A. S., Mehrabian, Z., Nicholls, D. G., and Polster, B. M.** Real-time visualization of cytoplasmic calpain activation and calcium deregulation in acute glutamate excitotoxicity. *Journal of neurochemistry* 110, 990-1004 (2009)

129. **Stains, J. P., and Gay, C. V.** Asymmetric distribution of functional sodium-calcium exchanger in primary osteoblasts. *Journal of bone and mineral research : the official journal of the American Society for Bone and Mineral Research* 13, 1862-1869 (1998)

130. **Simchowitz, L., and Cragoe, E. J., Jr.** Na+-Ca2+ exchange in human neutrophils. *The American journal of physiology* 254, C150-164 (1988)

131. **Wacholtz, M. C., Cragoe, E. J., Jr., and Lipsky, P. E.** A Na(+)-dependent Ca2+ exchanger generates the sustained increase in intracellular Ca2+ required for T cell activation. *Journal of immunology* 149, 1912-1920 (1992)

132. **Heise, N., Shumilina, E., Nurbaeva, M. K., Schmid, E., Szteyn, K., Yang, W., Xuan, N. T., Wang, K., Zemtsova, I. M., Duszenko, M., and Lang, F.** Effect of dexamethasone on Na+/Ca2+ exchanger in dendritic cells. *American journal of physiology. Cell physiology* 300, C1306-1313 (2011)

133. **Elbaz, B., Alperovitch, A., Gottesman, M. M., Kimchi-Sarfaty, C., and Rahamimoff, H.** Modulation of Na+-Ca2+ exchanger expression by immunosuppressive drugs is isoform-specific. *Molecular pharmacology* 73, 1254-1263 (2008)

134. **Rahamimoff, H., Elbaz, B., Valitsky, M., Khatib, M., Eskin-Schwartz, M., and Elmaz, D.** Immunosuppressive drugs, immunophilins, and functional expression of NCX isoforms. *Advances in experimental medicine and biology* 961, 275-287 (2013)

135. **Boscia, F., D'Avanzo, C., Pannaccione, A., Secondo, A., Casamassa, A., Formisano, L., Guida, N., Sokolow, S., Herchuelz, A., and Annunziato, L.** Silencing or knocking out the Na(+)/Ca(2+) exchanger-3 (NCX3) impairs oligodendrocyte differentiation. *Cell death and differentiation* 19, 562-572 (2012)

136. **Gabellini, N.** Transcriptional regulation by cAMP and Ca2+ links the Na+/Ca2+ exchanger 3 to memory and sensory pathways. *Molecular neurobiology* 30, 91-116 (2004)

137. **Gabellini, N., Bortoluzzi, S., Danieli, G. A., and Carafoli, E.** Control of the Na+/Ca2+ exchanger 3 promoter by cyclic adenosine monophosphate and Ca2+ in differentiating neurons. *J Neurochem* 84, 282-293 (2003)

138. **Gomez-Villafuertes, R., Torres, B., Barrio, J., Savignac, M., Gabellini, N., Rizzato, F., Pintado, B., Gutierrez-Adan, A., Mellstrom, B., Carafoli, E., and Naranjo, J. R.** Downstream regulatory element antagonist modulator regulates Ca2+ homeostasis and viability in cerebellar neurons. *J Neurosci* 25, 10822-10830 (2005)

139. **Molinaro, P., Viggiano, D., Nistico, R., Sirabella, R., Secondo, A., Boscia, F., Pannaccione, A., Scorziello, A., Mehdawy, B., Sokolow, S., Herchuelz, A., Di Renzo, G. F., and Annunziato, L.** Na+ -Ca2+ exchanger (NCX3) knock-out mice display an impairment in hippocampal long-term potentiation and spatial learning and memory. *The Journal of neuroscience : the official journal of the Society for Neuroscience* 31, 7312-7321 (2011)

140. **Stys, P. K., Waxman, S. G., and Ransom, B. R.** Ionic mechanisms of anoxic injury in mammalian CNS white matter: role of Na+ channels and Na(+)-Ca2+ exchanger. *The Journal of neuroscience : the official journal of the Society for Neuroscience* 12, 430-439 (1992)

141. **Amoroso, S., Tortiglione, A., Secondo, A., Catalano, A., Montagnani, S., Di Renzo, G., and Annunziato, L.** Sodium nitroprusside prevents chemical hypoxia-induced cell death through iron ions stimulating the activity of the Na+-Ca2+ exchanger in C6 glioma cells. *Journal of neurochemistry* 74, 1505-1513 (2000)

142. **Matsuda, T., Takuma, K., Nishiguchi, E., Hashimoto, H., Azuma, J., and Baba, A.** Involvement of Na+-Ca2+ exchanger in reperfusion-induced delayed cell death of cultured rat astrocytes. *The European journal of neuroscience* 8, 951-958 (1996)

143. **Pignataro, G., Gala, R., Cuomo, O., Tortiglione, A., Giaccio, L., Castaldo, P., Sirabella, R., Matrone, C., Canitano, A., Amoroso, S., Di Renzo, G., and Annunziato, L.** Two sodium/calcium exchanger gene products, NCX1 and NCX3, play a major role in the development of permanent focal cerebral ischemia. *Stroke* 35, 2566-2570 (2004)

144. **Molinaro, P., Cuomo, O., Pignataro, G., Boscia, F., Sirabella, R., Pannaccione, A., Secondo, A., Scorziello, A., Adornetto, A., Gala, R., Viggiano, D., Sokolow, S., Herchuelz, A., Schurmans, S., Di Renzo, G., and Annunziato, L.** Targeted disruption of Na+/Ca2+ exchanger 3 (NCX3) gene leads to a worsening of ischemic brain damage. *J Neurosci* 28, 1179-1184 (2008)

145. **Pignataro, G., Boscia, F., Esposito, E., Sirabella, R., Cuomo, O., Vinciguerra, A., Di Renzo, G., and Annunziato, L.** NCX1 and NCX3: two new effectors of delayed preconditioning in brain ischemia. *Neurobiology of disease* 45, 616-623 (2012)

146. **Cross, J. L., Boulos, S., Shepherd, K. L., Craig, A. J., Lee, S., Bakker, A. J., Knuckey, N. W., and Meloni, B. P.** High level over-expression of different NCX isoforms in HEK293 cell lines and primary neuronal cultures is protective following oxygen glucose deprivation. *Neuroscience research* 73, 191-198 (2012)

147. **Mohammadi, E., and Bigdeli, M. R.** Effects of preconditioning with normobaric hyperoxia on Na(+)/Ca(2)(+) exchanger in the rat brain. *Neuroscience* 237, 277-284 (2013)

148. **Martinez, Y., and N'Gouemo, P.** Blockade of the sodium calcium exchanger exhibits anticonvulsant activity in a pilocarpine model of acute seizures in rats. *Brain research* 1366, 211-216 (2010)

149. **N'Gouemo, P.** Probing the role of the sodium/calcium exchanger in pentylenetetrazole-induced generalized seizures in rats. *Brain research bulletin* 90, 52-57 (2013)

150. **Pannaccione, A., Secondo, A., Molinaro, P., D'Avanzo, C., Cantile, M., Esposito, A., Boscia, F., Scorziello, A., Sirabella, R., Sokolow, S., Herchuelz, A., Di Renzo, G., and Annunziato, L.** A new concept: Abeta1-42 generates a hyperfunctional proteolytic NCX3 fragment that delays caspase-12 activation and neuronal death. *The Journal of neuroscience : the official journal of the Society for Neuroscience* 32, 10609-10617 (2012)

151. **Deval, E., Levitsky, D. O., Constantin, B., Raymond, G., and Cognard, C.** Expression of the sodium/calcium exchanger in mammalian skeletal muscle cells in primary culture. *Experimental cell research* 255, 291-302 (2000)

152. **Leoty, C.** Sodium withdrawal contractures in rat slow twitch skeletal muscle. *General physiology and biophysics* 3, 413-429 (1984)

153. **Zhao, X., Moloughney, J. G., Zhang, S., Komazaki, S., and Weisleder, N.** Orai1 mediates exacerbated Ca(2+) entry in dystrophic skeletal muscle. *PloS one* 7, e49862 (2012)

154. **Deval, E., Levitsky, D. O., Marchand, E., Cantereau, A., Raymond, G., and Cognard, C.** Na(+)/Ca(2+) exchange in human myotubes: intracellular calcium rises in response to external sodium depletion are enhanced in DMD. *Neuromuscular disorders : NMD* 12, 665-673 (2002)

155. **Kramerova, I., Kudryashova, E., Wu, B., Ottenheijm, C., Granzier, H., and Spencer, M. J.** Novel role of calpain-3 in the triad-associated protein complex regulating calcium release in skeletal muscle. *Human molecular genetics* 17, 3271-3280 (2008)

156. **Wakimoto, K., Kuro-o, M., Yanaka, N., Komuro, I., Nabeshima, Y. I., and Imai, Y.** Expression of Na+/Ca(2+) exchanger (NCX1) gene in the developmental mouse embryo and adult mouse brain. *Comparative biochemistry and physiology. Part B, Biochemistry & molecular biology* 130, 191-198 (2001)

157. **Amoroso, S., De Maio, M., Russo, G. M., Catalano, A., Bassi, A., Montagnani, S., Renzo, G. D., and Annunziato, L.** Pharmacological evidence that the activation of the Na(+)-Ca2+ exchanger protects C6 glioma cells during chemical hypoxia. *British journal of pharmacology* 121, 303-309 (1997)

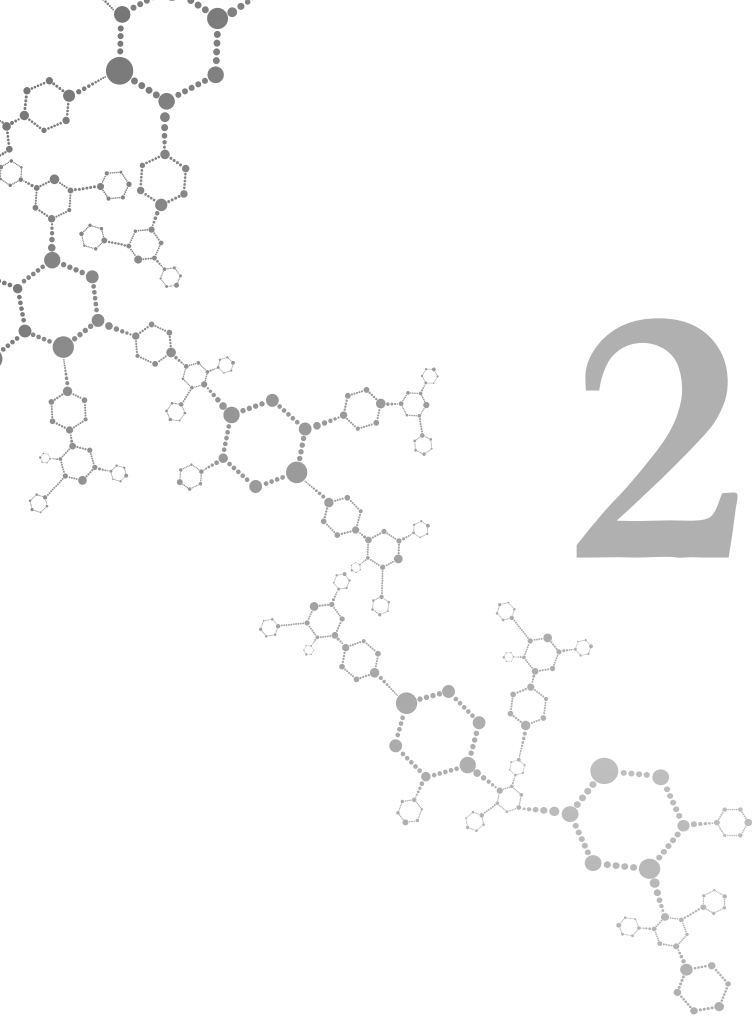

2

Function and regulation of the Na^+-Ca^{2+} exchanger NCX3 splice variants in brain and skeletal muscle

Lauriane Y.M. Michel[1,2], Sjoerd Verkaart[1], Werner J.H. Koopman[2,3], Peter H.G.M. Willems[2,3], Joost G.J. Hoenderop[1], René J.M. Bindels[1,2]

[1] Department of Physiology, Radboud University Medical Center, The Netherlands

[2] Centre for System Biology and Bioenergetics, Radboud University Medical Center, The Netherlands

[3] Department of Biochemistry, Radboud University Medical Center, The Netherlands

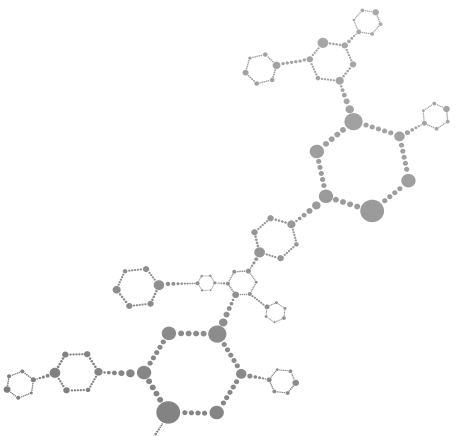

J Biol Chem 289, 11293-11303 (2014)

Abstract

Isoform 3 of the Na^+-Ca^{2+} exchanger (NCX3) is crucial for maintaining intracellular calcium ($[Ca^{2+}]_i$) homeostasis in excitable tissues. In this sense NCX3 plays a key role in neuronal excitotoxicity and Ca^{2+} extrusion during skeletal muscle relaxation. Alternative splicing generates two variants (NCX3-AC and NCX3-B). Here we demonstrated that NCX3 variants display a tissue-specific distribution in mice, with NCX3-B as mostly expressed in brain and NCX3-AC as predominant in skeletal muscle. Using Fura-2-based Ca^{2+} imaging, we measured the capacity and regulation of the two variants during Ca^{2+} extrusion and uptake in different conditions. Functional studies revealed that, although both variants are activated by intracellular sodium ($[Na^+]_i$), NCX3-AC has a higher $[Na^+]_i$ sensitivity, as Ca^{2+} influx is observed in the presence of extracellular Na^+. This effect could be partially mimicked for NCX3-B by mutating several glutamate residues in its cytoplasmic loop. In addition, NCX3-AC displayed a higher capacity of both Ca^{2+} extrusion and uptake compared to NCX3-B, together with an increased sensitivity to intracellular Ca^{2+}. Strikingly, substitution of Glu^{580} in NCX3-B with its NCX3-AC equivalent Lys^{580} recapitulated the functional properties of NCX3-AC regarding Ca^{2+} sensitivity, Lys^{580} presumably acting through a structure stabilization of the Ca^{2+}-binding site. The higher Ca^{2+} uptake capacity of NCX3-AC compared to NCX3-B is in line with the necessity to restore Ca^{2+} levels in the sarcoplasmic reticulum during prolonged exercise. The latter result, consistent with the high expression in the slow-twitch muscle, suggests that this variant may contribute to the Ca^{2+} handling beyond that of extruding Ca^{2+}.

Keywords: Sodium-calcium exchange, excitotoxicity, forward-mode, alternative splicing, reverse-mode, Ca^{2+} transport, plasma membrane, endoplasmic reticulum (ER), NCX, muscle fatigue.

Introduction

The Na^+-Ca^{2+} exchanger (NCX) is a plasma membrane transporter that plays a major role in the maintenance of Ca^{2+} homeostasis in various cell types (1,2). NCX catalyzes the exchange of Na^+ and Ca^{2+} with a 3:1 stoichiometry (3). Depending on the electrochemical gradient across the plasma membrane NCX can either extrude intracellular Ca^{2+} in its forward-mode or take up extracellular Ca^{2+} in its reverse-mode. The NCX protein contains 10 transmembrane segments and a large central intracellular loop (4-6). The latter was shown to be responsible for the allosteric modulation of the exchanger by Na^+ and Ca^{2+} (7). A high intracellular Na^+ concentration ($[Na^+]_i$) or low intracellular Ca^{2+} concentration ($[Ca^{2+}]_i$) inactivates the reverse-mode of the exchanger (7-9).

In mammals, the NCX family consists of three separate genes: *NCX1*, *NCX2* and *NCX3* (10). NCX1 is predominantly expressed in heart, kidney and brain (11), NCX2 is most abundantly expressed in brain (12) and NCX3 is expressed in excitable tissues such as brain and skeletal muscle (13). Numerous splice-variants of NCX1 exist in various species while there is only a single variant described for NCX2 (12). Finally, for NCX3, six variants have been described in human (12,14). In mice two variants of NCX3 have been identified, but data regarding their expression pattern is lacking. It has, therefore, been hypothesized that expression of mouse NCX3 variants follows the same tissue distribution as that observed in rat (12). This would imply that in mice NCX3-B is expressed in brain and NCX3-AC expression is restricted to the adult skeletal muscle. These two NCX3 variants are derived from an alternative splicing of the exons A, B and C. Given the fact that exons A and B are mutually exclusive, the alternative splicing introduces a difference of 24 residues between the NCX3-B and NCX3-AC variants. All of these residues are located within the cytoplasmic regulatory loop known to regulate the activity of the exchanger (12).

The role of NCX3 in the brain has been extensively studied. In neurons, NCX3 plays an important role in pathological situations such as ischemia and excitotoxicity (15,16). In skeletal muscle, NCX3 action constitutes the major Ca^{2+} extrusion mechanism during the relaxation process (17). Its absence induces muscle necrosis and aberrant Ca^{2+} homeostasis (18). However, little is known about the regulation and functional properties of NCX3-B and NCX3-AC.

The aim of the present study was to gain insight into the properties and physiological role of NCX3-B and NCX3-AC. To this end, the expression of both variants in various mouse tissues was assessed. Next, we investigated whether the amino acid differences in the regulatory loop of both NCX3 variants have functional consequences. Therefore, NCX3-AC and NCX3-B were expressed at the plasma membrane in Human Embryonic Kidney (HEK293T) cells. Subsequently, the regulation of the NCX3 variants by $[Ca^{2+}]_i$ and $[Na^+]_i$ was studied using Fura-2-based Ca^{2+} imaging. Finally, the same approach was applied to site-directed mutants to investigate the molecular mechanisms that give rise to the differences in exchange activity.

Materials and methods

cDNA Cloning

Murine NCX3-B (kindly provided by Prof. Geerten Vuister, Leicester, UK) was subcloned into the *Xho*I and *Nhe*I sites of the bicistronic mammalian vector pCINeo containing an internal ribosome entry site (IRES) and enhanced green fluorescent protein (eGFP). An HA-Tag was added to the N-terminus of the NCX protein. Fragments corresponding to exons AC or B were obtained by amplification of cDNA from mice hindlimb skeletal muscle using a high fidelity DNA polymerase (Phusion, Thermo Fisher). The uncut fragment, containing only NCX3-AC, after digestion with *Xmn*I was subcloned into the *Blp*I and *Xho*I sites of NCX3-B pCINeo vector. The D1ER calcium sensor targeted to the endoplasmic reticulum (ER) (www.addgene.org/36325) was inserted in a pcDNA3. Following transformation, the plasmids were tested by the action of two-cutter restriction enzymes and subsequently checked by sequencing.

Mutagenesis

All NCX3-B mutants were generated using a QuikChange Site-directed mutagenesis kit (Stratagene, La Jolla, CA) following the manufacturer's instruction. All mutants were subsequently validated by Sanger sequencing.

Expression profile and quantitative real-time polymerase chain reaction analysis

Three C57BL/6 mice were sacrificed. The brain, heart, and four different skeletal muscles from the hindlimb were collected: Gastrocnemius, Soleus, Extensor digitorum longus (EDL) and Tibialis anterior (TA). Tissue RNA was extracted using Trizol total RNA Isolation Reagent (Life technologies BRL, Breda, The Netherlands). After DNAse treatment (Promega, Madison, WI) 1 µg of RNA was reverse-transcribed by Molony-Murine Leukemia Virus-Reverse Transcriptase (Invitrogen, Carlsbad, CA) as previously described (19). Using a CFX96 Real time PCR detection system (Bio-Rad), three calibration curves corresponding to NCX3-AC, NCX3-B and total NCX3 were realized using serial dilutions of pCINeo-NCX3-B and pCINeo-NCX3-AC. The cDNA from tissues were used to measure the absolute copy number per µg of mRNA. The sequences were amplified using the following primers: Total NCX3 Forward 5'-ATATGGGGAGCTGGAGTTCA-3', Total NCX3 Reverse 5'-CTGGAGATAACAGGAGCGC-3', NCX3-AC Forward 5'-GGGCCCCCGCATGGTGGATA-3', NCX3-AC Reverse 5'-CAGCTTCCTGTCTGTCACTTCTGGA-3', NCX3-B Forward 5'-GCATATGGGGAGCTGGAGT-3', NCX3-B Reverse 5'-GTTCACCAAGGGCAATGAAG-3'.

Expression of the Na^+/Ca^{2+} exchanger in Human Embryonic Kidney cells

Human Embryonic Kidney cells (HEK293T) were grown in Dulbecco's modified Eagle's medium (Bio Whittaker-Europe, Verviers, Belgium) containing 10% (v/v) fetal calf serum,

2 mM L-glutamine at 37ºC with 5% (v/v) CO_2. The cells were seeded on a 6 well-plate and transiently transfected with the respective constructs (2 µg/well) using polyethylenimine cationic polymer PEI (Polysciences Inc., Warrington, PA) in accordance with the manufacturer's instructions. The HEK293T cells were used for the experiments 48h after transfection.

Cell surface biotinylation

Cell surface labeling with biotin was performed using the sulfo-NHS-LC-LC-biotin (0.5 mg/mL,Thermo Fisher Scientific, Rockford, IL) as described previously (20). Cells from each 6-well plate were homogenized on ice in 0.5 ml of lysis buffer (150 mM NaCl, 5 mM EDTA, 0.5% (v/v) Triton X-100 (v/v), proteases inhibitors, 50 mM Tris/HCl, pH 7.5) to prevent endo- and exocytosis, as described previously (21). Subsequently 5% (v/v) of the total protein amount was collected as an input sample. Next, biotinylated proteins (plasma membrane fraction) were precipitated using Neutravidin-agarose beads (Thermo Fisher). Biotinylated fractions were eluted in 2 x Laemmli buffer containing 100 mM dithiothreitol and proteinase inhibitors (22). Finally, samples were denatured for 30 min at 37ºC. NCX3-B and NCX3-AC expression was analyzed by immunoblot analysis for the input and the plasma membrane fraction (23).

Immunoblot analysis

Lysates were subjected to SDS–PAGE 8% (w/v) and electroblotted onto PVDF membranes. Blots were incubated with 5% (w/v) non-fat dried milk in TBS-T (137 mM NaCl, 0.2% (v/v) Tween-20 and 20 mM Tris/HCl, pH 7.6). Immunoblots were incubated overnight at 4ºC with a rabbit anti-NCX3 antibody (1:3000) (kindly provided by Prof. Kenneth Philipson, UCLA, USA) (24) diluted in 1% (w/v) milk in TBS-T. PVDF membranes were incubated 1 hour at room temperature with a sheep horseradish peroxidase-conjugated anti-rabbit (1:10000) (Sigma, MO, USA) in TBS-T. Afterwards, blots were visualized using the enhanced chemiluminescence system (ECL, Thermo Fisher).

$[Ca^{2+}]_i$ and $[Ca^{2+}]_{ER}$ measurements

48h after transfection, cells were loaded with 3 µM Fura-2 acetoxymethyl ester (Fura-2/AM) and 0.01% (v/v) Pluronic F-127 for 20 min at 37 °C in Krebs solution (5.5 mM KCl, 147 mM NaCl, 1.2 mM $MgCl_2$, 1.5 mM $CaCl_2$, 10 mM glucose, and 10 mM HEPES/NaOH, pH 7.4). Then, the cells were washed with Krebs medium for 10 min. Finally the coverslips were placed into a perfusion chamber mounted onto the stage of an inverted microscope (Zeiss Axiovert 200M, Carl Zeiss, Jena, Germany). Changes in medium and addition of inhibitors were facilitated using a perfusion system. $[Ca^{2+}]_i$ was monitored by exciting Fura-2 with monochromatic light of wavelength 340 and 380 nm (Polychrome IV, TILL Photonics, Gräfelfing, Germany). Fluorescence emission light was directed by a 415DCLP dichroic mirror (Omega Optical, Inc., Brattleboro, VT) through a 510WB40 emission filter

(Omega Optical, Inc.) onto a CoolSNAP HQ monochrome CCD-camera (Roper Scientific, Vianen, the Netherlands). The integration time of the CCD-camera was set at 200 ms with a sampling interval of 3 s. $[Ca^{2+}]_{ER}$ was monitored on cells co-expressing D1ER in a pcDNA3 vector and NCX3 variants in a pCINeo vector lacking the internal ribosome entry site enhanced GFP. Cerulean fluorescent protein (CFP) was excited with monochromatic light at 450 nm. Fluorescent emission light was directed by a 455DRLP Dichroic mirror (Omega Optical Inc.) through a 480AF30 and 535AF26 emission filters. All hardware was controlled with Metafluor software (version 6.0, Universal Imaging Corp., Downingtown, PA). During Fura-2 measurements enhanced GFP-positive cells were selected as transfected cells. During D1ER measurements, CFP-positive cells were selected as cotransfected cells (25). For each wavelength, the mean fluorescence intensity was monitored in an intracellular region and, for purpose of background correction, in an extracellular region of identical size. After background correction, the fluorescence emission ratio (340nm/380nm) and (530nm/480nm) was calculated to determine the Fura-2 and the D1ER ratios respectively. Eight to fifteen individual cells were selected and monitored simultaneously from each coverslip. NCX activity was evaluated as Ca^{2+} uptake through the reverse-mode by switching the normal Krebs medium to a Na^+-free NMDG medium containing: 5.5 mM KCl, 147 mM *N*-methyl glucamine, 1.2 mM $MgCl_2$, 1.5 mM $CaCl_2$, 10 mM glucose, and 10 mM HEPES/HCl, pH 7.4 (15). The effect of an increase in $[Ca^{2+}]_i$ and $[Na^+]_i$ was investigated by applying an irreversible and selective inhibitor of the sarcoplasmic reticulum Ca^{2+}-ATPase (thapsigargin, 1 µM) or using an inhibitor of the Na^+-K^+ ATPase (ouabain, 1 µM) incubated 60 min prior to the experiment and perfused during recordings as described previously (15). Additionally, the forward-mode of the exchanger was evaluated by measuring the capacity to perform Ca^{2+} extrusion after an increase induced by acute addition of the Ca^{2+} ionophore (ionomycin, 1 µM) in Ca^{2+}-free conditions. Osmolality of all buffers has been measured to ensure a difference smaller than 5 mOsm. All buffers were kept at 37 °C.

Analysis of the $[Ca^{2+}]_i$ measurements

After initiation of the reverse-mode, varying Ca^{2+} uptakes were observed in the different conditions. For each condition, the baseline value was calculated as an average of the first 60 s of recording. During investigation of the forward-mode, the baseline Fura-2 ratio recorded in mock-expressing cells in Ca^{2+}-free medium was subtracted from the maximal Fura-2 ratio in the same cells after ionomycin treatment. This calculation represents the maximum amount of Ca^{2+} that is present in the ER and that could potentially be extruded via NCX3. Next, the experimental extrusion of Ca^{2+} was calculated as follow: the difference between the mock and the given condition (NCX3-AC, NCX3-B or mock) both after addition of ionomycin. This difference was reported as a percentage of the theoretical maximum extrusion value described above. This difference is subsequently expressed as a percentage of the theoretical maximal value. During the experiments in absence of

thapsigargin or ouabain, the cells responding to a removal of extracellular Na^+ were quantified, by taking the Fura-2 ratio value of 0.4 as a threshold of responsiveness.

Drugs and chemicals

Ionomycin and thapsigargin were purchased from Sigma Chemical; Ouabain from MP biomedicals; Fura-2-AM and pluronic acid from Invitrogen. All were dissolved in dimethyl sulfoxide (DMSO). The final concentration of DMSO was 0.1% (v/v) and had no effect on $[Ca^{2+}]_i$.

Statistical analysis

All results are based on at least three different sessions of experiments. The Fura-2 ratio is an average of ≥ 65 individual cells. Values are expressed as means ± S.E.M. Statistical significance ($P < 0.05$) was determined using One-way ANOVA with the Bonferroni's procedure.

Results

Expression profile of NCX3-B and NCX3-AC in excitable tissues

In order to elucidate the expression of NCX3 variants in excitable tissues, the mRNA expression of NCX3-B and NCX3-AC was quantified in brain, heart and skeletal muscles. Type I and type II skeletal muscle fibers confer slow-twitch and fast-twitch properties to the myofibers respectively. In this study, four different skeletal muscles were selected; Soleus and Extensor digitorum longus (EDL) for their predominantly constitution of type I and type II fibers respectively, Tibialis anterior (TA) and Gastrocnemius for their mixed constitution of fibers in mammals (26). Due to high sequence homology between the two variants, primers were designed to anneal specifically to the alternatively spliced regions corresponding to exons B and AC (**Figures 1A and 1B**). A third set of primers was designed to measure the expression of both NCX3 variants. Quantification of total NCX3 expression showed low levels in cardiac tissue whereas a high expression was measured in brain (**Figure 1C**). Among the different skeletal muscles, NCX3 was more abundantly found in the slow-twitch muscle fibers constitutive of the soleus than in the fast-twitch or mixed fibers with a 6 to 10-fold difference. In the brain, the expression of NCX3-B was 3-fold higher than NCX3-AC (**Figure 1C**). In soleus, the opposite trend was observed with NCX3-AC being 3-fold higher than NCX3-B. In the fast-twitch skeletal muscles NCX3-B was poorly expressed while NCX3-AC expression levels appeared to be more than 6-fold higher.

Both NCX3 variants display reverse-mode exchange activity

Next, the investigation of NCX3 functional activity was performed using HEK293T cells transfected with NCX3-AC, NCX3-B or empty vector (mock). The activity of these exchangers was assessed by measuring changes in $[Ca^{2+}]_i$ using the ratiometric probe

Fura-2. Under resting conditions, basal $[Ca^{2+}]_i$ was similar in NCX3-AC, NCX3-B and mock transfected cells (**Figure 2A**). Thapsigargin has been shown to induce a rise in $[Ca^{2+}]_i$ and consequently fully activates NCX (27). Addition of thapsigargin (1 μM) increased $[Ca^{2+}]_i$ in all three conditions (**Figure 2A**). However, this increase was significantly lower in cells expressing NCX3-AC (**Figure 2B**) compared to the other conditions. Removal of extracellular Na^+ was used to energize Ca^{2+} uptake via the reverse-mode of NCX. This protocol yielded an increase in $[Ca^{2+}]_i$ in cells expressing NCX3-AC and NCX3-B (**Figure 2C**), indicating reverse-mode of exchange activity. Strikingly, the increase in $[Ca^{2+}]_i$ was 3-fold higher in cells expressing NCX3-AC than NCX3-B. Mock-transfected cells failed to respond, indicating that the endogenous NCX expressed in HEK293T cells could not be detected with our method. Cell surface quantification of NCX3 confirmed that both variants were similarly expressed at the plasma membrane (**Figure 2D**).

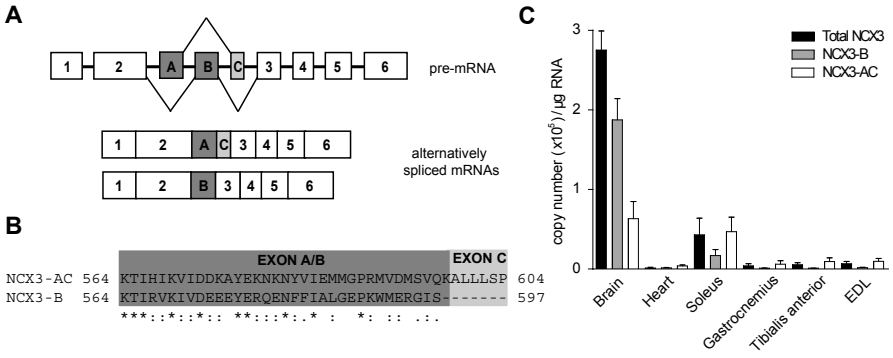

Figure 1 NCX3 splice-variants and their tissue expression.

A, Alternative splicing of the mice Na^+/Ca^{2+} exchanger isoform 3 pre-mRNA and the two variants obtained after alternative splicing of the exons A, B and C. **B**, Alignment of amino acid sequences in alternatively spliced NCX3 exons in the mice NCX3-AC and NCX3-B using ClustalW software. Missing residues are indicated by dashes. Symbols below the sequence indicate conserved (.) highly conserved (:) and identical residues (*). **C**, NCX3 mRNA levels in different mice tissues. Total NCX3 (black), NCX3-B (grey) and NCX3-AC (white) transcripts expression levels were quantified by real-time PCR. mRNA copy numbers were calculated from the NCX3 standard curves generated by using a diluted pCINeo-IRES-eGFP-mNCX3-AC and pCINeo-IRES-eGFP-mNCX3-B vectors. Heart has been used as a negative control to show the absence of NCX3.

Forward exchange activity of NCX3-AC is most sensitive to intracellular Ca^{2+}

Further, to explain the reduced increase in $[Ca^{2+}]_i$ upon addition of thapsigargin in NCX3-AC expressing cells (**Figure 2B**), we hypothesized that the forward-mode of NCX3-AC would be more active, leading to a smaller apparent increase in $[Ca^{2+}]_i$ compared to NCX3-B-expressing cells. In the absence of extracellular Na^+ and Ca^{2+}, conditions under which the forward-mode is abolished, the Ca^{2+} level in the ER and the change in $[Ca^{2+}]_i$ in response to thapsigargin, were similar in all cells (**Figure 3A-D**).

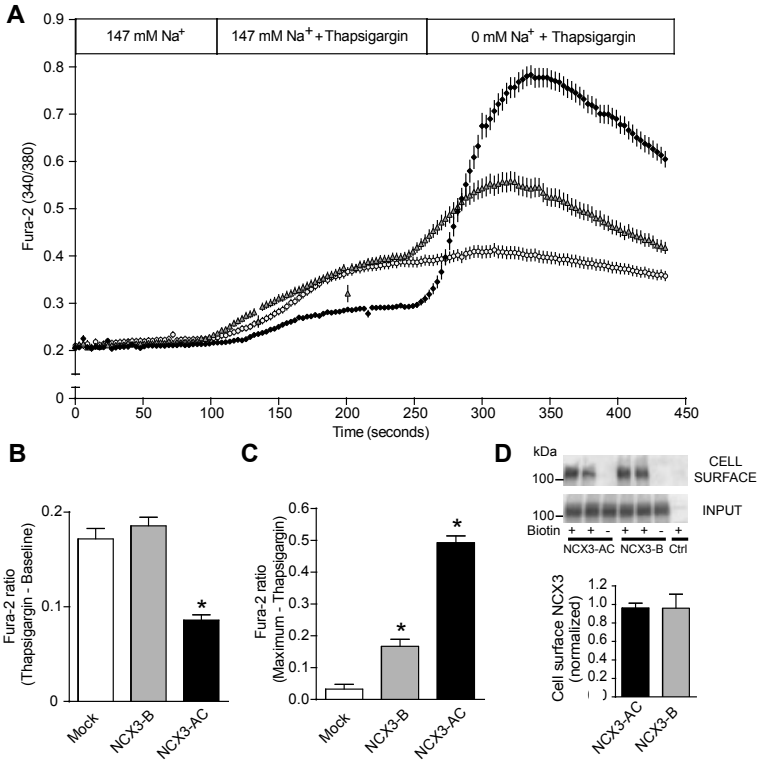

Figure 2 NCX3 variants exhibit functional differences in their reverse-mode.

A, Ca^{2+} influx in HEK293T cells expressing NCX3-AC (♦), NCX3-B (▲) or an empty vector (○) and loaded with Fura-2-AM. Cells were perfused with Krebs medium (147 mM Na^+). At 100 seconds, internal Ca^{2+} stores were depleted by applying 1 µM thapsigargin. At 245 seconds, reverse NCX mode was initiated by perfusing with a Na^+-free medium (NMDG medium). The 340/380nm emission ratios are shown. Each point represents the mean of the data, studied in three independent experimental sessions for a number (n) of cells monitored. Mock, n=126; NCX3-B, n=96; NCX3-AC, n=106. **B**, Mean values of the maximum Fura-2 ratio after addition of thapsigargin (1 µM) shown in A. **C**, Mean values of the maximum Fura-2 fluorescence, shown in A, after removal of extracellular Na^+. For **B** and **C** *$P < 0.05$. **D**, Quantification and representative immunoblots of total cellular NCX3 at the plasma membrane (Cell surface) and in the total cell lysates (Input) in cells expressing NCX3-AC, NCX3-B or an empty vector (Ctrl). For each condition, cells that were not treated with biotin are included for comparison. (n=4 per condition).

In order to strengthen our hypothesis, the forward-mode was triggered by perfusing the cells with the Ca^{2+} ionophore ionomycin (1 µM) in the presence of extracellular Na^+. Under these conditions ionomycin allows for a complete release of Ca^{2+} in a fast manner from the ER to the cytoplasm, thereby inducing an activation of NCX in its forward-mode of exchange. Upon addition of ionomycin, an increase in $[Ca^{2+}]_i$ was recorded in the

control condition (**Figure 3E**). This rise in $[Ca^{2+}]_i$ was greatly diminished in both variants of NCX3 confirming the extrusion of Ca^{2+} via the forward-mode of the exchanger. The forward-mode activity, expressed as the ability to extrude Ca^{2+}, was significantly larger for NCX3-AC than for NCX3-B (78 ± 9% and 47 ± 11%, respectively, P<0.05) (**Figure 3F**).

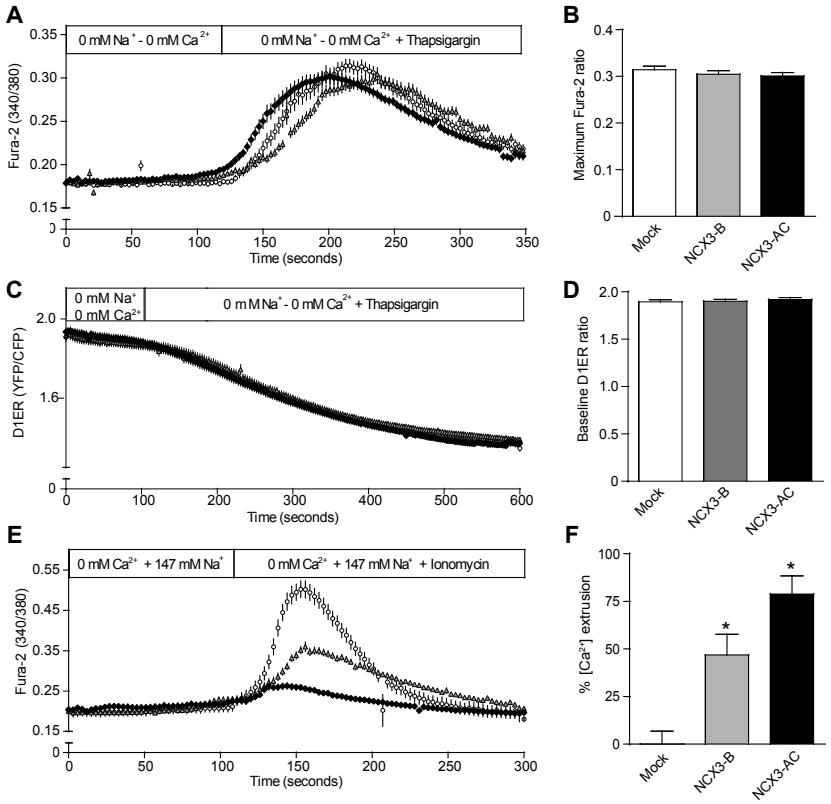

Figure 3 Differences in threshold of activation of the NCX3 variants in the forward-mode.

A-D, Release of Ca^{2+} from the ER in HEK293T cells expressing NCX3-AC (♦), NCX3-B (▲) or an empty vector (○) during perfusion of thapsigargin (1 μM) in Na^+ and Ca^{2+}-free conditions **A**, after loading and recording of the Fura-2 ratio (340nm/380nm) and **C**, after recording of the D1ER sensor. Each point represents the mean (± S.E.M.) of the data, for a number (n) of cells monitored. **A**, Mock, n=72; NCX3-B, n=85; NCX3-AC, n=114 and **C**, Mock, n=119; NCX3-B, n=99; NCX3-AC, n=150. **B**, Mean values of the maximum Fura-2 ratio after addition of thapsigargin (1 μM) shown in A. **D**, Average value of the baseline YFP/CFP ratio shown in C. **E**, Fura-2 ratio (340nm/380nm) in HEK293T cells expressing NCX3-AC (♦), NCX3-B (▲) or an empty vector (○) during perfusion of ionomycin (1 μM) in Ca^{2+} -free conditions. Each point represents the mean of the data, for a number (n) of cells monitored. Mock, n=111; NCX3-B, n= 78; NCX3-AC, n=94. **F**, Percentage of $[Ca^{2+}]$ extrusion after addition of ionomycin (1 μM) shown in A and calculated as described in the experimental procedures. *P < 0.05

The activity of NCX3-AC in reverse exchange is higher than NCX3-B

Figure 2A and 2C show that NCX3-B and NCX3-AC can both operate in the reverse-mode and that NCX3-AC induces a larger increase in $[Ca^{2+}]_i$. The capacity of the reverse-mode of the NCX3 variants was then investigated by adding thapsigargin in the absence of extracellular Na^+, thus preventing a contribution from NCX3 in its forward-mode. In these conditions, $[Ca^{2+}]_i$ rose (**Figure 4A**) in accordance with the pattern seen previously after addition of thapsigargin (**Figure 2A**). The increase in $[Ca^{2+}]_i$ observed after the switch to the Na^+-free condition was significantly higher in NCX3-AC compared to NCX3-B-expressing cells (**Figure 4B**), pinpointing either a lower sensitivity of NCX3-B to $[Ca^{2+}]_i$ or a poor sensitivity to extracellular $[Na^+]$.

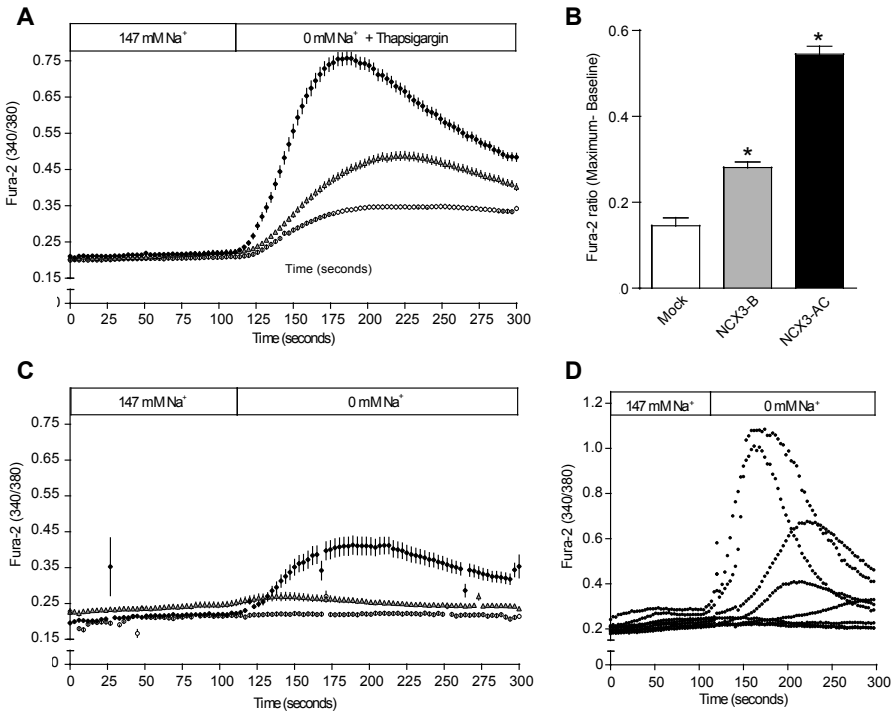

Figure 4 Differences in properties of NCX3-B and NCX3-AC in the reverse-mode of exchange.

A, Ca^{2+} influx in HEK293T cells expressing NCX3-AC (♦), NCX3-B (▲) or an empty vector (○) in Na^+-free conditions simultaneously with applying thapsigargin (1 µM), conditions for which forward-mode exchange is abolished. Mock, n=158; NCX3-B, n= 153; NCX3-AC, n=139. **B**, Mean values of the maximum Fura-2 ratio after the switch to Na^+-free medium containing 1 µM thapsigargin shown in A with $^*P < 0.05$. **C**, Fura-2 ratio in cells expressing NCX3-AC (♦), NCX3-B (▲) or an empty vector (○) in Na^+-free conditions in absence of thapsigargin. Each point represents the mean of the data, for a number (n) of cells monitored. Mock, n=88; NCX3-B, n=66; NCX3-AC, n=104. **D**, Representative recording of eight HEK293T cells expressing NCX3-AC during removal of extracellular Na^+ in absence of thapsigargin.

Nevertheless, the Ca^{2+} uptake observed in NCX3-B-expressing cells under removal of extracellular Na^+ (**Figure 4A**) was not detected in the absence of thapsigargin (**Figure 4C**) demonstrating the importance of intracellular Ca^{2+} in the activation of this variant. In the case of NCX3-AC, a low average was observed (**Figure 4C**), suggesting a poor activation of the reverse-mode. Nevertheless, considering the cells separately, 45% of the NCX3-AC-expressing cells appeared to respond strongly to a change in Na^+ gradient (**Figure 4D**). This effect was less frequent for NCX3-B and mock cells, a response being observed in 7% and 1% of measured cells, respectively (data not shown).

High sensitivity of NCX3-AC reverse-mode to intracellular Na^+

To investigate the regulation of NCX3 in the reverse-mode by intracellular $[Na^+]$, Fura-2 ratios were recorded following incubation of NCX3-AC and NCX3-B-expressing cells with ouabain (1 µM, 60 min), a Na^+-K^+-ATPase inhibitor which has been shown to induce a rise in $[Na^+]_i$ (28). An activity in reverse-mode was observed for both variants upon removal of extracellular Na^+. In both cases, this activity was higher than the one recorded during activation by the increased $[Ca^{2+}]_i$ (**Figure 4A and 5A**). Additionally, the maximum Fura-2 ratio of NCX3-AC in these conditions was found to be significantly higher than recorded in the variant B (**Figure 5C**).

Surprisingly, after incubation with ouabain, the basal $[Ca^{2+}]_i$ measured in NCX3-AC-expressing cells was found to be very close to the maximum value recorded in the absence of extracellular Na^+ (**Figure 5A**), as demonstrated by the low increase in $[Ca^{2+}]_i$ provoked by the removal of extracellular Na^+. The Fura-2 ratio in the presence of extracellular Na^+ was observed to be already 4-times greater than NCX3-B (**Figure 5B**). This effect was not observed upon activation by intracellular Ca^{2+} (**Figure 4A**) or in the NCX3-B-expressing cells for which removal of extracellular Na^+ seems to be required for the activation of the exchanger. The activation of NCX3-AC by intracellular $[Na^+]$, in high extracellular Na^+ condition, demonstrates a much greater sensitivity than NCX3-B to intracellular Na^+.

Molecular determinants of the Na^+ and Ca^{2+} sensitivity of NCX3 variants

The data recorded in Figure 4 and 5 demonstrated that the NCX3-AC variant is more sensitive to intracellular Ca^{2+} and Na^+. To get a better understanding of the molecular mechanisms responsible for this increased sensitivity, the role of several residues of the alternatively spliced region of NCX3 variants was investigated. This region, located in the intracellular loop, within the Ca^{2+}-binding domain 2 (CBD2) of the protein, differs significantly from one variant to the other. For instance, negatively charged residues such as glutamate and aspartate found in NCX3-B sequence are absent in NCX3-AC (**Figure 6A**). These residues have been shown to participate in the formation of the Ca^{2+}-binding site of NCX1 (29). Furthermore at these positions several positively charged residues are present in the variant AC, residues that are described in the case of NCX1 as critical for stabilization of the tertiary structure of the CBD2 (30,31).

To study the possible role of these residues in the regulation of the exchanger, site-directed NCX3-B mutants were generated targeting different glutamate residues (**Figure 6A**) E573D, E574K, E575A, E580K and E588G. The different mutants were subjected to recording of the forward and the reverse-mode by applying the similar protocols as described in the aforementioned paragraphs. Interestingly, E580K NCX3-B displayed similar properties compared to NCX3-AC in both forward and reverse-mode (**Figures 6B and 6C**) triggered by an elevation in $[Ca^{2+}]_i$. With respect to the activation of the reverse-mode through a rise in $[Na^+]_i$, the measurements of the Fura-2 ratio at basal and maximum level revealed a significant increase in the sensitivity to $[Na^+]_i$ in Na^+ conditions for four out of the five mutants tested (**Figure 6D**). In the absence of extracellular Na^+, only mutation E573D showed a significant increase in the maximum $[Ca^{2+}]_i$ recorded (**Figure 6E**). However, the four mutations accounting for the increase seen in Figure 6D displayed, in Na^+-free conditions, a trend toward a Ca^{2+} influx similar to NCX3-AC. Furthermore, the comparison between NCX3-AC and the three mutations E573D, E574K and E580K did not reveal any significant difference. To be noted, in all four conditions, E588G NCX3-B showed no difference in its capacities compared to NCX3-B.

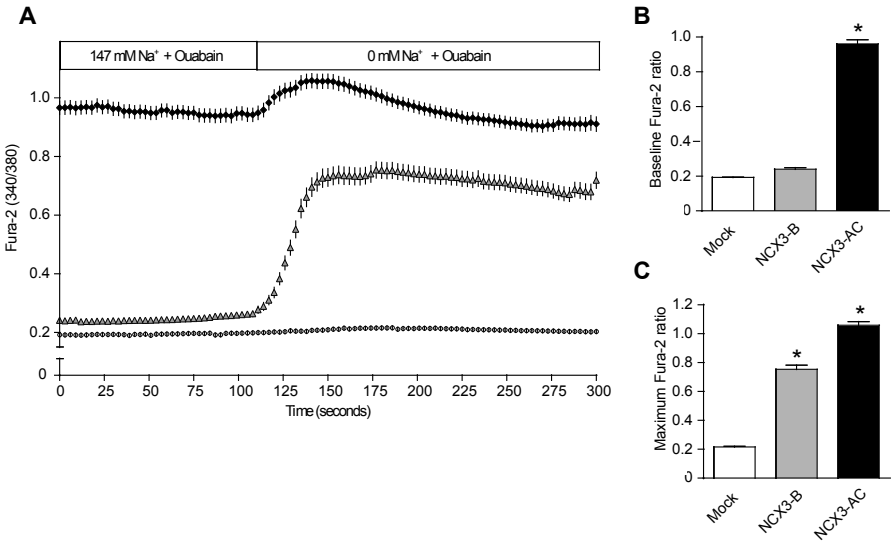

Figure 5 NCX3 variants exhibit distinct sensitivities to $[Na^+]_i$.

A, Fura-2 ratio (340nm/380nm) in HEK293T cells expressing NCX3-AC (♦), NCX3-B (▲) or an empty vector (○) after one-hour treatment with ouabain (1 μM). Each point represents the mean of the data, for a number (n) of cells monitored. Mock, n=124; NCX3-B, n=152; NCX3-AC, n=176. **B-C**, Mean values of Fura-2 ratio recorded at the baseline **B**; Average of the first 60 seconds of the experiment shown in A, in 147 mM Na^+ medium, and **C**, maximum Fura-2 ratio recorded after the switch to Na^+-free medium shown in A with *P < 0.05.

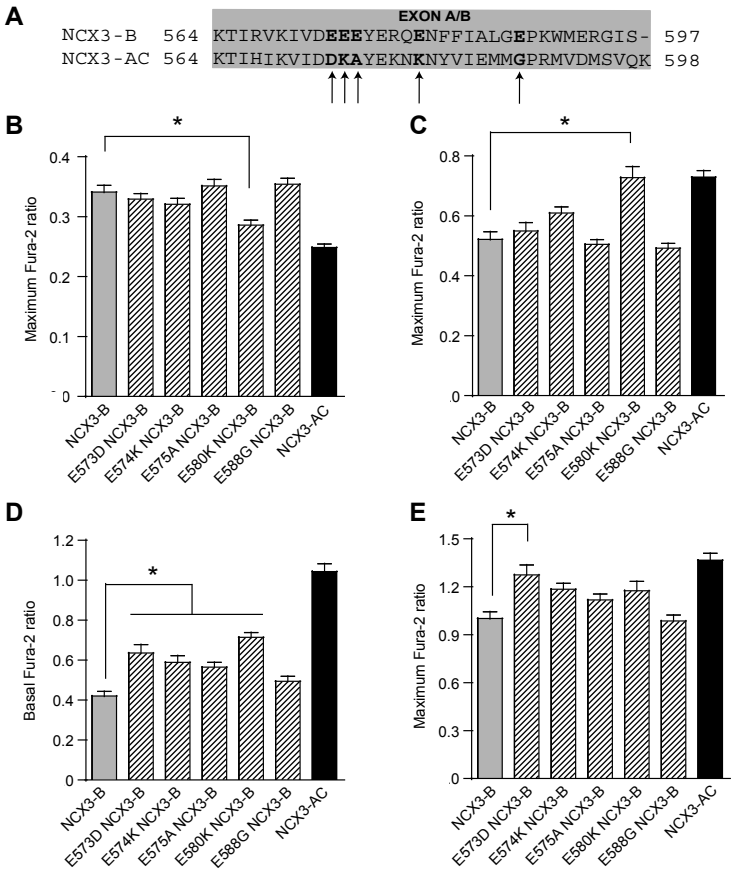

Figure 6 Glutamate residues: key regulators of Ca^{2+} and Na^{+} sensitivity in NCX3-AC.

A, Alignment of the amino acid sequences of the mutually exclusive exon A/B of NCX3-B to NCX3-AC. Missing residues are indicated by dashes. Specific NCX3-B single mutants were generated from corresponding amino acid of NCX3-AC (indicated by an arrow). For B to E, *P < 0.05. **B**, Mean values of the maximum Fura-2 ratio recorded during forward-mode followed by the addition of ionomycin (1μM) in Ca^{2+}-free conditions in cells expressing NCX3-AC, NCX3-B or mutants of NCX3-B. NCX3-B, n= 108; NCX3-AC, n=116; E573D NCX3-B, n= 93; E574K NCX3-B, n= 110; E575A NCX3-B, n= 82; E580K NCX3-B, n= 90; E588G NCX3-B, n= 110; **C**, Mean values of the maximum Fura-2 ratio, in reverse-mode triggered by the switch to Na^{+}-free medium containing 1μM thapsigargin, values recorded in HEK293T cells expressing NCX3 variants and mutants of NCX3-B. NCX3-B, n= 102; NCX3-AC, n=120; E573D NCX3-B, n= 77; E574K NCX3-B, n= 110; E575A NCX3-B, n= 121; E580K NCX3-B, n= 86; E588G NCX3-B, n= 102; **D-E**, Fura-2 ratio recorded during reverse-mode triggered by one-hour treatment with ouabain (1μM) in NCX3-AC, NCX3-B and NCX3-B mutants expressing HEK293T cells. NCX3-B, n= 99; NCX3-AC, n=88; E573D NCX3-B, n= 86; E574K NCX3-B, n= 76; E575A NCX3-B, n= 122; E580K NCX3-B, n= 123; E588G NCX3-B, n= 99; **D**, Mean values of Fura-2 ratio at the baseline; Average of the first 60 seconds of the experiment, in 147mM Na^{+} medium. **E**, Mean values of the maximum Fura-2 ratio after the switch to Na^{+}-free medium during the same experiment as D.

Discussion

In the present study, we show, for the first time, functional recordings of the variant NCX3-AC. These recordings indicate a higher capacity of this variant in reverse and forward-mode of exchange compared to NCX3-B. A difference that can be fully attributed to the intrinsic properties of both variants considering that the plasma membrane expression in HEK293T cells did not differ between the two variants, and that the Ca^{2+} level in the endoplasmic reticulum were similar in these cells as proven by the thapsigargin addition in absence of extracellular Na^+ and Ca^{2+}. Furthermore, the reduced $[Ca^{2+}]_i$ measured in NCX3-AC-expressing cells upon thapsigargin addition compared to NCX3-B, together with the activation of NCX3-AC reverse-mode in absence of an elevation in $[Ca^{2+}]_i$ suggest a higher sensitivity of NCX3-AC to changes in $[Ca^{2+}]_i$. Thereby, a value slightly above the $[Ca^{2+}]_i$ recorded during the resting state is sufficient to trigger the exchanger.

The lower sensitivity of NCX3-B to $[Ca^{2+}]_i$, in both modes of exchange, could be suppressed by mutating the glutamate residue at position 580. This gain of sensitivity observed in the E580K NCX3-B mutant reveals that the activation by Ca^{2+} of the forward and reverse-mode of the exchanger is regulated through the same site for which the residue 580 represents a key residue. In NCX1, the equivalent residue Lys^{585} is involved in the formation of a salt bridge that, in Ca^{2+}-free conditions, stabilizes the Ca^{2+}-binding site I and II through the preservation of the tertiary structure (29,32). NCX1 mutation of this lysine into a glutamate causes a drop in the Ca^{2+} affinity (29,32). In NCX3-AC, Lys^{580} confers to the site I of the CBD2 a high affinity for Ca^{2+} (31-33). In contrast, this variant has two Ca^{2+}-binding sites in its Ca^{2+}-binding domain 2 whereas ITC (isothermal titration calorimetry) measurements showed that NCX3-B has three Ca^{2+}-binding sites (30,33). However, none of these Ca^{2+} sites featured a high affinity for Ca^{2+} (33). Our data concurs with the literature in suggesting that during a rise in $[Ca^{2+}]_i$, the high-affinity site I of NCX3-AC CBD2 will bind Ca^{2+} at a lower concentration than NCX3-B. This could result in a disruption of the salt bridge at Lys^{580} as hypothesized for NCX1 (29) and, therefore, in an activation of the exchanger at lower $[Ca^{2+}]_i$.

Another important finding from the current study is that NCX3-B displayed a higher Na^+-dependent inactivation, given that only the reverse-mode of NCX3-AC could be activated, during a rise in $[Na^+]_i$ in presence of extracellular Na^+. The partial suppression of this effect by mutating glutamate residues suggests that the hydrophilic domain found between the position 572 and 580 in the CBD2 domain is involved in this inactivation. For NCX1, it has been demonstrated that the alternative splicing of the same region can alleviate the Na^+-dependent inactivation (34,35). Moreover, D578R and K585C mutations in NCX1, corresponding to the position 573 and 580 in NCX3, reversed the Na^+-dependent inactivation in a complete and partial manner, respectively (36). The emerging hypothesis concerning the functioning of this Na^+-dependent inactivation is a

regulation by the Ca^{2+}-binding site of the CBD2 through proximity with the catenin-like domain of the protein (CLD) (32). This domain, formed by residues of the intracellular loop outside CBD1 and CBD2, would control the Na^+-dependent inactivation. Our results are consistent with the hypothesis predicting that E573D, E574K, E575A and E580K NCX3-B are responsible for the partial disruption of a Ca^{2+}-binding site that will alter the interaction with the CLD and, therefore, lower the Na^+-dependent inactivation.

The tissue-specific distribution observed for the two variants of NCX3, NCX3-B being mostly expressed in the brain and NCX3-AC being the main variant detected in skeletal muscle, is consistent with the functional properties measured for these variants. In neurons, NCX3-B and its low capacity to perform Ca^{2+} uptake would have a protective effect against severe Ca^{2+} overload, a phenomenon that could have dramatic consequences on neurons. With this respect, the low sensitivity to an increase in $[Na^+]_i$ would confer this preservation during the firing of neurons. In the same manner, activation of the forward-mode of NCX3-B requires a substantial rise in $[Ca^{2+}]_i$. This feature would have the same protective effect and yet will not interfere with the synaptic activity, highly dependent on $[Ca^{2+}]_i$ (37).

In skeletal muscle, sensitivity to $[Ca^{2+}]_i$ and the high capacity of NCX3-AC in the forward-mode corroborates with the necessity in such fibers to activate the Ca^{2+} extrusion as soon as the contraction starts. Moreover, the high sensitivity of NCX3-AC to changes in $[Na^+]_i$ and its high capacity to perform Ca^{2+} uptake in reverse-mode suggest that NCX3-AC might have additional implications via its reverse-mode. The operation and relevance of the reverse mode has been previously observed for several members of the NCX family in numerous tissues, in both physiological (38-40) and pathological situations (41,42). From another angle, during prolonged exercise, extracellular Ca^{2+} has been shown to have a beneficial effect on the resistance to muscle fatigue, an effect that could only be observed in slow-twitch muscle, like soleus, dedicated to this type of prolonged exercise (43,44). Together with the high expression of NCX3-AC observed in soleus, these results suggest that NCX3-AC might be implicated in Ca^{2+} influx in slow-twitch muscle, a hypothesis consistent with the findings from the Danieli-Betto's group (44). Here, the Ca^{2+} free conditions provoke a dramatic increase of muscle fatigue in soleus, an effect also obtained by inhibition of NCX. This is also in accordance with the increased fatigability observed in $NCX3^{-/-}$ mice (18). The underlying mechanism linking Ca^{2+} uptake and muscle fatigue is still poorly understood but presumably involves a refilling of the SR Ca^{2+}. Many variants of the NCX family are already known to contribute to this latter process (45,46), particularly in excitable cells (47-49). Therefore, NCX3 could in principle be involved in this process in slow-twitch muscle. Nevertheless, our study was only performed in HEK 293 cells, albeit a well-used cell model to study mechanistic properties and ionic regulation of NCX isoforms (35,50,51). Therefore, confirmation of the latter hypothesis needs further investigations using muscular excitable tissue, in particular in soleus.

In conclusion, two variants of NCX3, which depict a tissue-specific distribution among excitable tissues, have distinct properties with regard to capacity of exchange and sensitivity to $[Ca^{2+}]_i$ and $[Na^+]_i$, NCX3-AC functioning with a greater capacity in all situations. Our data indicated that NCX3-AC is the main variant expressed in skeletal muscle with a high expression in soleus, a muscle in which NCX have been shown to be implicated in the resistance to fatigue (44). Additionally, our results are, to the best of our knowledge, the first functional recordings of NCX3-AC and provides evidence of a high capacity to achieve Ca^{2+} influx that can be triggered by a simple increase in $[Na^+]_i$. This exchanger might, therefore, play a role in the resistance to muscle fatigability observed in the slow-twitch muscle. Altogether, this study provides insights into the ionic regulation of NCX3 through its alternative splicing in a tissue specific manner. In fact, the two variants may contribute to Ca^{2+} handling beyond their role in Ca^{2+} extrusion.

Acknowledgements

This research was supported by an equipment grant of NWO (Netherlands Organization for Scientific Research, No: 911-02-008) and the CSBR (Centre for Systems Biology Research) initiative from the Netherlands Organization for Scientific Research (NWO; No: CSBR09/013V).

Author contribution

LYM, JGH and RJB conceived the study. LYM designed, performed and analyzed the experiments and wrote the manuscript. All authors discussed the results and revised critically the manuscript. All authors reviewed the results and approved the final version of the manuscript.

References

1. **Crespo, L. M., Grantham, C. J., and Cannell, M. B.** Kinetics, stoichiometry and role of the Na-Ca exchange mechanism in isolated cardiac myocytes. *Nature* 345, 618-621 (1990)
2. **Kimura, J., Noma, A., and Irisawa, H.** Na-Ca exchange current in mammalian heart cells. *Nature* 319, 596-597 (1986)
3. **Hinata, M., Yamamura, H., Li, L., Watanabe, Y., Watano, T., Imaizumi, Y., and Kimura, J.** Stoichiometry of Na+-Ca2+ exchange is 3:1 in guinea-pig ventricular myocytes. *The Journal of physiology* 545, 453-461 (2002)
4. **Liao, J., Li, H., Zeng, W., Sauer, D. B., Belmares, R., and Jiang, Y.** Structural insight into the ion-exchange mechanism of the sodium/calcium exchanger. *Science* 335, 686-690 (2012)
5. **Szerencsei, R. T., Kinjo, T. G., and Schnetkamp, P. P.** The topology of the C-terminal sections of the NCX1 Na (+) /Ca (2+) exchanger and the NCKX2 Na (+) /Ca (2+) -K (+) exchanger. *Channels (Austin)* 7, 109-114 (2013)
6. **John, S. A., Liao, J., Jiang, Y., and Ottolia, M.** The cardiac Na+-Ca2+ exchanger has two cytoplasmic ion permeation pathways. *Proc Natl Acad Sci U S A* 110, 7500-7505 (2013)
7. **Hilgemann, D. W.** Regulation and deregulation of cardiac Na(+)-Ca2+ exchange in giant excised sarcolemmal membrane patches. *Nature* 344, 242-245 (1990)
8. **Matsuoka, S., Nicoll, D. A., Hryshko, L. V., Levitsky, D. O., Weiss, J. N., and Philipson, K. D.** Regulation of the cardiac Na(+)-Ca2+ exchanger by Ca2+. Mutational analysis of the Ca(2+)-binding domain. *J Gen Physiol* 105, 403-420 (1995)
9. **Hilgemann, D. W., Matsuoka, S., Nagel, G. A., and Collins, A.** Steady-state and dynamic properties of cardiac sodium-calcium exchange. Sodium-dependent inactivation. *J Gen Physiol* 100, 905-932 (1992)
10. **Cai, X., and Lytton, J.** The cation/Ca(2+) exchanger superfamily: phylogenetic analysis and structural implications. *Mol Biol Evol* 21, 1692-1703 (2004)
11. **Kofuji, P., Hadley, R. W., Kieval, R. S., Lederer, W. J., and Schulze, D. H.** Expression of the Na-Ca exchanger in diverse tissues: a study using the cloned human cardiac Na-Ca exchanger. *Am J Physiol* 263, C1241-1249 (1992)
12. **Quednau, B. D., Nicoll, D. A., and Philipson, K. D.** Tissue specificity and alternative splicing of the Na+/Ca2+ exchanger isoforms NCX1, NCX2, and NCX3 in rat. *Am J Physiol* 272, C1250-1261 (1997)
13. **Nicoll, D. A., Quednau, B. D., Qui, Z., Xia, Y. R., Lusis, A. J., and Philipson, K. D.** Cloning of a third mammalian Na+-Ca2+ exchanger, NCX3. *J Biol Chem* 271, 24914-24921 (1996)
14. **Lindgren, R. M., Zhao, J., Heller, S., Berglind, H., and Nister, M.** Molecular cloning and characterization of two novel truncated isoforms of human Na+/Ca2+ exchanger 3, expressed in fetal brain. *Gene* 348, 143-155 (2005)
15. **Secondo, A., Staiano, R. I., Scorziello, A., Sirabella, R., Boscia, F., Adornetto, A., Valsecchi, V., Molinaro, P., Canzoniero, L. M., Di Renzo, G., and Annunziato, L.** BHK cells transfected with NCX3 are more resistant to hypoxia followed by reoxygenation than those transfected with NCX1 and NCX2: Possible relationship with mitochondrial membrane potential. *Cell Calcium* 42, 521-535 (2007)
16. **Pannaccione, A., Secondo, A., Molinaro, P., D'Avanzo, C., Cantile, M., Esposito, A., Boscia, F., Scorziello, A., Sirabella, R., Di Renzo, G., and Annunziato, L.** A New Concept: Abeta1-42 Generates a Hyperfunctional Proteolytic NCX3 Fragment That Delays Caspase-12 Activation and Neuronal Death. *J Neurosci* 32, 10609-10617 (2012)
17. **Huerta, M., Muniz, J., Vasquez, C., Marin, J. L., and Trujillo, X.** Sodium/calcium exchange in tonic skeletal muscle fibers of the frog. *Jpn J Physiol* 41, 933-944 (1991)

18. **Sokolow, S., Manto, M., Gailly, P., Molgo, J., Vandebrouck, C., Vanderwinden, J. M., Herchuelz, A., and Schurmans, S.** Impaired neuromuscular transmission and skeletal muscle fiber necrosis in mice lacking Na/Ca exchanger 3. *J Clin Invest* 113, 265-273 (2004)

19. **Hoenderop, J. G., Hartog, A., Stuiver, M., Doucet, A., Willems, P. H., and Bindels, R. J.** Localization of the epithelial Ca(2+) channel in rabbit kidney and intestine. *Journal of the American Society of Nephrology : JASN* 11, 1171-1178 (2000)

20. **van de Graaf, S. F., Hoenderop, J. G., Gkika, D., Lamers, D., Prenen, J., Rescher, U., Gerke, V., Staub, O., Nilius, B., and Bindels, R. J.** Functional expression of the epithelial Ca(2+) channels (TRPV5 and TRPV6) requires association of the S100A10-annexin 2 complex. *EMBO J* 22, 1478-1487 (2003)

21. **Gkika, D., Topala, C. N., Hoenderop, J. G., and Bindels, R. J.** The immunophilin FKBP52 inhibits the activity of the epithelial Ca2+ channel TRPV5. *Am J Physiol Renal Physiol* 290, F1253-1259 (2006)

22. **Kamsteeg, E. J., Wormhoudt, T. A., Rijss, J. P., van Os, C. H., and Deen, P. M.** An impaired routing of wild-type aquaporin-2 after tetramerization with an aquaporin-2 mutant explains dominant nephrogenic diabetes insipidus. *EMBO J* 18, 2394-2400 (1999)

23. **Chang, Q., Hoefs, S., van der Kemp, A. W., Topala, C. N., Bindels, R. J., and Hoenderop, J. G.** The beta-glucuronidase klotho hydrolyzes and activates the TRPV5 channel. *Science* 310, 490-493 (2005)

24. **Thurneysen, T., Nicoll, D. A., Philipson, K. D., and Porzig, H.** Sodium/calcium exchanger subtypes NCX1, NCX2 and NCX3 show cell-specific expression in rat hippocampus cultures. *Brain Res Mol Brain Res* 107, 145-156 (2002)

25. **Lambers, T. T., Weidema, A. F., Nilius, B., Hoenderop, J. G., and Bindels, R. J.** Regulation of the mouse epithelial Ca2(+) channel TRPV6 by the Ca(2+)-sensor calmodulin. *J Biol Chem* 279, 28855-28861 (2004)

26. **Armstrong, R. B., and Phelps, R. O.** Muscle fiber type composition of the rat hindlimb. *Am J Anat* 171, 259-272 (1984)

27. **Balasubramanyam, M., Rohowsky-Kochan, C., Reeves, J. P., and Gardner, J. P.** Na+/Ca2+ exchange-mediated calcium entry in human lymphocytes. *J Clin Invest* 94, 2002-2008 (1994)

28. **Rose, C. R., and Ransom, B. R.** Intracellular sodium homeostasis in rat hippocampal astrocytes. *The Journal of physiology* 491 (Pt 2), 291-305 (1996)

29. **Besserer, G. M., Ottolia, M., Nicoll, D. A., Chaptal, V., Cascio, D., Philipson, K. D., and Abramson, J.** The second Ca2+-binding domain of the Na+ Ca2+ exchanger is essential for regulation: crystal structures and mutational analysis. *Proc Natl Acad Sci U S A* 104, 18467-18472 (2007)

30. **Hilge, M., Aelen, J., Perrakis, A., and Vuister, G. W.** Structural basis for Ca2+ regulation in the Na+/Ca2+ exchanger. *Annals of the New York Academy of Sciences* 1099, 7-15 (2007)

31. **Hilge, M., Aelen, J., Foarce, A., Perrakis, A., and Vuister, G. W.** Ca2+ regulation in the Na+/Ca2+ exchanger features a dual electrostatic switch mechanism. *Proc Natl Acad Sci U S A* 106, 14333-14338 (2009)

32. **Hilge, M., Aelen, J., and Vuister, G. W.** Ca2+ regulation in the Na+/Ca2+ exchanger involves two markedly different Ca2+ sensors. *Mol Cell* 22, 15-25 (2006)

33. **Breukels, V., Touw, W. G., and Vuister, G. W.** Structural and dynamic aspects of Ca2+ and Mg2+ binding of the regulatory domains of the Na+/Ca2+ exchanger. *Biochem Soc Trans* 40, 409-414 (2012)

34. **Dyck, C., Omelchenko, A., Elias, C. L., Quednau, B. D., Philipson, K. D., Hnatowich, M., and Hryshko, L. V.** Ionic regulatory properties of brain and kidney splice variants of the NCX1 Na(+)-Ca(2+) exchanger. *J Gen Physiol* 114, 701-711 (1999)

35. **Hurtado, C., Prociuk, M., Maddaford, T. G., Dibrov, E., Mesaeli, N., Hryshko, L. V., and Pierce, G. N.** Cells expressing unique Na+/Ca2+ exchange (NCX1) splice variants exhibit different susceptibilities to Ca2+ overload. *Am J Physiol Heart Circ Physiol* 290, H2155-2162 (2006)

36. **Dunn, J., Elias, C. L., Le, H. D., Omelchenko, A., Hryshko, L. V., and Lytton, J.** The molecular determinants of ionic regulatory differences between brain and kidney Na+/Ca2+ exchanger (NCX1) isoforms. *J Biol Chem* 277, 33957-33962 (2002)

37. **Fatt, P., and Katz, B.** Spontaneous subthreshold activity at motor nerve endings. *The Journal of physiology* 117, 109-128 (1952)

38. **Rebolledo, A., Speroni, F., Raingo, J., Salemme, S. V., Tanzi, F., Munin, V., Anon, M. C., and Milesi, V.** The Na+/Ca2+ exchanger is active and working in the reverse mode in human umbilical artery smooth muscle cells. *Biochemical and biophysical research communications* 339, 840-845 (2006)

39. **Minami, A., Xia, Y. F., and Zucker, R. S.** Increased Ca2+ influx through Na+/Ca2+ exchanger during long-term facilitation at crayfish neuromuscular junctions. *The Journal of physiology* 585, 413-427 (2007)

40. **Viatchenko-Karpinski, S., Terentyev, D., Jenkins, L. A., Lutherer, L. O., and Gyorke, S.** Synergistic interactions between Ca2+ entries through L-type Ca2+ channels and Na+-Ca2+ exchanger in normal and failing rat heart. *The Journal of physiology* 567, 493-504 (2005)

41. **Yamamura, H., Cole, W. C., Kita, S., Hotta, S., Murata, H., Suzuki, Y., Ohya, S., Iwamoto, T., and Imaizumi, Y.** Overactive bladder mediated by accelerated Ca2+ influx mode of Na+/Ca2+ exchanger in smooth muscle. *American journal of physiology. Cell physiology* 305, C299-308 (2013)

42. **Kitao, T., Takuma, K., Kawasaki, T., Inoue, Y., Ikehara, A., Nashida, T., Ago, Y., and Matsuda, T.** The Na+/Ca2+ exchanger-mediated Ca2+ influx triggers nitric oxide-induced cytotoxicity in cultured astrocytes. *Neurochemistry international* 57, 58-66 (2010)

43. **Cairns, S. P., Hing, W. A., Slack, J. R., Mills, R. G., and Loiselle, D. S.** Role of extracellular [Ca2+] in fatigue of isolated mammalian skeletal muscle. *Journal of applied physiology* 84, 1395-1406 (1998)

44. **Germinario, E., Esposito, A., Midrio, M., Peron, S., Palade, P. T., Betto, R., and Danieli-Betto, D.** High-frequency fatigue of skeletal muscle: role of extracellular Ca(2+). *European journal of applied physiology* 104, 445-453 (2008)

45. **Jung, S. Y., Park, Y. J., Park, Y. J., Cha, S. H., Lee, M. Z., and Suh, C. K.** Na+-Ca2+ exchanger modulates Ca2+ content in intracellular Ca2+ stores in rat osteoblasts. *Experimental & molecular medicine* 39, 458-468 (2007)

46. **Hirota, S., Pertens, E., and Janssen, L. J.** The reverse mode of the Na(+)/Ca(2+) exchanger provides a source of Ca(2+) for store refilling following agonist-induced Ca(2+) mobilization. *American journal of physiology. Lung cellular and molecular physiology* 292, L438-447 (2007)

47. **Huang, J., Hove-Madsen, L., and Tibbits, G. F.** SR Ca2+ refilling upon depletion and SR Ca2+ uptake rates during development in rabbit ventricular myocytes. *American journal of physiology. Cell physiology* 293, C1906-1915 (2007)

48. **Piacentino, V., 3rd, Margulies, K. B., and Houser, S. R.** Ca influx via the Na/Ca exchanger maintains sarcoplasmic reticulum Ca content in failing human myocytes. *Annals of the New York Academy of Sciences* 976, 476-477 (2002)

49. **Sirabella, R., Secondo, A., Pannaccione, A., Scorziello, A., Valsecchi, V., Adornetto, A., Bilo, L., Di Renzo, G., and Annunziato, L.** Anoxia-induced NF-kappaB-dependent upregulation of NCX1 contributes to Ca2+ refilling into endoplasmic reticulum in cortical neurons. *Stroke; a journal of cerebral circulation* 40, 922-929 (2009)

50. **Iwamoto, T., and Shigekawa, M.** Differential inhibition of Na+/Ca2+ exchanger isoforms by divalent cations and isothiourea derivative. *Am J Physiol* 275, C423-430 (1998)

51. **John, S. A., Ribalet, B., Weiss, J. N., Philipson, K. D., and Ottolia, M.** Ca2+-dependent structural rearrangements within Na+-Ca2+ exchanger dimers. *Proc Natl Acad Sci U S A* 108, 1699-1704 (2011)

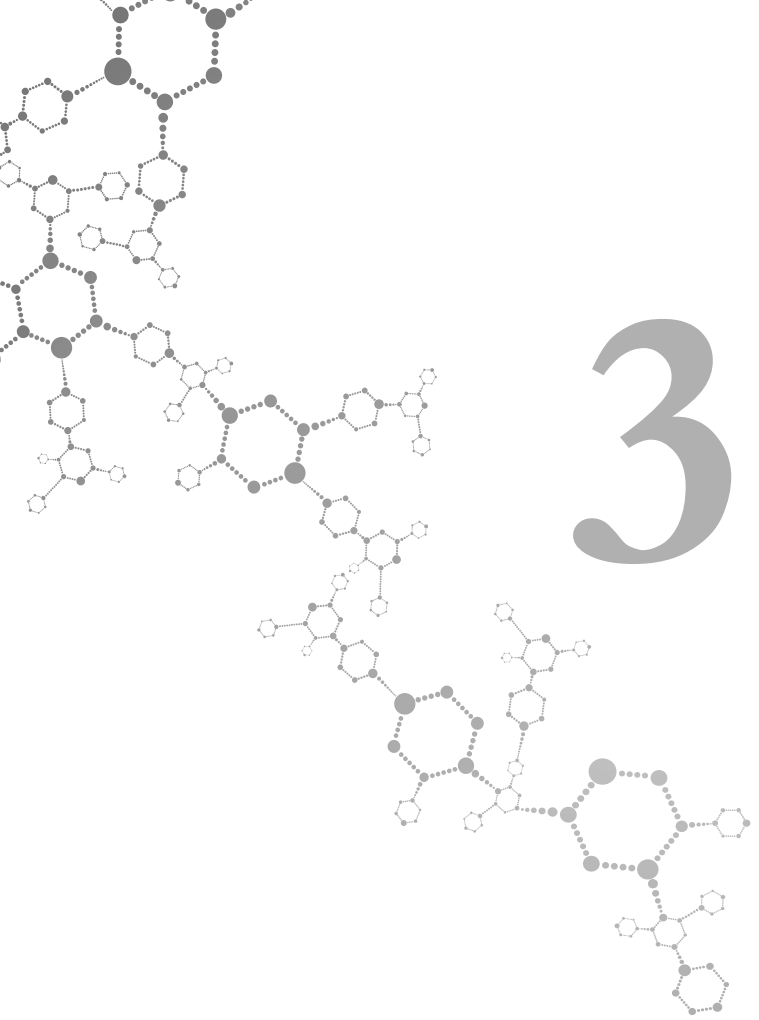

3

Differential regulation of the Na^{+}-Ca^{2+} exchanger NCX3 by protein kinase PKC and PKA

Lauriane Y.M. Michel[1,2], Sjoerd Verkaart[1], Joost G.J. Hoenderop[1], René J.M. Bindels[1,2]

[1] Department of Physiology, Radboud University Medical Center, The Netherlands

[2] Centre for System Biology and Bioenergetics, Radboud University Medical Center, The Netherlands

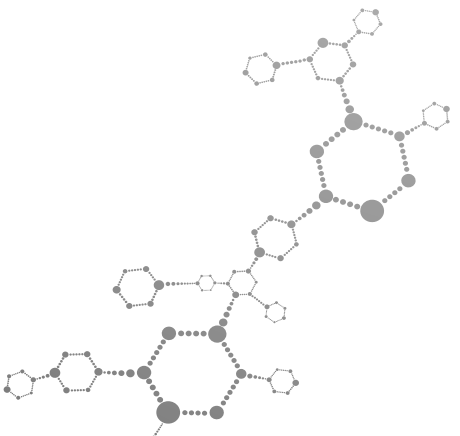

Submitted for publication

Abstract

Isoform 3 of the Na^+-Ca^{2+} exchanger (NCX3) participates in the Ca^{2+} fluxes across the plasma membrane. Among the NCX family, NCX3 carries out a peculiar role due to its specific functions in skeletal muscle and the immune system and to its neuroprotective effect under stress exposure. In this context, proper understanding of the regulation of NCX3 is primordial to consider its potential use as a drug target. In this study, we demonstrated the regulation of NCX3 by protein kinase A (PKA) and C (PKC). Disparity in regulation has been previously reported among the splice variants of NCX3 therefore the activity of Ca^{2+} uptake and extrusion of the two murine variants was measured using fura-2-based Ca^{2+} imaging and revealed that both variants are similarly regulated. PKC stimulation diminished the Ca^{2+} uptake performed by NCX3 in the reverse mode, triggered by a rise in $[Ca^{2+}]_i$ or $[Na^+]_i$, whereas an opposite response was observed upon PKA stimulation, with a significant increase of the Ca^{2+} uptake after a rise in $[Ca^{2+}]_i$. For both kinases, the Ca^{2+} extrusion capacity remained unaffected. Next, using site-directed mutagenesis, the sensitivity of NCX3 to PKC was abolished by singly mutating its predicted phosphorylation sites T529 or S695. The sensitivity to PKC might be due to the influence of T529 phosphorylation on the Ca^{2+}-binding domain 1. Additionally, we showed that stimulation of NCX3 by PKA occurred through residue S524. This effect may well participate in the fight-or-flight response in skeletal muscle and the long-term potentiation in hippocampus.

Keywords: Sodium-calcium exchange, Ca^{2+} transport, phosphorylation, skeletal muscle, reverse mode, forward mode, plasma membrane, NCX, Ca^{2+}-binding domain, long-term potentiation

Introduction

The plasma membrane family of Na^+-Ca^{2+} exchangers (NCX) consists of low-affinity/high-capacity ion transporters that play a crucial role in the control of intracellular Ca^{2+} homeostasis. NCX family members are involved in diverse physiological processes such as Ca^{2+} re-absorption in the kidney (1), heartbeat development in cardiac tissue (2,3), vasoconstriction in smooth muscle (4) and spatial learning in neurons (5). Of the four isoforms of the NCX family, three are expressed in mammals (6). Constituted of two clusters of five transmembrane domains separated by a large cytoplasmic loop, NCX isoforms function in a similar manner, allowing Ca^{2+} translocation in exchange of Na^+ with a stoichiometry of 1:3, respectively (7). Depending on the membrane potential and the transmembrane concentration gradient for Na^+ and Ca^{2+}, NCX can either perform Ca^{2+} uptake or efflux, referred as reverse mode and forward mode, respectively.

The third member of the NCX family, NCX3, was originally found solely in brain and skeletal muscle (8). Later on, however, it was also detected in the immune system (9,10) and osseous tissue (11,12). Its peculiar tissue distribution is associated with specific physiological functions of these tissues. Thus, NCX3 is required for neuronal development (13) and long-term potentiation in the hippocampus, a process involved in spatial learning and memory (14). In skeletal muscle, Ca^{2+} disturbances observed in the absence of NCX3 give rise to electromyographic abnormalities and muscle necrosis (15). Furthermore, NCX3 has been implicated in Ca^{2+} refilling of the sarcoplasmic reticulum (16). More recently, NCX3 was found to be involved in TNFα production in macrophages (9) and in the bone formation and resorption (12).

In the past few years, growing attention has been devoted to NCX3, not only because of its role in the immune system and osseous tissues but also because recent studies highlighted its involvement in cellular Ca^{2+} handling in stress situations (17,18). For example, in hypoxia (19-22) and anoxia (23,24), NCX3 upregulation has been associated with neuroprotection. Such effect is also seen in excitotoxic cell death. The initial Ca^{2+} influx that occurs during glutamate and β-amyloid peptide exposure has been demonstrated to induce calpain-mediated cleavage of the intracellular loop of NCX3 thus causing the exchanger to become hyperfunctional (17,18). These findings demonstrate the potential of NCX3 as a relevant target for disease treatment. However, rational drug development requires detailed understanding of the molecular mechanisms underlying the post-translational regulations of its activity.

Although the first NCX member, NCX1, has been extensively studied (25-27), the information obtained in regard to post-translational regulation cannot simply be extrapolated to NCX3. First, the intracellular loop carrying the regulatory sites shows a low sequence homology of about 60% between NCX1 and NCX3 with some regions sharing only 55% homology, whereas the remainder of the two exchangers is 70% to 80% identical. This lack of conservation in the regulatory sites may suggest the existence

of different post-translational regulatory mechanisms. Consistent with this idea is the observation that regulation by calpain cleavage appears to be limited to NCX3 (17).

Phosphorylation of NCX can affect its plasma membrane stability, proteolysis, protein-protein interactions or directly alters its exchange activity. The protein kinase A and C (PKA and PKC) are serine/threonine protein kinases that play a significant role in the regulation of the activity of Ca^{2+} transporters (6,28), particularly ion exchangers (29-33). Strong evidence supports the importance of NCX phosphorylation in the modulation of its activity (25,34). However, the exact mechanism remains largely unknown.

In this study, we addressed the potential of PKC and/or PKA phosphorylation to alter NCX3 activity. To this end, cells treated with either PMA (PKC activator) or forskolin (PKA activator) were loaded with the fluorescent Ca^{2+} indicator fura-2, after which the changes in fura-2 emission ratio, reflecting the changes in cytosolic free Ca^{2+} concentration ($[Ca^{2+}]_i$), were monitored under conditions that specifically activate either the forward or reverse exchange activity of NCX3 (16). As variants of NCX3 are differentially regulated by intracellular ionic concentrations (16) and post-translational modifications such as calpain cleavage (35), both murine variants NCX3-AC and NCX3-B were investigated following transient expression in HEK293T cells. Both PKC and PKA activation independently altered NCX3 activity. Therefore, as a next step, the potential phosphorylation sites of PKC and PKA were identified and one by one subjected to site-directed mutagenesis into an alanine to assess their contribution to the effects of PKC and PKA activation on NCX3 activity.

Materials and methods

cDNA Cloning

Coding sequences of murine NCX3-AC and NCX3-B (16) were subcloned into a bicistronic mammalian vector pCINeo containing an internal ribosome entry site and enhanced green fluorescent protein (eGFP). A HA tag was added to the N-terminus of the NCX protein and plasmids were subsequently checked by Sanger sequencing.

Site-directed Mutagenesis

All NCX3-AC mutants were generated using a Quikchange site-directed mutagenesis kit (Stratagene, la Jolla, CA) according to the manufacturer's instructions. All mutations were subsequently validated by Sanger sequencing.

Expression of NCX3 in Human Embryonic Kidney Cells

Human Embryonic Kidney Cells (HEK293T) were cultured in a Dulbecco's modified Eagle's medium (BioWhittaker-Europe, Verviers, Belgium) containing 10 % (v/v) fetal calf serum and 2 mM L-Glutamine at 37 ºC and 5 % (v/v) CO_2. The cells were seeded on a glass

coverslip coated with 50 µg/mL fibronectin (Roche, Mannheim, Germany) in a six-well plate. 24 hours after seeding and 48 hours prior to measurement, cells in six-well plate were transiently transfected with the respective constructs (2 µg/well) using polyethylenimine cationic polymer PEI (Polysciences, Inc, Warrington, PA) in accordance with the manufacturer's instructions.

$[Ca^{2+}]_i$ measurements

30 minutes prior to measurement, cells were loaded with 3 µM fura-2 acetoxymethyl ester (fura-2/AM) and 0.01 % (v/v) Pluronic F-127 for 20 min at 37 °C in Krebs solution (5.5 mM KCl, 147 mM NaCl, 1.2 mM $MgCl_2$, 1.5 mM $CaCl_2$, 10 mM glucose, and 10 mM HEPES/NaOH, pH 7.4). After a 10 min wash in Krebs medium, coverslips were placed into a perfusion chamber mounted onto the stage of an inverted microscope (Zeiss Axiovert 200M, Carl Zeiss, Jena, Germany). Addition of compounds and changes of solution were facilitated using a perfusion system. $[Ca^{2+}]_i$ was monitored by alternately exciting fura-2 with monochromatic light of wavelength 340 and 380 nm (Polychrome IV, TILL Photonics, Gräfelfing, Germany). Fluorescence emission light was directed by a 415DCLP dichroic mirror (Omega Optical, Inc., Brattleboro, VT) through a 510WB40 emission filter (Omega Optical, Inc.) onto a CoolSNAP HQ monochrome CCD-camera (Roper Scientific, Vianen, the Netherlands). The integration time of the CCD-camera was set at 200 ms with a sampling interval of 3 s. All hardware was controlled with Metafluor software (version 6.0, Universal Imaging Corp., Downingtown, PA). Prior to measurements, eGFP-positive cells were selected as transfected cells. Eight to 18 individual cells were selected and monitored simultaneously from each coverslip. For each wavelength, the mean fluorescence intensity was monitored in an intracellular region and, for purpose of background correction, in an extracellular region of identical size. After background correction, the fluorescence emission ratio (340 nm/380 nm) was calculated as a measure of $[Ca^{2+}]_i$.

Measurement of Na^+-Ca^{2+} exchange activity

Both the Ca^{2+} extrusion and Ca^{2+} uptake activity were compared between the two NCX3 variants and following activation of PKA and PKC. The activators of PKA (10 µM forskolin) and PKC (100 nM phorbol 12-myristate 13-acetate (PMA)) were added 10 min and 15 min, respectively, prior to the onset and perfused during the measurement. In its reverse mode, NCX activity was evaluated as the peak fura-2 ratio increase after changing to Na^+-free NMDG medium (5.5 mM KCl, 147 mM *N*-methyl glucamine, 1.2 mM $MgCl_2$, 1.5 mM $CaCl_2$, 10 mM glucose, and 10 mM HEPES/HCl, pH 7.4 (36)) containing the irreversible and selective inhibitor of the sarcoplasmic reticulum Ca^{2+}-ATPase, thapsigargin (1 µM), to increase $[Ca^{2+}]_i$ (16). To increase the intracellular ($[Na^+]_i$), cells were treated with the Na^+-K^+ ATPase inhibitor, ouabain (1 µM), for 60 min prior to the onset of the measurement and during the measurement (16). The forward-mode of the exchanger was evaluated by

measuring the Ca^{2+} extrusion activity after an acute increase induced in $[Ca^{2+}]_i$ evoked by addition of the Ca^{2+} ionophore, ionomycin, (1 μM), in Ca^{2+}-free medium (5.5 mM KCl, 147 mM NaCl, 1.2 mM $MgCl_2$, 10 mM glucose, and 10 mM HEPES/NaOH, pH 7.4). All buffers were kept at 37 ºC. Osmolality of all buffers has been measured to ensure a difference smaller than 5 mOsm.

Drugs and chemicals

Ionomycin, thapsigargin, forskolin and PMA were purchased from Sigma; ouabain from MP Biomedicals; and fura-2-AM and pluronic acid from Invitrogen. All were dissolved in dimethyl sulfoxide. During Ca^{2+} recordings, thapsigargin, ionomycin and ouabain were used at a final concentration of 1 μM. PMA and forskolin were used at final concentration of 100 nM and 10 μM respectively. The final concentration of dimethyl sulfoxide was 0.1 % (v/v) and had no effect on $[Ca^{2+}]_i$.

Statistical analysis

All results are based on at least three independent sessions of experiments. The fura-2 ratio shown is an average of ≥ 50 individual cells. Values are expressed as means ± S.E.M. Statistical significance ($P < 0.05$) was determined using One-Way ANOVA or Two-ways ANOVA followed by the Bonferroni's procedure.

Results

HEK293T cells transiently expressing the murine NCX3 variants NCX3-AC, NCX3-B or an empty vector (mock), were loaded with the ratiometric fluorescent Ca^{2+} indicator fura-2 to monitor the changes in cytosolic free Ca^{2+} concentration ($[Ca^{2+}]_i$) under conditions of forward and reverse exchange activity and to assess the effects of PKC and PKA activation thereupon.

Forward mode of NCX3 is unaffected by PKC stimulation

NCX3 forward exchange activity was induced by addition of the Ca^{2+} ionophore ionomycin (1 μM) in the absence of extracellular Ca^{2+}. Ionomycin evoked a rapid increase in $[Ca^{2+}]_i$, which, because of the absence of extracellular Ca^{2+}, is entirely due to the leak of Ca^{2+} from intracellular stores (**Figure 1A**). The peak fura-2 ratio value was 1.3-fold higher in NCX3-B as compared to NCX3-AC expressing cells (**Figures 1A and 1B**), which is consistent with a higher forward exchange activity of NCX3-AC (see also, (16)). In neither case, pretreatment with PMA (100 nM) altered the peak fura-2 value, indicating that the forward exchange activity of these two NCX3 variants is insensitive to PKC activation. PMA itself has no effect on $[Ca^{2+}]_i$ as can be judged from the observation that during the period before the addition of ionomycin the fura-2 ratio signal is similar between untreated and PMA-treated cells.

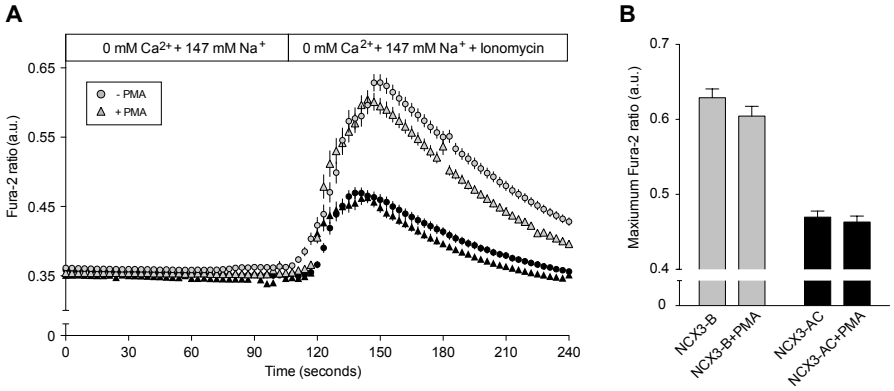

Figure 1 Influence of PKC activation on the forward mode activity of NCX3.

A, At 48 hours post-transfection, HEK293T cells expressing NCX3-B (grey symbols) and NCX3-AC (black symbols) were loaded with fura-2 ratio. The 340/380nm excitation ratio for fura-2 was recorded in transfected cells in absence (circles) or after (triangles) PKC activation by PMA (100 nM) for 15 minutes. At 100 s after the onset of recordings, Ca^{2+} extrusion via Na^+-Ca^{2+} exchange was initiated after depletion of the intracellular Ca^{2+} stores by acute addition of ionomycin (1 μM) in Ca^{2+}-free medium (16). Each data point represents the mean (± S.E.M.) of at least 100 cells for each condition monitored in four independent experimental sessions. **B**, Mean (± S.E.M.) of the maximum fura-2 ratio values recorded after replacement to ionomycin containing medium from the recordings shown in A.

Reverse exchange activity of NCX3 variants is reduced upon PKC stimulation

In a first series of measurements, NCX3 reverse exchange activity was induced by a simultaneous rise in $[Ca^{2+}]_i$ by thapsigargin (1 μM) inhibition of SERCA activity and removal of extracellular Na^+ (37). This condition, evoked a rapid increase in $[Ca^{2+}]_i$ (**Figure 2A**). Compared to mock transfected cells, which lack endogenous NCX activity (16), the peak value of the fura-2 ratio increase was 2.1- and 1.4-fold higher in NCX3-AC and NCX3-B expressing cells, respectively (**Figure 2B**). Pretreatment with PKC for 15 min, significantly reduced this value by 32% and 27% in NCX3-AC and NCX3-B expressing cells, respectively (**Figures 2A and 2B**). This reduction was not observed in the mock-transfected cells and, therefore, specific for NCX3. PMA treatment did not detectably alter the fura-2 ratio signal under normal conditions of extracellular Na^+ (**Figure 1A**).

In a second series of measurements, NCX3 reverse exchange activity was induced by a rise in $[Na^+]_i$ by pretreatment with the Na^+-K^+ ATPase inhibitor ouabain (1 μM) for 60 min. Under normal conditions of extracellular Na^+, the fura-2 ratio signal was not altered in mock-transfected cells, whereas a 4.3- and 2.6-fold increase as compared to mock-transfected cells was observed in NCX3-AC and NCX3-B expressing cells, respectively (**Figures 3A and 3B**). Subsequent removal of extracellular Na^+ evoked a further increase

in fura-2 ratio, the magnitude of which was greater in NCX3-B than NCX3-AC expressing cells (**Figure 3A**). Mock-transfected cells showed a delayed and relatively small increase in $[Ca^{2+}]_i$. Pretreatment with PMA significantly decreased the elevated $[Ca^{2+}]_i$ under normal conditions of extracellular Na^+ in both NCX3-AC and NCX3-B expressing cells (**Figures 3A and 3B**). Nevertheless, PMA treatment did not detectably alter the magnitude of the ratio increase evoked by subsequent extracellular Na^+ removal (**Figure 3C**).

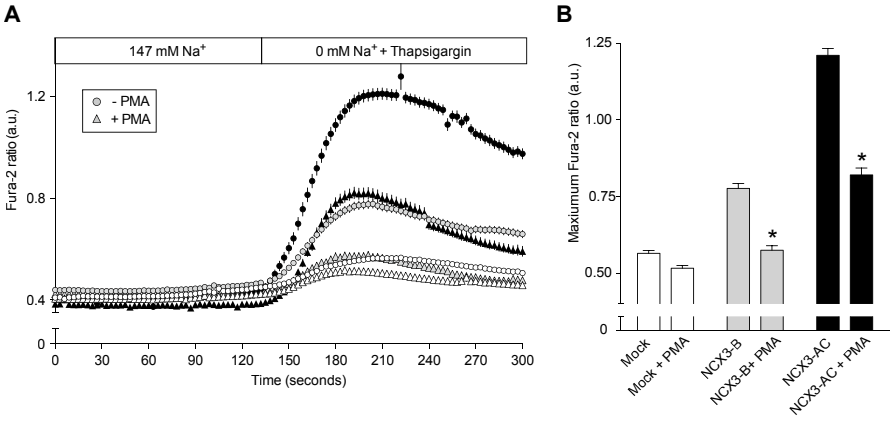

Figure 2 Influence of PKC activation on the reverse mode activity of NCX3 induced by intracellular Ca^{2+} mobilization.

A, At 48 hours post-transfection, HEK293T cells transiently expressing NCX3-AC (black symbols), NCX3-B (grey symbols) or empty vector (white symbols) were loaded with fura-2-AM, after 15 minutes incubation with 100 nM PMA (triangles) or in absence of treatment (circles), and transferred to the stage of the microscope for fluorescence emission recording. At 130 s after the onset of recording, Na^+-containing perfusion medium (147 mM Na^+) was replaced by a Na^+-free medium (NMDG medium) containing 1 μM thapsigargin for induction of reverse NCX3 activity. The 340/380nm excitation ratios for fura-2 are shown. Each data point represents the mean (± S.E.M.), of at least 140 cells monitored per condition in six independent recordings. **B**, Mean (± S.E.M.) of the maximum fura-2 ratio values after addition of thapsigargin (1 μM) and removal of extracellular Na^+ shown in A. *$P < 0.05$.

Identification of PKC phosphorylation site

The recordings presented in Figures 2 and 3 demonstrate that PKC activation decreases the reverse mode of exchange of NCX3. In order to identify the potential phosphorylation site(s) responsible for this regulation, we first aligned the amino acid sequences of the intracellular loop of NCX3 in several species (*Danio rerio, Gallus gallus, Bos Taurus, Rattus norvegicus, Callithrix jacchus, Homo sapiens, Mus musculus*), region where most of the regulation of the NCX family occurs, more specifically in the Ca^{2+}-binding domains 1 and 2 (**Figure 4A**). Phosphorylation sites located in the alternatively spliced region were excluded

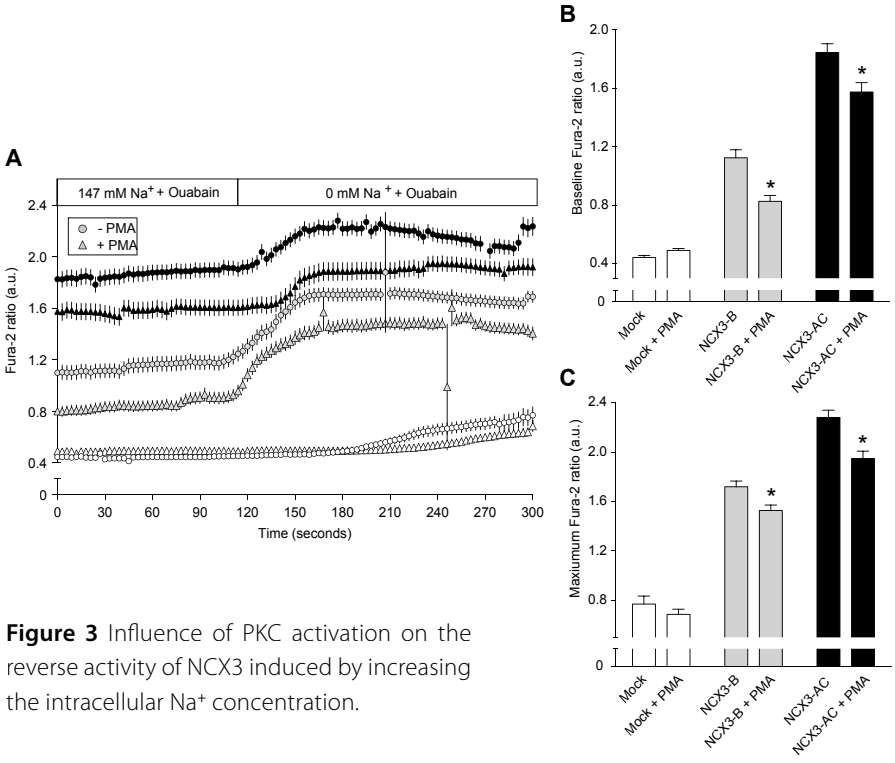

Figure 3 Influence of PKC activation on the reverse activity of NCX3 induced by increasing the intracellular Na^+ concentration.

A, At 48 hours post-transfection, HEK293T cells transiently expressing NCX3-AC (black symbols), NCX3-B (grey symbols) or empty vector (white symbols) were treated with the Na^+-K^+-ATPase inhibitor ouabain (1 µM) for 60 minutes and loaded with fura-2. The 340/380nm excitation ratio for fura-2 was recorded in transfected cells after PKC stimulation (triangles) for 15 minutes with PMA (100 nM) or in absence of stimulation (circles). At 120 s after the onset of recording, Na^+-containing perfusion medium was replaced by Na^+-free medium (NMDG medium) for induction of reverse NCX3 activity. Each data point represents the mean (± S.E.M.), of at least 70 cells monitored in each condition and in three independent experimental sessions. **B**, Mean (± S.E.M.) of the baseline fura-2 ratio during the first 60 s of the recordings shown in A. **C**, Mean (± S.E.M.) of the maximum fura-2 ratio in Na^+-free conditions taken from the recordings shown in A. *$P < 0.05$.

as PMA affected both NCX3-AC and NCX3-B in a similar manner. In the intracellular loop of NCX3, eight serine and threonine residues were predicted by the programs NetPhosK (38) and NetPhos 2.0 (39) as putative PKA and/or PKC phosphorylation sites for both variants. Site-directed mutagenesis was performed on the six PKA and/or PKC sites conserved in all mammals and predicted with the highest probability of phosphorylation according to NetPhos 2.0. Selected serine and threonine residues of NCX3-AC were mutated into alanine to prevent phosphorylation. Subsequently, the reverse mode was triggered by simultaneous addition of thapsigargin and extracellular Na^+ removal. The NCX3-AC exchangers carrying the mutated residues T529A and S695A, exhibited no sensitivity to PKC activation since the maximum fura-2 ratio was not significantly diminished after PMA treatment (**Figures 4B and 4C**).

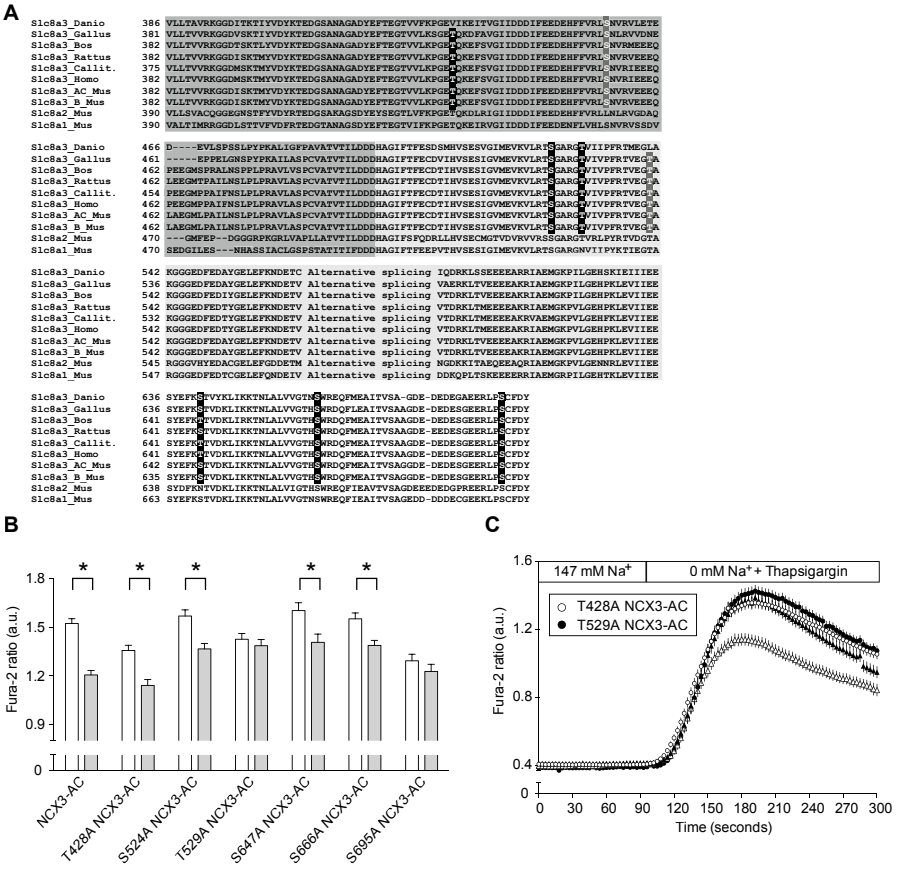

Figure 4 Identification of the PKC phosphorylation sites in NCX3-AC responsible for the reduced reverse activity induced by PKC activation.

A, Alignment of the amino acid sequences of the intracellular loop of NCX3 (Slc8a3) in several species from top to bottom: *Danio rerio, Gallus gallus, Bos Taurus, Rattus norvegicus, Callithrix jacchus, Homo sapiens and Mus musculus*. For comparison, sequences of murine NCX1 (Slc8a1) and NCX2 (Slc8a2) are included. The catenin-like domain (CLD) is shown in white and the Ca^{2+}-binding domains (CBD) are represented in dark grey (CBD1) and light grey (CBD2). Serine and threonine residues of the intracellular loop that are predicted for PKC and/or PKA phosphorylation according to both NetphosK and Netphos2.0 programs are highlighted. Phosphorylation sites predicted with a score lower than 0.8 (NetPhos2.0) are represented in dark grey. The residues, shown in black, for which phosphorylation was predicted with a score above 0.8 (NetPhos2.0) have been mutated into Alanine in NCX3-AC. **B**-**C**, At 48 hours post-transfection, HEK293T cells transiently expressing the indicated NCX3-AC single mutant were loaded with fura-2. Fura-2 excitation ratios (340/380nm) were recorded in transfected cells in absence (white) or after (grey) PKC activation by PMA (100 nM) for 15 minutes. **B**, Mean of the maximum fura-2 ratio after switching to Na^+-free medium containing 1 µM thapsigargin. **C**, The 340/380nm excitation ratios for fura-2 of HEK293T cells expressing the single mutants T428A NCX3-AC (white symbols) or T529A NCX3-AC (black symbols) are shown in absence (circle) or following a treatment with PMA (triangle). Each data point represents (± S.E.M.), of at least 60 cells per condition recorded in four independent experimental sessions. *P < 0.05.

Forward mode of action of NCX3 is unaffected by PKA stimulation

To investigate the effect of PKA activation on NCX3 exchange activity, cells were pretreated with the PKA activator, forskolin (10 μM) for 10 min. Similarly to PMA, forskolin did not alter the forward exchange activity of the two NCX3 variants as determined after acute addition of ionomycin in the absence of extracellular Ca^{2+} (**Figure 5A**).

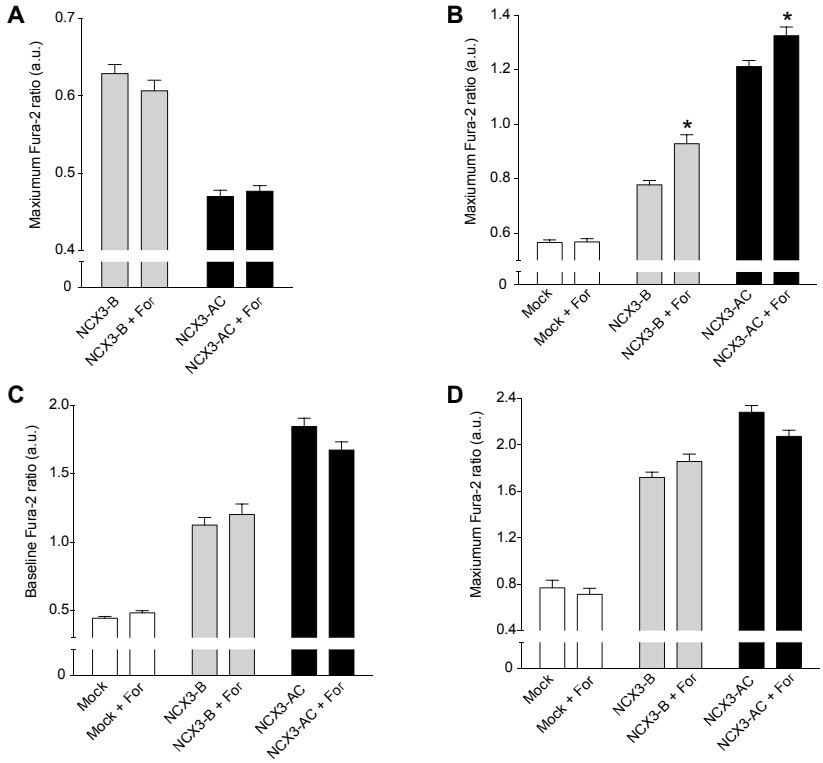

Figure 5 Influence of PKA activation on the reverse and forward mode of NCX3.

A-D, Mean of the values (± S.E.M.) of fura-2 ratio measured in cells transiently expressing NCX3-AC (black bars), NCX3-B (grey bars) or mock (white bars), loaded with fura-2 in absence or following a treatment with PKA activator, forskolin (10 μM) for 10 min prior to the experiments. **A**, Forward mode activity of NCX3 induced by acute addition of ionomycin (1 μM) in Ca^{2+}-free medium. Each bar represents the mean (± S.E.M.) of the maximum fura-2 ratio of at least 80 cells monitored during four different recording sessions. **B**, Reverse mode activity was induced by the replacement of Na^+-containing perfusion medium (147 mM Na^+) by a Na^+-free medium (NMDG medium) containing 1 μM thapsigargin. Each bar represents the mean (± S.E.M.) of the maximum fura-2 ratio of at least 130 cells per condition recorded in five independent experimental sessions. *$P < 0.05$ **C-D**, Reverse mode of NCX3 induced by ouabain treatment (1 μM) for 60 minutes measured in three independent recordings for at least 63 cells in each conditions. **C**, Mean (± S.E.M.) of the baseline fura-2 ratio during the first 60 s of recording. **D**, Mean (± S.E.M.) of the maximum fura-2 ratio values after switching to Na^+-free medium (NMDG medium).

Reverse exchange activity of NCX3 variants is increased upon PKA stimulation

When the NCX3 reverse exchange activity was assessed after a rise in $[Ca^{2+}]_i$ by simultaneous thapsigargin addition and extracellular Na^+ removal, a significant increase in peak value of the fura-2 ratio was observed in forskolin-treated NCX3-AC and NCX3-B expressing cells (**Figure 5B**). Similarly to PMA, forskolin did not alter the small increase in fura-2 ratio observed in mock-transfected cells. Additionally, forskolin did not alter the increase in baseline $[Ca^{2+}]_i$ evoked by ouabain in the presence of extracellular Na^+ (**Figure 5C**) or after subsequent removal of extracellular Na^+ (**Figure 5D**).

Molecular determinants involved in PKA-dependent increase in reverse NCX3 exchange activity

To identify the molecular determinants underlying the increase of NCX3 exchange capacity by PKA activation seen uniquely in the reverse mode activated by simultaneous addition of thapsigargin and removal of extracellular Na^+, we first selected six predicted PKA and/or PKC phosphorylation sites based on their conservation in NCX3 in all mammals, as mentioned above (**Figure 4A**) and mutated these into an alanine. Assessment of their forskolin sensitivity revealed that only the exchanger expressing the S524A mutation had become insensitive to PKA activation (**Figures 6A and 6B**).

Discussion

The present study dissected for the first time the molecular mechanisms underlying the PKC and PKA regulation of NCX3. The data presented demonstrate that while PKC and PKA alter the Ca^{2+} uptake performed by NCX3 in the reverse mode, on the contrary, neither PKC nor PKA affect the $[Ca^{2+}]_i$-stimulated forward exchange activity of the two NCX3 variants, NCX3-AC and NCX3-B, as assessed by ionomycin addition in the presence of extracellular Na^+ but absence of extracellular Ca^{2+}.

The reverse exchange activity of these exchangers is not (NCX3-B) or only slightly (NCX3-AC) activated at normal intracellular $[Na^+]_i$ and $[Ca^{2+}]_i$, as revealed by the effect of extracellular Na^+ removal (16). However, upon subsequent release of Ca^{2+} from intracellular stores induced by thapsigargin, or increase in $[Na^+]_i$ by ouabain incubation, a marked stimulation of the reverse mode occurs. Here, we show that PKC and PKA exert opposite effects on the reverse exchange activity of the two NCX3 variants. Upon Ca^{2+} release from the intracellular stores PKC activation decreases, whereas PKA activation increases NCX3 activity. Furthermore, for both variants, activation of PKC, but not PKA resulted in a significant reduction of the reverse exchange activity induced by a drastic increase in $[Na^+]_i$. Nonetheless, after a rise in $[Na^+]_i$ PKC activation reduced the Ca^{2+} uptake exclusively in presence of extracellular Na^+; as the difference of uptake observed

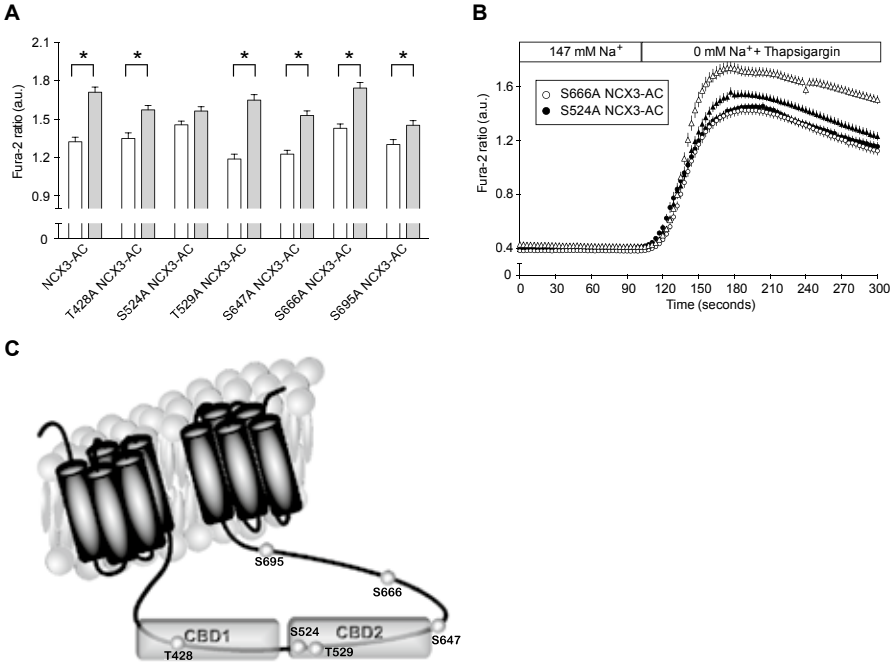

Figure 6 Targeting PKA phosphorylation sites in NCX3-AC responsible for the PKA-mediated increase of NCX3 activity in reverse mode.

A-B, 48 hours after transfection, HEK293T cells transfected with NCX3-AC exchanger mutated for a single residue were loaded with fura-2. Fluorescence emission recordings of fura-2 were performed in cells in absence (white bars) or following a treatment with PKA activator, forskolin (10 µM) (grey bars) for 10 min prior to the experiments. **A**, Maximum fura-2 ratio values after a switch to Na^+-free medium containing 1 µM thapsigargin were calculated as the mean (± S.E.M.) of at least 60 cells in each condition and during three independent experimental sessions. *$P < 0.05$. **B**, The 340/380nm excitation ratios for fura-2 of HEK293T cells expressing the single mutants S524A NCX3-AC (black symbols) or S666A NCX3-AC (white symbols) are shown in absence (circle) or following a treatment with forskolin (triangle). **C**, Schematic representation of NCX3 depicting the PKC and PKA regulatory sites mutated. The 10 transmembrane domains of the NCX3 exchanger are represented here, together with its large intracellular loop. Localization of the residues predicted as phosphorylation sites and mutated by site-directed mutagenesis are indicated by the motif P. S524 appears to be involved in the stimulatory effect of PKA on NCX3 reverse exchange activity, whereas T529 and S695 are implicated in the inhibitory effect of PKC.

in presence of extracellular Na^+ between the PMA-treated and non-treated cells was not further increased in Na^+-free conditions.

Consequently, using site-directed mutagenesis we were able to abrogate the inhibitory effect of PKC by the mutation of a single residue of the intracellular loop, the threonine at

position 529 (T529) or the serine located at position 695 (S695) (**Figure 6C**). Mutating these residues singly into an alanine completely reversed the inhibitory effect of PKC activation on the increase in $[Ca^{2+}]_i$ induced by simultaneous addition of thapsigargin and removal of extracellular Na^+. As for PKA phosphorylation, its stimulatory effect on the Ca^{2+} uptake capacity by NCX3 after a rise in $[Ca^{2+}]_i$ was lost when mutating a unique residue S524.

The loss of sensitivity to PKC and PKA stimulation of the two mutants T529A and S524A NCX3-AC, respectively pinpointed the presence of two phosphorylation sites. Phosphorylation can modify the capacity of exchange of NCX3 by triggering a conformational change or by modifying its interactions with other proteins thereby affecting its stability at the plasma membrane or its interaction with other intracellular factors. Nevertheless, the latter would affect reverse and forward mode in a similar manner. Therefore, the absence of changes in the forward mode of NCX3 after PKC or PKA stimulation suggests a modulation via structural changes of the intracellular loop, a region known to regulate the exchanger.

Regarding the structural aspects, the two phosphorylation sites are located in the Ca^{2+}-binding domain 2 (CBD2) (**Figure 6C**), T529 at the beginning of the third β-strand of the β-sandwich that constitutes CBD2 while S524, few residues apart, is located before this third β-strand (40,41). Within the CBD2 structure, the location of both residues is diametrically opposed to the Ca^{2+}-binding site (40). Therefore, it is unlikely that phosphorylation in this region interacts with the Ca^{2+}-binding sites or influences the number or the stability of those sites. A direct impact of phosphorylation on NCX3 capacity of exchange could therefore occur through interaction with CBD1. Such interactions have never been investigated. Nevertheless, crystal and NMR structure of the two Ca^{2+}-binding domains of NCX1, CBD12, reported an antiparallel arrangement of the two β-sandwich of CBD1 and CBD2 that extended to NCX3 would bring the T529 in the proximity and S524 even closer of the Ca^{2+}-binding sites of CBD1 (42,43).

As for the S695 site, the mutant S695A NCX3-AC was not only insensitive to PKC but showed as well a low sensitivity to PKA as the increase in ratio measured after forskolin in NCX3-AC S695A was lower than the other mutants. These observations suggest rather than a direct phosphorylation, a disruption in the signal integration. Nevertheless, it remains unclear whether the mutation disrupts the structure of the intracellular loop or whether the serine 695 is a key residue involved in the signal transmission to the transmembrane domains. The latter is more likely when taking into consideration the high level of conservation of the region flanking S695 among the NCX family and among species (42) and that S695 is located in the catenin-like domain (CLD) (44), a region previously linked to the relay of information to the transmembrane domains (45).

The stimulation of PKC enhanced the reverse mode activated by Ca^{2+}. Nevertheless, it also increased the reverse mode activated by Na^+, a mode mainly governed by the Na^+-dependent inactivation common to the entire NCX family. Therefore, one might hypothesize that PKC phosphorylates T529 and thus decreases the reverse mode

through an interaction with S695 residue and potentially a change of Ca^{2+}-binding affinity of CBD1, thereby affecting the reverse mode triggered by both ions. While PKA phosphorylation at S524, located closer to the Ca^{2+}-binding sites of CBD1 would increase the affinity for Ca^{2+} (42). However disruption of structure caused by the substitution S695A might reduce the probability of phosphorylation at S524 and in a larger extend at T529. In this regard, the investigation of the NCX structure in its phosphorylated state and the measure of the affinity of CBD1 for Ca^{2+} is required to confirm our hypothesis.

The specificity of the site T529 for PKC was further confirmed by the absence of sensitivity of the site to PKA. Interestingly, this site is conserved in NCX2 but absent in the ubiquitously expressed isoform, NCX1. T529 is predicted with a high probability for PKC phosphorylation in NCX3 (0.82), notably because of the hydrophobic residue (V530) at position +1 and the basic residue at -2 (R527), an optimal phosphorylation site for all PKC isozymes (46). The involvement of the phosphorylation of NCX3 by PKC in physiological conditions remains puzzling due to the lack of information on the implications of NCX3 in the different neuronal and muscular pathways and the multiple roles carried out by PKC in cell signaling. As for PKA, the lack of hydrophobic residue at +1 after S524 together with the basic residue at -2 fit the consensus for PKA phosphorylation (30). The eight residues flanking the phosphorylation sites, from -4 to +4, are conserved in NCX2 and in all variants of NCX1 (47). Surprisingly, phosphorylation of NCX1 by PKA is a matter of controversy (27,48-50) while our findings suggest that, in absence of other post-translational modifications, NCX1 can be phosphorylated by PKA leading, most likely, to an increase in the reverse mode activity.

In skeletal muscle where NCX3 is expressed, PKA is activated downstream of the β-adrenergic signaling pathway (51). For instance, during the fight-or-flight response activated under stress and intense exercise, epinephrine is released from the sympathetic nervous system and binds the β-Adrenergic Receptor. The subsequent rise in cAMP activates PKA and leads to metabolic changes and potentiation of Ca^{2+}-mediated contraction by acting on several Ca^{2+} transporters to rapidly sustain muscle exercise (52). In this context, the increased activity of NCX3 phosphorylated by PKA contributes to the Ca^{2+} entry and contraction required to develop force rapidly. On the other side, the relaxation of the myofiber would not be favored by this stimulation, as Ca^{2+} extrusion by NCX3 remains unchanged.

In the hippocampus, the synaptic enhancement known as long-term potentiation (LTP), essential for the formation of memory and learning, (53,54) is dependent on the activation of multiple kinases such as PKA and CaMKII but also the capacity to perform a strong Ca^{2+} influx via NMDA and other transporters (55). In such case, the increased capacity of NCX3, expressed in hippocampus, for Ca^{2+} influx after PKA stimulation could be involved in the Ca^{2+} entry. In fact, this role has been previously implied, as reduction of learning and memory observed in the mice lacking NCX3 has been attributed to an impaired long-term potentiation (14).

Acknowledgments

This research was supported by an equipment grant of NWO (Netherlands Organization for Scientific Research, No: 911-02-008) and the CSBR (Centre for Systems Biology Research) initiative from the Netherlands Organization for Scientific Research (NWO; No: CSBR09/013V).

Author contribution

LYM, RJB and JGH conceived the study. LYM designed, performed, analyzed the experiments and wrote the manuscript. SV performed the mutagenesis. JGH and RJB revised critically the manuscript. All authors reviewed the results and approved the final version of the manuscript.

References

1. **Talor, Z., and Arruda, J. A.** Partial purification and reconstitution of renal basolateral Na+-Ca2+ exchanger into liposomes. *The Journal of biological chemistry* 260, 15473-15476 (1985)
2. **Ottolia, M., Torres, N., Bridge, J. H., Philipson, K. D., and Goldhaber, J. I.** Na/Ca exchange and contraction of the heart. *Journal of molecular and cellular cardiology* 61, 28-33 (2013)
3. **Pott, C., Philipson, K. D., and Goldhaber, J. I.** Excitation-contraction coupling in Na+-Ca2+ exchanger knockout mice: reduced transsarcolemmal Ca2+ flux. *Circulation research* 97, 1288-1295 (2005)
4. **Zhang, J., Ren, C., Chen, L., Navedo, M. F., Antos, L. K., Kinsey, S. P., Iwamoto, T., Philipson, K. D., Kotlikoff, M. I., Santana, L. F., Wier, W. G., Matteson, D. R., and Blaustein, M. P.** Knockout of Na+/Ca2+ exchanger in smooth muscle attenuates vasoconstriction and L-type Ca2+ channel current and lowers blood pressure. *American journal of physiology. Heart and circulatory physiology* 298, H1472-1483 (2010)
5. **Jeon, D., Yang, Y. M., Jeong, M. J., Philipson, K. D., Rhim, H., and Shin, H. S.** Enhanced learning and memory in mice lacking Na+/Ca2+ exchanger 2. *Neuron* 38, 965-976 (2003)
6. **de Groot, T., Lee, K., Langeslag, M., Xi, Q., Jalink, K., Bindels, R. J., and Hoenderop, J. G.** Parathyroid hormone activates TRPV5 via PKA-dependent phosphorylation. *Journal of the American Society of Nephrology : JASN* 20, 1693-1704 (2009)
7. **Eisner, D. A., and Lederer, W. J.** Na-Ca exchange: stoichiometry and electrogenicity. *The American journal of physiology* 248, C189-202 (1985)
8. **Quednau, B. D., Nicoll, D. A., and Philipson, K. D.** Tissue specificity and alternative splicing of the Na+/Ca2+ exchanger isoforms NCX1, NCX2, and NCX3 in rat. *The American journal of physiology* 272, C1250-1261 (1997)
9. **Staiano, R. I., Granata, F., Secondo, A., Petraroli, A., Loffredo, S., Frattini, A., Annunziato, L., Marone, G., and Triggiani, M.** Expression and function of Na+/Ca2+ exchangers 1 and 3 in human macrophages and monocytes. *European journal of immunology* 39, 1405-1418 (2009)
10. **Nurbaeva, M. K., Schmid, E., Szteyn, K., Yang, W., Viollet, B., Shumilina, E., and Lang, F.** Enhanced Ca(2)(+) entry and Na+/Ca(2)(+) exchanger activity in dendritic cells from AMP-activated protein kinase-deficient mice. *FASEB journal : official publication of the Federation of American Societies for Experimental Biology* 26, 3049-3058 (2012)
11. **Li, J. P., Kajiya, H., Okamoto, F., Nakao, A., Iwamoto, T., and Okabe, K.** Three Na+/Ca2+ exchanger (NCX) variants are expressed in mouse osteoclasts and mediate calcium transport during bone resorption. *Endocrinology* 148, 2116-2125 (2007)
12. **Sosnoski, D. M., and Gay, C. V.** NCX3 is a major functional isoform of the sodium-calcium exchanger in osteoblasts. *Journal of cellular biochemistry* 103, 1101-1110 (2008)
13. **Boscia, F., D'Avanzo, C., Pannaccione, A., Secondo, A., Casamassa, A., Formisano, L., Guida, N., Sokolow, S., Herchuelz, A., and Annunziato, L.** Silencing or knocking out the Na(+)/Ca(2+) exchanger-3 (NCX3) impairs oligodendrocyte differentiation. *Cell death and differentiation* 19, 562-572 (2012)
14. **Molinaro, P., Viggiano, D., Nistico, R., Sirabella, R., Secondo, A., Boscia, F., Pannaccione, A., Scorziello, A., Mehdawy, B., Sokolow, S., Herchuelz, A., Di Renzo, G. F., and Annunziato, L.** Na+ -Ca2+ exchanger (NCX3) knock-out mice display an impairment in hippocampal long-term potentiation and spatial learning and memory. *The Journal of neuroscience : the official journal of the Society for Neuroscience* 31, 7312-7321 (2011)
15. **Sokolow, S., Manto, M., Gailly, P., Molgo, J., Vandebrouck, C., Vanderwinden, J. M., Herchuelz, A., and Schurmans, S.** Impaired neuromuscular transmission and skeletal muscle fiber necrosis in mice lacking Na/Ca exchanger 3. *The Journal of clinical investigation* 113, 265-273 (2004)

16. **Michel, L. Y., Verkaart, S., Koopman, W. J., Willems, P. H., Hoenderop, J. G., and Bindels, R. J.** Function and regulation of the Na+-Ca2+ exchanger NCX3 splice variants in brain and skeletal muscle. *The Journal of biological chemistry* 289, 11293-11303 (2014)

17. **Bano, D., Young, K. W., Guerin, C. J., Lefeuvre, R., Rothwell, N. J., Naldini, L., Rizzuto, R., Carafoli, E., and Nicotera, P.** Cleavage of the plasma membrane Na+/Ca2+ exchanger in excitotoxicity. *Cell* 120, 275-285 (2005)

18. **Pannaccione, A., Secondo, A., Molinaro, P., D'Avanzo, C., Cantile, M., Esposito, A., Boscia, F., Scorziello, A., Sirabella, R., Sokolow, S., Herchuelz, A., Di Renzo, G., and Annunziato, L.** A new concept: Abeta1-42 generates a hyperfunctional proteolytic NCX3 fragment that delays caspase-12 activation and neuronal death. *The Journal of neuroscience : the official journal of the Society for Neuroscience* 32, 10609-10617 (2012)

19. **Amoroso, S., De Maio, M., Russo, G. M., Catalano, A., Bassi, A., Montagnani, S., Renzo, G. D., and Annunziato, L.** Pharmacological evidence that the activation of the Na(+)-Ca2+ exchanger protects C6 glioma cells during chemical hypoxia. *British journal of pharmacology* 121, 303-309 (1997)

20. **Boscia, F., Gala, R., Pignataro, G., de Bartolomeis, A., Cicale, M., Ambesi-Impiombato, A., Di Renzo, G., and Annunziato, L.** Permanent focal brain ischemia induces isoform-dependent changes in the pattern of Na+/Ca2+ exchanger gene expression in the ischemic core, periinfarct area, and intact brain regions. *Journal of cerebral blood flow and metabolism : official journal of the International Society of Cerebral Blood Flow and Metabolism* 26, 502-517 (2006)

21. **Matsuda, T., Takuma, K., Nishiguchi, E., Hashimoto, H., Azuma, J., and Baba, A.** Involvement of Na+-Ca2+ exchanger in reperfusion-induced delayed cell death of cultured rat astrocytes. *The European journal of neuroscience* 8, 951-958 (1996)

22. **Pignataro, G., Tortiglione, A., Scorziello, A., Giaccio, L., Secondo, A., Severino, B., Santagada, V., Caliendo, G., Amoroso, S., Di Renzo, G., and Annunziato, L.** Evidence for a protective role played by the Na+/Ca2+ exchanger in cerebral ischemia induced by middle cerebral artery occlusion in male rats. *Neuropharmacology* 46, 439-448 (2004)

23. **Sirabella, R., Secondo, A., Pannaccione, A., Scorziello, A., Valsecchi, V., Adornetto, A., Bilo, L., Di Renzo, G., and Annunziato, L.** Anoxia-induced NF-kappaB-dependent upregulation of NCX1 contributes to Ca2+ refilling into endoplasmic reticulum in cortical neurons. *Stroke; a journal of cerebral circulation* 40, 922-929 (2009)

24. **Stys, P. K., Waxman, S. G., and Ransom, B. R.** Ionic mechanisms of anoxic injury in mammalian CNS white matter: role of Na+ channels and Na(+)-Ca2+ exchanger. *The Journal of neuroscience : the official journal of the Society for Neuroscience* 12, 430-439 (1992)

25. **Iwamoto, T., Pan, Y., Wakabayashi, S., Imagawa, T., Yamanaka, H. I., and Shigekawa, M.** Phosphorylation-dependent regulation of cardiac Na+/Ca2+ exchanger via protein kinase C. *The Journal of biological chemistry* 271, 13609-13615 (1996)

26. **Mene, P., Pugliese, F., and Cinotti, G. A.** Regulation of Na(+)-Ca2+ exchange in cultured human mesangial cells. *The American journal of physiology* 261, F466-473 (1991)

27. **Ruknudin, A., He, S., Lederer, W. J., and Schulze, D. H.** Functional differences between cardiac and renal isoforms of the rat Na+-Ca2+ exchanger NCX1 expressed in Xenopus oocytes. *The Journal of physiology* 529 Pt 3, 599-610 (2000)

28. **Chappe, V., Hinkson, D. A., Zhu, T., Chang, X. B., Riordan, J. R., and Hanrahan, J. W.** Phosphorylation of protein kinase C sites in NBD1 and the R domain control CFTR channel activation by PKA. *The Journal of physiology* 548, 39-52 (2003)

29. **Liaw, Y. S., Yang, P. C., Yu, C. J., Kuo, S. H., Luh, K. T., Lin, Y. J., and Wu, M. L.** PKC activation is required by EGF-stimulated Na(+)-H+ exchanger in human pleural mesothelial cells. *The American journal of physiology* 274, L665-672 (1998)

30. **Alrefai, W. A., Scaglione-Sewell, B., Tyagi, S., Wartman, L., Brasitus, T. A., Ramaswamy, K., and Dudeja, P. K.** Differential regulation of the expression of Na(+)/H(+) exchanger isoform NHE3 by PKC-alpha in Caco-2 cells. *American journal of physiology. Cell physiology* 281, C1551-1558 (2001)

31. **Yang, X., and Lytton, J.** Purinergic stimulation of K+-dependent Na+/Ca2+ exchanger isoform 4 requires dual activation by PKC and CaMKII. *Bioscience reports* 33(2013)

32. **He, S., Ruknudin, A., Bambrick, L. L., Lederer, W. J., and Schulze, D. H.** Isoform-specific regulation of the Na+/Ca2+ exchanger in rat astrocytes and neurons by PKA. *The Journal of neuroscience : the official journal of the Society for Neuroscience* 18, 4833-4841 (1998)

33. **Honegger, K. J., Capuano, P., Winter, C., Bacic, D., Stange, G., Wagner, C. A., Biber, J., Murer, H., and Hernando, N.** Regulation of sodium-proton exchanger isoform 3 (NHE3) by PKA and exchange protein directly activated by cAMP (EPAC). *Proceedings of the National Academy of Sciences of the United States of America* 103, 803-808 (2006)

34. **Schulze, D. H., Muqhal, M., Lederer, W. J., and Ruknudin, A. M.** Sodium/calcium exchanger (NCX1) macromolecular complex. *The Journal of biological chemistry* 278, 28849-28855 (2003)

35. **Michel, L. Y., Hoenderop, J. G., and Bindels, R. J.** Calpain-3-mediated regulation of the Na-Ca exchanger isoform 3. *Pflugers Archiv : European journal of physiology* (2015)

36. **Secondo, A., Staiano, R. I., Scorziello, A., Sirabella, R., Boscia, F., Adornetto, A., Valsecchi, V., Molinaro, P., Canzoniero, L. M., Di Renzo, G., and Annunziato, L.** BHK cells transfected with NCX3 are more resistant to hypoxia followed by reoxygenation than those transfected with NCX1 and NCX2: Possible relationship with mitochondrial membrane potential. *Cell Calcium* 42, 521-535 (2007)

37. **Balasubramanyam, M., Rohowsky-Kochan, C., Reeves, J. P., and Gardner, J. P.** Na+/Ca2+ exchange-mediated calcium entry in human lymphocytes. *The Journal of clinical investigation* 94, 2002-2008 (1994)

38. **Blom, N., Sicheritz-Ponten, T., Gupta, R., Gammeltoft, S., and Brunak, S.** Prediction of post-translational glycosylation and phosphorylation of proteins from the amino acid sequence. *Proteomics* 4, 1633-1649 (2004)

39. **Blom, N., Gammeltoft, S., and Brunak, S.** Sequence and structure-based prediction of eukaryotic protein phosphorylation sites. *Journal of molecular biology* 294, 1351-1362 (1999)

40. **Breukels, V., Touw, W. G., and Vuister, G. W.** NMR structure note: solution structure of Ca(2)(+) binding domain 2B of the third isoform of the Na(+)/Ca(2)(+) exchanger. *Journal of biomolecular NMR* 54, 115-121 (2012)

41. **Besserer, G. M., Ottolia, M., Nicoll, D. A., Chaptal, V., Cascio, D., Philipson, K. D., and Abramson, J.** The second Ca2+-binding domain of the Na+ Ca2+ exchanger is essential for regulation: crystal structures and mutational analysis. *Proceedings of the National Academy of Sciences of the United States of America* 104, 18467-18472 (2007)

42. **Hilge, M., Aelen, J., Perrakis, A., and Vuister, G. W.** Structural basis for Ca2+ regulation in the Na+/Ca2+ exchanger. *Annals of the New York Academy of Sciences* 1099, 7-15 (2007)

43. **Ottolia, M., Nicoll, D. A., John, S., and Philipson, K. D.** Interactions between Ca2+ binding domains of the Na+-Ca2+ exchanger and secondary regulation. *Channels* 4, 159-162 (2010)

44. **Hilge, M., Aelen, J., and Vuister, G. W.** Ca2+ regulation in the Na+/Ca2+ exchanger involves two markedly different Ca2+ sensors. *Molecular cell* 22, 15-25 (2006)

45. **Hilge, M., Aelen, J., Foarce, A., Perrakis, A., and Vuister, G. W.** Ca2+ regulation in the Na+/Ca2+ exchanger features a dual electrostatic switch mechanism. *Proceedings of the National Academy of Sciences of the United States of America* 106, 14333-14338 (2009)

46. **Nishikawa, K., Toker, A., Johannes, F. J., Songyang, Z., and Cantley, L. C.** Determination of the specific substrate sequence motifs of protein kinase C isozymes. *The Journal of biological chemistry* 272, 952-960 (1997)

47. **Breukels, V., Touw, W. G., and Vuister, G. W.** Structural and dynamic aspects of Ca2+ and Mg2+ binding of the regulatory domains of the Na+/Ca2+ exchanger. *Biochemical Society transactions* 40, 409-414 (2012)

48. **Wanichawan, P., Louch, W. E., Hortemo, K. H., Austbo, B., Lunde, P. K., Scott, J. D., Sejersted, O. M., and Carlson, C. R.** Full-length cardiac Na+/Ca2+ exchanger 1 protein is not phosphorylated by protein kinase A. *American journal of physiology. Cell physiology* 300, C989-997 (2011)

49. **Lin, X., Jo, H., Sakakibara, Y., Tambara, K., Kim, B., Komeda, M., and Matsuoka, S.** Beta-adrenergic stimulation does not activate Na+/Ca2+ exchange current in guinea pig, mouse, and rat ventricular myocytes. *American journal of physiology. Cell physiology* 290, C601-608 (2006)

50. **Ginsburg, K. S., and Bers, D. M.** Isoproterenol does not enhance Ca-dependent Na/Ca exchange current in intact rabbit ventricular myocytes. *Journal of molecular and cellular cardiology* 39, 972-981 (2005)

51. **Dietz, M. R., Chiasson, J. L., Soderling, T. R., and Exton, J. H.** Epinephrine regulation of skeletal muscle glycogen metabolism. Studies utilizing the perfused rat hindlimb preparation. *The Journal of biological chemistry* 255, 2301-2307 (1980)

52. **Johnson, B. D., Brousal, J. P., Peterson, B. Z., Gallombardo, P. A., Hockerman, G. H., Lai, Y., Scheuer, T., and Catterall, W. A.** Modulation of the cloned skeletal muscle L-type Ca2+ channel by anchored cAMP-dependent protein kinase. *The Journal of neuroscience : the official journal of the Society for Neuroscience* 17, 1243-1255 (1997)

53. **Jay, T. M., Gurden, H., and Yamaguchi, T.** Rapid increase in PKA activity during long-term potentiation in the hippocampal afferent fibre system to the prefrontal cortex in vivo. *The European journal of neuroscience* 10, 3302-3306 (1998)

54. **Kim, M., Huang, T., Abel, T., and Blackwell, K. T.** Temporal sensitivity of protein kinase a activation in late-phase long term potentiation. *PLoS computational biology* 6, e1000691 (2010)

55. **Malenka, R. C., Kauer, J. A., Perkel, D. J., Mauk, M. D., Kelly, P. T., Nicoll, R. A., and Waxham, M. N.** An essential role for postsynaptic calmodulin and protein kinase activity in long-term potentiation. *Nature* 340, 554-557 (1989)

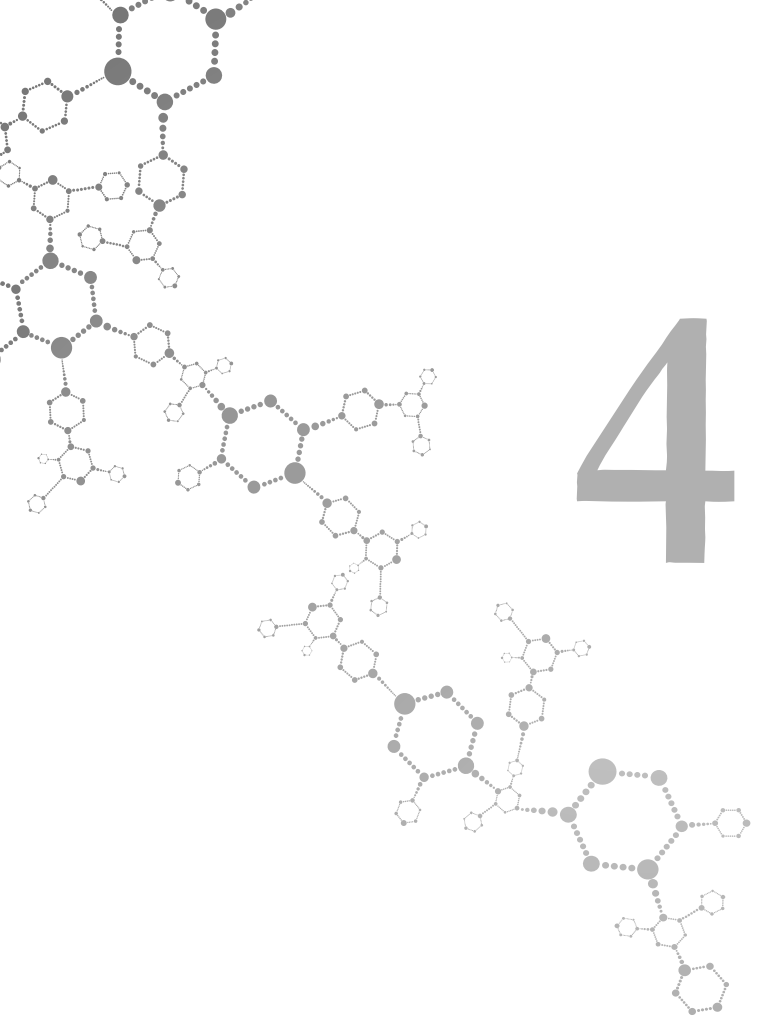

4

Calpain-3-mediated regulation of the Na^+-Ca^{2+} exchanger NCX3

Lauriane Y.M. Michel[1,2], Joost G.J. Hoenderop[1], René J.M. Bindels[1,2]

[1] Department of Physiology, Radboud University Medical Center, The Netherlands
[2] Centre for System Biology and Bioenergetics, Radboud University Medical Center, The Netherlands

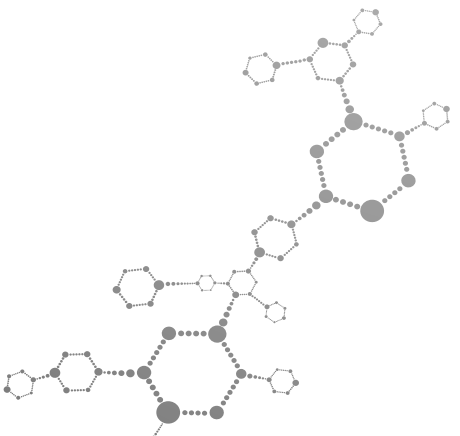

Pflügers Archiv 468, 243-255 (2016)

Abstract

Ca^{2+} disturbances are observed when Ca^{2+}-dependent cysteine proteases malfunction, causing muscle weakness and wasting. For example, loss of calpain-3 (CAPN3) activity leads to limb-girdle muscular dystrophy 2A (LGMD2A). In neuronal excitotoxicity, the cleavage of the Na^{+}-Ca^{2+} exchanger isoform 3 (NCX3) has been associated with an increase in activity and elevation of the Ca^{2+} content in the endoplasmic reticulum (ER). Since NCX3 is expressed in skeletal muscle, we evaluated the cleavage of different NCX3 splice variants by CAPN1 and CAPN3. Using Fura-2-based cellular Ca^{2+} imaging, we showed for the first time that CAPN3 increases NCX3 activity and that only NCX3-AC, the variant predominantly expressed in skeletal muscle, is sensitive to calpain. The silencing of the endogenous CAPN1 and the expression of the inactive form of CAPN3 (C129S CAPN3) confirmed the specificity for CAPN1 and CAPN3. Functional studies revealed that cellular Ca^{2+} uptake through the reverse mode of NCX3 was significantly increased independently of the mode of activation of the exchanger by either a rise in intracellular Ca^{2+} ($[Ca^{2+}]_i$) or Na^{+} ($[Na^{+}]_i$). Subsequently, the sensitivity to CAPN1 and CAPN3 could be abrogated by removal of the six residues coded in exon C of NCX3-AC. Additionally, mutation of the Leu^{600} and Leu^{601} suggested the presence of a cleavage site at Leu^{602}. The increased Ca^{2+} uptake of NCX3 might participate in the Ca^{2+} refilling of the sarcoplasmic reticulum (SR) after the excitation-contraction uncoupling following exercise and therefore be implicated in the impaired reticular Ca^{2+} storage observed in LGMD2A.

Keywords: Sodium-calcium exchange, alternative splicing, calpain-3, muscular dystrophy, muscle fatigue, exercise

Introduction

The calpain proteases (CAPN) are Ca^{2+}-dependent cysteine proteases expressed throughout the entire body. A compromised function of one of the calpain family members can lead to diverse pathologies such as embryonic lethality, gastropathy, muscular dystrophy, or platelet dysfunction (1). In the human genome, 15 members of the calpain family have been found (CAPN1 to CAPN15) (2). The distinctive characteristic of calpain lies in its activation by a rise in intracellular Ca^{2+} levels ($[Ca^{2+}]_i$). This phenomenon triggers the autolysis of the protease. The cytosolic concentration of Ca^{2+} required for this activation differs between isoforms. The targets of its proteolysis are difficult to predict as the calpain family recognizes a tertiary structure and not the primary sequence unlike many conventional proteases (3).

Contrary to CAPN1 and CAPN2 that are ubiquitously expressed, the third isoform CAPN3 is restricted to the skeletal muscle. Interestingly, nanomolar levels of Ca^{2+} are sufficient to activate CAPN3 while CAPN1 and CAPN2 require micromolar and millimolar concentrations, respectively (4). In physiological conditions, CAPN3 is activated when local Ca^{2+} levels are higher than 200 nM over a long period. Such requirements are met following eccentric contractions (5,6). However, in tetanic and concentric contractions, CAPN3 remains in its inactive state, which makes CAPN3 activity specific to certain types of contractions.

CAPN3 dysfunction causes the limb-girdle muscular dystrophy (LGMD) 2A also called calpainopathy, which is the most common type of LGMD, with 30% of the patients (7). The LGMD2A is an autosomal recessive form of muscular dystrophy characterized by muscle weakness of the proximal limb-girdle muscles eventually leading to a loss of ambulation. It derives from a single mutation of CAPN3 causing a defect in CAPN3 function. As of now, 97 distinct mutations have been identified as a cause of LGMD2A (8).

Among many peculiarities, CAPN3 is not freely present in the cytoplasm like CAPN1 and CAPN2 but tightly bound to the N2 region of the myofiber (9) and to the triad (10) formed by a central t-tubule and two terminal cisternae of the sarcoplasmic reticulum (SR). In this region where many Ca^{2+} transporters are present, a tight control of the Ca^{2+} fluxes is maintained during excitation-contraction coupling by connecting the SR to the sarcolemma (11). The absence of CAPN3 or its impaired function is linked with Ca^{2+} disturbances within the myofibers including a decrease in Ca^{2+} release from the SR (10). Such impairments could well contribute to the clinical phenotype of the LGMD2A. Therefore, the investigation of the role of CAPN3 on the Ca^{2+} fluxes occurring at the triad is of great interest.

Recently, the Na^{+}-Ca^{2+} exchanger family (NCX) has been shown to be a substrate of CAPN1 and CAPN2 (12). The third member of the family, NCX3, was revealed to be the only isoform specifically cleaved during excitotoxic conditions (12). NCX cleavage modifies its activity and the resulting Ca^{2+} influx (13). Interestingly, NCX3 is also expressed

in the skeletal muscles and has been found at the triad (14) where it extrudes Ca^{2+} across the sarcolemma prior to relaxation. Recently, NCX3 was hypothesized to be involved in the regulation of Ca^{2+} beyond Ca^{2+} extrusion, and several studies have suggested a role for NCX3 in Ca^{2+} re-entry into the SR (15,16) during prolonged exercise.

The expression of NCX3 can give rise to different variants (17) due to an alternative splicing. Two variants have been described in mice NCX3-AC and NCX3-B. Previous work from our group showed that these variants have different capacities of exchange in physiological situations (15). It is however unclear whether the calpain family cleaves both variants and how the cleavage affects their functional properties.

In the present study, we investigated for the first time the sensitivity of the different NCX3 variants to calpain using Fura-2-based Ca^{2+} imaging in presence of the calpain inhibitor calpastatin. The results were confirmed by the use of a siRNA targeting specifically CAPN1. By expressing both CAPN3 and its inactive form (C129S CAPN3), a novel regulation of NCX3 variants by the skeletal muscle CAPN3 was found. These properties were further compared with the expression pattern of the two variants among the different myofiber types. Finally, the combination of data concerning the reverse mode triggered by $[Ca^{2+}]_i$ and by $[Na^+]_i$, together with the use of site-directed mutagenesis, enabled a full characterization of the transport capacities of the exchanger upon regulation by calpain and provided a new insight into the molecular determinants responsible for this sensitivity.

Materials and Methods

Animal model

Four C57BL/6 mice were sacrificed and subsequently, the skeletal muscles from the left and right hind limbs were dissected and directly frozen in liquid nitrogen in order to obtain the gastrocnemius, the tibialis anterior (TA), the extensor digitorum longus, and the soleus. The heart sample used as a negative control was removed from four C57BL/6 mice.

Cell lines and transfection

The Human Embryonic Kidney cells HEK293T, were cultured in a Dulbecco's modified Eagle medium (Bio Whittaker-Europe, Verviers, Belgium) containing 10% (v/v) fetal calf serum, 2 mM L-glutamine at 37ºC with 5% (v/v) CO2. 48 hours prior to experiments cells were seeded on a six well-plate and transiently transfected. For double transfections, cells received 1 µg of each constructs for a total of 2 µg/well, using polyethylenimine cationic polymer PEI (Polysciences Inc., Warrington, PA) in accordance with the manufacturer's instructions.

Cloning and mutagenesis

Coding sequence of the human calpastatin (hCAST) was obtained from Dharmacon Research Inc. (Lafayette, CO). Human calpain-3 (hCAPN3) (kindly provided by Dr. van der Maarel, Leiden, The Netherlands) was subcloned into a pCINeo IRES-mCherry backbone. The subcloning of the mice NCX3-AC and NCX3-B into pCINeo IRES-GFP vectors with a HA-Tag fused at the N-terminus of the protein has been previously described in detail (15). Calpain cleavage sites were predicted using the group base prediction system-calpain cleavage detector (GPS-CCD) 1.0 prediction tool (18). The variant specific cleavage site was mutated using site-directed mutagenesis, performed on NCX3-AC leading to the following mutation: LL-600601-WW NCX3-AC targeting the cleavage sites. Additionally, the exon C consisting of the –ALLLSP- region could be removed to NCX3-AC (NCX3-A) and the C129S mutation inserted in hCAPN3 using a Quick-change site-directed mutagenesis kit (Stratagene, La Jolla, CA).

Expression profile and quantitative real-time polymerase chain reaction analysis

Tissue RNA was extracted using TRIzol total RNA Isolation Reagent (Life technologies BRL, Breda, The Netherlands). After DNAse treatment (Promega, Madison, WI), 1.5 µg of RNA was reverse-transcribed by Moloney-Murine Leukemia Virus-Reverse Transcriptase (Invitrogen, Carlsbad, CA) as previously described (19). Using a CFX96 real time PCR detection system (Bio-Rad, Hercules, CA), the relative quantification of NCX3 and the calpain isoforms were measured in the cDNA from tissues and normalized according to the Livak method on GAPDH expression. Absolute quantification of the variants NCX3-AC and NCX3-B was calculated thanks to NCX3 standard curves generated by using a diluted pCINeo-IRES-eGFP-mNCX3-AC and pCINeo-IRES-eGFP-mNCX3-B vectors. Calculations were performed as previously described (15,20) in order to obtain the absolute copy number for each variant. Sequences were amplified using the validated primers described in the table below (**Table 1**).

Table 1 Primers sets for relative and absolute quantification by RT-PCR

Name primers	Forward (5′→ 3′)	Reverse (5′→ 3′)
Total mNCX3	GAGCTGGAGTTCAAGAATG	CTTCCTGTCTGTCACTTC
mNCX3-AC	GAAACAGTCAAAACAATTCACATC	GTCACTTCTGGAGATAACAGGAG
mNCX3-B	GAAACAGTGAAAACCATAAGGG	CTGTCACTTCTGATATTCC
mCAPN1	ACCACATTTTACGAGGGCAC	GGATCTTGAACTGGGGGTTT
mCAPN2	ACATGCGTACTCTGTCACCG	GCTGGGGCAATTGTCATTCC
mCAPN3	ACAACAATCAGCTGGTTTTCACC	CAAAAAACTCTGTCACCCCTCC
mGAPDH	TAACATCAAATGGGGTGAGG	GGTTCACACCCATCACAAAC

Each set of primers amplified a fragment of 70 bp to 150 bp and has been tested and validated beforehand.

Silencing of calpain-1

Downregulation of CAPN1 expression was performed using siRNA targeting human calpain-1 and consisting of three to five target-specific 19-25 nt siRNAs (Santacruz, Dallas, TX) and a control siRNA (Dharmacon Research Inc., Lafayette, CO). 24 hours after plating, HEK293T cells were transfected with an optimized concentration of 30 nM of siRNA and 1 µg/well of the NCX3 construct, NCX3-AC or NCX3-B, and 1 µg/well of mock vector using Lipofectamine. Functional experiments were performed 72 h after transfection, time required for an optimal downregulation with such siRNA.

Immunoblot analysis

HEK293T cells were lysed at 4 ºC in a solution of 150 mM NaCl, 5 mM EGTA, 50 mM Tris, pH adjusted to 7.5 with NaOH, Triton X-100 0.5% (v/v) and protease inhibitors (1 mM PMSF, 5 µg/mL leupeptin, 1 µg/mL aprotinin, 1 µg/mL pepstatin). After centrifugation at 12,000 x g for 10 min, 5x Laemmli buffer containing 100 nM dithiothreitol was added to the supernatant. Lysates were subjected to SDS–PAGE 8% (w/v) and electroblotted onto polyvinylidene difluoride (PVDF) membranes. Blots were incubated with 5% (w/v) non-fat dried milk in TBS-T (137 mM NaCl, 0.2% (v/v) Tween-20, and 20 mM Tris/HCl, pH 7.6). Immunoblots were incubated overnight at 4 ºC with either a mouse anti-Beta-actin antibody (1:1,000) (Sigma, MO, USA) or a goat anti-calpain-1 (1:150) (Santacruz, Dallas, TX) diluted in 1% (w/v) milk in TBS-T. PVDF membranes were incubated one hour at room temperature with a sheep horseradish peroxidase-conjugated anti-goat (1:2,000) or anti-mouse (1:10,000) antibody (Sigma, MO, USA) in TBS-T. Afterwards, blots were visualized using the enhanced chemiluminescence system (ECL, Thermo Fisher).

Fura-2 measurements

NCX3 activity was measured by recording intracellular Ca^{2+} level. HEK293T cells were seeded on coverslips coated with fibronectin (Roche, Mannheim, Germany) prior to transfection. 48 hours after transfection the cells were loaded for 20 min at 37 ºC with the ratiometric probe Fura-2-AM 3 µM and 0.01% (v/v) pluronic acid F-127 (Invitrogen, Carlsbad, CA) in Krebs solution (5.5 mM KCl, 147 mM NaCl, 1.2 mM $MgCl_2$, 1.5 mM $CaCl_2$, 10 mM glucose, and 10 mM HEPES/NaOH, pH 7.4). After a 10-min wash, coverslips were mounted onto a stage of an inverted microscope (Zeiss Axiovert 200M, Carl Zeiss, Jena, Germany). Changes in medium and addition of compounds were facilitated using a perfusion system. $[Ca^{2+}]_i$ was monitored by exciting Fura-2 with monochromatic light of wavelength 340 and 380 nm (Polychrome IV, TILL Photonics, Gräfelfing, Germany). Fluorescence emission was directed by a 415DCLP dichroic mirror (Omega Optical, Inc., Brattleboro, VT) through a 510WB40 emission filter (Omega Optical, Inc.) onto a CoolSNAP HQ monochrome charge-coupled device (CCD) camera (Roper Scientific, Vianen, The Netherlands). The integration time of the CCD camera was set at 200 ms with a sampling interval of 3 s. All hardware was controlled with Metafluor software (version 6.0, Universal

Imaging Corp., Downingtown, PA). For each wavelength, the mean fluorescence intensity was monitored in an intracellular region and, for purpose of background correction, in an extracellular region of identical size. After background correction, the fluorescence emission ratio (340 nm/380 nm) was calculated to determine the Fura-2 ratios. Ten to nineteen individual GFP-positive cells were selected and monitored simultaneously from each coverslip. After double transfection of CAPN3 and NCX3, only cells positive for both GFP and mCherry were selected. The reverse mode of NCX activity was evaluated using the Ca^{2+} uptake that follows the removal of extracellular Na^+ using a NMDG solution (5.5 mM KCl, 147 mM *N*-methyl glucamine, 1.2 mM MgCl2, 1.5 mM CaCl2, 10 mM glucose, and 10 mM HEPES/HCl, pH 7.4) (21). All buffers were kept at 37 ºC and the variability in osmolality was lower than 5 mOsm. The activation of the reverse mode of the exchanger was achieved by either raising the $[Ca^{2+}]_i$ using the sarcoplasmic reticulum Ca^{2+}-ATPase inhibitor thapsigargin (1 µM) simultaneously with the Na^+ removal, or raising the $[Na^+]_i$ with a 60-min incubation in presence of the inhibitor of the Na^+-K^+ ATPase ouabain (1 µM) (21) prior to the experiments with a perfusion during recordings.

Statistical analysis

All results are based on at least three different sessions of experiments. The Fura-2 ratio is an average of ≥ 50 individual cells. Values are expressed as means ± S.E.M. Statistical significance ($P < 0.05$) was determined using One-way ANOVA with the Bonferroni's procedure.

Results

Expression of calpains and NCX3 in skeletal muscle

Using RT-PCR, mRNA levels of the calpain family members were measured in cardiac tissues and skeletal muscles of different fiber types: slow-twitch fibers predominant in the soleus, fast-twitch fibers dominant in the extensor digitorum longus (EDL), or mixed fibers such as those found in the gastrocnemius and the tibialis anterior (TA). The measurements revealed that calpains were highly expressed in soleus, showing 2.3-, 2.9- and 3.3- fold increases for CAPN1, CAPN2, and CAPN3, respectively, compared to the other skeletal muscles (**Figure 1A-C**). Expression of CAPN1 in the heart was somewhat lower with a 1.3 fold increase expression compared to the gastrocnemius, while CAPN2 was increased by a factor of 4.1. Finally, CAPN3 expression in cardiac tissue was more than 55 times lower than in skeletal muscle. A similar expression pattern was observed for NCX3, which confirmed the specific enrichment of both CAPN3 and NCX3 in the skeletal muscle (**Figure 1D**). NCX3 expression was highest in the EDL, followed by the soleus, the TA, and the gastrocnemius. Using an absolute quantification method, we were able to obtain the percentage of the different variants of NCX3, NCX3-AC containing

both exons A and C, and NCX-B containing only the exon B (**Figure 1E**). These data revealed the predominance of NCX3-AC in all fiber types. However, in the soleus, NCX3-AC was 72% of the total NCX3 while for the other fiber-type this percentage was higher than 94%.

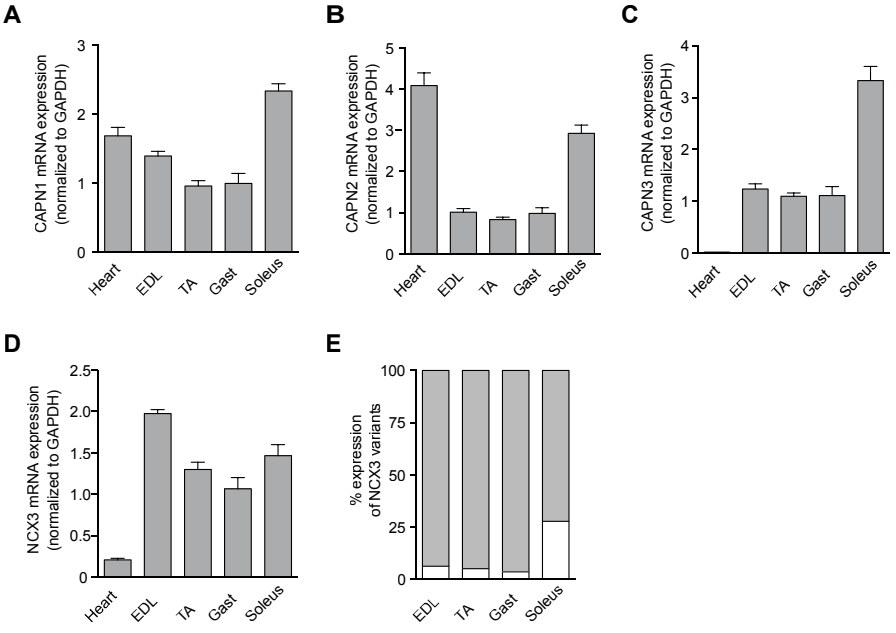

Figure 1 NCX3 and calpain expression in mice skeletal muscle.

A, CAPN1, **B**, CAPN2, **C**, CAPN3 and **D**, NCX3 expression at mRNA levels in several types of skeletal muscle. Values are normalized on the housekeeping gene GAPDH. **E**, The percentage of each NCX3 variants represented as the absolute copy number of either NCX3-B (white) and NCX3-AC (grey) compared to the sum of both quantifications. For clarity, S.E.M. of value < 3 % in each case is not depicted.

Effect of CAPN on NCX3 activity

The effect of calpain activation on NCX3 reverse activity was investigated using the ratiometric Fura-2 probe. The reverse mode of exchange, where Ca^{2+} enters the cell, was triggered by the switch to a Na^+-free medium together with a rise in either $[Na^+]_i$ or $[Ca^{2+}]_i$. In order to elevate the Ca^{2+} levels, the cells were perfused with a Na^+-free medium containing thapsigargin. Thapsigargin inhibits the SERCA ATPase and therefore prevents the re-uptake of Ca^{2+} in the endoplasmic reticulum (ER). As the ER constitutively leaks Ca^{2+}, the Ca^{2+} stocks were emptied in a slow manner. $[Na^+]_i$ was elevated by incubating cells with ouabain in a Na^+-rich medium prior to the measurements. By blocking the Na^+-

K^+-ATPase, ouabain causes a gradual rise in intracellular Na^+ until similar concentrations across the plasma membrane are reached. The activity of both variants of NCX3 was recorded in HEK293T cells expressing an NCX3 variant together with an empty vector (Mock) or the calpain inhibitor calpastatin (CAST). Importantly, our group previously determined the plasma membrane localization of NCX3 in transfected HEK293T cells by cell surface biotinylation. Importantly, NCX3-AC and NCX3-B were both expressed at the plasma membrane in similar amount (15).

In NCX3-B expressing cells, exchange activity remained unchanged by the expression of calpastatin, while the exchange capacity of NCX3-AC was decreased (**Figures 2A and 2C**). Thus, in the reverse mode, the calpastatin expression caused a significant decrease in the maximum Ca^{2+} levels measured in the NCX3-AC expressing cells under Na^+-free conditions (**Figures 2B and 2E**), regardless of whether intracellular Ca^{2+} or Na^+ was increased. Furthermore, the expression of the calpain inhibitor significantly diminished the initial Ca^{2+} uptake observed in NCX3-AC expressing cells in presence of extracellular Na^+ and ouabain (**Figure 2D**).

Silencing of CAPN1 and the NCX3 Ca^{2+} uptake

CAPN1, CAPN2, and CAPN3 are the three major isoforms of calpains found in skeletal muscle. CAPN1 and CAPN2 are also ubiquitously expressed and therefore endogenously expressed in HEK293T. Due to their different thresholds of activation by Ca^{2+}, CAPN1 was more likely to be the unique isoform activated during our functional assays as its threshold is in the micromolar range and CAPN2 is activated by Ca^{2+} fluxes in the millimolar range. Incubating the cells with thapsigargin resulted in a mild rise of $[Ca^{2+}]_i$ in the micromolar range. In a similar manner, the incubation of cells expressing NCX3 with ouabain gradually raised Na^+ levels and triggered a Ca^{2+} influx that was able to activate CAPN1 (22). In order to investigate the potential role of CAPN1 on the activity of NCX3 variants, CAPN1 was silenced using siRNA specifically targeting CAPN1 in HEK293T. The expression of CAPN1 was measured by immunoblotting 72 h after transfection (**Figure 3E**). CAPN1 has an electrophoretic mobility of 80 kDa (23). The quantification revealed a significant downregulation of 50 %. As with the cells transfected with calpastatin, the direct silencing of CAPN1 had no effect on NCX3-B activity in reverse mode activated by either $[Na^+]_i$ or $[Ca^{2+}]_i$ (**Figures 3A and 3D**). Nonetheless, in the reverse mode conditions triggered by intracellular Ca^{2+}, silencing CAPN1 significantly decreased the maximum Ca^{2+} uptake of the NCX3-AC expressing cells compared to the untargeted siRNA conditions (**Figure 3B**). This effect is also observed when $[Na^+]_i$ is increased, where intracellular Ca^{2+} uptake is significantly decreased during perfusion with a Na^+-rich medium (**Figure 3D**).

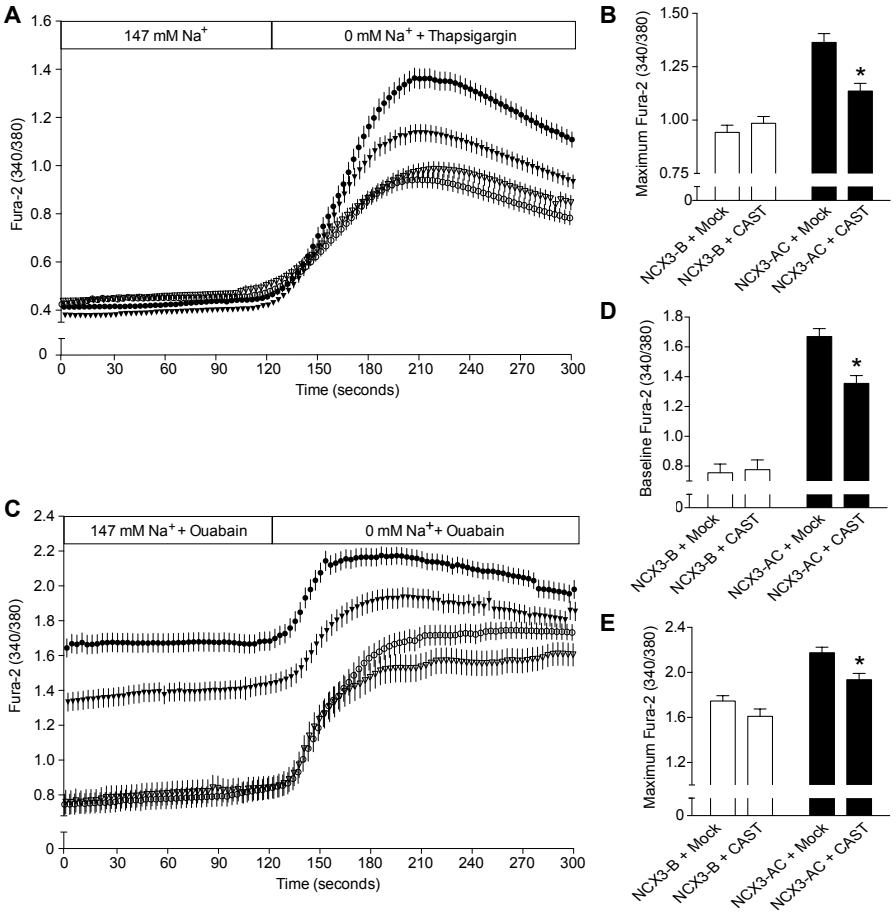

Figure 2 Influence of the calpain inhibitor calpastatin on the reverse mode of exchange of NCX3.

The reverse mode of exchange of NCX3 was measured by recording the ratio 340/380 nm in HEK293T cells loaded by Fura-2-AM. Ca^{2+} influx was measured in HEK293T cells expressing NCX3-AC (filled) and NCX3-B (open) after double transfection with an empty vector (circle) or calpastatin (triangle). Cells were perfused with a Na^+-rich medium (147 mM Na^+). **A**, At 120 s, reverse NCX mode was initiated by perfusing with a Na^+-free medium and depleting the internal Ca^{2+} stores by applying 1 µM thapsigargin. **B**, Mean values of the maximum Fura-2 ratio, shown in A, after removal of Na^+. **C**, Reverse NCX mode was recorded after rising intracellular Na^+ by a 60-min incubation with the Na^+-K^+ ATPase inhibitor ouabain and at 120 s by perfusing the cells with a Na^+-free medium. The 340/380 nm emission ratios are shown representing for each point the mean of the data, after three independent experimental sessions for a number (n) of cells (n > 71). **D**, Baseline of Fura-2 ratio after incubation with ouabain shown in C. **E**, maximum values of Fura-2 ratio after removal of extracellular Na^+, shown in C.

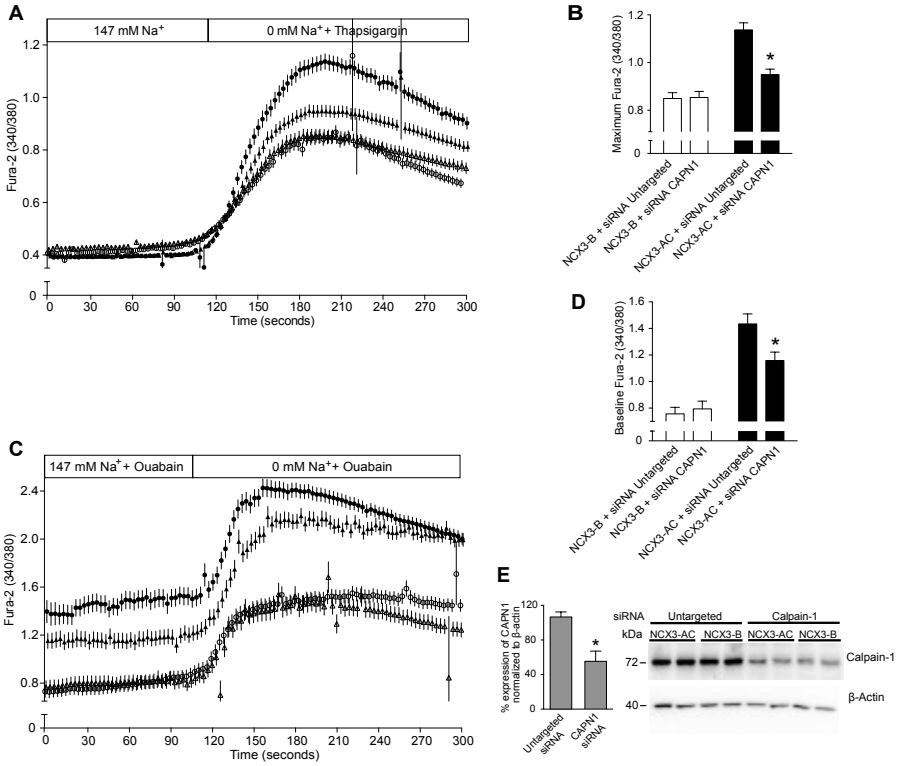

Figure 3 Ca^{2+} influx by NCX3 after silencing of CAPN1.

Ca^{2+} influx measured in HEK293T cells loaded with Fura-2-AM and exposed for 72 h to either the CAPN1 siRNA (triangle), either the untargeted siRNA (circle) and simultaneously transfected with NCX3-AC (filled) or NCX3-B (open). **A**, Ca^{2+} uptake was triggered by an increase in intracellular Ca^{2+} caused by exposure to a Na^+-free medium together with thapsigargin (1 µM) and **C**, by an increase in intracellular Na^+ obtained after 60 min incubation with ouabain (1 µM) followed by the exposure to Na^+-free medium after 120 s. The ratios are shown representing for each point the mean of the data, after three independent experimental sessions for a number (n) of cells (n > 70). **B**, Mean values of the maximum Fura-2 ratio after addition of thapsigargin (1 µM) shown in A. **D**, Mean values of the baseline of Fura-2 ratio after exposure to ouabain, the first 60 s of measurements are averaged. **E**, Representative immunoblots of the downregulation of CAPN1 expression 72 h after exposure to siRNA. β-actin is used as a loading control. Percentage of downregulation of CAPN1 was normalized on β-actin expression and data were measured on four different experiments and for both cells expressing NCX3-B and NCX3-AC.

Influence of the proteolytic activity of CAPN3 on NCX3 capacity

The third isoform of calpain, CAPN3, was not expressed in our cell model and was therefore transfected together with NCX3 variants. The overexpression resulted in an increase in the maximum intracellular Ca^{2+} levels recorded in NCX3-AC expressing cells

in both thapsigargin and ouabain conditions (**Figure 4**). Additionally, the baseline measured after ouabain incubation was significantly elevated compared to the normal conditions revealing a higher Ca^{2+} uptake in presence of extracellular Na^{+} (**Figure 4D**). In both conditions, the exchange capacity of the NCX3-B expressing cells remained unchanged.

Site-directed mutagenesis was used to introduce a C129S mutation in the CAPN3 sequence. This mutation inactivated the catalytic site of CAPN3 (24). In cells expressing C129S CAPN3, the function of NCX3-B measured in both ouabain and thapsigargin conditions was unchanged while the increase in Ca^{2+} uptake observed for NCX3-AC was abrogated (**Figures 4B, 4D and 4E**).

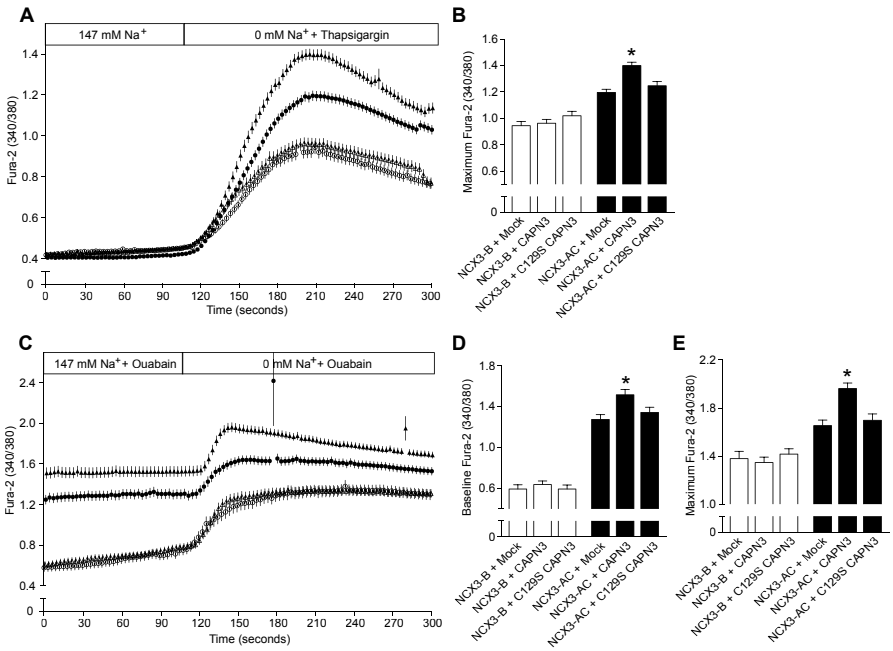

Figure 4 The reverse mode of NCX3 and the skeletal muscle-specific CAPN3.

The reverse mode of NCX3 was measured in HEK293T cells by recording the 340/380 nm ratio after loading the cells with Fura-2. Cells were transfected with NCX3-AC (filled) and NCX3-B (open) after double transfection with an empty vector (circle), CAPN3 (triangle) or C129S CAPN3, an inactive form of CAPN3. For clarity, the recordings of C129S CAPN3 have not been included in A and C. The reverse mode was triggered by the removal of extracellular Na^{+} **A**, simultaneously with a rise in intracellular Ca^{2+} by thapsigargin or **C**, after 60 min incubation with ouabain. The ratios are shown representing for each point the mean of the data, after three independent experimental sessions for a number (n) of cells (n > 47). **B and E**, Mean values of the maximum Fura-2 ratio after removal of Na^{+} and **D**, at the baseline that includes the first 60 s of measurements shown in A and C, respectively, and the C129S CAPN3.

Targeting the molecular determinants of the regulation by calpain

The data recorded in Figure 2, 3, and 4 clearly demonstrated that NCX3-AC activity is regulated by different calpains. Additionally, one of the cleavage sites for calpain predicted by the software program *Group base prediction system - calpain cleavage detector* (GPS-CCD 1.0) (18) is located in the exon C of NCX3-AC, between the Leu^{601} and Leu^{602} (**Figure 5A**). Next, exon C was removed by site-directed mutagenesis. The mutant NCX3-A had a significantly lower Ca^{2+} uptake when incubated with thapsigargin than NCX3-AC (**Figures 5B and 5C**). This decrease corresponded to the observed effect of silencing of CAPN1 and remained significantly higher than NCX3-B activity. Furthermore, expression of CAST or CAPN3 had no significant effect on the Ca^{2+} uptake recorded for NCX3-A expressing cells (**Figures 5B and 5C**), which confirms that the exon C is directly implicated in the regulation by calpain possibly by cleavage.

The positions -1 and -2 of a cleavage site are of major importance for the recognition of the site by calpain (25). Therefore, the residues Leu^{600} and Leu^{601} were mutated into Trp^{600} and Trp^{601}, residues carrying the lowest probability of occurrence in a calpain cleavage site (25), and unlikely to be recognized by the calpain. In the reverse mode activated by an increase in $[Ca^{2+}]_i$, the capacity of the LL600601WW-NCX3-AC mutant was significantly decreased compared to NCX3-AC and similar to NCX3-A (**Figures 5B and 5C**). In a similar manner, during reverse activation by an increase in $[Na^+]_i$, the highest intracellular Ca^{2+} value of LL600601WW-NCX3-AC in Na^+-free conditions is decreased compared to NCX3-AC expressing cells (**Figures 5D and 5F**). In Na^+-rich conditions the exchange capacity of LL600601WW-NCX3-AC mutant as observed by the baseline of Fura-2 during ouabain exposure was decreased compared to NCX3-AC (**Figure 5E**), but it was identical to NCX3-AC in the presence of calpastatin while remaining, significantly higher than NCX3-B. The LL600601WW-NCX3-AC activity remained unchanged in CAST and CAPN3 conditions in both thapsigargin and ouabain conditions, similarly to NCX3-A. Thereby, the mutation of the two residues abrogated the regulation of the exchanger by both CAPN1 and CAPN3.

Discussion

The present study unraveled for the first time the influence of the muscle-specific CAPN3 on the activity of NCX3. Furthermore, this study revealed the specificity of CAPN1 and CAPN3 for the variant NCX3-AC, predominant in skeletal muscle, as an increase of the reverse mode of exchange is observed solely for this variant and implicates the presence of the exon C to be responsible for the CAPN effect. First, the muscle-specific CAPN3 elevated the Ca^{2+} uptake performed by NCX3-AC in its reverse mode triggered by a rise in either $[Ca^{2+}]_i$ or $[Na^+]_i$. Such an increase was absent in NCX3-B expressing cells.

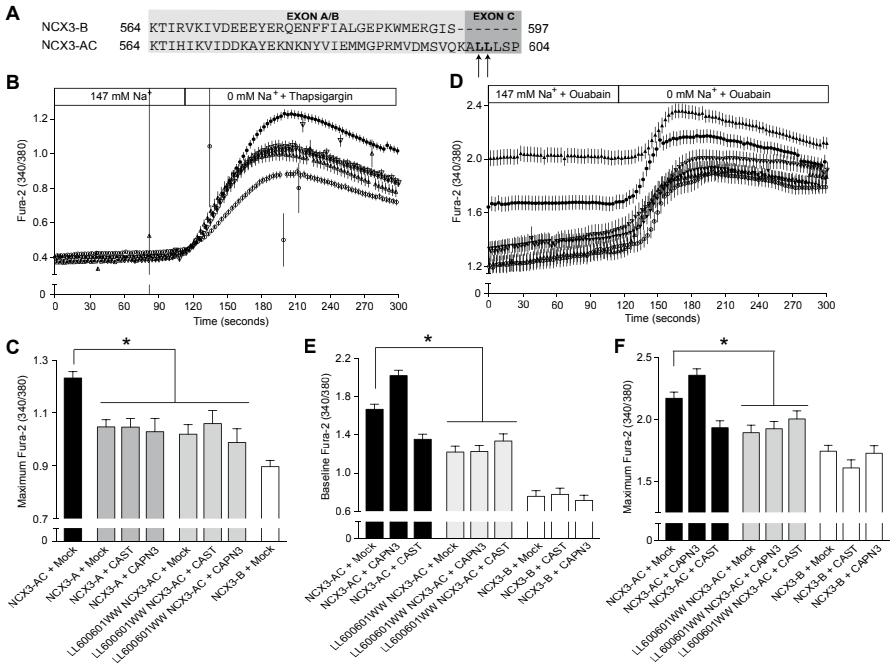

Figure 5 Targeting the calpain cleavage site of NCX3-AC

A, Alignment of amino acid sequence of the alternatively spliced exons A, B and C of the two variants NCX3-AC and NCX3-B using ClustalW software. Mutated residues are indicated by arrows and missing residues by dashes. The predicted calpain cleavage site is located after the second arrow. **B-F**, 340/380 nm ratios recorded in HEK293T cells transfected loaded with Fura-2-AM during the reverse mode of NCX3 after removal of extracellular Na^+, B and D together with the exposure to thapsigargin (1 µM) and D to F, after 60 min exposure to ouabain (1 µM). **B**, Fura-2 ratio of cells expressing NCX3-AC (black), NCX3-A (grey) and NCX3-B (white) together with an empty vector (circle), calpastatin (down-pointing triangle), CAPN3 (up-pointing triangle). For clarity, the recordings of the mutant LL600601WW NCX3-AC are not shown. **C**, Mean values of the maximum Fura-2 ratio after removal of Na^+ in all recorded conditions. **D**, The Ca^{2+} influx has been measured by recording the 340/380 nm ratio in cells loaded with Fura-2 ratio and expressing NCX3-AC (black) or LL600601WW NCX3-AC (grey) together with an empty vector (circle), calpastatin (down-pointing triangle), CAPN3 (up-pointing triangle). For clarity, the recordings of NCX3-B variant have not been included. **E and F**, Mean values of the baseline and maximum Fura-2 ratio, respectively. The baseline represents the mean values for the first 60 s of the measurements. All ratios represent for each point the mean of the data, after three independent experimental sessions for a number (n) of cells (n > 54).

The involvement of CAPN3 catalytic activity was further demonstrated by the lack of effect with the inactive form of CAPN3, the C129S mutant. Secondly, the inhibition by calpastatin of multiple proteases such as CAPN1 and CAPN2 decreased Ca^{2+} uptake by

NCX3-AC, an effect unique to this variant. The silencing of CAPN1 confirmed this effect, thereby suggesting that CAPN2 and additional intracellular proteases inhibited by calpastatin have no influence on NCX3 activity (26). Together, these results help to unravel the roles of CAPN1 and CAPN3 in increasing the reverse mode capacity of NCX3.

In the present experiments, the NCX3 activity was triggered by a Na^+ removal in the extracellular medium, which lead to a strong intracellular Ca^{2+} entry. Such entry provokes CAPN1 autolysis as this process can be rapidly achieved following a strong Ca^{2+} rise, although in diverse cell types CAPN1 can also be found in its autolyzed form at resting state (27,28). In this regard, previous study from our group has shown that Ca^{2+} levels in HEK293T cells expressing NCX3-AC and NCX3-B were unchanged in both cytoplasm and ER at resting state(15). Therefore, CAPN1 activation in this study is expected to be similar in all conditions.

Additionally, this study identified the molecular determinants of the calpain sensitivity. Among the predicted sites for calpain cleavage, a variant-specific site was predicted in exon C, and the activity of NCX3-A, a mutant missing the exon C, was measured. NCX3-A had an activity similar to the one recorded under CAPN1 inhibition by either calpastatin or siRNA, thereby demonstrating the loss of the calpain sensitivity. The two key residues of the hypothesized calpain cleavage site, Leu^{600} and Leu^{601}, were mutated into Trp^{600} and Trp^{601}, respectively. These mutations diminished the Ca^{2+} uptake performed in the reverse mode of exchange by NCX3-AC. The similarity to NCX3-A activity confirmed the implication of the two residues Leu^{601} and Leu^{602} in the regulation of NCX3-AC by calpain, which possibly occurs by cleavage. However, the decreased activity of NCX3-AC in the absence of calpain can not fully explain the differences observed between the variant NCX3-AC and NCX3-B, as the mutations of Leu^{600} and Leu^{601} are not sufficient to obtain the properties of NCX3-B. The difference between the two variants has been previously attributed to the mutually exclusive exons A and B and their influence on the Ca^{2+}-binding domain 2 (CBD2) of the intracellular loop of NCX3. However, the exon C, responsible for the sensitivity to calpain, most likely contributes as well to the functional differences between the two variants. This additional effect of exon C could explain the inability of any of the mutations targeting the CBD2 in exon B of NCX3-B to fully reproduce NCX3-AC activity in the reverse mode activated by intracellular Na^+ (15).

Calpain recognizes its cleavage site by the primary sequence as well as the tertiary structure, which complicates the identification of a consensus sequence for the calpain cleavage site. Tompa *et al*. attempted to pinpoint the residues necessary for cleavage in 11 amino acids (25). The exon C, where a calpain cleavage site is predicted at Leu^{602}, carries only six residues –ALLLSP- that have a high occurrence in calpain cleavage sites (25). Here, the investigation of the potential cleavage of NCX3-AC at Leu^{602} and detection of its generated fragments would be needed to confirm whether or not the exon C is carrying a cleavage site for calpain. Furthermore, the neighboring sequence at the end of exon A and at the beginning of exon 5 is of importance as well for the recognition by

calpain. The point mutation of each residue of this region would provide further information on which residues are necessary for the recognition by calpain.

Interestingly, the three Leucine residues located next to the predicted cleavage site are conserved within the NCX family. NCX2, expressed in the brain also expresses the exon C of sequence –ALLLNQ-. In NCX1, the exon C of sequence –ALLLNEL- (17) is alternatively spliced. The splice variants of NCX1 carrying the exon C are detected in excitable tissues (17,29,30). Additionally, the cleavage of NCX by the calpain family has only been reported in excitable tissues (12,31,32). Therefore, the implication of the exon C in the regulation of both NCX1 and NCX2 and its potential cleavage by calpain at position Leu^{602} warrants further exploration.

The cleavage of NCX3 by CAPN1, leading to a hyperactive exchanger has been reported previously (13). The description by Bano *et al*. of the cleavage sites in neurons did not describe a site located on the exon C (12). Furthermore, NCX3-B is predominant in neuronal tissues, but in our experiments, NCX3-B was unaffected by CAPN1. This could be explained by the different cellular model used and conditions of experiments that would lead to diverse status of the cells. It has been found that several types of post-translational regulation, such as calmodulin binding (33,34), phosphorylation (35,36), and phosphoinositide binding (37), can be involved in protecting the cleavage site of the target protein or favor a specific site of cleavage. From these different studies, some common mechanisms arise. First, the intracellular loop of NCX3 is of significant importance for NCX3 regulation. Secondly, in NCX3 as well as in diverse Ca^{2+} channels (38,39) and transporters (40,41), the proteolytic activity of the calpain family goes beyond its role in protein degradation and provides an additional Ca^{2+}-dependent regulatory mechanism in order to adjust the Ca^{2+} fluxes of the cells.

In this study, we have shown that CAPN1, CAPN2, and the muscle-specific CAPN3 are expressed in skeletal muscle. Unlike CAPN2, CAPN1 and CAPN3 can be activated under physiological conditions in myofibers. CAPN1, freely present in the sarcoplasm, is autolyzed and activated during the prolonged elevation of $[Ca^{2+}]_i$ to micromolar levels such as that following eccentric exercise. In these conditions, a disruption of the excitation-contraction (EC) coupling can occur, caused by the decrease in Ca^{2+} release from the SR that could lead to post-exercise fatigue and contribute to the muscle weakness observed in several muscular pathologies (42). In the myocardium, the CAPN1 activation observed during an ischemic event affects the SR Ca^{2+} content and release capacity leading to a cardiac contractile dysfunction (43). Therefore, the increased activity of NCX3-AC caused by CAPN1 could either constitute a protective attempt to refill the intracellular Ca^{2+} stores in skeletal muscle and to delay the E-C uncoupling or to compete with the Ca^{2+} re-uptake into the SR by an enhanced Ca^{2+} extrusion. The low rate of $[Ca^{2+}]_i$ increase during these specific uncoupling events greatly favors the activation of the reverse mode. Furthermore, the capacity of NCX to refill the SR Ca^{2+} levels has been observed in several excitable tissues such as cardiomyocytes (44), slow-twitch fibers (16),

and smooth muscle cells (45,46). Additionally, both an elevated CAPN1 activity (47) and an increased capacity of exchange by NCX (48) were observed in the *mdx* model of Duchenne muscular dystrophy, where higher sarcoplasmic Ca^{2+} levels were found. Finally, the cleavage of NCX3 by calpain in neurons provoked a significant increase in ER Ca^{2+} content and delayed the caspase activation during neuronal excitotoxicity (13).

Regarding CAPN3 in the myofiber, the protease is tightly bound at the myofibril and at the triad, a privileged region for Ca^{2+} fluxes responsible for the EC coupling. The conditions necessary for CAPN3 activation are not yet fully understood. Its activation seems to occur from 24 to 48 hours following eccentric exercise (49), a phase of intense sarcomeric remodeling where the SR Ca^{2+} content slowly rises again until it reaches normal levels 48 h after exercise (50). The increase in NCX3 activity following CAPN3 cleavage could, therefore, be involved in the persistent increase in the Ca^{2+} content of the SR during the days following eccentric exercise. This hypothesis is consistent with the Ca^{2+} disturbances (10,51), such as a low Ca^{2+} release from the SR, observed in the CAPN3 knock-out (KO) fibers mimicking the LGMD2A condition. Additionally, while several potential substrates of CAPN3 appear to be affected by the protease through non-proteolytic action (52), the proteolytically inactive CAPN3 (C129S CAPN3) was not shown to have any effect on NCX3-AC activity, further demonstrating that CAPN3 modulates NCX3-AC through cleavage. It has to be noted that in our study the CAPN3 is expressed in high levels and freely present in the cytoplasm of the HEK cells, therefore more prone to activation at lower $[Ca^{2+}]_i$. This might well explain the activation of CAPN3 in our experiments despite the specific requirements for its activation, described by others, in terms of $[Ca^{2+}]_i$ and exercise. Our study has been performed in HEK cells, as a well-used cell model for the investigation of the capacity of exchange and the ionic regulations of the NCX family (53,54). The study of the regulation of NCX3 by calpain in the dense cellular organization of the myofiber would be essential in order to conclude on the role of NCX3 in the Ca^{2+} disturbances of LGMD2A.

In conclusion, a novel target sensitive to the muscle-specific CAPN3 was identified. This sensitivity was found to be restricted to the skeletal muscle variant NCX3-AC. The site located in the exon C was identified as implicated in the regulation of the exchanger by CAPN1 and CAPN3, possibly by a direct cleavage and might be involved with other Ca^{2+} transporters in the Ca^{2+} refilling of the SR, subsequent to the EC uncoupling. The loss of regulation of NCX3 by CAPN3 could therefore be implicated in diverse muscular pathologies such as the LGMD2A.

Acknowledgments

This research was supported by an equipment grant of NWO (Netherlands Organization for Scientific Research, No: 911-02-008) and the CSBR (Centre for Systems Biology Research) initiative from the Netherlands Organization for Scientific Research (NWO; No: CSBR09/013V).

Author contribution

All three authors conceived the study. LYM designed, performed and analyzed all the experiments and wrote the manuscript. JGH and RJB revised critically the manuscript. All authors reviewed the results and approved the final version of the manuscript.

References

1. **Hata, S., Abe, M., Suzuki, H., Kitamura, F., Toyama-Sorimachi, N., Abe, K., Sakimura, K., and Sorimachi, H.** Calpain 8/nCL-2 and calpain 9/nCL-4 constitute an active protease complex, G-calpain, involved in gastric mucosal defense. *PLoS genetics* 6, e1001040 (2010)

2. **Sorimachi, H., Hata, S., and Ono, Y.** Impact of genetic insights into calpain biology. *Journal of biochemistry* 150, 23-37 (2011)

3. **McDermott, J. R., Mantle, D., Biggins, J. A., Kidd, A. M., Davison, K., Lauffart, B., and Pennington, R. J.** Specificity of neuropeptide degradation by two calcium-activated neutral proteases from human skeletal muscle. *Life sciences* 37, 725-730 (1985)

4. **Branca, D., Gugliucci, A., Bano, D., Brini, M., and Carafoli, E.** Expression, partial purification and functional properties of themuscle-specific calpain isoform p94. *European journal of biochemistry / FEBS* 265, 839-846 (1999)

5. **Murphy, R. M., Verburg, E., and Lamb, G. D.** Ca2+ activation of diffusible and bound pools of mu-calpain in rat skeletal muscle. *The Journal of physiology* 576, 595-612 (2006)

6. **Murphy, R. M., and Lamb, G. D.** Calpain-3 is activated following eccentric exercise. *Journal of applied physiology* 106, 2068; author reply 2069 (2009)

7. **Richard, I., Broux, O., Allamand, V., Fougerousse, F., Chiannilkulchai, N., Bourg, N., Brenguier, L., Devaud, C., Pasturaud, P., Roudaut, C., and et al.** Mutations in the proteolytic enzyme calpain 3 cause limb-girdle muscular dystrophy type 2A. *Cell* 81, 27-40 (1995)

8. **Richard, I., Roudaut, C., Saenz, A., Pogue, R., Grimbergen, J. E., Anderson, L. V., Beley, C., Cobo, A. M., de Diego, C., Eymard, B., Gallano, P., Ginjaar, H. B., Lasa, A., Pollitt, C., Topaloglu, H., Urtizberea, J. A., de Visser, M., van der Kooi, A., Bushby, K., Bakker, E., Lopez de Munain, A., Fardeau, M., and Beckmann, J. S.** Calpainopathy-a survey of mutations and polymorphisms. *American journal of human genetics* 64, 1524-1540 (1999)

9. **Keira, Y., Noguchi, S., Minami, N., Hayashi, Y. K., and Nishino, I.** Localization of calpain 3 in human skeletal muscle and its alteration in limb-girdle muscular dystrophy 2A muscle. *Journal of biochemistry* 133, 659-664 (2003)

10. **Kramerova, I., Kudryashova, E., Wu, B., Ottenheijm, C., Granzier, H., and Spencer, M. J.** Novel role of calpain-3 in the triad-associated protein complex regulating calcium release in skeletal muscle. *Human molecular genetics* 17, 3271-3280 (2008)

11. **Al-Qusairi, L., and Laporte, J.** T-tubule biogenesis and triad formation in skeletal muscle and implication in human diseases. *Skeletal muscle* 1, 26 (2011)

12. **Bano, D., Young, K. W., Guerin, C. J., Lefeuvre, R., Rothwell, N. J., Naldini, L., Rizzuto, R., Carafoli, E., and Nicotera, P.** Cleavage of the plasma membrane Na+/Ca2+ exchanger in excitotoxicity. *Cell* 120, 275-285 (2005)

13. **Pannaccione, A., Secondo, A., Molinaro, P., D'Avanzo, C., Cantile, M., Esposito, A., Boscia, F., Scorziello, A., Sirabella, R., Sokolow, S., Herchuelz, A., Di Renzo, G., and Annunziato, L.** A new concept: Abeta1-42 generates a hyperfunctional proteolytic NCX3 fragment that delays caspase-12 activation and neuronal death. *The Journal of neuroscience : the official journal of the Society for Neuroscience* 32, 10609-10617 (2012)

14. **Sacchetto, R., Margreth, A., Pelosi, M., and Carafoli, E.** Colocalization of the dihydropyridine receptor, the plasma-membrane calcium ATPase isoform 1 and the sodium/calcium exchanger to the junctional-membrane domain of transverse tubules of rabbit skeletal muscle. *European journal of biochemistry / FEBS* 237, 483-488 (1996)

15. **Michel, L. Y., Verkaart, S., Koopman, W. J., Willems, P. H., Hoenderop, J. G., and Bindels, R. J.** Function and regulation of the Na+-Ca2+ exchanger NCX3 splice variants in brain and skeletal muscle. *The Journal of biological chemistry* 289, 11293-11303 (2014)

16. **Germinario, E., Esposito, A., Midrio, M., Peron, S., Palade, P. T., Betto, R., and Danieli-Betto, D.** High-frequency fatigue of skeletal muscle: role of extracellular Ca(2+). *European journal of applied physiology* 104, 445-453 (2008)

17. **Quednau, B. D., Nicoll, D. A., and Philipson, K. D.** Tissue specificity and alternative splicing of the Na+/Ca2+ exchanger isoforms NCX1, NCX2, and NCX3 in rat. *The American journal of physiology* 272, C1250-1261 (1997)

18. **Liu, Z., Cao, J., Gao, X., Ma, Q., Ren, J., and Xue, Y.** GPS-CCD: a novel computational program for the prediction of calpain cleavage sites. *PloS one* 6, e19001 (2011)

19. **Hoenderop, J. G., Hartog, A., Stuiver, M., Doucet, A., Willems, P. H., and Bindels, R. J.** Localization of the epithelial Ca(2+) channel in rabbit kidney and intestine. *Journal of the American Society of Nephrology : JASN* 11, 1171-1178 (2000)

20. **Whelan, J. A., Russell, N. B., and Whelan, M. A.** A method for the absolute quantification of cDNA using real-time PCR. *J Immunol Methods* 278, 261-269 (2003)

21. **Secondo, A., Staiano, R. I., Scorziello, A., Sirabella, R., Boscia, F., Adornetto, A., Valsecchi, V., Molinaro, P., Canzoniero, L. M., Di Renzo, G., and Annunziato, L.** BHK cells transfected with NCX3 are more resistant to hypoxia followed by reoxygenation than those transfected with NCX1 and NCX2: Possible relationship with mitochondrial membrane potential. *Cell Calcium* 42, 521-535 (2007)

22. **Harwood, S. M., Allen, D. A., Chesser, A. M., New, D. I., Raftery, M. J., and Yaqoob, M. M.** Calpain is activated in experimental uremia: is calpain a mediator of uremia-induced myocardial injury? *Kidney international* 63, 866-877 (2003)

23. **Yoshimura, N., Kikuchi, T., Sasaki, T., Kitahara, A., Hatanaka, M., and Murachi, T.** Two distinct Ca2+ proteases (calpain I and calpain II) purified concurrently by the same method from rat kidney. *The Journal of biological chemistry* 258, 8883-8889 (1983)

24. **Herasse, M., Ono, Y., Fougerousse, F., Kimura, E., Stockholm, D., Beley, C., Montarras, D., Pinset, C., Sorimachi, H., Suzuki, K., Beckmann, J. S., and Richard, I.** Expression and functional characteristics of calpain 3 isoforms generated through tissue-specific transcriptional and posttranscriptional events. *Molecular and cellular biology* 19, 4047-4055 (1999)

25. **Tompa, P., Buzder-Lantos, P., Tantos, A., Farkas, A., Szilagyi, A., Banoczi, Z., Hudecz, F., and Friedrich, P.** On the sequential determinants of calpain cleavage. *The Journal of biological chemistry* 279, 20775-20785 (2004)

26. **Ali, M. A., Stepanko, A., Fan, X., Holt, A., and Schulz, R.** Calpain inhibitors exhibit matrix metalloproteinase-2 inhibitory activity. *Biochemical and biophysical research communications* 423, 1-5 (2012)

27. **Noma, H., Kato, T., Fujita, H., Kitagawa, M., Yamano, T., and Kitagawa, S.** Calpain inhibition induces activation of the distinct signalling pathways and cell migration in human monocytes. *Immunology* 128, e487-496 (2009)

28. **Campbell, J. S., and Hallett, M. B.** Active calpain in phagocytically competent human neutrophils: electroinjection of fluorogenic calpain substrate. *Biochemical and biophysical research communications* 457, 341-346 (2015)

29. **Long, Y., Wang, W. P., Yuan, H., Ma, S. P., Feng, N., Wang, L., and Wang, X. L.** Functional comparison of the reverse mode of Na+/Ca2+ exchangers NCX1.1 and NCX1.5 expressed in CHO cells. *Acta pharmacologica Sinica* 34, 691-698 (2013)

30. **Kuroda, H., Sobhan, U., Sato, M., Tsumura, M., Ichinohe, T., Tazaki, M., and Shibukawa, Y.** Sodium-calcium exchangers in rat trigeminal ganglion neurons. *Molecular pain* 9, 22 (2013)

31. **Atherton, J., Kurbatskaya, K., Bondulich, M., Croft, C. L., Garwood, C. J., Chhabra, R., Wray, S., Jeromin, A., Hanger, D. P., and Noble, W.** Calpain cleavage and inactivation of the sodium calcium exchanger-3 occur downstream of Abeta in Alzheimer's disease. *Aging cell* 13, 49-59 (2014)

32. **Wanichawan, P., Hafver, T. L., Hodne, K., Aronsen, J. M., Lunde, I. G., Dalhus, B., Lunde, M., Kvaloy, H., Louch, W. E., Tonnessen, T., Sjaastad, I., Sejersted, O. M., and Carlson, C. R.** Molecular basis of calpain cleavage and inactivation of the sodium-calcium exchanger 1 in heart failure. *The Journal of biological chemistry* 289, 33984-33998 (2014)

33. **Iwamoto, N., Lu, R., Tanaka, N., Abe-Dohmae, S., and Yokoyama, S.** Calmodulin interacts with ATP binding cassette transporter A1 to protect from calpain-mediated degradation and upregulates high-density lipoprotein generation. *Arteriosclerosis, thrombosis, and vascular biology* 30, 1446-1452 (2010)

34. **Sivanandam, A., Murthy, S., Chinnakannu, K., Bai, V. U., Kim, S. H., Barrack, E. R., Menon, M., and Reddy, G. P.** Calmodulin protects androgen receptor from calpain-mediated breakdown in prostate cancer cells. *Journal of cellular physiology* 226, 1889-1896 (2011)

35. **Nicolas, G., Fournier, C. M., Galand, C., Malbert-Colas, L., Bournier, O., Kroviarski, Y., Bourgeois, M., Camonis, J. H., Dhermy, D., Grandchamp, B., and Lecomte, M. C.** Tyrosine phosphorylation regulates alpha II spectrin cleavage by calpain. *Molecular and cellular biology* 22, 3527-3536 (2002)

36. **Zhang, S., Kim, T. S., Dong, Y., Kanazawa, S., Kawaguchi, M., Gao, N., Minato, H., Takegami, T., Nojima, T., Asai, K., and Miura, Y.** AT motif binding factor 1 (ATBF1) is highly phosphorylated in embryonic brain and protected from cleavage by calpain-1. *Biochemical and biophysical research communications* 427, 537-541 (2012)

37. **Sprague, C. R., Fraley, T. S., Jang, H. S., Lal, S., and Greenwood, J. A.** Phosphoinositide binding to the substrate regulates susceptibility to proteolysis by calpain. *The Journal of biological chemistry* 283, 9217-9223 (2008)

38. **Sandoval, A., Oviedo, N., Tadmouri, A., Avila, T., De Waard, M., and Felix, R.** Two PEST-like motifs regulate Ca2+/calpain-mediated cleavage of the CaVbeta3 subunit and provide important determinants for neuronal Ca2+ channel activity. *The European journal of neuroscience* 23, 2311-2320 (2006)

39. **Kaczmarek, J. S., Riccio, A., and Clapham, D. E.** Calpain cleaves and activates the TRPC5 channel to participate in semaphorin 3A-induced neuronal growth cone collapse. *Proceedings of the National Academy of Sciences of the United States of America* 109, 7888-7892 (2012)

40. **James, P., Vorherr, T., Krebs, J., Morelli, A., Castello, G., McCormick, D. J., Penniston, J. T., De Flora, A., and Carafoli, E.** Modulation of erythrocyte Ca2+-ATPase by selective calpain cleavage of the calmodulin-binding domain. *The Journal of biological chemistry* 264, 8289-8296 (1989)

41. **Shoshan-Barmatz, V., Weil, S., Meyer, H., Varsanyi, M., and Heilmeyer, L. M.** Endogenous, Ca(2+)-dependent cysteine-protease cleaves specifically the ryanodine receptor/Ca2+ release channel in skeletal muscle. *The Journal of membrane biology* 142, 281-288 (1994)

42. **Lamb, G. D.** Mechanisms of excitation-contraction uncoupling relevant to activity-induced muscle fatigue. *Applied physiology, nutrition, and metabolism = Physiologie appliquee, nutrition et metabolisme* 34, 368-372 (2009)

43. **Singh, R. B., Chohan, P. K., Dhalla, N. S., and Netticadan, T.** The sarcoplasmic reticulum proteins are targets for calpain action in the ischemic-reperfused heart. *Journal of molecular and cellular cardiology* 37, 101-110 (2004)

44. **Hove-Madsen, L., and Tort, L.** Characterization of the relationship between Na+ -Ca2+ exchange rate and cytosolic calcium in trout cardiac myocytes. *Pflugers Archiv : European journal of physiology* 441, 701-708 (2001)

45. **Lemos, V. S., Poburko, D., Liao, C. H., Cole, W. C., and van Breemen, C.** Na+ entry via TRPC6 causes Ca2+ entry via NCX reversal in ATP stimulated smooth muscle cells. *Biochemical and biophysical research communications* 352, 130-134 (2007)

46. **Davis, K. A., Samson, S. E., Hammel, K. E., Kiss, L., Fulop, F., and Grover, A. K.** Functional linkage of Na+-Ca2+-exchanger to sarco/endoplasmic reticulum Ca2+ pump in coronary artery: comparison of smooth muscle and endothelial cells. *Journal of cellular and molecular medicine* 13, 1775-1783 (2009)

47. **Zhao, X., Moloughney, J. G., Zhang, S., Komazaki, S., and Weisleder, N.** Orai1 mediates exacerbated Ca(2+) entry in dystrophic skeletal muscle. *PloS one* 7, e49862 (2012)

48. **Deval, E., Levitsky, D. O., Marchand, E., Cantereau, A., Raymond, G., and Cognard, C.** Na(+)/Ca(2+) exchange in human myotubes: intracellular calcium rises in response to external sodium depletion are enhanced in DMD. *Neuromuscular disorders : NMD* 12, 665-673 (2002)

49. **Murphy, R. M., Goodman, C. A., McKenna, M. J., Bennie, J., Leikis, M., and Lamb, G. D.** Calpain-3 is autolyzed and hence activated in human skeletal muscle 24 h following a single bout of eccentric exercise. *Journal of applied physiology* 103, 926-931 (2007)

50. **Chen, W., Ruell, P. A., Ghoddusi, M., Kee, A., Hardeman, E. C., Hoffman, K. M., and Thompson, M. W.** Ultrastructural changes and sarcoplasmic reticulum Ca2+ regulation in red vastus muscle following eccentric exercise in the rat. *Experimental physiology* 92, 437-447 (2007)

51. **Dayanithi, G., Richard, I., Viero, C., Mazuc, E., Mallie, S., Valmier, J., Bourg, N., Herasse, M., Marty, I., Lefranc, G., Mangeat, P., and Baghdiguian, S.** Alteration of sarcoplasmic reticulum ca release in skeletal muscle from calpain 3-deficient mice. *International journal of cell biology* 2009, 340346 (2009)

52. **Ojima, K., Ono, Y., Ottenheijm, C., Hata, S., Suzuki, H., Granzier, H., and Sorimachi, H.** Non-proteolytic functions of calpain-3 in sarcoplasmic reticulum in skeletal muscles. *Journal of molecular biology* 407, 439-449 (2011)

53. **Hurtado, C., Prociuk, M., Maddaford, T. G., Dibrov, E., Mesaeli, N., Hryshko, L. V., and Pierce, G. N.** Cells expressing unique Na+/Ca2+ exchange (NCX1) splice variants exhibit different susceptibilities to Ca2+ overload. *American journal of physiology. Heart and circulatory physiology* 290, H2155-2162 (2006)

54. **John, S. A., Ribalet, B., Weiss, J. N., Philipson, K. D., and Ottolia, M.** Ca2+-dependent structural rearrangements within Na+-Ca2+ exchanger dimers. *Proceedings of the National Academy of Sciences of the United States of America* 108, 1699-1704 (2011)

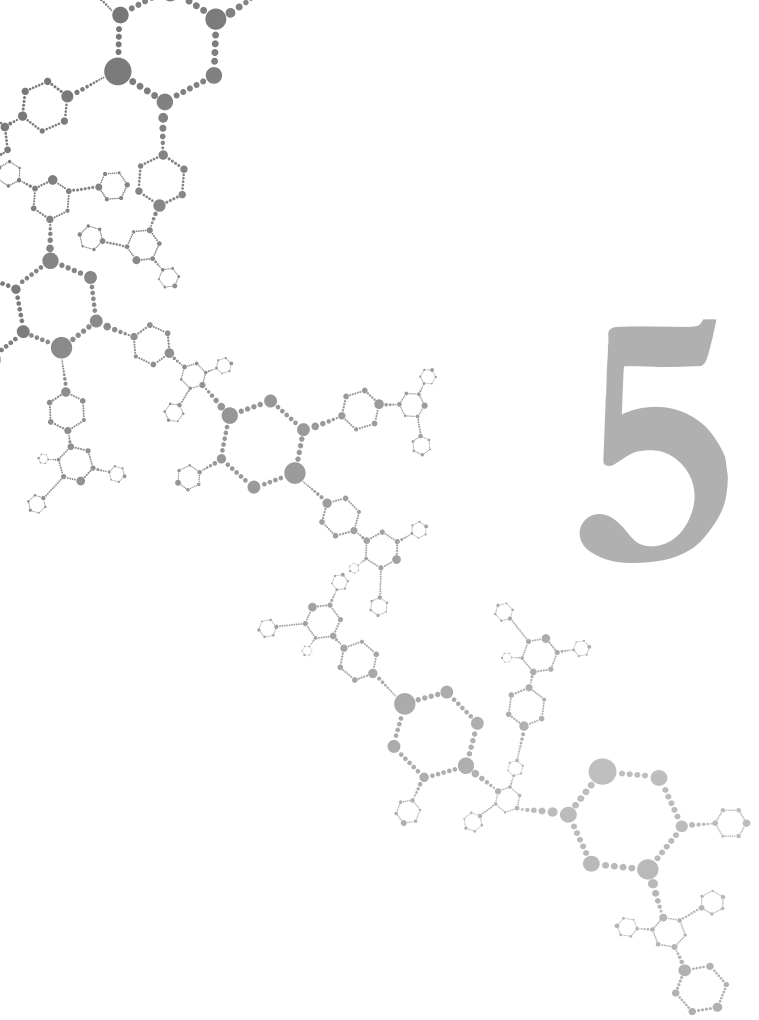

5

Brain region-specific NCX1 and NCX3 expression in mice models of neuronal excitotoxicity

Lauriane Y.M. Michel[1,2], Elias K. Michaelis[3], Ranu Pal[3], Dongwei Hui[3], Amanda J. Kiliaan[4], Joost G.J. Hoenderop[1], René J.M. Bindels[1,2]

[1] Department of Physiology, Radboud University Medical Center, The Netherlands

[2] Centre for System Biology and Bioenergetics, Radboud University Medical Center, The Netherlands

[3] Department of Pharmacology and Toxicology and the Higuchi Biosciences Center, University of Kansas, Lawrence, KS, USA

[4] Department of Anatomy, Donders Institute for Brain, Cognition and Behaviour, Radboud University Medical Center, The Netherlands

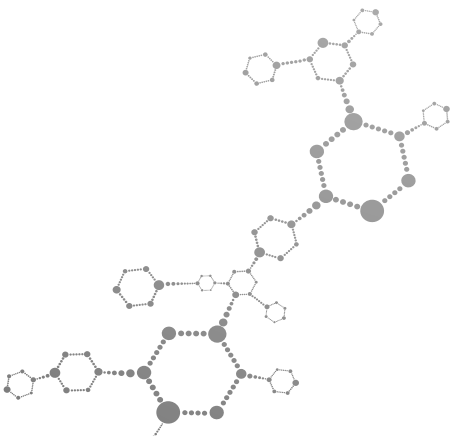

Submitted for publication

Abstract

The NCX family of Na^+-Ca^{2+} exchangers significantly contributes to maintenance of Ca^{2+} homeostasis throughout the body. In addition to their role in neuronal differentiation, long-term potentiation and memory, NCX1 and NCX3, are crucially involved in neuroprotection during excitotoxicity and neuronal injury. Importantly, brain region-specific expression of these isoforms remains unknown. Furthermore, the influence of excitotoxicity on NCX expression has never been examined. Here, we report that in hippocampus, prefrontal and parietal cortex the NCX1 transcript is more abundantly expressed than the NCX3 transcript in two mice strains, while both exchangers are equally expressed in striatum, cerebellum and brain stem. Next, we quantified, for the first time, the brain-specific expression of NCX3 splice variants and observed that in all regions NCX3-B expression was higher than that of NCX3-BC, while NCX3-AC transcripts were barely detectable. NCX3-BC is held responsible for the neuroprotective action of NCX3. Therefore, regions, such as brain stem, expressing most of this variant, might be less prone to neuronal death during excitotoxicity. Finally, NCX expression was quantified in brain regions of Glud1 and $A\beta PP_{swe}/PS1_{dE9}$ transgenic mice, facing hyper-glutamatergic and excitotoxic conditions due to respectively glutamate over-stimulation and Alzheimer's pathology. None of the two models showed significant alterations in NCX1 and NCX3 transcript expression compared to WT, while significant changes were reported following ischemic preconditioning. Furthermore, expression levels of NCX3 splice variants remained likewise unaffected. Together these findings suggest that neurons may differentially respond to distinct types of stress and injuries.

Keywords: Sodium-calcium exchange, alternative splicing, Ca^{2+} transport, absolute quantification, neuronal stress, excitotoxicity, Alzheimer's disease

Introduction

One of the primary and most common cell responses to stress conditions such as hypoxia (1), anoxia (2), or toxic exposure (3,4) originates from the ability of the cell to trigger a strong Ca^{2+} influx. This mechanism is found in many tissues including liver (4), muscle (5), cardiac tissues (6), or neurons (7). Ca^{2+} overload can lead to cellular damage by activation of many enzymes involved in protein and DNA/RNA breakdown (8,9). Furthermore Ca^{2+} influx, by increasing ROS production (10), is extremely toxic for the cell and an overload of mitochondria with Ca^{2+} might trigger cell death (11). In neurons, the initial Ca^{2+} transient occurring upon excitotoxic conditions is followed by a secondary gradual rise in intracellular Ca^{2+} levels (12). The primary rise of intraneural Ca^{2+} has been attributed to several mechanisms including activation of nicotinic, NMDA and AMPA receptors (13-15). However the exact mechanisms underlying the secondary rise in intracellular Ca^{2+} content and its role in cellular stress responses are not fully understood.

The family of Na^{+}-Ca^{2+} exchangers, NCX, is found in all cell types and members of this family are highly expressed in the brain (16). NCX is implicated in the Ca^{2+} fluxes across the plasma membrane and its exchange capacity is activated by anoxic and hypoxic conditions (17-19). Therefore, NCX was originally hypothesized to be responsible for the secondary Ca^{2+} influx following exposure to stress. However, previous studies revealed that the first and the third isoforms, NCX1 and NCX3, showed a neuroprotective capacity during ischemia (20,21) and are involved in preconditioning phenomena (22).

In excitotoxic conditions, the exposure of neurons to high concentrations of glutamate or to amyloid peptide, as seen in Alzheimer's disease, leads to a rise in intracellular Ca^{2+} levels. In such pathological conditions, NCX is also found to play a neuroprotective role, in particular NCX3. Originally thought to exert its action via efflux of Ca^{2+}, a recent study on the third isoform of the NCX family, NCX3, has revealed that the exchanger achieves neuroprotection by maintaining the ER Ca^{2+} levels via a Ca^{2+} uptake in its reverse mode of exchange, thus leading to a delay in caspase activation and prevention of neuronal cell death (23). The neuroprotective capacity is further augmented by the cleavage of NCX3 by the calpain proteases (23,24).

Although NCX expression in hypoxia and anoxia has been extensively studied, little is known about changes in the expression of NCX3 under excitotoxic conditions in different regions of the brain. In particular, it remains unclear whether NCX expression is upregulated during excitotoxicity, as it is the case following ischemic preconditioning and postconditioning (25,26). Furthermore, we recently showed that specific variants of NCX3 can be cleaved by calpain (24). Therefore, the investigation of the expression of NCX3 variants and their distribution in the brain is of great interest to fully understand the extent to which NCX3 can be neuroprotective in each brain region. Additionally, despite the multiple studies dedicated to NCX in the brain, a quantitative description of the regional distribution of NCX1 and NCX3 in the healthy brain is missing and would be

important in attempting to comprehend the physiological roles of NCX isoforms in each region of the brain, and their action during stress.

In this study, we performed a comparative investigation of the expression of NCX isoforms in several brain regions in healthy and excitotoxic situations. We first characterized and compared the expression of NCX in healthy WT animals from two mouse strains. By means of absolute quantification, the expression of the different isoforms NCX1 and NCX3 was compared in six regions of the brain. Next, by using two mouse models, Glud1 and $A\beta PP_{swe}/PS1_{dE9}$ (AβPP/PS1) transgenic mice, we measured the variation in the expression of NCX isoforms in murine brains that were under stress conditions. These mouse models allowed us to compare NCX expression in brain regions under conditions of a moderate increase in synaptic concentration of glutamate measured in Glud1 mice (27) with that under strong excitotoxic conditions as seen in the AβPP/PS1 mice (28), and thus characterize the effect of hyper-excitation and excitotoxicity on NCX expression levels in the brain. Finally, by using primers specifically designed to detect single variants of NCX3, the mRNA levels of NCX3 splice variants in the brain were quantified in Wild-type (WT), Glud1, and AβPP/PS1 mice with specific attention paid to the exon C-containing variants, suggested to be implicated in neuroprotection.

Materials and Methods

Animal model

Glud1 transgenic mice were generated by the introduction of the glutamate dehydrogenase 1 *Glud1* gene under the control of the neuron-specific enolase promoter in C57BL6/SJL mice. The Glud1 mice have been crossbred with C57BL/6 mice for over 40 generations. Overexpression of glutamate dehydrogenase in these mice results in excessive release of glutamate at synapses of central nervous system (CNS) neurons (27). Six Glud1 transgenic (Tg Glud1) male mice and six littermate C57BL/6 male mice (WT Glud1) were sacrificed when 7-months old. Subsequently the brains were microdissected in order to collect specifically the following regions: cerebellum, hippocampus, prefrontal cortex, striatum, parietal cortex and brain stem. The $A\beta PP_{swe}/PS1_{dE9}$ (AβPP/PS1) mouse model of Alzheimer's disease was originally obtained from John Hopkins University, Baltimore, MD, USA (28) and a colony was established at the Central Animal Facility of the Radboud University Medical Centre, Nijmegen, The Netherlands. This double transgenic model was created by co-injection of chimeric mouse/human $A\beta PP_{swe}$ (mouse AβPP695 harboring a human Aβ domain and mutations K595N and M596L linked to Swedich familial Alzheimer's disease pedigrees) and human mutated presenilin-1 PS1-dE9 (deletion of exon 9) vectors controlled by independent mouse prion protein promotor elements. The two transfected genes co-integrate and co-segregate as a single locus (29). This line was originally maintained in a hybrid background by backcrossing to C3HeJ

x C57BL6/J F1 mice for nine generations. For the present work, five AβPP-PS1 transgenic mice (Tg AβPP/PS1) and five of their wild type littermate controls (WT AβPP/PS1), all at 10 months of age were sacrificed. To reduce the variability of the data only male mice were used for the experiment. After microdissection, brain regions were collected. The experiments were performed according to Dutch federal regulations for animal protection and were approved by the Veterinary Authority of the Radboud University Medical Centre.

RNA extraction

Tissues were homogenized and subsequently total RNA was extracted using TRIzol total RNA isolation reagent (Life technologies BRL, Breda, The Netherlands). After DNAse treatment (Promega, Madison, WI) to prevent genomic DNA contamination, DNAse action was stopped by the DNAse stop buffer (Promega) at 65 ºC for 10 min and RNA concentrations were determined by measuring the ratio of the UV absorbance at 260 and 280 nm using the Nanodrop 2000c (Thermoscientific, Wilmington, DE). Thereafter, 1.5 µg of RNA was reverse-transcribed by Moloney-Murine Leukemia Virus-Reverse Transcriptase (Invitrogen, Carlsbad, CA) in a 30 µL mix and incubated at 37 ºC for 1.5 hours as previously described (30). cDNA obtained was diluted 10 times and used to determine mRNA expression levels of the genes of interest.

Cloning

The subcloning of NCX1-BD into pCINeo IRES GFP vector and NCX3-AC and NCX3-B into pCINeo IRES GFP vectors with an HA-Tag fused at the N-terminus of the protein was described in detail previously (24,31). Next, the NCX3-BC was generated by insertion of the exon-C into NCX3-B using a Quick-change site-directed mutagenesis kit (Stratagene, La Jolla, CA). Subsequently, all constructs were validated by Sanger sequencing.

Expression profile and quantitative real-time polymerase chain reaction analysis

Using a CFX96 Real time PCR detection system (Bio-Rad, Hercules, CA), 2.5 µL of sample was mixed with the Power SYBR Green PCR master mix (Applied Biosystems, Foster City, CA) and exon-overlapping primers against the gene of interest in a 96-well plate. Samples were included in duplicate and all samples were measured on three independent experimental sessions. To ensure purity of the sample and the absence of contamination from genomic DNA, a negative control for each sample in which reverse transcriptase was performed in the absence of the enzyme, was tested during the first measurement. Sequences were amplified using the primers described in the **Table 1**. Prior to RT-qPCR, dynamic range ($R^2 > 0.99$) and efficiency (90-110) were evaluated for each set of primers. Sets of primers targeting the variants of NCX3 were also tested to ensure that detection was restricted to only the variant targeted. Additionally, to allow absolute quantification,

five-fold serial dilutions of each vector were performed starting from a set concentration of 200 µg DNA/µL. Ten serial dilutions of the vector carrying the gene of interest were included in duplicate on each plate to determine a reference curve starting from a concentration of 0.32 µg DNA/µL.

Table 1 Primers sets for relative and absolute quantification by RT-PCR

Name primers	Forward (5'→ 3')	Reverse (5'→ 3')
mNCX1	TCGGTGCCAGACACATTTGC	CAGCATTGCTTCCAGTGACAT
mNCX3	GAGCTGGAGTTCAAGAATG	CTTCCTGTCTGTCACTTC
mNCX3-AC	GAAACAGTCAAAACAATTCACATC	GTCACTTCTGGAGATAACAGGAG
mNCX3-B	GAAACAGTGAAAACCATAAGGG	CTGTCACTTCTGATATTCC
mNCX3-BC	GAAACAGTGAAAACCATAAGGG	GTCACTTCTGGAGATAACAGGAG

Each set of primers amplified a fragment of 70 bp to 150 bp and has been tested and validated beforehand.

Normalization Transgenic on WT mice

Expression of the transgenic mice Tg Glud1 and Tg AβPP/PS1 were normalized on the expression of their WT littermates, WT Glud1 and WT AβPP/PS1, respectively. Normalization was expressed in percentage of variation compared to WT expression.

Absolute quantification

For each plate, the cycle thresholds of detection (CT) of the reference samples were plotted to obtain a standard curve of CT values as a function of log [concentration of RNA (copynumber/µL)]. First, the molecular weight of each construct was calculated using the following formula:

weight (g/mol) = (bp size of vector) x (weight of a bp (Da)) where bp=base pair

As the constructs used were of about 9600 ± 20 bp, and a base pair weight is 660 Da, the molecular weight was of 6336000 g/mol of each construct. Hence, the number of copies/g was calculated as follows:

Mass of copies (molecules/g) = (Avogadro's number)/weight

Therefore each gram of construct contained 9.50×10^{16} molecules. Additionally, for each standard, the concentration of DNA in ng/µL was calculated based on the extrapolation of the nanodrop values according to the serial dilution. This value was subsequently multiplied by the number of copies/ng to obtain the concentration of copies in a µL.

Finally the logarithm of this value was plotted to obtain the standard curve. Next, the equation of the calibration curve was used to determine from the CT value of RT-qPCR obtained from each sample, the exact copy number of mRNA/µL. By taking into account the dilution of samples during the reverse transcriptase phase, the final value of copy number/µg RNA could be determined as previously described (24,32) and results could be compared intra-experimentally during data analysis.

Statistical analysis

All results are based on at least three independent sessions of experiments and on 5 (AβPP/PS1) or 6 (Glud1) mice in each condition. Values are expressed as means ± S.E.M. or in percentage of WT expression ± S.E.M. Statistical significance was determined using One-Way ANOVA or two-way ANOVA followed by the Bonferroni's procedure ($P < 0.05$).

Results

Brain region-specific expression of NCX transcripts in healthy mice

Quantification of NCX transcripts in different regions of the brain of WT littermates of Glud1 transgenic mice revealed that NCX1 expression was highest in the parietal cortex (854 ± 49 copies/ng RNA), and was significantly higher than in the brain stem, cerebellum, and striatum in which the expression was 408 ± 63 copies/ng RNA (**Figure 1A**). NCX3 transcript expression was highest in the brain stem (589 ± 243 copies/ng RNA) and lowest in the parietal cortex (261 ± 127 copies/ng RNA). In three brain regions, hippocampus, prefrontal and parietal cortex, transcript levels of NCX1 were markedly higher than those of NCX3, while these levels were equal in cerebellum, striatum and brainstem. Essentially the same brain region-specific expression pattern of NCX transcripts was observed in the WT littermates of AβPP/PS1 mice (**Figure 1B**). In these mice, the expression levels of NCX1 transcripts in the hippocampus, prefrontal and parietal cortex were significantly higher than those of NCX3 in the same regions.

Brain region-specific expression of NCX3 variant transcripts in healthy mice

To investigate the expression of NCX3 variants, primers were designed to specifically amplify the mouse variants NCX3-AC, NCX3-B, and NCX3-BC. This latter variant was described previously as being expressed in rat brain (16) but its presence in mouse brain has never been examined. Our analysis revealed that this variant is present in all regions of the mouse brain in both WT littermates of Glud1 and WT littermates of AβPP/PS1 (**Figures 2A and 2B** respectively). On the other hand with a copy number below 5/ng RNA, NCX3-AC was hardly detectable. NCX3-B transcript levels did not differ significantly among the different brain regions and, in all regions, they were significantly higher than those of NCX3-BC. In both mouse models, the highest levels of expression of NCX3-BC transcript were measured in the brain stem. Transcript levels of NCX3-BC measured in

the brain stem were significantly higher than those in the hippocampus, prefrontal and parietal cortex of WT littermates of AβPP/PS1 mice and significantly higher than those of all other brain regions of WT littermates of Glud1 mice.

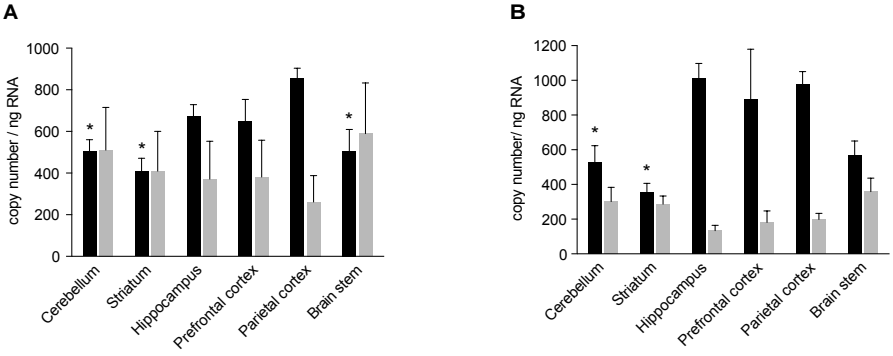

Figure 1 Expression of NCX1 and NCX3 in six brain regions of the WT littermates of both Glud1 (WT Glud1) and AβPP/PS1 mice (WT AβPP/PS1).

Absolute quantification of the Na^{+}-Ca^{2+} exchanger NCX1 (black) and NCX3 (grey) transcripts in six brain regions of the healthy brain microdissected from **A**, WT Glud1 (C57BL6) mice and **B**, WT AβPP/PS1 mice (C3HeJ x C57BL6/J). Results shown represent the mean of the data ± S.E.M. for the following number (n) of mice: WT Glud1 n=6, WT AβPP/PS1 n=5. Expression has been quantified in three independent experiments for each mouse. Values for each NCX isoform are compared to the parietal cortex with $P < 0.05$.

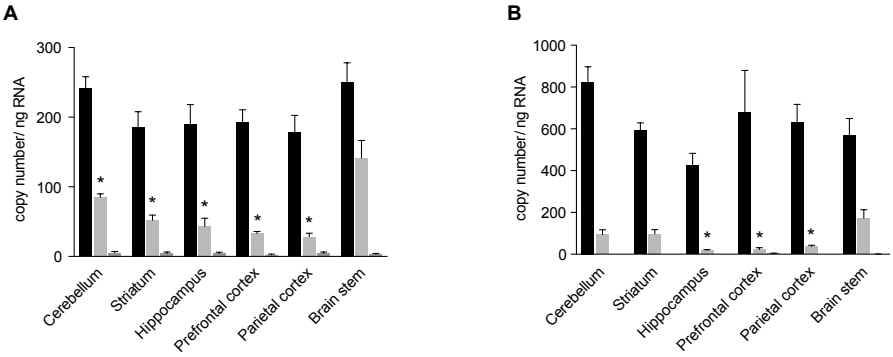

Figure 2 Quantification of transcripts of NCX3 splice variants in different brain regions of WT littermates of both Glud1(WT Glud1) and AβPP/PS1 mice (WT AβPP/PS1).

The copy number per ng of RNA of several NCX3 splice variant transcripts was quantified in six brain regions of the brain from **A**, WT Glud1 (C57BL6) mice and **B**, WT AβPP/PS1 mice (C3HeJ x C57BL6/J). NCX3-B (black) NCX3-BC (light grey) and NCX3-AC (dark grey). Results represent the mean of the data ± S.E.M. for the following number (n) of mice: WT Glud1 n=6, WT AβPP/PS1 n=5. Expression has been quantified in three independent experiments for each mice. Values for each NCX3 variant are compared to the brain stem with $P < 0.05$.

Effect of chronic glutamate-induced neuronal hyper-excitation on NCX expression

In order to investigate whether neuronal stress induced by higher than normal activation of synaptic glutamate receptors might affect the expression of NCX proteins, similar measurements to those done on WT mouse brains were conducted on Tg Glud1 mice. Due to the introduction of the glutamate dehydrogenase gene under a neuronal promoter, these mice are subjected to moderate excess of synaptic release of glutamate from glutamatergic neurons in the CNS (27). No significant differences in NCX1 (**Figure 3A**) or NCX3 (**Figure 3B**) transcript levels were observed in the different brain regions between WT and Tg Glud1 mice. Similarly, measurement of mRNA expression levels of the NCX3 variants revealed, once again, no significant differences between Tg mice and their WT littermates. Of note were the higher levels of NCX3-B and NCX3-BC in the striatum of the Tg Glud1 mice as compared with those of the WT littermates (**Figure 3C**). NCX3-AC transcripts were hardly detectable (data not shown).

Effect of severe excitotoxicity associated with Alzheimer's disease on NCX expression

Alzheimer's disease is associated with high levels of excitotoxicity. To investigate a possible effect of an excitotoxic state on NCX protein expression, we determined NCX transcript levels in the AβPP/PS1 mouse model of Alzheimer's disease. Transgenic AβPP/PS1 (Tg AβPP/PS1) mice carry mutations of both presenilin-1 and AβPP genes leading to the development of Alzheimer's pathology and the neuronal accumulation of amyloid peptide already at 6 months of age (33). NCX1 (**Figure 4A**) and NCX3 (**Figure 4B**) transcript levels in the different brain regions did not differ significantly between Tg AβPP/PS1 mice and their WT littermates. Similarly, quantification of the levels of expression of NCX3 variants mRNAs showed no significant differences in transcript expression (**Figure 4C**). The NCX3-AC variant was not detected in most samples (data not shown).

Discussion

The present study quantified, for the first time, the Na^+-Ca^{2+} exchanger NCX1 and NCX3 transcripts in different regions of the murine brain in two WT mice strains. The WT littermates of Glud1 and AβPP/PS1 mice had a similar pattern of expression of NCX isoforms. NCX1 mRNA levels were higher than NCX3 levels in all regions of the WT mouse brains. Furthermore, whereas NCX1 transcripts were highly expressed in both paleo- and neocortex, i.e., in hippocampus, prefrontal cortex, and parietal cortex, a significantly lower expression of NCX3 was detected in these regions. On the other hand, NCX3 expression was highest in the brain stem. A similar level of expression of NCX1 and NCX3 was observed in striatum. Additionally, brain expression of the three NCX3 variants:

NCX3-AC, NCX3-B, and NCX3-BC were measured and revealed a low level of expression for NCX3-AC. NCX3-BC and NCX3-B were detected in all regions of the brain with NCX3-B expression being higher than NCX3-BC. Thereafter, NCX expression was quantified in hyper-glutamatergic and excitotoxic conditions using the Glud1 Tg mouse model in which CNS neurons are subjected to chronic glutamate over-stimulation, and the AβPP/PS1 mouse model of Alzheimer's disease (AD), mice that develop β-amyloid deposits as early as 6 months of age (33). Comparison of the NCX isoforms expression with WT mice revealed no significant changes in NCX1 and NCX3 expression in Glud1 and AβPP/PS1 mouse model. Similarly, the expression of NCX3 variants was unchanged in both transgenic mouse models.

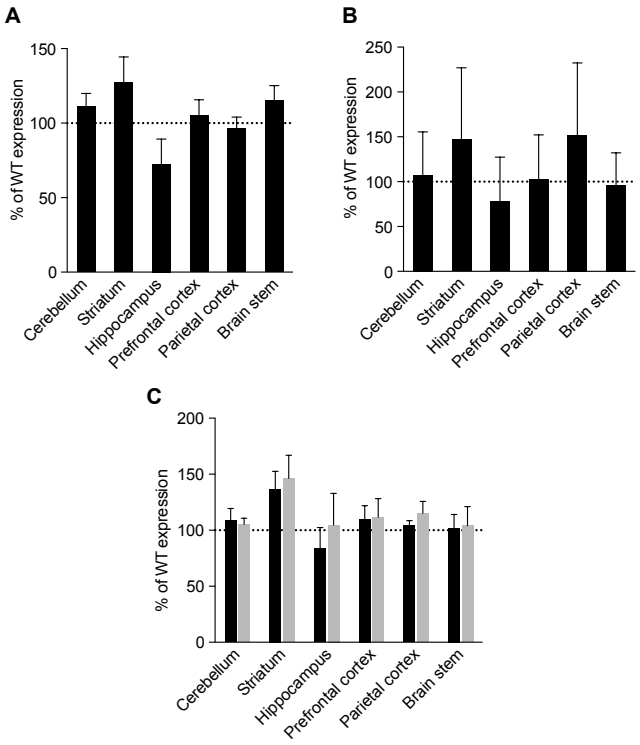

Figure 3 Effect of chronic excess of synaptic glutamate release on NCX expression in different brain regions of the transgenic Glud1 mice.

Percentage of difference of **A**, NCX1 expression, **B**, NCX3 expression, and **C**, NCX3-B (black) and NCX3-BC (grey) expression between transgenic Glud1 mice and their WT littermates in six regions of the brain. Copy number quantification in each condition has been performed in three independent experimental sessions for each mouse. Results of the Tg Glud1 are represented as the percentage ± S.E.M. of the expression measured in their WT littermates, for a number (n) of mice in each conditions (n=6).

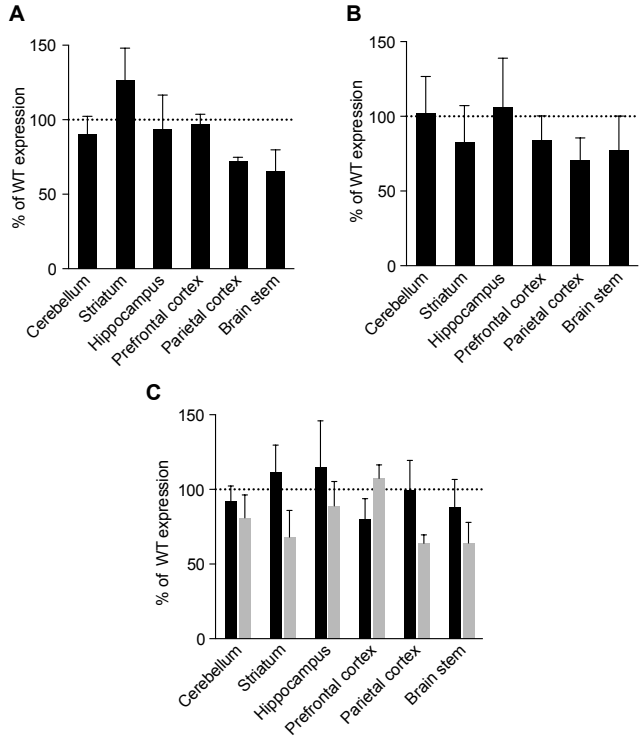

Figure 4 Impact of a severe excitotoxicity on NCX expression in different brain regions of the transgenic AβPP/PS1 mice.

Percentage of difference in transcripts levels corresponding to **A**, expression of NCX1, **B**, NCX3, **C**, NCX3-B (black) and NCX3-BC (grey) from the brain of transgenic AβPP/PS1 mice compared to their WT littermates. Expression between transgenic AβPP/PS1 mice and their WT littermates and is quantified in six independent regions of the microdissected brain. Copy number quantification in each condition has been performed in three independent experimental sessions for each mouse. Results of the Tg AβPP/PS1 are represented as the percentage ± S.E.M. of the expression measured in their WT littermates, for a number (n) of mice (n=5).

While the high expression in WT of NCX1 in hippocampus and NCX3 in the striatum and cerebellum has been previously reported (34,35), the expression quantified in our experiments differs in several regions from previous studies of the Annunziato's group (35,36) where high levels were found in cerebellum and NCX3 was predominantly expressed in hippocampus (36). These conflicting results might be due to different analysis techniques or related to the variation among animal models, our study being performed on mouse brain whereas Papa *et al*. studied NCX isoforms in rat brain (36). The

former explanation for the disparities is most likely as tissue distribution is in many cases conserved among rodents (37). Additionally, while previous studies investigated NCX isoforms at the RNA levels in the detailed regions of the brain, quantitative measurements were not performed and therefore NCX isoforms expression were not accurately measured nor compared.

The specific isoform distribution together with the different properties attributed to each isoform in terms of Ca^{2+} uptake and extrusion suggest an isoform-specific role in each brain region. In this regard, one phenomenon regulated by NCX fluxes is the differentiation and maturation of neuronal cells (38,39). By modulating intracellular Ca^{2+} levels, NCX isoforms affect the role of Ca^{2+} as a second messenger in the different signaling pathways implicated in neuronal differentiation. In this manner, high expression of NCX1 has been linked with neuronal differentiation (40). However, for oligodendrocyte differentiation, NCX3 upregulation is required (38) together with a downregulation of NCX1. This observation confirms the specificity of the NCX isoforms for the different physiological situations to which each cell type is adapted. These specificities have however not been fully investigated in each brain region, thus most of them remain largely unknown. A recent study, pointed out the implications of NCX3 in the long-term potentiation and the spatial learning and memory formation in the hippocampus (41), a finding consistent with our study where NCX3 was detected in hippocampus. However, several regions showed higher NCX3 expression levels such as the striatum, cerebellum and brain stem. NCX3 is, therefore, expected in such regions to be implicated as well in important physiological situations. Although so far its involvement in brain stem and striatum has not been investigated, NCX3 has been suggested to participate in the ability of cerebellar neurons to sustain and buffer the repetitive Ca^{2+} entry resulting from the firing of mossy fibers (42).

Quantification of the transcripts of NCX3 variants revealed in mice the presence of NCX3-BC, a variant described until now solely in rat (16). NCX3-BC was expressed in all regions of the mouse brain, as was also NCX3-B. Of these two variants, NCX3-B was expressed more highly than NCX3-BC, while the NCX3-AC variant was expressed at very low levels. These results were in line with the tissue distribution described in rat, where NCX3-AC is predominantly expressed in skeletal muscle and the remaining variants restricted to the brain (16). The quantification of the NCX3 variant in the different areas of the brain is of importance in fully understanding their function in neuronal physiology. The properties of both NCX3-B and NCX3-AC have been previously examined in mice (43), while the activity of NCX3-BC has yet to be characterized.

Numerous studies have focused on the implications of NCX activity during neuronal stress and pointed out a neuroprotective role for NCX1 and NCX3 in hypoxic and anoxic conditions linked to an upregulation of both exchangers following ischemic preconditioning (20,21,25,26,44,45). Furthermore, the neuroprotective action of NCX3 has been associated with its cleavage by the calpain protease leading to a hyperactive

exchanger (23). Such process was observed following the induction of neuronal hypoxia as well as upon severe excitotoxic conditions, such as those present in Alzheimer's disease and following glutamate overexposure. Additionally, the increase in the Ca^{2+} uptake via NCX in its reverse mode of exchange, following ischemic preconditioning and exposure to β-amyloid peptide, has been shown to participate in the maintenance of ER Ca^{2+} levels and leading to a delay in caspase activation and neuronal death (23,26), thus suggesting the neuroprotective action of NCX3 originates from a common cellular response to neuronal injury (46).

Surprisingly, either exposure to a moderate synaptic hyper-excitation of neurons as is observed in transgenic Glud1 mice or to a severe excitotoxicity condition as is the case in the AD mouse model AβPP/PS1, did not lead to significant changes in NCX1 and NCX3 expression. This lack of an apparent transcriptional response to glutamate hyperactivity and excitotoxicity in NCX1/3 expression contrasted with the upregulation induced by hypoxic conditions (22). Altogether, these data suggest that implications of NCX in neuroprotection result from stimulation of distinct signaling pathways depending on whether neurons are facing hypoxic stress or exposure to an excitotoxic molecule such as glutamate or β-amyloid peptide. Consistently with this hypothesis, the Glud1 mice exhibit a partial resistance to *in vivo* cerebral ischemia, i.e., a glutamate-induced "pre-conditioning"-like effect (47) observed in absence of a significant upregulation of NCX1/3 expression between WT and transgenic mice. The molecular pathways of neuroprotection induced by synaptic glutamate hyperactivity are not fully defined (48) and may implicate certain isoforms of NCX, if not in terms of changes in expression, possibly in terms of changes in post-translational modifications and activation of the exchanger.

Additionally, recent investigations suggested that exon C, alternatively spliced in NCX3 variants and present in NCX3-AC and NCX3-BC, is responsible for calpain cleavage by carrying a cleavage site (43). Therefore, rearrangement of NCX3 variants expression levels in the various brain regions would be expected under conditions of hyper-excitability or excitotoxicity leading to a potential enrichment of NCX3-BC or NCX3-AC. However, no significant changes in the expression levels of NCX3 variants were observed suggesting that the plasma membrane expression of NCX is not increased under conditions of high glutamate synaptic activity or excitotoxicity and that the hyperactive state of the cleaved exchanger is exclusively accountable for the increased Ca^{2+} fluxes. To confirm these observations, the measures investigating RNA levels of the two variants should be supplemented by a quantitative approach at protein levels. Such method can unfortunately not be applied yet to splice variants sharing such degree of similarity in both size and sequence. Finally, a neuroprotective effect of NCX3 restricted solely to NCX3-BC after calpain cleavage would provide further protection to the area of the brain expressing high levels of NCX3-BC such as the cerebellum, striatum, and, particularly, the brain stem where NCX3-BC levels were significantly higher than in other brain regions. On the contrary the remaining areas would be more sensitive to excitotoxic stress and

prone to injury. Consistent with this hypothesis, a lower susceptibility to ischemia-induced cell damage is observed in brain stem compared with the remaining regions of the brain, while the neocortex and the hippocampus are more prone to neuronal injury (49).

In conclusion, our study reports a high expression of NCX1 in hippocampus, prefrontal and parietal cortex and a high expression of NCX3 in striatum, cerebellum and brain stem of the mouse brain. Such differential expression patterns for these two NCX isoforms are probably an indication of the role that the exchangers play in the regulation of physiological activities in these regions. The neuroprotective action that has been attributed to NCX1 and NCX3 could provide these regions a higher protection against neurotoxicity and neuronal injury. However, in contrast to what has been observed following hypoxic conditions, NCX expression as well as the distribution of NCX3 variants remained unchanged under conditions of glutamate synaptic hyperactivity or excitotoxicity. These results indicate a differential response of neurons to distinct types of stress stimuli. Finally, we showed for the first time in the present study, the specific expression of NCX3 variants in mouse brain regions. NCX3-AC was barely expressed, and NCX3-BC and NCX3-B were detected in all regions of the brain with NCX3-B expression being higher than NCX3-BC. The expression of NCX3-BC correlated with the tolerance to ischemia found in the different regions of the WT brain. As NCX3-BC is suggested to be exclusively responsible for the neuroprotective action of NCX3, the study of the expression and post-translational modifications of NCX3-BC, following ischemic and hyper-glutamatergic conditioning, would be of great interest to understand the different mechanisms by which NCX3 prevents neuronal cell death.

Acknowledgments

This research was supported by an equipment grant of The Netherlands Organization for Scientific Research (NWO, No. 911-02-008) and the Centre for Systems Biology Research (CSBR) initiative from the NWO (No. CSBR09/013V), and by grants AG12993 and AG035982 from the National Institute on Aging, and grant HD002528 from the Eunice Kennedy Shriver National Institute on Child Health and Human Development, the United States National Institutes of Health. The authors thank Dr. Peter Willems for critical reading of the manuscript.

Author contribution

LYM, RJB and JGH conceived the study. AJK provided the $A\beta PP_{swe}/PS1_{dE9}$ transgenic and wild type mice. EKM, RP, and DH provided the Glud1 transgenic and wild type mice and microdissected the brain regions. LYM designed, performed, analyzed the experiments and wrote the manuscript. AJK, EM, JGH, and RJB revised critically the manuscript. All authors reviewed the results and approved the final version of the manuscript.

References

1. **Zhu, W. H., Conforti, L., Czyzyk-Krzeska, M. F., and Millhorn, D. E.** Membrane depolarization in PC-12 cells during hypoxia is regulated by an O2-sensitive K+ current. *The American journal of physiology* 271, C658-665 (1996)
2. **Snowdowne, K. W., Freudenrich, C. C., and Borle, A. B.** The effects of anoxia on cytosolic free calcium, calcium fluxes, and cellular ATP levels in cultured kidney cells. *The Journal of biological chemistry* 260, 11619-11626 (1985)
3. **Mattson, M. P., Cheng, B., Davis, D., Bryant, K., Lieberburg, I., and Rydel, R. E.** beta-Amyloid peptides destabilize calcium homeostasis and render human cortical neurons vulnerable to excitotoxicity. *The Journal of neuroscience : the official journal of the Society for Neuroscience* 12, 376-389 (1992)
4. **Rees, K. R., Sinha, K. P., and Spector, W. G.** The pathogenesis of liver injury in carbon tetrachloride and thioacetamide poisoning. *The Journal of pathology and bacteriology* 81, 107-118 (1961)
5. **Rivet-Bastide, M., Imbert, N., Cognard, C., Duport, G., Rideau, Y., and Raymond, G.** Changes in cytosolic resting ionized calcium level and in calcium transients during in vitro development of normal and Duchenne muscular dystrophy cultured skeletal muscle measured by laser cytofluorimetry using indo-1. *Cell calcium* 14, 563-571 (1993)
6. **Puceat, M., Clement, O., Scamps, F., and Vassort, G.** Extracellular ATP-induced acidification leads to cytosolic calcium transient rise in single rat cardiac myocytes. *The Biochemical journal* 274 (Pt 1), 55-62 (1991)
7. **Choi, D. W.** Glutamate neurotoxicity and diseases of the nervous system. *Neuron* 1, 623-634 (1988)
8. **Leonard, J. P., and Salpeter, M. M.** Agonist-induced myopathy at the neuromuscular junction is mediated by calcium. *The Journal of cell biology* 82, 811-819 (1979)
9. **Scoltock, A. B., Bortner, C. D., St, J. B. G., Putney, J. W., Jr., and Cidlowski, J. A.** A selective requirement for elevated calcium in DNA degradation, but not early events in anti-Fas-induced apoptosis. *The Journal of biological chemistry* 275, 30586-30596 (2000)
10. **Dykens, J. A.** Isolated cerebral and cerebellar mitochondria produce free radicals when exposed to elevated CA2+ and Na+: implications for neurodegeneration. *Journal of neurochemistry* 63, 584-591 (1994)
11. **Durant, S., Homo, F., and Duval, D.** Calcium and A23187-induced cytolysis of mouse thymocytes. *Biochemical and biophysical research communications* 93, 385-391 (1980)
12. **Randall, R. D., and Thayer, S. A.** Glutamate-induced calcium transient triggers delayed calcium overload and neurotoxicity in rat hippocampal neurons. *The Journal of neuroscience : the official journal of the Society for Neuroscience* 12, 1882-1895 (1992)
13. **Chin, J. H., Tse, F. W., Harris, K., and Jhamandas, J. H.** Beta-amyloid enhances intracellular calcium rises mediated by repeated activation of intracellular calcium stores and nicotinic receptors in acutely dissociated rat basal forebrain neurons. *Brain cell biology* 35, 173-186 (2006)
14. **Alberdi, E., Sanchez-Gomez, M. V., Cavaliere, F., Perez-Samartin, A., Zugaza, J. L., Trullas, R., Domercq, M., and Matute, C.** Amyloid beta oligomers induce Ca2+ dysregulation and neuronal death through activation of ionotropic glutamate receptors. *Cell calcium* 47, 264-272 (2010)
15. **Berridge, M. J.** Calcium hypothesis of Alzheimer's disease. *Pflugers Archiv : European journal of physiology* 459, 441-449 (2010)
16. **Quednau, B. D., Nicoll, D. A., and Philipson, K. D.** Tissue specificity and alternative splicing of the Na+/Ca2+ exchanger isoforms NCX1, NCX2, and NCX3 in rat. *The American journal of physiology* 272, C1250-1261 (1997)

17. **Stys, P. K., Waxman, S. G., and Ransom, B. R.** Ionic mechanisms of anoxic injury in mammalian CNS white matter: role of Na+ channels and Na(+)-Ca2+ exchanger. *The Journal of neuroscience : the official journal of the Society for Neuroscience* 12, 430-439 (1992)

18. **Matsuda, T., Takuma, K., Nishiguchi, E., Hashimoto, H., Azuma, J., and Baba, A.** Involvement of Na+-Ca2+ exchanger in reperfusion-induced delayed cell death of cultured rat astrocytes. *The European journal of neuroscience* 8, 951-958 (1996)

19. **Amoroso, S., Tortiglione, A., Secondo, A., Catalano, A., Montagnani, S., Di Renzo, G., and Annunziato, L.** Sodium nitroprusside prevents chemical hypoxia-induced cell death through iron ions stimulating the activity of the Na+-Ca2+ exchanger in C6 glioma cells. *Journal of neurochemistry* 74, 1505-1513 (2000)

20. **Pignataro, G., Gala, R., Cuomo, O., Tortiglione, A., Giaccio, L., Castaldo, P., Sirabella, R., Matrone, C., Canitano, A., Amoroso, S., Di Renzo, G., and Annunziato, L.** Two sodium/calcium exchanger gene products, NCX1 and NCX3, play a major role in the development of permanent focal cerebral ischemia. *Stroke; a journal of cerebral circulation* 35, 2566-2570 (2004)

21. **Molinaro, P., Cuomo, O., Pignataro, G., Boscia, F., Sirabella, R., Pannaccione, A., Secondo, A., Scorziello, A., Adornetto, A., Gala, R., Viggiano, D., Sokolow, S., Herchuelz, A., Schurmans, S., Di Renzo, G., and Annunziato, L.** Targeted disruption of Na+/Ca2+ exchanger 3 (NCX3) gene leads to a worsening of ischemic brain damage. *The Journal of neuroscience : the official journal of the Society for Neuroscience* 28, 1179-1184 (2008)

22. **Pignataro, G., Boscia, F., Esposito, E., Sirabella, R., Cuomo, O., Vinciguerra, A., Di Renzo, G., and Annunziato, L.** NCX1 and NCX3: two new effectors of delayed preconditioning in brain ischemia. *Neurobiology of disease* 45, 616-623 (2012)

23. **Pannaccione, A., Secondo, A., Molinaro, P., D'Avanzo, C., Cantile, M., Esposito, A., Boscia, F., Scorziello, A., Sirabella, R., Sokolow, S., Herchuelz, A., Di Renzo, G., and Annunziato, L.** A new concept: Abeta1-42 generates a hyperfunctional proteolytic NCX3 fragment that delays caspase-12 activation and neuronal death. *The Journal of neuroscience : the official journal of the Society for Neuroscience* 32, 10609-10617 (2012)

24. **Michel, L. Y., Verkaart, S., Koopman, W. J., Willems, P. H., Hoenderop, J. G., and Bindels, R. J.** Function and regulation of the Na+-Ca2+ exchanger NCX3 splice variants in brain and skeletal muscle. *The Journal of biological chemistry* 289, 11293-11303 (2014)

25. **Pignataro, G., Esposito, E., Cuomo, O., Sirabella, R., Boscia, F., Guida, N., Di Renzo, G., and Annunziato, L.** The NCX3 isoform of the Na+/Ca2+ exchanger contributes to neuroprotection elicited by ischemic postconditioning. *Journal of cerebral blood flow and metabolism : official journal of the International Society of Cerebral Blood Flow and Metabolism* 31, 362-370 (2011)

26. **Sisalli, M. J., Secondo, A., Esposito, A., Valsecchi, V., Savoia, C., Di Renzo, G. F., Annunziato, L., and Scorziello, A.** Endoplasmic reticulum refilling and mitochondrial calcium extrusion promoted in neurons by NCX1 and NCX3 in ischemic preconditioning are determinant for neuroprotection. *Cell death and differentiation* 21, 1142-1149 (2014)

27. **Bao, X., Pal, R., Hascup, K. N., Wang, Y., Wang, W. T., Xu, W., Hui, D., Agbas, A., Wang, X., Michaelis, M. L., Choi, I. Y., Belousov, A. B., Gerhardt, G. A., and Michaelis, E. K.** Transgenic expression of Glud1 (glutamate dehydrogenase 1) in neurons: in vivo model of enhanced glutamate release, altered synaptic plasticity, and selective neuronal vulnerability. *The Journal of neuroscience : the official journal of the Society for Neuroscience* 29, 13929-13944 (2009)

28. **Borchelt, D. R., Ratovitski, T., van Lare, J., Lee, M. K., Gonzales, V., Jenkins, N. A., Copeland, N. G., Price, D. L., and Sisodia, S. S.** Accelerated amyloid deposition in the brains of transgenic mice coexpressing mutant presenilin 1 and amyloid precursor proteins. *Neuron* 19, 939-945 (1997)

29. **Jankowsky, J. L., Slunt, H. H., Ratovitski, T., Jenkins, N. A., Copeland, N. G., and Borchelt, D. R.** Co-expression of multiple transgenes in mouse CNS: a comparison of strategies. *Biomolecular engineering* 17, 157-165 (2001)

30. **Hoenderop, J. G., Hartog, A., Stuiver, M., Doucet, A., Willems, P. H., and Bindels, R. J.** Localization of the epithelial Ca(2+) channel in rabbit kidney and intestine. *Journal of the American Society of Nephrology : JASN* 11, 1171-1178 (2000)

31. **van der Hagen, E. A., van Loon, E. P., Verkaart, S., Latta, F., Bindels, R. J., and Hoenderop, J. G.** The Na+/Ca2+ Exchanger 1 (NCX1) Variant 3 as the Major Extrusion System in Renal Distal Tubular Transcellular Ca2+-Transport. *Nephron* 131, 145-152 (2015)

32. **Whelan, J. A., Russell, N. B., and Whelan, M. A.** A method for the absolute quantification of cDNA using real-time PCR. *Journal of immunological methods* 278, 261-269 (2003)

33. **Garcia-Alloza, M., Robbins, E. M., Zhang-Nunes, S. X., Purcell, S. M., Betensky, R. A., Raju, S., Prada, C., Greenberg, S. M., Bacskai, B. J., and Frosch, M. P.** Characterization of amyloid deposition in the APPswe/PS1dE9 mouse model of Alzheimer disease. *Neurobiology of disease* 24, 516-524 (2006)

34. **Wakimoto, K., Kuro-o, M., Yanaka, N., Komuro, I., Nabeshima, Y. I., and Imai, Y.** Expression of Na+/Ca(2+) exchanger (NCX1) gene in the developmental mouse embryo and adult mouse brain. *Comparative biochemistry and physiology. Part B, Biochemistry & molecular biology* 130, 191-198 (2001)

35. **Canitano, A., Papa, M., Boscia, F., Castaldo, P., Sellitti, S., Taglialatela, M., and Annunziato, L.** Brain distribution of the Na+/Ca2+ exchanger-encoding genes NCX1, NCX2, and NCX3 and their related proteins in the central nervous system. *Annals of the New York Academy of Sciences* 976, 394-404 (2002)

36. **Papa, M., Canitano, A., Boscia, F., Castaldo, P., Sellitti, S., Porzig, H., Taglialatela, M., and Annunziato, L.** Differential expression of the Na+-Ca2+ exchanger transcripts and proteins in rat brain regions. *The Journal of comparative neurology* 461, 31-48 (2003)

37. **Prasad, A., Kumar, S. S., Dessimoz, C., Bleuler, S., Laule, O., Hruz, T., Gruissem, W., and Zimmermann, P.** Global regulatory architecture of human, mouse and rat tissue transcriptomes. *BMC genomics* 14, 716 (2013)

38. **Boscia, F., D'Avanzo, C., Pannaccione, A., Secondo, A., Casamassa, A., Formisano, L., Guida, N., Sokolow, S., Herchuelz, A., and Annunziato, L.** Silencing or knocking out the Na(+)/Ca(2+) exchanger-3 (NCX3) impairs oligodendrocyte differentiation. *Cell death and differentiation* 19, 562-572 (2012)

39. **Gabellini, N., Bortoluzzi, S., Danieli, G. A., and Carafoli, E.** Control of the Na+/Ca2+ exchanger 3 promoter by cyclic adenosine monophosphate and Ca2+ in differentiating neurons. *Journal of neurochemistry* 84, 282-293 (2003)

40. **Secondo, A., Esposito, A., Sirabella, R., Boscia, F., Pannaccione, A., Molinaro, P., Cantile, M., Ciccone, R., Sisalli, M. J., Scorziello, A., Di Renzo, G., and Annunziato, L.** Involvement of the Na+/Ca2+ exchanger isoform 1 (NCX1) in neuronal growth factor (NGF)-induced neuronal differentiation through Ca2+-dependent Akt phosphorylation. *The Journal of biological chemistry* 290, 1319-1331 (2015)

41. **Molinaro, P., Viggiano, D., Nistico, R., Sirabella, R., Secondo, A., Boscia, F., Pannaccione, A., Scorziello, A., Mehdawy, B., Sokolow, S., Herchuelz, A., Di Renzo, G. F., and Annunziato, L.** Na+ -Ca2+ exchanger (NCX3) knock-out mice display an impairment in hippocampal long-term potentiation and spatial learning and memory. *The Journal of neuroscience : the official journal of the Society for Neuroscience* 31, 7312-7321 (2011)

42. **Gomez-Villafuertes, R., Torres, B., Barrio, J., Savignac, M., Gabellini, N., Rizzato, F., Pintado, B., Gutierrez-Adan, A., Mellstrom, B., Carafoli, E., and Naranjo, J. R.** Downstream regulatory element antagonist modulator regulates Ca2+ homeostasis and viability in cerebellar neurons. *The Journal of neuroscience : the official journal of the Society for Neuroscience* 25, 10822-10830 (2005)

43. **Michel, L. Y., Hoenderop, J. G., and Bindels, R. J.** Calpain-3-mediated regulation of the Na-Ca exchanger isoform 3. *Pflugers Archiv : European journal of physiology* (2015)

44. **Secondo, A., Staiano, I. R., Scorziello, A., Sirabella, R., Boscia, F., Adornetto, A., Canzoniero, L. M., Di Renzo, G., and Annunziato, L.** The Na+/Ca2+ exchanger isoform 3 (NCX3) but not isoform 2 (NCX2) and 1 (NCX1) singly transfected in BHK cells plays a protective role in a model of in vitro hypoxia. *Annals of the New York Academy of Sciences* 1099, 481-485 (2007)

45. **Vinciguerra, A., Formisano, L., Cerullo, P., Guida, N., Cuomo, O., Esposito, A., Di Renzo, G., Annunziato, L., and Pignataro, G.** MicroRNA-103-1 selectively downregulates brain NCX1 and its inhibition by anti-miRNA ameliorates stroke damage and neurological deficits. *Molecular therapy : the journal of the American Society of Gene Therapy* 22, 1829-1838 (2014)

46. **Bano, D., Young, K. W., Guerin, C. J., Lefeuvre, R., Rothwell, N. J., Naldini, L., Rizzuto, R., Carafoli, E., and Nicotera, P.** Cleavage of the plasma membrane Na+/Ca2+ exchanger in excitotoxicity. *Cell* 120, 275-285 (2005)

47. **Badawi, Y., Pal, R., Hui, D., Michaelis, E. K., and Shi, H.** Ischemic tolerance in an in vivo model of glutamate preconditioning. *Journal of neuroscience research* (2014)

48. **Hardingham, G. E., and Bading, H.** Synaptic versus extrasynaptic NMDA receptor signalling: implications for neurodegenerative disorders. *Nat Rev Neurosci* 11, 682-696 (2010)

49. **Sieber, F. E., Palmon, S. C., Traystman, R. J., and Martin, L. J.** Global incomplete cerebral ischemia produces predominantly cortical neuronal injury. *Stroke; a journal of cerebral circulation* 26, 2091-2095; discussion 2096 (1995)

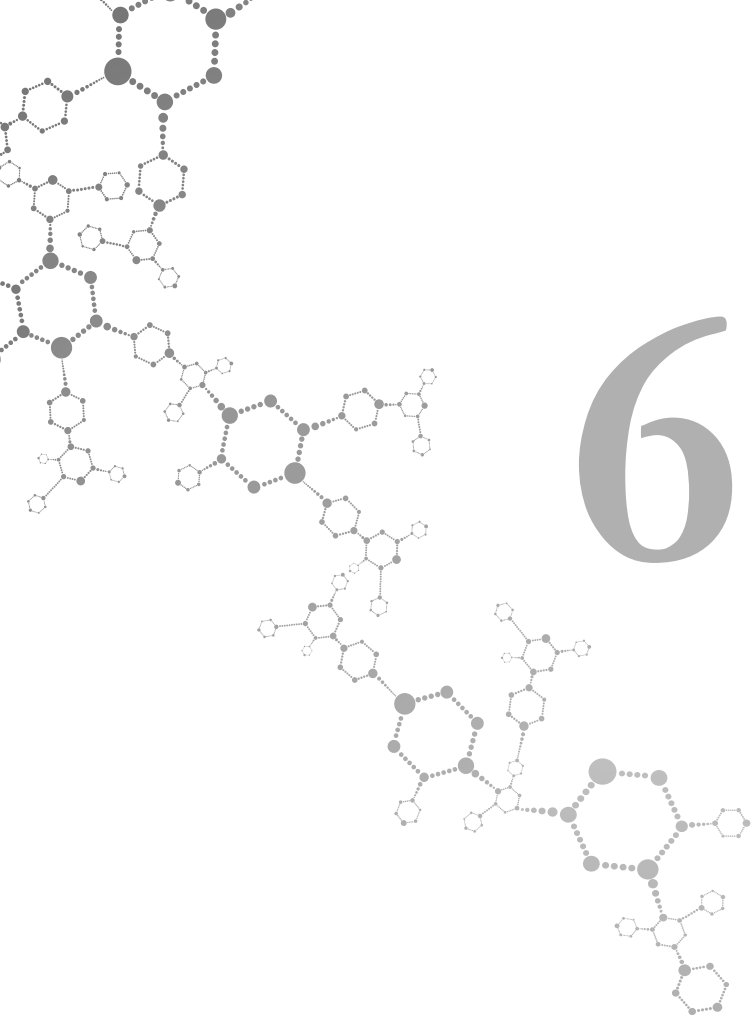

6

General discussion and summary

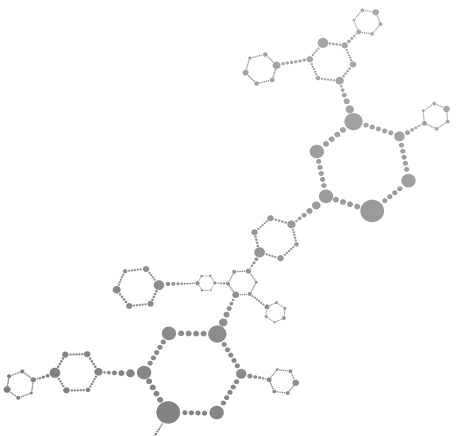

Introduction

The NCX family of plasma membrane Na^+-Ca^{2+} exchangers significantly contributes to the control of the intracellular Ca^{2+} concentration ($[Ca^{2+}]_i$) and are implicated in a wide range of physiological processes such as blood pressure regulation, heartbeat development and insulin secretion. The diversity of these functions is paralleled by a tight control of isoform expression and regulation. This is achieved *i*) at the transcriptional level, in the nucleus, where the activation of the promotor and the alternative splicing of the messenger RNA lead to a specific distribution of each splice variant and isoform, *ii*) at the post-translational level, in the endoplasmic reticulum and Golgi apparatus and at the plasma membrane, where modifications affect the ionic regulation and the capacity of exchange.

The third member of the NCX family, NCX3, is essential for numerous and diverse physiological functions. The exchanger is responsible for bone resorption in osseous tissue and inflammatory processes throughout the body. In excitable tissues, for instance in skeletal muscle, NCX3 contributes to muscle relaxation and neuromuscular transmission. In the central nervous system, spatial learning and memory are impaired in its absence. Furthermore, NCX3 has a crucial role in pathological situations such as brain injury and excitotoxicity. In contrast to the extensively studied first isoform NCX1, the molecular basis of the modulation of NCX3 activity remains poorly understood. Therefore, this thesis aimed to elucidate novel regulatory mechanisms of NCX3 and its molecular determinants with primary interest devoted to the alternatively spliced region through the study of the tissue distribution and function of NCX3 splice variants.

Methodologies for live cell measurements of Na^+-Ca^{2+} exchange

NCX isoforms can perform both influx and efflux of Ca^{2+} across the plasma membrane via the so-called reverse and forward mode, respectively. Since its first identification, Na^+-Ca^{2+} exchange has proven to be challenging to measure because of its bidirectional exchange mode and its tight control by multiple intracellular factors such as ions, metabolic intermediates, nucleotides and proteins. The use of an appropriate technique to study the activity of the NCX isoforms is of great importance in order to fully unravel the subtleties of their regulations. Methodological approaches should enable the study of both modes of exchange in order to detect potential asymmetrical regulations and identify the underlying regulatory mechanisms. With this aim three cell-based techniques have been designed *i*) $^{45}Ca^{2+}$ measurement of Ca^{2+} influx and efflux, *ii*) whole-cell current recordings and *iii*) fluorophore-based intracellular Ca^{2+} imaging.

$^{45}Ca^{2+}$ measurements

In 1967, Reuter and Seitz designed the first functional assay making use of the beta-emitter Ca^{2+} isotope, $^{45}Ca^{2+}$, to study the mechanism of Ca^{2+} efflux across the plasma membrane. By demonstrating its dependence on extracellular Na^+, they provided the first evidence of a Na^+-driven antiporter, referred to as the Na^+-Ca^{2+} exchanger or NCX (1-3). In the subsequent 50 years, $^{45}Ca^{2+}$ assays have been used frequently to investigate the exchange of Ca^{2+} across the plasma membrane by the NCX family. In these assays Na^+-Ca^{2+} exchange is initiated by a change in plasma membrane electrochemical gradients of Na^+ and/or Ca^{2+} in combination with intracellular activation of the exchanger. Depending on the mode of exchange, the former is achieved by removal or lowering of extracellular Na^+ or Ca^{2+}. Thus, Ca^{2+} uptake via reverse exchange is assayed in Na^+-free Ca^{2+}-containing medium, while Ca^{2+} efflux in the forward mode is determined in Na^+-containing Ca^{2+}-free medium. Intracellular activation of NCX requires the manipulation of intracellular ionic concentrations, most frequently by increasing the intracellular Na^+ concentration ($[Na^+]_i$). Na^+ loading was initially achieved in the presence of the ionophore, nystatin (4,5). However, the selectivity of the ionophore for monovalent ions is problematic as, in addition to increasing $[Na^+]_i$, nystatin also impairs the plasma membrane electrochemical gradients of Cl^- and K^+ (6). Nowadays, the combination of the Na^+-specific ionophore monensin and the Na^+-K^+-ATPase inhibitor ouabain is preferred (7-9). Ca^{2+} influx is initiated by replacement of extracellular NaCl-containing medium with a Na^+-free solution containing $^{45}Ca^{2+}$ and either N-methyl D-Glucamine (NMDG) or choline chloride to replace Na^+. Measurement of Ca^{2+} efflux requires preloading of the cells with $^{45}Ca^{2+}$ for 4 hours (10,11) or for one minute in presence of the Ca^{2+} ionophore, ionomycin (7,12). $^{45}Ca^{2+}$ efflux is favored by exposing the cells to the SERCA inhibitor thapsigargin. To lower the relative contribution of other Ca^{2+} transporters, $^{45}Ca^{2+}$ efflux is often measured in NCX overexpressing cells (13). $^{45}Ca^{2+}$ efflux is compared to that obtained in Ca^{2+}- and Na^+-free medium in which no efflux takes place. Finally, Ca^{2+} efflux and uptake are calculated thanks to the $^{45}Ca^{2+}$measured in the cells and the extracellular medium using liquid scintillation counting. Overall, $^{45}Ca^{2+}$ assays provide, in a rapid manner, an averaged capacity of exchange for a high number of cells. However, the capacity of exchange is obtained in the absence of many parameters such as confluency, cell morphology and intracellular parameters and, most importantly from a regulatory point of view, in the absence of any information regarding $[Ca^{2+}]_i$.

Whole-cell current recordings

The development of the patch-clamp technique in 1976 by Neher and Sackmann (14) revolutionized the cellular physiology research by enabling the study of individual ion channels and transporters. The high-resolution recording of cell currents is applicable to all channels and transporters, providing that the transport is electrogenic - resulting in a change in net charge across the membrane (15). All three mammalian NCX isoforms

exchange Na^+ against Ca^{2+} with a 3:1 stoichiometry, respectively, and are therefore electrogenic. Soon after the initial design of the patch clamp technique, procedures have been developed to study NCX.

Electrophysiological measurements of NCX are performed by recording cell current using the whole-cell configuration. Patch-clamp experiments offer low-noise and precise current recordings together with the possibility to control both intracellular and extracellular environment, providing insights into the intrinsic properties of the exchanger. Interestingly in the investigation of the NCX family, patch-clamp can be combined with intracellular Ca^{2+} measurements by means of Ca^{2+} probes. Currents recordings are performed following depolarization of the membrane potential (-80mV to +80mV). At +80mV, an outward current corresponding to a Ca^{2+} influx via the so-called reverse mode of exchange is favored. On the contrary, the NCX inward current associated with Ca^{2+} efflux occurring in the forward mode is recorded in a constant holding potential of -80mV (16,17). Pretreatment with diverse compounds is achieved prior and/or during the recordings to eliminate the contribution of others Ca^{2+} transporters and trigger sufficient Ca^{2+} release from the endoplasmic reticulum to activate NCX using the activator of the Ryanodine Receptor (RyR), caffeine and ryanodine, the SERCA ATPase inhibitor, thapsigargin or the Na^+-K^+-ATPase inhibitor ouabain to increase $[Na^+]_i$ (17,18). Additionally, a train of prepulses (-80mV to 0mV) prior to the measure of inward current is often performed in order to normalize the SR Ca^{2+} load. Limitations in the patch-clamp approach directly stems from the intrinsic properties of this technique. The manipulation of the intracellular solution is of great help to test the effect of specific compounds on NCX but also affects intracellular regulations of the exchanger through changes in the intracellular composition such as the absence of second messenger, presence of buffers (19) or modification of the ionic concentrations. Furthermore, the recording of a single cell current with the high-resolution measurements remains time-consuming, which ultimately reduces drastically the number of cells measured by conditions.

Intracellular Ca^{2+} imaging

Since the discovery in 1963, of the first Ca^{2+}-sensitive bioluminescent protein *aequorin* from jellyfish (20), new fluorescent and bioluminescent indicators of intracellular Ca^{2+} have been engineered and have become available for the study of Ca^{2+} fluxes in living cell. The first measurements of NCX using Ca^{2+} indicators were performed in the 80's, when only the reverse mode could be measured by fluorimetry. The exchanger was triggered in cells in suspension by the replacement of Na^+ by Li^+ in the extracellular medium (21). In the past 30 years, considerable advances have been made in microscopy and imaging techniques and we are nowadays able to combine the measure of $[Ca^{2+}]_i$ with live cell imaging in order to monitor dynamic changes in up to 30 attached cells using a ratiometric probe. To ensure membrane permeability, commercially available

Ca^{2+} indicators often carry an additional acetoxymethyl (AM) group, removed following cell entry by cellular enzymes, as it is the case for the most commonly used Ca^{2+} probe, Fura-2. Despite these advances, in certain cell types the loading of the dye can remain problematic because of the low permeability of the cell membrane, the strong extrusion mechanism of the indicator and its incomplete hydrolysis or its sequestration in non-cytoplasmic organelles. Since the first use of Ca^{2+} indicators in the investigation of NCX, many modifications have been made to the original approach due to novel findings. For example, Li+, often used to replace NaCl in Na^+-free medium, was recently found to be transported by the mitochondrial NCLX (22) and hypothesized to be in a smaller extend transported by other plasma membrane NCX isoforms notably in skeletal muscle (23,24), therefore the replacement of Na^+ by the N-methyl D-glucamine (NMDG) or Choline chloride is nowadays favored over Li^+ (8,25). In **chapter 2**, novel protocols have been designed in order to measure both mode of exchange of NCX using the Fura-2 based Ca^{2+} imaging (**Table 1**). Ca^{2+} uptake by NCX3 in the reverse mode is recorded upon removal of extracellular Na^+ and replacement by NMDG medium. The exchanger is activated by a rise in either $[Ca^{2+}]_i$ or $[Na^+]_i$. On one hand, the acute addition of thapsigargin blocks the re-uptake of Ca^{2+} by the SERCA ATPase and lead to a rise in $[Ca^{2+}]_i$ due to the intrinsic Ca^{2+} leak from the ER. On the other hand, a rise in $[Na^+]_i$ is obtained after a 60-minutes incubation with ouabain inhibiting the Na^+-K^+-ATPase inhibitor and thereby preventing Na^+ extrusion. The ionophore monensin formerly employed to elevate $[Na^+]_i$ is no longer used. Although specific to Na^+ ions, monensin forms a Na^+-H^+ exchanger that impacts pH intra and extracellularly, a parameter that greatly affects the capacity of exchange of NCX (26). The forward mode of exchange is measured in Ca^{2+}-free extracellular medium during a fast release of Ca^{2+} achieved by the acute addition of ionomycin, a Ca^{2+} ionophore that permeabilizes membranes from all cellular Ca^{2+} stores (ER, mitochondria) (27,28). The specificity of this approach for the forward mode of NCX was tested by the absence of exchange in Na^+ and Ca^{2+}-free conditions and by monitoring the Ca^{2+} load in the ER to insure a similar Ca^{2+} level in the different conditions as reported in **chapter 2**. Thanks to the design of this latter protocol, NCX activity and the regulations by $[Ca^{2+}]_i$ or $[Na^+]_i$ can be examined by Ca^{2+} imaging in both modes of exchange, similarly to $^{45}Ca^{2+}$ assays and patch-clamp recordings (**Table 1**). Overall intracellular Ca^{2+} recordings are qualitatively more accurate than radioactive measurements as living cells can be selected based on morphology, transfection, etc. and $[Ca^{2+}]_i$ can be monitored over time. Furthermore Fura-2 based Ca^{2+} imaging enables a higher throughput than whole-cell current recordings and therefore offer a great combination for the study of the NCX family. This is why this technique has been selected and used further in the investigation of NCX3 variants in **chapters 2, 3 and 4**.

Regulation of NCX3 by its intracellular loop

The intracellular loop: a decisive region

Na^+ and Ca^{2+} are translocated across the biological membrane by the Na^+-Ca^{2+} exchanger expressed in all living beings. This process occurs thanks to the 10 transmembrane domains of the exchanger anchored in the phospholipidic bilayer. While the intracellular loop located after the five first transmembrane segments could appear to have a secondary role, its importance is actually central for the regulation of the exchanger by its environment (**Figure 1**).

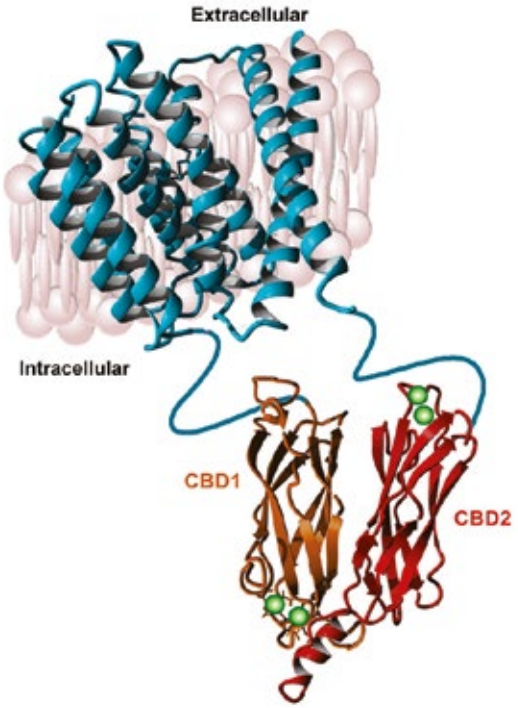

Figure 1 Structural features of NCX3.

Structural model of the Na^+-Ca^{2+} exchanger NCX3 representing the transmembrane domain (blue) as the crystal structure of the bacterial NCX_Mj (29). Ca^{2+}-binding domains are depicted as NMR structure of NCX1-CBD1 (orange) and NCX3-B-CBD2 (red) with bound Ca^{2+} ions (green) (30). NCX1-CBD1 and NCX3-CBD2 structures have been obtained independently; the two CBD domains are arranged similarly to NCX1-CBD1/2 structure (31). NMR structure of NCX3-CBD2 domain has been obtained in absence of bound Ca^{2+}. Ca^{2+} ions have been represented according to the described Ca^{2+}-binding sites of NCX3-B. (30) (Protein Data Bank PDB accession numbers: NCX_Mj: 3V5S; NCX1-CBD: 2FWS; NCX3-CBD2: 2LT9)

Since the isolation of the first isoform of NCX, NCX1, in 1988, physiological and molecular studies have identified many regulators of NCX1 including ionic factors such as $[Ca^{2+}]_i$, $[Na^+]_i$, pH, several molecules and proteins as well as numerous post-translational modifications. Most of the factors identified for NCX1 exert their regulatory action by directly acting on its cytoplasmic domain. The diversity of the intracellular sequence modulates further the influence of the factors on each isoform of the NCX family. Due to alternative splicing events, the cytoplasmic loop differs within splice variants of a same isoform, leading to different regulatory mechanisms. The studies presented in **chapters 2, 3 and 4** of this thesis extend our knowledge on several regulatory factors of NCX3. The roles of factors regulating NCX1 have been investigated and confirmed in NCX3 and a new pathway has been described. The ionic regulation of NCX3 and their links with alternative splicing was investigated in **chapter 2**. Regulatory mechanisms of NCX3 activity by post-translational modifications, in particular PKC and PKA phosphorylation and calpain cleavage were identified in **chapters 3 and 4**, respectively (**Table 2**).

Ionic regulation and exchange capacity

Exerting a tight control on NCX function, $[Ca^{2+}]_i$ and $[Na^+]_i$ insure the NCX activity to be in balance with each cell type requirements. The role of the intracellular loop in the regulation by ions of NCX was originally unraveled by the exposition to a low concentration of α-chymotrypsin. Ultimately disrupting the cytoplasmic loop, α-chymotrypsin induced an apparent loss of modulatory effect by both Ca^{2+} and Na^+ (32-34). Distinction has to be made between the Na^+ and Ca^{2+} ions binding at regulatory sites of the cytoplasmic loop, exclusively involved in its regulations, and the transported Na^+ and Ca^{2+} ions. Difficulties to fully comprehend the modulation of NCX function by Ca^{2+} and Na^+ taking place in this loop derives from the impossibility to measure the capacity of exchange in his native form independently of the ionic regulation, these two remain closely intertwined. NCX1, found in numerous cell types such as cardiomyocytes, neurons and smooth muscle cells and first cloned isoform of the NCX family, has been extensively studied and a strong dependence to Ca^{2+} and Na^+ was shown. While thermodynamic considerations would suggest a low $[Ca^{2+}]_i$ to favor Ca^{2+} entry mode, a rise in $[Ca^{2+}]_i$ is actually required to operate in reverse mode. (35). This phenomenon has been attributed to the binding of Ca^{2+} ions at the two Ca^{2+}-binding domains CBD1 and CBD2 (36). Similarly, raising $[Na^+]_i$ activates the Ca^{2+} entry mode (37,38). An additional counterintuitive regulation, the so-called Na^+-dependent inactivation, enables the $[Na^+]_i$- and time-dependent reduction of the Ca^{2+} entry mode in response to an increase in cytoplasmic Na^+ (39) and is attributed to the CBD2 domain (36). Transmission of the ionic regulations to the transmembrane domain responsible for ion translocation is postulated to be carried out by the Catenin-like domain (CLD)(11,39,40).

Despite the low sequence homology between the cytoplasmic loop of the NCX isoforms (about 60%), the conservation of key residues leads to a similar structure of the

cytoplasmic loop among NCX isoforms with two distinct Ca^{2+}-binding domains CBD1 and CBD2 formed in β-sandwiches and arranged together in a antiparallel fashion (**Figure 1**) (30). In **chapter 2**, the modulation of NCX3 function by $[Ca^{2+}]_i$ and $[Na^+]_i$ was confirmed and further investigated. The large intracellular loop is responsible for the ionic regulation as can be seen from the distinct regulations of NCX3 variants, alternatively spliced in the CBD2. The Ca^{2+} uptake via the reverse mode of exchange requires a elevation in either $[Ca^{2+}]_i$ or $[Na^+]_i$ for activation and similarly to NCX1 and NCX2, NCX3 is subjected to Na^+-dependent inactivation. As with the reverse mode, the forward mode is highly dependent on the Na^+ and Ca^{2+} concentrations on either side of the membrane providing a fine-tuning of the Ca^{2+} fluxes. In all these aspects, alternative splicing of the NCX3 exchanger represents an additional regulatory mechanism for each isoforms of NCX.

Alternative splicing, variants and NCX activity

During alternative splicing, alternative exons are retained or spliced out of the messenger RNA, a process resulting in multiple variants. Splicing events are mainly controlled by the core splicing machinery together with multiple sequence-specific RNA binding proteins that are cell-type dependent. The unique sequence obtained after splicing confers distinct properties and capacities to each splice variant of the NCX family. More than twelve variants of the first isoform, NCX1, have been detected while no splicing event was observed for NCX2 (41). In the case of NCX3, since its first cloning in 1996 by Philipson et al (42), three variants have been described in rat (41). In the mice only two variants, NCX3-AC and NCX3-B, have been originally found and a third variant NCX3-BC was identified in **chapter 5** (**Figure 2**). Similarly to NCX1, exon A and B in NCX3 are mutually exclusive while exon C is optional in both isoforms. The so-called exons D, E and F are only present and spliced in NCX1(43).

The function of the two NCX3 variants, NCX3-B and NCX3-AC, has been dissected in **chapter 2** (**Table 1**) and great disparities in their capacities of exchange were brought to light as the two variants differ greatly in both forward and reverse mode. In term of primary amino acid sequence, NCX3-AC and NCX3-B differ for only 24 residues located within the CBD2, which alters tremendously their capacity of exchange and their regulation by ions. In reverse mode, NCX3-AC capacity of Ca^{2+} uptake is significantly higher (>80%) with a faster rate of uptake compared to NCX3-B. As for the forward mode, while both variants perform Ca^{2+} efflux, NCX3-AC has a 60% higher Ca^{2+} efflux in forward mode (44).

Table 1 Activation and modes of exchange of NCX3 depending on $[Na^+]$ and $[Ca^{2+}]$.

Mode of exchange	Extracellular conditions	Intracellular conditions			Activity	Remarks
	$[Na^+]_e$ or $[Ca^{2+}]_e$	Type of ions	Applied changes	Compound used		
Reverse mode	**$[Na^+]_e$ = 0 mM**	Resting levels	none	none	+/-	Solely in NCX3-AC with a partial activation
		$[Ca^{2+}]_i$	moderate increase	Thapsigargin	+	In both variants. Higher in NCX3-AC
		$[Na^+]_i$	increase	Ouabain	+++	In both variants. Higher in NCX3-AC
	$[Na^+]_e$ = 147 mM	$[Na^+]_i$	increase	Ouabain	++	In both variants. Higher in NCX3-AC
Forward mode	**$[Ca^{2+}]_e$ = 0 mM**	$[Ca^{2+}]_i$	Fast increase	Ionomycin	++	In both variants. Higher in NCX3-AC
	$[Ca^{2+}]_e$ = 1,5 mM	$[Ca^{2+}]_i$	moderate increase	Thapsigargin	+	Observed solely in NCX3-AC

Conditions necessary for the activation of NCX3 splice variants. These conditions were applied in **Chapter 2** by Fura-2-based $[Ca^{2+}]_i$ measurements and validated for the two variants tested: NCX3-B and NCX3-AC. With reverse and forward mode corresponding to Ca^{2+} uptake and efflux, respectively. Extracellular concentration of Na^+ and Ca^{2+} are reported as $[Na^+]_e$ and $[Ca^{2+}]_e$, respectively. Compounds used at a final concentration of 1 μM.

In terms of regulation by $[Ca^{2+}]_i$ and $[Na^+]_i$, NCX3-AC is activated at a lower threshold of $[Ca^{2+}]_i$ than NCX3-B expressed predominantly in the brain in both forward and reverse modes due to an increased affinity for Ca^{2+} of the CBD2 (44,45). Besides, NCX3-AC elicits an increased sensitivity to intracellular Ca^{2+} (44) caused by the structural stabilization of the Ca^{2+}-binding site of the CBD2 by Lys^{580} (**Table 2**). Consistently, in NCX1 the equivalent residue, Lys^{585}, is implicated in the stabilization of the Ca^{2+}-binding site (31,46) (**Figure 2**). As for the reverse mode, a rise in $[Na^+]_i$ triggers Ca^{2+} uptake in both NCX3 variants. However NCX3-AC presents a stronger sensitivity to intracellular Na^+, since in such

conditions a stronger Ca^{2+} influx occurs even in presence of extracellular Na^{+} (44). Moreover the Na^{+}-dependent inactivation of the reverse mode could be alleviated by NCX3-AC but not by NCX3-B, an effect presumably attributed to the interaction between the mutually exclusive exons A/B and the CLD. Similarly, in NCX1 splice variants, stronger Na^{+}-dependent inactivation was observed in the B-containing variant NCX1-BD, compared to the exon A-containing variants NCX1-AD and NCX1-ACDEF (47). Resemblances in the implications of exons A/B in NCX1 and NCX3 suggests that despite a low conservation of the mutually exclusive exons between isoforms (50% for exon B and 64% for exon A) and some variations in the degree of Na^{+}-dependent inactivation, their role in shaping the ionic regulations in particular the Na^{+}-dependence is conserved within the NCX family (40).

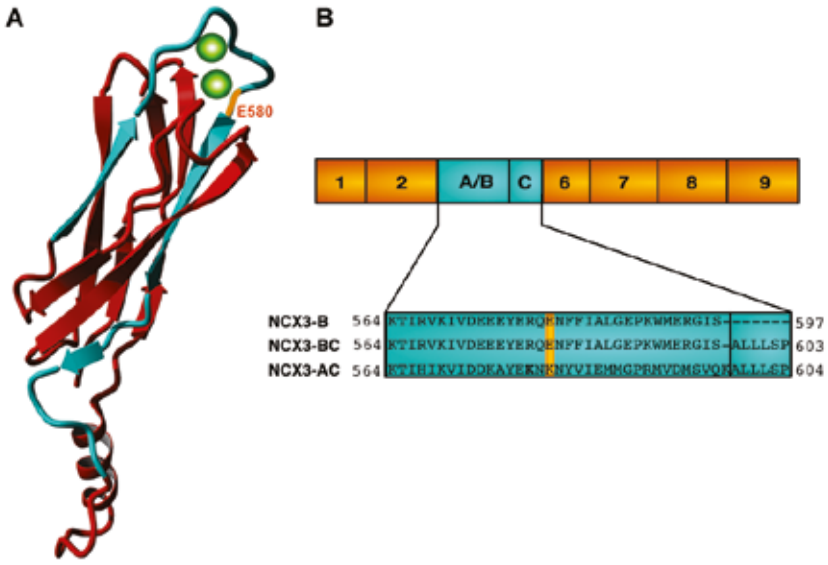

Figure 2 Alternative splicing of NCX3.

A, NMR structure of the Ca^{2+}-binding domain 2 of NCX3-B (PDB accession number 2LT9). Alternatively spliced region is shown in blue. **B**, The nine exons constituting the nucleotide sequence of NCX3 with a focus on the alternatively spliced region (blue) and its corresponding amino acids, coded by exons A, B and C. **A-B**, In orange is highlighted the position of the residue 580, responsible for the modulation of the sensitivity of NCX3 variants to Ca^{2+} (Lys^{580} in NCX3-AC)

The variant NCX3-BC reported in mice brain for the first time in **chapter 5** is similar in sequence to the variant NCX3-BC found in rat by Philipson *et al.* (41). Functional characterization of NCX3-BC in both species has not yet been performed. Nevertheless,

NCX3-BC is expected to have a strong Na^+-dependent inactivation alike NCX3-B. While NCX3-BC could be expected to have identical regulation by ions as NCX3-B, the exon C much as the entire cytoplasmic loop is subjected to post-translational modifications that confer additional regulation to NCX3-BC compared to NCX3-B such as its possible cleavage by the calpain proteases.

Phosphorylation by PKC and PKA

Among the most common post-translational modifications of eukaryotic proteins, phosphorylation leads to numerous regulations of targets proteins. In this regard, phosphorylation of Ca^{2+} transporters can affect its interactions with other proteins, plasma membrane stability, proteolysis or even directly influence its transport activity (48,49). As for the NCX family, multiple consensus sites for several kinases are present in the sequence, hence a large number of predicted phosphorylation sites for each isoform. The kinases predicted to phosphorylate NCX3 include two important kinase families activated by intracellular second messengers; the protein kinase A (PKA) activated by cyclic AMP (cAMP) and the protein kinase C (PKC) regulated by both Ca^{2+} and diacylglycerol (DAG). PKA and PKC are playing primordial roles in various signal transduction cascades and are implicated in many physiological processes such as vasoconstriction, glycogenolysis and lipolysis. PKA and PKC consensus phosphorylation sites share a requirement for basic residues upstream and hydrophilic residue downstream of the phosphorylated Serine/Threonine.

Contrary to PKA, for which phosphorylation of NCX1 remains controversial (49,50), phosphorylation of NCX1 by PKC has been previously shown, although its impact on NCX1 activity remains unclear. As for NCX3, data measured by means of fura-2 based Ca^{2+} imaging shown in **chapter 3** confirmed the modulation of NCX3 activity by both PKA and PKC phosphorylation (**Table 2**). The stimulation of PKC by phorbol 12-myristate 13-acetate (PMA) diminished the Ca^{2+} uptake of the NCX3-expressing HEK293T cells. On the contrary, PKA activation by forskolin increased significantly the capacity for Ca^{2+} uptake. PKC and PKA influenced in a similar manner the two murine variants tested, NCX3-B and NCX3-AC. For its part, Ca^{2+} efflux unaffected by PMA and forskolin provided evidence that PKA and PKC exert a direct action on the capacity of exchange of NCX3 independently of plasma membrane expression. Single mutation of potential phosphorylation sites by site-directed mutagenesis suggested that PKA and PKC act on NCX3 by phosphorylating the residues S524 and T529, respectively (**Table 2**). Both sites are located in a region of the CBD2 not subjected to alternative splicing. Therefore, the additional variant NCX3-BC is expected to be similarly affected by PKA and PKC. The two phosphorylation sites are diametrically opposed to the Ca^{2+}-binding site of CBD2 (**Figure 3**). Nevertheless, due to the antiparallel arrangement of the two CBD1 and CBD2 domains, phosphorylation is more likely to modulate the affinity of the CBD1 Ca^{2+}-binding sites. The close proximity of the two phosphorylation sites and the diametrically

opposite effect of the two kinases on the reverse mode of NCX3 attest to the complex interplay between the two CBDs and the transmembrane domains (**Figure 3**). Differences in proximity of the phosphorylated residues to the Ca^{2+}-binding site and possible interaction with the CLD might be accountable for this opposite effect of the two kinases. Nonetheless the determination of NCX3 structure in its phosphorylated state is necessary to fully comprehend these regulatory mechanisms.

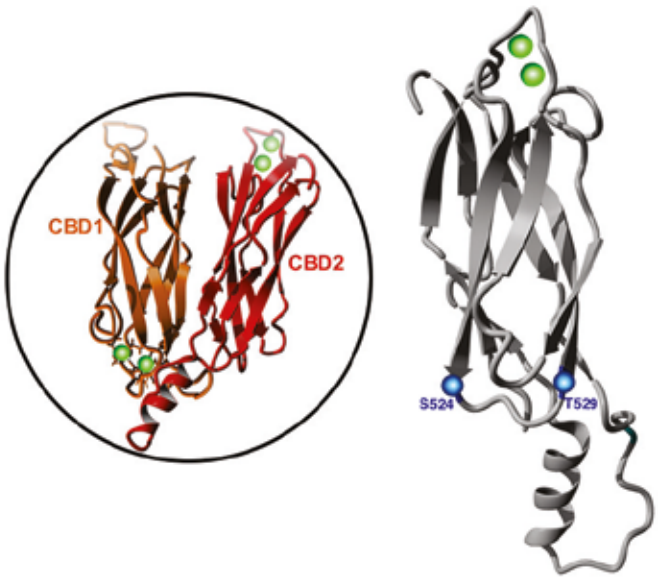

Figure 3 Phosphorylation sites of NCX3.

NMR structure of the CBD2 of NCX3-B where the localization of the two phosphorylation sites of NCX3 is highlighted in blue. The domain is rotated compared to the arranged form CBD1/2 (circle). The two residues S524 and T529, conserved among mammals, have been identified in **Chapter 3** as being responsible for PKA and PKC modulation of NCX3 activity, respectively. For clarity, the antiparallel arrangement of the two β-sandwiches of CBD1 and CBD2 is reminded (circle) to highlight the proximity of CBD1 Ca^{2+}-binding sites with the phosphorylation sites identified. (PDB accession number 2LT9)

Cleavage by the Ca^{2+}-dependent protease calpain

Modulatory proteolysis constitutes an additional post-translational regulation and impacts the length and/or the three-dimensional arrangement of the protein by a direct cleavage. In the past 20 years, research showed that as multiple proteases are primarily involved in proteolysis and protein degradation, several proteases are implicated in modulatory proteolysis that regulates the activity of the target proteins as it is the case

for the Ca^{2+}-dependent cysteine proteases of the calpain family (CAPN). Expressed throughout the entire body, calpains are involved in very diverse physiological processes such as cellular response to neuronal injury and gastric defense. Calpain proteases are inactive in their native conformation. Calpain proenzymes autolyse rapidly, upon a rise in $[Ca^{2+}]_i$, each isoforms requiring distinct Ca^{2+} levels to become catalytically active. Among their numerous substrates calpain proteins cleave multiple ion transporters and are strongly implicated in the regulation of ionic fluxes across the plasma and organelles membranes (endoplasmic, mitochondrial…). **Chapter 4** provides evidence for a variant-dependent regulation of NCX3 by the Ca^{2+}-dependent protease calpain 1 (CAPN1) and identified NCX3 as a novel target of the muscle-specific calpain, CAPN3 (**Table 2**).

In neurons, specific cleavage of NCX3 was previously reported following glutamate and β-amyloid peptides exposure (51). This cleavage, associated with a hyperfunctionality of the exchanger in the reverse mode lead to a significant increase in Ca^{2+} uptake. Consistently, data presented in **chapter 4** indicates a stronger capacity for Ca^{2+} influx in presence of calpain. This effect was not restricted to neuronal calpains, as similar effect was induced by the muscle-specific isoform of calpain, CAPN3. Importantly, while both NCX3-B and NCX3-AC were subjected to Fura-2 based Ca^{2+} imaging, sensitivity to CAPN1 and CAPN3 was restricted to NCX3-AC. Removal of the exon C from NCX3-AC by mutagenesis abolished CAPN3-mediated increase of activity and thereby confirmed the implication of this exon in the sensitivity to calpain, possibly by a direct cleavage since the increase activity of NCX3 was lost during expression of the catalytically inactive CAPN3. Similarly, the variant-specific decrease in Ca^{2+} uptake capacity observed for NCX3-AC in presence of the endogenous CAPN1 inhibitor calpastatin or the silencing of CAPN1 indicated a stronger sensitivity for the C-containing exons. This further suggests that the variant NCX3-BC described in **chapter 5** would be, similarly to NCX3-AC, more prone to calpain cleavage than NCX3-B.

Fura-2 based Ca^{2+} imaging measurements of NCX3 performed in **chapter 4** in presence of the catalytically inactive CAPN3 demonstrated a direct cleavage of the exchanger within the exon C located in the CBD2 without excluding additional cleavage sites. In fact, Nicotera's group (52) identified several cleavage sites in NCX3-B in the brain located on either side of the CBD1 and for which cleavage would result in the loss of the entire domain (**Table 2**). Both results do not exclude each other as **chapter 4** postulates a cleavage of NCX3 in exon-C containing variants, namely NCX3-BC in the brain as reported in **chapter 5**. Nicotera's group investigated exclusively the intracellular loop of NCX3-B and therefore could not detect the cleavage site postulated in exon C. These differences might be indicative of various sensitivities or a joint action between the different sites reported. This discrepancy might as well be caused by differences in cell types investigated causing distinct protections of the cleavage sites by post-translational modifications as it is seen with phosphorylation and calmodulin binding of NCX. On the other hand, one might be puzzled by the capacity of the cleaved NCX3 to retain its

Table 2 Overview of the regulatory factors of NCX3.

Type of regulation	Regulation		Effect on NCX3 activity	Residues targeted	Remarks / References
	Type	Actors			
Ionic	**$[Ca^{2+}]_i$**	↗	activation	Lys^{580}	Activation of forward or reverse mode dependent on $[Ca^{2+}]_i$ (**Chapter 2**)
	$[Na^+]_i$	↗	activation inhibition	exons A/B/C	Activation until a certain extend At high $[Na^+]_i$ NCX is inhibited
	$[H^+]_i$	↗	Inhibition	CBD1/2	Competition with Ca^{2+} for binding at CBD1/2 (53-55)
Post-translational modifications	**Phospho-rylation**	PKA	↗	S524	Increase NCX3 reverse mode (**Chapter 3**)
		PKC	↘	T529	Decrease NCX3 reverse mode (**Chapter 3**)
	Cleavage	Signal peptidase	Insertion	1-30 at the N-terminal	Predicted by SignalP 3.0 Insertion in the plasma membrane
		Calpain 1, 2, 3	↗	• Leu^{602} * • Lys^{370} • Asn^{504} • Arg^{510} • Val^{512}	Hyperactive reverse mode *Leu^{602} tested in functional studies (**Chapter 4**) Other sites identified by cleavage *in vitro* of NCX3 intracellular loop (52)
	Dimerization	-	Trafficking	CBD1	Postulated to participate with Ca^{2+} in trafficking to the plasma membrane (56)

Overview of the regulatory mechanisms of the exchange activity of NCX3 by intracellular ionic concentrations and post-translational modifications.

exchange activity particularly due to the separation of the intracellular loop holding together the two clusters of transmembrane domains. In this respect, the first mechanistic studies of NCX, already revealed that disruption of the cytoplasmic loop, for instance

following α-chymotrypsin treatment, still enabled proper Na^+-Ca^{2+} exchange although ionic regulation is lifted. This capacity is attributed to a close proximity of the transmembrane segments and the tightly packed core containing eight of the 10 transmembrane helices as indicated by the recent cristallization of the transmembrane region of the exchanger (29). Finally, the cleavage of the site located in exon C and identified in **chapter 4** would disrupt the CBD2 Ca^{2+}-binding site and result in a loss of interaction between the CBD2 and the downstream CLD. This loss would therefore abolish the Na^+-dependent inactivation as it is observed in NCX3-AC. For this reason the higher capacity of NCX3-AC for Ca^{2+} uptake in reverse mode compared to NCX3-B can not be solely attributed to the alternative splicing of the mutually exclusive exon A/B and is more likely to result from a combined effect of the modulation of NCX3 activity by Na^+ and Ca^{2+} of exon A together with an increased capacity due to the cleavage of exon C upon $[Ca^{2+}]_i$ increase and calpain activation. In this context, the functional characterization of the newly identified variant NCX3-BC compared to NCX3-B would be of great interest to confirm the role of exon C in the regulation of NCX3.

Intracellular loop: adaptive regulation to (patho) physiological processes

Tissue expression

Splicing events, by modifying the messenger RNA coding for a given protein, shape the amino-acid sequence of each protein to match its tissue requirements. In the case of NCX3, alternative splicing confers distinct properties and capacities to each splice variant with respect to ionic regulation and post-translational modifications. Therefore, a better understanding of the tissue distribution of NCX3 splice variants is of great interest to comprehend the implications of NCX3 to meet the requirements of the different tissues. Numerous studies investigated alternative splicing events to unravel the factors that enable tissue-specific splicing. Although several family of proteins have been implicated in this process in several tissues such as the exonic/intronic splicing silencers/enhancers and the SR (Ser-Arg) nuclear factors (57,58), none of them has been directly correlated to the splicing of NCX isoforms. Given the similarity of sequence and the presence of mutually exclusive exons A and B in both NCX1 and NCX3, the splicing of both isoforms is most likely guided by a similar splicing protein and/or machinery.

Data presented in **chapter 2**, established the predominance of the splice variant NCX3-AC in mice skeletal muscle, consistently with its expression in rat muscle (41). Furthermore, the study demonstrated the 6 to 10-fold enrichment of NCX3 expression in slow-twitch muscle fibers compared to mixed and fast-twitch fibers. The ratio calculated in **chapter 4** confirmed the predominance of NCX3-AC in all fiber types as this variant represented 72% of the total NCX3 in soleus and more than 94% in extensor digitorum

longus (EDL), gastrocnemius and tibialis anterior. Nevertheless the high expression of NCX3 found in the fast-twitch muscle (EDL) in **chapter 4** is in disagreement with the expression levels found in **chapter 2**. In addition, NCX3 expression in mixed fibers varies between the two measurements. This puzzling difference might well be due to the use of the "housekeeping" gene, GAPDH, for normalization of the NCX3 expression performed in **chapter 4**. Absolute quantification is more suitable to direct comparison of different tissues and/or organs, because of the discrepancy in expression of "housekeeping" genes such as GAPDH and β-actin between tissues, presumably because of their different energetic status, metabolism and cellular proliferation (59,60). However, GAPDH expression was assumed to be constant in similar tissues such as skeletal muscles types. This assumption has been recently rejected by evidences of the fiber type dependence of GAPDH expression (61). Normalized expression of NCX3 in skeletal muscle shown in **chapter 4** is therefore less relevant than results shown in **chapter 2** for which total NCX3 measurements are consistent with the expression of NCX3-AC together with NCX3-B. As for NCX3-BC, the expression of the newly described variant has not been measured in skeletal muscles, NCX3-BC being unknown in mice until its recent description as indicated in **chapter 5**. Contrary to primers used in **chapters 4 and 5**, primers detecting NCX3-B and NCX3-AC in **chapter 2** were not tested for unspecific amplification of NCX3-BC. Therefore, NCX3-BC could contribute to the measure of one of the two variants presented in **chapter 2**, most likely in a negligible extent, as this variant was not detected in rat skeletal muscle.

With respect to the murine brain, expression of NCX3 and its variants has been first determined in **chapter 2**, where high expression of NCX3 could be measured with 6.5 to 68–fold enrichment compared to skeletal muscle. Moreover, NCX3-B appeared to be highly expressed compared to NCX3-AC. Importantly, the study performed in **chapter 5** represents the first investigation of NCX3-BC and measured, by absolute quantification of messenger RNA, the expression of NCX3 variants in brain regions of two independent WT mice strains. NCX3-BC could be detected in every region although from 1.7 to 6.3-fold lower compared to NCX3-B. Despite variations between the two mouse strains, a similar NCX3-B distribution was observed with a higher expression in brain stem, cerebellum and striatum compared to prefrontal, parietal cortex and hippocampus. NCX3-BC depicted a similar pattern (**Table 3**). Neuronal detection of NCX3-AC in **chapter 2** indicated a higher expression than measured in **chapter 5**. This effect could well be linked with unspecific detection of NCX3-BC by the primers used in the former study, as in subsequent investigations, performed with highly specific primers, NCX3-AC expression was negligible in any regions and mice strains tested. To conclude, the predominance of exon-B-containing variants in the brain and restriction of NCX3-AC to the skeletal muscle demonstrates the variant specific tissue distribution of NCX3. Similarly to NCX1, each splice variants elicits unique ionic regulation providing a better adaptation of NCX3 to each tissue and suggests new implications for NCX3 in physiological processes in health and disease.

Intracellular, sarcoplasmic and mitochondrial Ca^{2+} levels

The study of the forward and reverse exchange activity of NCX3 by Fura-2 Ca^{2+} recordings evidenced the inactive state of NCX3 in resting conditions as firstly reported in **chapter 2** and confirmed in **chapters 3 and 4**. Investigations of NCX3 activation, consistently with previous examinations of NCX1, corroborated the absolute requirement for either a $[Ca^{2+}]_i$ and/or $[Na^+]_i$ elevation (35). Furthermore, NCX3-AC, having the lowest requirement for $[Ca^{2+}]_i$ and $[Na^+]_i$, is only partially active in absence of extracellular Na^+, demonstrating that intracellular requirement can not be fully lifted by extracellular ionic concentration. Thereby these properties limit NCX roles to physiological situations implicating dynamic changes in intracellular ionic levels. In **chapter 2**, both modes of exchange have been separately examined to obtain a better understanding of their activation in physiological situations. Activation of reverse exchange is dependent on $[Ca^{2+}]_i$ and $[Na^+]_i$ while the forward mode depends exclusively on $[Ca^{2+}]_i$. Upon $[Ca^{2+}]_i$ elevation, the mode of exchange favored is determined by extracellular Na^+ levels. Lower $[Na^+]_e$ will triggers Ca^{2+} uptake while in normal serum Na^+ levels (135 to 145 mM), Ca^{2+} efflux is activated. Because of these properties, researchers have for long thought that NCX exerted its physiological role solely via its forward mode, particularly in excitable tissues by extruding Ca^{2+} across the plasma membrane following an action potential as the electrochemical gradient across the plasma membrane would not favor a reversal of NCX.

Reversal of NCX has been matter of debate in the past decades, as several groups observed NCX Ca^{2+} uptake in both pathological and physiological conditions (62-64) while it was originally thought that the electrochemical gradient across the plasma membrane in physiological conditions could not favor NCX reversal. In this regard, Ca^{2+} uptake dependence to $[Na^+]_i$ is of great importance, as sufficiently high $[Na^+]_i$ would thermodynamically favor reversal of NCX at the resting membrane potential (65) As evidenced in **chapter 2**, elevation of $[Na^+]_i$, generated by incubation of HEK293T cells with the Na^+-K^+ ATPase inhibitor, ouabain, induced Ca^{2+} uptake via reverse exchange of NCX3 at physiological serum Na^+ levels. $[Na^+]_i$ is dynamic during many processes in particular in excitable tissues, as action potentials triggers a Na^+ transient, such as in neurons and skeletal muscle where NCX3 is typically expressed. If in most cases, $[Na^+]_i$ is quickly restored in excitable tissues by the Na^+-K^+ ATPase, a prolonged and severe $[Na^+]_i$ rise can occur in physiological situations such as during a prolonged exercise of slow-twitch muscles, the bursting in motor neurons and the long-term potentiation of hippocampal neurons (62,66). These modifications in $[Na^+]_i$ would enable reversal of the exchanger and induce Ca^{2+} uptake (**Figure 4**).

In addition to reversal of activity, NCX is localized at the plasma membrane next to the junctional sarcoplasmic/endoplasmic reticulum (SR/ER) in numerous cell types (67-71) and its capacity to regulate Ca^{2+} levels in the ER and SR subsequently to the reversal of its mode of exchange has been confirmed in multiple occasions e.g. in smooth muscle cells (72-74), in postnatal cardiomyocytes (75,76) in neurons during hypoxia (77,78), and in

failing cardiomyocytes (79). As for NCX3 in reverse mode, the exchanger could influence the ER Ca^{2+} pool in multiple ways. First, the influx of Ca^{2+} by the reverse mode of NCX3 could trigger the Ca^{2+} release from the SR, by contributing to the Ca^{2+}-induced Ca^{2+}-release (CICR) together with the plasma membrane L-type Ca^{2+} channels as it is observed for NCX1 in cardiac myocytes (64,80). Because CICR does not contribute to Ca^{2+} release in skeletal muscle, where NCX3 is highly expressed, the direct participation of NCX3 in CICR is very unlikely (81). Secondly, an opposite relationship has been postulated for NCX1 with regard to the store-operated Ca^{2+} entry (SOCE), suggesting that NCX-mediated Ca^{2+} entry would be directly induced by ER/SR Ca^{2+} release. SOCE has been originally described as a ubiquitous pathway in non-excitable tissues for store-dependent Ca^{2+} entry. One of its main functions lies in its capacity to replenish ER Ca^{2+} store. In the past 15 years, convincing results have indicated that SOCE mechanisms can be extended to excitable tissues such as skeletal muscle (82), neurons (83), and vascular smooth muscle cells (VSMC) (84). Furthermore, Stim and Orai, main actors of the SOCE pathways are also expressed in excitable tissues. The first argument in favor of NCX Ca^{2+} uptake being part of SOCE is that NCX1 and NCX3 are both activated by store depletion following SERCA ATPase inhibition or RyR stimulation. However no valid experiments has proven yet that NCX activation truly results from ER Ca^{2+} depletion and not cytoplasmic elevation of Ca^{2+}. Additionally, several studies reported the close proximity of Orai with NCX in SMC, and some data suggested their coupling at the plasma membrane (84). Furthermore, refilling of the SR Ca^{2+} levels has been observed in several cell types expressing NCX3 as in slow-twitch fibers (85) osteoclasts (86) and neurons (25). However exact mechanisms by which NCX would be part of the SOCE system remain extremely unclear. On the contrary, some studies provided evidence that NCX is not directly implicated in SOCE in cardiomyocytes (87) but rather activated by the store-operated channels as evidenced by Blaustein's group. Interestingly, by examining the role of NCX in relation to the store operated Ca^{2+} entry in vascular smooth muscle cells (VSMC), Blaustein's group proposed two Ca^{2+} permeable entry, the first one, as previously described, would consist of a SOCE pathway with the transient potential (TRP) store-operated channel (SOC) that enables not only Ca^{2+} but also Na^{+} influx. This latter Na^{+} influx mediated by SOC channels would induce NCX activation in its reverse mode, hence this second Ca^{2+} entry through NCX, refilling Ca^{2+} in the SR (**Figure 4**) (88). Such hypothesis has been later confirmed in VSMC (89) and airways SMC (90) and hold truth as well in epithelial cells (91) and platelets (92,93) and is consistent with the increased colocalization between SERCA and NCX upon SR depletion in VSMC (94). As for skeletal muscle, neurons and other cell types where NCX3 is highly expressed, the role of SOCE is until now unclear. In the light of this recent hypothesis, investigation of Na^{+} influx by SOC and its potential role in activating NCX3 reverse mode might well unravel new regulatory pathways of physiological mechanisms.

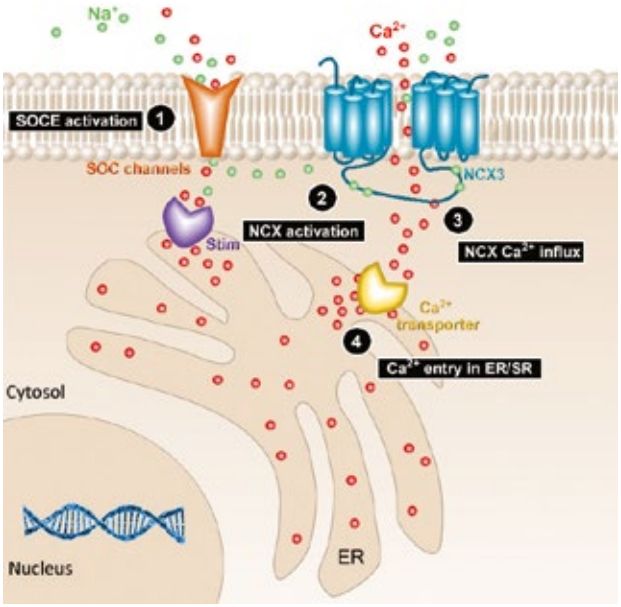

Figure 4 Proposed molecular mechanisms for Ca^{2+} refilling of the ER/SR via NCX3.

Schematic representation of the postulated pathway implicated in the refilling of the ER/SR Ca^{2+} store via the reverse mode of NCX3. First, depletion of Ca^{2+} from the ER/SR activates SOC channels thanks to their proximity. While the resulting Ca^{2+} influx is taken up by the ER/SR through Stim, Na^+ influx participates to increase $[Na^+]_i$ and to activate NCX3 in its reverse mode via Na^+-binding at the CBD1-CBD2. NCX3-mediated Ca^{2+} uptake is transported into the lumen of the ER/SR via an unknown mechanism that would presumably consist of a Ca^{2+} transporter such as SERCA located within close proximity of NCX.

In the past 10 years, in addition to the mitochondrial exchanger NCLX (22), NCX isoforms have also been hypothesized to participate and interfere with mitochondrial processes. In particular, NCX3 has been demonstrated to be implicated in the mitochondrial Ca^{2+} extrusion pathways during hypoxia (12,95). Very recently, NCX3 was further shown to reduce the mitochondrial Ca^{2+} concentration ($[Ca^{2+}]_{mito}$) during preconditioning protecting neurons during injury (78). This crucial mechanism in stress conditions remains poorly understood but would, most likely, involve a relationship between the plasma membrane NCX and the mitochondria through a common interacting partner or a signaling pathway that might implicate as well ER Ca^{2+} store. A direct localization of NCX3 at the outer membrane of the mitochondria as previously proposed is less probable as the presence of multiple α-helical proteins is rather rare at the outer membrane of the mitochondria and requires a pre-sequence recognized by the

translocase of the outer membrane (96) that is absent in NCX3. In fact, the first transmembrane segment of NCX3 presumably serves as a signal peptide routing this polytopic protein to the plasma membrane, similarly to NCX1.

The knowledge gained in this thesis on the regulation of the Na^+-Ca^{2+} exchange capacity in both forward and reverse mode together with the novel functions proposed for NCX3 in Ca^{2+} handling throughout the cell participate to a better understanding of the role of NCX3 in skeletal muscle and neuronal cells where the exchanger is highly expressed. In such tissues, the variant-specific distribution reported in **chapters 2 and 5** together with the newly described regulatory mechanisms of each variant reported in **chapters 2**, **3 and 4** suggest novel physiological implications for the exchanger in both tissues.

Novel implications in skeletal muscle physiology

Since its discovery, the NCX family has been postulated to participate in the Ca^{2+} clearance in skeletal muscle fibers following contraction, by extruding Ca^{2+} across the plasma membrane jointly with the re-uptake of Ca^{2+} by the SERCA ATPase in the SR to enable muscle relaxation. However, very little information is available on the role of each isoform and splice variant in this process. Both NCX1 and NCX3 have been repeatedly detected in skeletal muscle fiber (41,97). Messenger RNA expression presented in **chapters 2 and 3** indicated the enrichment of NCX3-AC in all skeletal muscle. The activation of NCX3-AC in its Ca^{2+} efflux mode at low levels of Ca^{2+} as demonstrated in **chapter 2** corroborates with its postulated role in relaxation. Nevertheless, if solely responsible for Ca^{2+} extrusion, a higher NCX3-AC expression would be expected in muscle predominantly constituted of fast-twitch fibers, such as EDL, where fast contraction/relaxation process occurs. On the contrary, higher expression of NCX3 is reported in slow-twitch muscles suggesting the implication of an additional NCX isoform in Ca^{2+} efflux, NCX1. In this regard, NCX1-ACDEF is the predominant variant of NCX1 among the four detected in muscles (NCX1-ACDEF, NCX1-BDE, NCX1-BCD, NCX1-BD) and the only A-containing variant (41). As greater activation of NCX1 by Ca^{2+} is observed in A-containing variant compared to the B-counterparts (47), the presence of the exon-A containing variant may suggest capacity for the forward mode comparable to NCX3-AC. Furthermore, NCX1 expression is higher at both protein and RNA levels in fast-twitch and mixed muscle fibers compared to slow-twitch muscle (97) which would compensate for lower NCX3 expression in these fiber types.

NCX3-AC enrichment in slow-twitch muscle, combined with its properties in reverse mode, evokes additional roles in Ca^{2+} homeostasis for the variant. During action potential (AP), the acetylcholine released from the neuromuscular junction (NMJ) triggers at the sarcolemma a transient Na^+ current by the voltage-dependent Na^+ channel $Na_{v1.4}$ (98,99) leading to depolarization event. This event activates the voltage dependent Ca^{2+} channel DHPR located at the t-tubule and mechanically coupled to RyR at the SR membrane and

results in SR Ca^{2+} release and thus initiates the contraction. During a single AP, rise in $[Na^+]_i$ is quickly compensated by K^+ efflux and intracellular resting levels are quickly reestablished by Na^+-K^+ exchange via Na^+-K^+ ATPase so that the reverse exchange of NCX is not activated. However in slow-twitch muscle, prolonged exercise induces over time a significant rise in $[Na^+]_i$. Murphy *et al.*, have shown that after a 60-min training, $[Na^+]_i$ is increased of 80% in soleus, while this effect is absent in EDL (100). Under those conditions, $[Na^+]_i$ would enable reversal of the NCX3-AC to favor Ca^{2+} uptake as indicated by the data presented in **chapter 2**. Ca^{2+} influx observed in slow-twitch muscle has been linked to the higher resistance of slow-twitch fibers to muscle fatigue (85,101). This beneficial effect has been fully attributed to NCX (85) and the increased fatigability observed in $NCX3^{-/-}$ mice suggests a direct involvement of NCX3 in this mechanism (102). In this pathway, NCX-mediated Ca^{2+} influx would be accountable for the strengthening of the contraction by a stronger Ca^{2+} recruitment and would enable the replenishment of SR Ca^{2+} store.

In some cases the repeated elevation in triadic Ca^{2+} levels occurring during a prolonged exercise, in particular an eccentric exercise, leads to uncouple the DHPR and the RyR (103). This uncoupling, also called excitation-contraction (EC) uncoupling, triggers the depletion of Ca^{2+} store that underlies muscle fatigue and weakness (104), a phenomenon also observed upon uncoupling induced by pathological RyR mutations in ryanodinopathies (104). Upon EC uncoupling, Ca^{2+} release in the sarcoplasm activates the Ca^{2+} dependent protease CAPN1 having many substrates including NCX3-AC. The cleaved NCX3-AC exchanger showed higher capacity of Ca^{2+} uptake with a high sensitivity to Na^+ levels, as reported in **chapter 4**, and performs stronger Ca^{2+} increase therefore having an increased efficiency to replenish the Ca^{2+} store. Such phenomena would be protective by an attempt to counteract the store depletion and more prone in slow-twitch muscles, muscles often subjected to prolonged exercise. Consistently, a similar effect of CAPN1 on SR Ca^{2+} content is observed during cardiac dysfunction (105). Furthermore, in Duchenne muscular dystrophy mice model (Mdx), an increased activity of SOCE has been observed that leads to CAPN1 activation (106). In such conditions, a significant enhancement of Ca^{2+} entry via Na^+-Ca^{2+} exchange is detected in Mdx myotubes together with an upregulation of NCX3 and an increased sarcoplasmic Ca^{2+} (24,106). Altogether, these data corroborates the hypothesis mentioned above according to which the activation of the reverse mode of NCX3, as a consequence of Ca^{2+} and Na^+ entry via the SOCE and CAPN1 activation, contributes to the increase in the SR Ca^{2+} storage (**Figure 4**). In such pathology a better understanding of the role of NCX3 in relation with the SR would be of great importance. In addition to muscle fatigue, this could suggest a beneficial effect of NCX3 in pathologies where failure in EC coupling is observed such as ryanodinopathies as well as age-related decline in muscle force.

In addition to CAPN1, NCX3-AC is a target for CAPN3 cleavage, as demonstrated in **chapter 4**. CAPN-mediated regulation of NCX3 seems to occur through the same site for

CAPN1 and CAPN3 and thereby has similar effect on the exchange capacity of NCX3. Mutations of CAPN3 affecting its catalytic activity cause the limb-girdle muscular dystrophy 2A (LGMD2A). Although the conditions under which CAPN3 is activated are still controversial (107,108), the decrease in sarcoplasmic Ca^{2+} content and the increased phenotype in slow-twitch compared to fast-twitch muscles reported in CAPN3 KO mice could well be linked with an impaired refilling of the SR caused by a loss of NCX3-AC cleavage (109,110). In this regard, the investigation of the role of NCX3 on restoring SR Ca^{2+} levels in muscle fiber is crucial to conclude on its involvement in muscular pathologies such as the LGMD2A.

Finally, during the fight-or-flight response occurring during stress and intense exercise, the activation of PKA caused by epinephrine release, enhances Ca^{2+}-mediated contraction by modifying the activity of numerous Ca^{2+} transporters (111). In this regard the increased activity of NCX3 variants upon PKA activation reported in **chapter 3** suggests an increased Ca^{2+} uptake via NCX during the fight-or-flight response. It has to be noted that the PKA-mediated increase of the reverse mode is exclusively present upon high $[Ca^{2+}]_i$ together with low extracellular Na^+ levels. Therefore, for this mode to be activated would imply a decrease in plasma $[Na^+]$ or a decrease in $[Na^+]$ in the vicinity of the sarcolemma. In absence of information concerning these extracellular $[Na^+]$ during fight-or-flight response it is not possible to conclude on the participation of the phosphorylation of NCX3 in the enhancement of Ca^{2+}-mediated contraction.

Novel physiological implications in the central nervous system

In **chapter 5**, the absolute quantification of NCX3 splice variants in mice brain indicated the expression of exon-B-containing variants exclusively. In all regions investigated, both NCX3-B and NCX3-BC were detected, NCX3-B being predominant. NCX3 expression in adult brain suggests physiological implications in addition to the previously reported role in cell differentiation (112-115). Similarly to skeletal muscle, the Na^+ transient via $Na_v1.1$, initiating the neuronal depolarization is not sufficient to trigger the activation of NCX3 in its reverse mode. Furthermore, the reversal of NCX3 is less likely to occur than in skeletal muscle given the low sensitivity of exon-B-containing variants to $[Na^+]_i$, as reported in **chapter 2**. Subsequently to the Na^+ transient, elevation in $[Ca^{2+}]_i$ enables neurotransmitter release at the synaptic nerve terminals. This rise in absence of changes in $[Na^+]_e$ triggers the activation of Ca^{2+} efflux via the forward activity of NCX. In this respect, NCX3-B could well participate in this process in combination with other NCX isoforms in order to maintain Ca^{2+} balance and enable subsequent action potential.

The roles of NCX3 might also differ among CNS regions due to diversity in action potential and physiological functions. This possibility has been investigated solely in hippocampus, the region involved in memory processes. NCX3 quantification in hippocampus reported in **chapter 5** indicated similar expression compared to other regions, contrary to the enrichment observed in earlier investigations (116). Nevertheless,

the significant impairment in spatial learning and memory observed in NCX3 KO mice and the enhanced memory resulting of the knockout of the transcriptional repressor of NCX3, DREAM, demonstrates specific functions for NCX3 in hippocampus (117,118). In this regard, the synaptic enhancement occurring in hippocampus also known as long-term potentiation (LTP) is directly involved in learning and memory formation (119,120). The molecular mechanisms behind LTP consist of a high frequencies neural activity leading to NMDA-mediated Na^+ transient inducing a long-lasting increase in $[Ca^{2+}]_i$ at postsynaptical terminal causing enhanced transmitter release (121). Interestingly, during LTP induction considerable Na^+ transient (over 100 mM) is measured locally, which rises threefold what is observed in short synaptic bursts (66). Therefore, hippocampal LTP provides optimal conditions for the reversal of NCX3 exchange activity. Additionally, large elevation of $[Ca^{2+}]_i$ during LTP triggers the activation of multiple kinases such as PKA and CaMKII. The stimulation of NCX3 capacity in the reverse mode by PKA, as indicated in **chapter 3**, further enhances its capacities and could contribute to sustain the Ca^{2+} requirement during LTP.

Mechanisms of LTP are in fact very similar to the mechanisms underlying epileptogenesis, as both require high-frequency neural activity (122). Furthermore, NCX3 appears to be implicated as well in pathologies where hyperexcitability state is observed such as epilepsia and seizures. Early, the importance of Na^+ and Ca^{2+} levels has been evidenced as both low $[Ca^{2+}]_e$ and high $[Na^+]_i$ induces seizures (123,124). Recently, Martinez *et al.* showed that the blockade of NCX3 reduces the severity and delays significantly the seizures (125,126). Detrimental role of NCX3 in such pathologies is presumably due to the inappropriate and untimely activation of several mechanisms of LTP, that are likely to implicate NCX3; an hypothesis consistent with the fact that the lowest seizure threshold of the brain is located in the hippocampus and with the recurrent memory impairment caused by seizures (127,128). On the other hand, in the light of the numerous cases of crosstalk of NCX3 with the SR/ER and the importance of Ca^{2+} refilling of the ER during LTP in hippocampus, the investigation of the possible implication of the NCX in ER/SR refilling is of great interest in the understanding of LTP molecular determinants as well as the development of therapies for pathological impairment of ER Ca^{2+} replenishment such as presenilin mutations causing early onset familial Alzheimer's disease where capacitative Ca^{2+} entry is impaired.

With regard to pathological situations, the activation of NCX3 upon strong variations of $[Na^+]_i$ or $[Ca^{2+}]_i$ make it a potent actor during stress conditions (**Figure 5**). The activation of NCX3 and NCX1 in hypoxia and anoxia, reported many times, has been linked with a decrease in hypoxia-induced cell death (12,129-132), a neuroprotective effect attributed solely to NCX3 and confirmed by the accentuated brain damage following ischemia observed in NCX3 KO mice (117,132). In hypoxia the rise in intracellular Na^+ due to a Na^+ influx via the voltage-dependent Na^+ channels, participates in the activation of NCX3 in its reverse mode and could well be responsible for the NCX-mediated secondary Ca^{2+}

rise observed following initial Ca^{2+} entry (133). Recently, Annunziato's group reported the calpain-mediated cleavage of NCX3 induced by amyloid β_{1-42} toxicity in mice and human (25,134). Interestingly, in excitotoxic conditions *in vivo* the Ca^{2+}-dependent proteases exclusively cleaved the third isoform of the NCX family. The initial study reporting this cleavage postulated a detrimental effect of NCX3 arguing for a defect in Ca^{2+} extrusion that would participate in the Ca^{2+} rise occurring upon stress conditions and precipitate cell death (52). However subsequent studies on the cleaved exchanger and its capacities of exchange evidenced (25) a neuroprotective effect for NCX3 as the exchanger showed hyperactive capacity in its Ca^{2+} uptake mode of exchange. These results, consistently with the CAPN1-mediated effect reported in **chapter 4**, suggest that NCX3 would participate to ER Ca^{2+} refilling and delay toxicity-induced cell death. This hypothesis is consistent with observations made 20 years ago on human post-mortem Alzheimer's disease brain and reporting the increased reverse activity of NCX (135) (**Figure 5**).

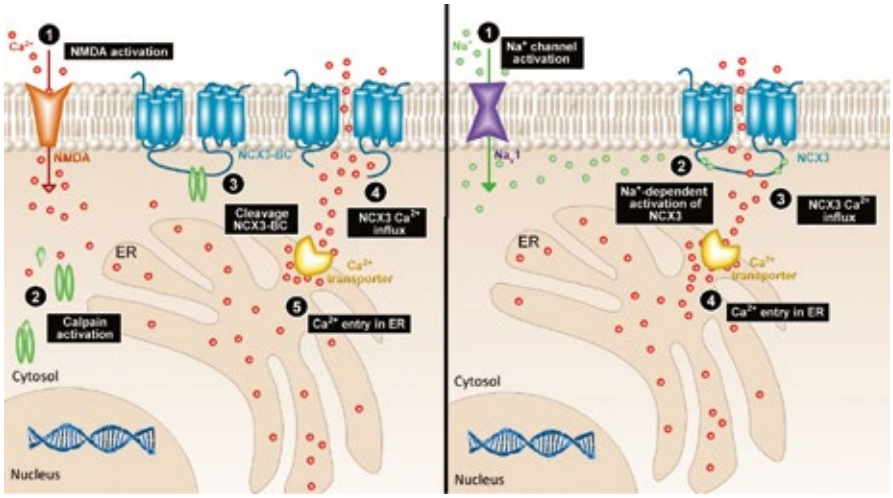

Figure 5 Postulated pathways for the neuroprotective role of NCX3 in hypoxic conditions.

Schematic representation of cellular pathways in hypoxic conditions leading to NCX3 activation due to primary Ca^{2+} and Na^+ entry. Left panel depicts the activation of the NMDA receptor upon hypoxic excitotoxic conditions triggering a primary Ca^{2+} entry into the cytoplasm, responsible for the activation of cytoplasmic proteases calpain 1 and 2. The cleavage by calpain of NCX3-BC (presumably at Leu^{602}) together with the rise in $[Ca^{2+}]_i$ triggers the reverse mode of NCX3. NCX3-mediated influx of Ca^{2+} intracellularly is transported into the ER. The right panel presents the Na^+ influx triggered in hypoxic conditions through the plasma membrane voltage-gated Na^+ channels. Intracellular Na^+ influx activates NCX3 by Na^+-binding at the intracellular loop and initiates the reverse mode of exchange. Ca^{2+} is then transported across the ER membrane by one of the ER Ca^{2+} transporters.

The study performed in 2005 by Carafoli's group reported for the first time the cleavage of NCX3 and identified *in vitro* several cleavage sites for calpain in the exchanger, leading to the disruption of the CBD1 of the intracellular loop (52). Data presented in **chapter 4** suggest that exon C-containing variants carry an additional calpain cleavage site within the CBD2 of the intracellular loop. This site is implicated as well in a calpain-mediated increase of the reverse mode capacity and is presumably more prone to cleavage (**Figure 5**). This cleavage site, besides providing an explanation for the evolutionary splicing of this 6-amino acids coding exon, could be of great importance in pathological situations that triggers calpain activation. In neurons, this would imply a higher capacity of cleavage for NCX3-BC providing a lesser vulnerability to injury. According to the absolute quantification reported in **chapter 5**, NCX3-BC expression in the different brain regions (**Table 3**) is inversely proportional to the vulnerability to ischemia observed in these regions, as hippocampus and neocortex are more sensitive than the striatum and the cerebellum; all regions in turn being by far more vulnerable to ischemia- induced damage than the brain stem (136,137). This correlation would suggest the involvement of the variant NCX3-BC in the resistance to hypoxia that has yet to be proven.

Table 3 NCX3 expression and resistance to hypoxia-induced damage in WT mice brain regions.

Brain regions	Expression NCX3 (% BS)	Expression NCX3-B (% BS)	Expression NCX3-BC (% BS)	Sensitivity to hypoxia
Hippocampus	37	75	**11**	
Neocortex	53	115	**17**	
Striatum	80	105	**57**	
Cerebellum	84	145	**55**	
Brain stem (BS)	100	100	**100**	

Percentages of RNA expression of NCX3 splice variants in various brain regions of C57BL6 WT mice compared to Brain stem (expression set at 100%). Percentages are calculated from copy number/ng RNA obtained in **Chapter 5**. Neocortex represents here the prefrontal and parietal cortex. Resistance to hypoxia is depicted as an arrow from the lowest resistance in hippocampus (black) to the lowest sensitivity (white) (137).

Neuroprotection via NCX3, common to multiple types of neuronal injuries such as shortage of nutrients and/or oxygen in hypoxia or anoxia and pathologies causing neurotoxicity such as Alzheimer's disease suggests a similar pathway by which NCX3 exerts its neuroprotective action. In this respect, both hyperglutamatergic and ischemic preconditioning provide additional protection preventing neuronal damage (138). However, while ischemic pre- and post-conditioning lead to a significant upregulation of

NCX3 reported in multiple mice models (12,130), the expression of the exchanger is unaffected by hyperglutamatergic conditions or amyloid $\beta_{1\text{-}42}$ toxicity in all brain regions tested, as reported in **chapter 5**. This finding indicates that the neuroprotective response of NCX3 results from distinct signaling pathways activated according to the type of neuronal insults. Nevertheless, while it is clear that only ischemic conditions trigger the upregulation of the exchanger, it remains unclear how post-translational modifications and activation of NCX3 participates in these differential responses and the role played by NCX3-BC in these pathways. Therefore, functions carried out by NCX3 in hypoxia cannot be translated as originally thought to other excitotoxic conditions where most likely different cellular pathways are implicated. Furthermore, the study of the differential cell responses to the diverse stress and injuries is of great interest in the understanding of the mechanisms of preconditioning and of the neuroprotective effect of NCX3.

Conclusion and future perspectives

The general aim of this thesis was to provide more insight in the physiological and molecular regulation of the Na^+-Ca^{2+} exchanger NCX3. Our studies illustrated the identification of regulators of NCX3 and their molecular mechanisms of action. A novel protocol was designed to enable the study of NCX3 in both modes of exchange by live-cell Ca^{2+} imaging and is applicable to all NCX isoforms. Using this approach, deeper insight was obtained in the functional properties of NCX3 splice variants. Furthermore, the regulation of NCX3 by PKA and PKC phosphorylation was unraveled as well as the variant-specific modulation mediated by CAPN1 and CAPN3. The studies identified the role of each spliced exon, the underlying molecular determinants and further pinpointed the crucial role of the intracellular loop in the regulation of NCX3 activity (**Table 2**). One of the future challenges in the comprehension of the NCX family would be to understand the signal transmission from the regulatory loop to the transmembrane domains responsible for ion translocation as well as the part played by the catenin-like domain in this process. A first step towards this goal has been the recent determination of the bacterial NCX crystal structure (29). Additionally, the ionic requirements for reversal of NCX3 identified and investigated in this thesis together with the studies performed in the past years demonstrating that these ionic requirements can be met in diverse cell types have proven that NCX3 can participate in Ca^{2+} entry in pathological but also in physiological conditions. Future studies should now aim to investigate the physiological roles of Ca^{2+} uptake via NCX3 and the interplay between this Ca^{2+} uptake, the store-operated channels and the Ca^{2+} storage in both SR/ER and mitochondria.

Altogether, the 'palette' of distinct regulatory mechanisms constitutes a fine-tuning of NCX activity to match the requirements of each tissue and cell type. The investigation described in this thesis demonstrated a tissue-specific expression of NCX3 splice variants

in skeletal muscle and brain in addition with various levels of expression in each fiber type and brain regions. In skeletal muscle, splicing, Ca^{2+} uptake capacity and calpain-mediated regulation of NCX3 suggest that the exchanger plays a more complex role than originally thought, by acting in both modes of exchange. This is of particular relevance in the comprehension of physiological events such as prolonged exercise and age-related muscular decline but also in several muscular pathologies where reticular Ca^{2+} imbalances are observed. Further studies focusing on the roles of NCX3 in skeletal muscle would be necessary. In this respect, the use of conditional knock-out models would be of great interest to decipher the roles of NCX3 in muscle fiber and at the neuromuscular junction. Finally, the neuroprotective role of NCX3 in neuronal injury and excitotoxicity is recognized. However examination of NCX3 expression performed in this thesis indicates differential stress-dependent responses that remain poorly understood. Future studies could make use of the recently developed CRISPR/Cas technique (139) to generate mice models with a deletion of the identified NCX3 cleavage sites. As NCX3 remains a promising drug target to reestablish Ca^{2+} balance, new insights on its implications could be of great help in pathologies causing intracellular Ca^{2+} disturbances such as epilepsia, muscular dystrophy or neuronal injury.

References

1. **Reuter, H., and Seitz, N.** Untersuchungen zur kinetik des 45Ca-efflux von meerschweinchwn vorhofen. *Naunyn-Schmiedeberg's Arch. Pharmacol. Exp. Pathol* 257, 324–325 (1967)

2. **Reuter, H., and Seitz, N.** The dependence of calcium efflux from cardiac muscle on temperature and external ion composition. *The Journal of physiology* 195, 451-470 (1968)

3. **Baker, P. F., Blaustein, M. P., Hodgkin, A. L., and Steinhardt, R. A.** The influence of calcium on sodium efflux in squid axons. *The Journal of physiology* 200, 431-458 (1969)

4. **Kasir, J., Ren, X., Furman, I., and Rahamimoff, H.** Truncation of the C terminus of the rat brain Na(+)-Ca(2+) exchanger RBE-1 (NCX1.4) impairs surface expression of the protein. *The Journal of biological chemistry* 274, 24873-24880 (1999)

5. **Nicoll, D. A., Longoni, S., and Philipson, K. D.** Molecular cloning and functional expression of the cardiac sarcolemmal Na(+)-Ca2+ exchanger. *Science* 250, 562-565 (1990)

6. **Akaike, N., and Harata, N.** Nystatin perforated patch recording and its applications to analyses of intracellular mechanisms. *Jpn J Physiol* 44, 433-473 (1994)

7. **Secondo, A., Pannaccione, A., Molinaro, P., Ambrosino, P., Lippiello, P., Esposito, A., Cantile, M., Khatri, P. R., Melisi, D., Di Renzo, G., and Annunziato, L.** Molecular pharmacology of the amiloride analog 3-amino-6-chloro-5-[(4-chloro-benzyl)amino]-n-[[(2,4-dimethylbenzyl)-amino] iminom ethyl]-pyrazinecarboxamide (CB-DMB) as a pan inhibitor of the Na+-Ca2+ exchanger isoforms NCX1, NCX2, and NCX3 in stably transfected cells. *The Journal of pharmacology and experimental therapeutics* 331, 212-221 (2009)

8. **Iwamoto, T., Kita, S., Zhang, J., Blaustein, M. P., Arai, Y., Yoshida, S., Wakimoto, K., Komuro, I., and Katsuragi, T.** Salt-sensitive hypertension is triggered by Ca2+ entry via Na+/Ca2+ exchanger type-1 in vascular smooth muscle. *Nature medicine* 10, 1193-1199 (2004)

9. **Nagano, T., Kawasaki, Y., Baba, A., Takemura, M., and Matsuda, T.** Up-regulation of Na(+)-Ca2+ exchange activity by interferon-gamma in cultured rat microglia. *Journal of neurochemistry* 90, 784-791 (2004)

10. **Iwamoto, T., and Kita, S.** YM-244769, a novel Na+/Ca2+ exchange inhibitor that preferentially inhibits NCX3, efficiently protects against hypoxia/reoxygenation-induced SH-SY5Y neuronal cell damage. *Molecular pharmacology* 70, 2075-2083 (2006)

11. **Iwamoto, T., Watano, T., and Shigekawa, M.** A novel isothiourea derivative selectively inhibits the reverse mode of Na+/Ca2+ exchange in cells expressing NCX1. *The Journal of biological chemistry* 271, 22391-22397 (1996)

12. **Secondo, A., Staiano, R. I., Scorziello, A., Sirabella, R., Boscia, F., Adornetto, A., Valsecchi, V., Molinaro, P., Canzoniero, L. M., Di Renzo, G., and Annunziato, L.** BHK cells transfected with NCX3 are more resistant to hypoxia followed by reoxygenation than those transfected with NCX1 and NCX2: Possible relationship with mitochondrial membrane potential. *Cell calcium* 42, 521-535 (2007)

13. **Blaustein, M. P., and Santiago, E. M.** Effects of internal and external cations and of ATP on sodium-calcium and calcium-calcium exchange in squid axons. *Biophysical journal* 20, 79-111 (1977)

14. **Neher, E., and Sakmann, B.** Single-channel currents recorded from membrane of denervated frog muscle fibres. *Nature* 260, 799-802 (1976)

15. **Neher, E., Sakmann, B., and Steinbach, J. H.** The extracellular patch clamp: a method for resolving currents through individual open channels in biological membranes. *Pflugers Archiv : European journal of physiology* 375, 219-228 (1978)

16. **Weber, C. R., Ginsburg, K. S., Philipson, K. D., Shannon, T. R., and Bers, D. M.** Allosteric regulation of Na/Ca exchange current by cytosolic Ca in intact cardiac myocytes. *J Gen Physiol* 117, 119-131 (2001)

17. **Reuter, H., Han, T., Motter, C., Philipson, K. D., and Goldhaber, J. I.** Mice overexpressing the cardiac sodium-calcium exchanger: defects in excitation-contraction coupling. *The Journal of physiology* 554, 779-789 (2004)

18. **Pott, C., Yip, M., Goldhaber, J. I., and Philipson, K. D.** Regulation of cardiac L-type Ca2+ current in Na+-Ca2+ exchanger knockout mice: functional coupling of the Ca2+ channel and the Na+-Ca2+ exchanger. *Biophysical journal* 92, 1431-1437 (2007)

19. **Mathias, R. T., Cohen, I. S., and Oliva, C.** Limitations of the whole cell patch clamp technique in the control of intracellular concentrations. *Biophysical journal* 58, 759-770 (1990)

20. **Shimomura, O., Johnson, F. H., and Saiga, Y.** Microdetermination of Calcium by Aequorin Luminescence. *Science* 140, 1339-1340 (1963)

21. **Pritchard, K., and Ashley, C. C.** Evidence for Na+/Ca2+ exchange in isolated smooth muscle cells: a fura-2 study. *Pflugers Archiv : European journal of physiology* 410, 401-407 (1987)

22. **Palty, R., Silverman, W. F., Hershfinkel, M., Caporale, T., Sensi, S. L., Parnis, J., Nolte, C., Fishman, D., Shoshan-Barmatz, V., Herrmann, S., Khananshvili, D., and Sekler, I. N**CLX is an essential component of mitochondrial Na+/Ca2+ exchange. *Proceedings of the National Academy of Sciences of the United States of America* 107, 436-441 (2010)

23. **Montezinho, L. P., C, B. D., Fonseca, C. P., Glinka, Y., Layden, B., Mota de Freitas, D., Geraldes, C. F., and Castro, M. M.** Intracellular lithium and cyclic AMP levels are mutually regulated in neuronal cells. *Journal of neurochemistry* 90, 920-930 (2004)

24. **Deval, E., Levitsky, D. O., Marchand, E., Cantereau, A., Raymond, G., and Cognard, C.** Na(+)/Ca(2+) exchange in human myotubes: intracellular calcium rises in response to external sodium depletion are enhanced in DMD. *Neuromuscular disorders : NMD* 12, 665-673 (2002)

25. **Pannaccione, A., Secondo, A., Molinaro, P., D'Avanzo, C., Cantile, M., Esposito, A., Boscia, F., Scorziello, A., Sirabella, R., Sokolow, S., Herchuelz, A., Di Renzo, G., and Annunziato, L.** A new concept: Abeta1-42 generates a hyperfunctional proteolytic NCX3 fragment that delays caspase-12 activation and neuronal death. *The Journal of neuroscience : the official journal of the Society for Neuroscience* 32, 10609-10617 (2012)

26. **Lichtshtein, D., Dunlop, K., Kaback, H. R., and Blume, A. J.** Mechanism of monensin-induced hyperpolarization of neuroblastoma-glioma hybrid NG108-15. *Proceedings of the National Academy of Sciences of the United States of America* 76, 2580-2584 (1979)

27. **Abramov, A. Y., and Duchen, M. R.** Actions of ionomycin, 4-BrA23187 and a novel electrogenic Ca2+ ionophore on mitochondria in intact cells. *Cell calcium* 33, 101-112 (2003)

28. **Morgan, A. J., and Jacob, R.** Ionomycin enhances Ca2+ influx by stimulating store-regulated cation entry and not by a direct action at the plasma membrane. *The Biochemical journal* 300 (Pt 3), 665-672 (1994)

29. **Liao, J., Li, H., Zeng, W., Sauer, D. B., Belmares, R., and Jiang, Y.** Structural insight into the ion-exchange mechanism of the sodium/calcium exchanger. *Science* 335, 686-690 (2012)

30. **Breukels, V., Touw, W. G., and Vuister, G. W.** NMR structure note: solution structure of Ca(2)(+) binding domain 2B of the third isoform of the Na(+)/Ca(2)(+) exchanger. *J Biomol NMR* 54, 115-121

31. **Hilge, M., Aelen, J., and Vuister, G. W.** Ca2+ regulation in the Na+/Ca2+ exchanger involves two markedly different Ca2+ sensors. *Mol Cell* 22, 15-25 (2006)

32. **Hilgemann, D. W.** Regulation and deregulation of cardiac Na(+)-Ca2+ exchange in giant excised sarcolemmal membrane patches. *Nature* 344, 242-245 (1990)

33. **Philipson, K. D., and Nishimoto, A. Y.** Na+-Ca2+ exchange in inside-out cardiac sarcolemmal vesicles. *The Journal of biological chemistry* 257, 5111-5117 (1982)

34. **Matsuoka, S., Nicoll, D. A., Reilly, R. F., Hilgemann, D. W., and Philipson, K. D.** Initial localization of regulatory regions of the cardiac sarcolemmal Na(+)-Ca2+ exchanger. *Proceedings of the National Academy of Sciences of the United States of America* 90, 3870-3874 (1993)

35. **DiPolo, R., and Beauge, L.** Characterization of the reverse Na/Ca exchange in squid axons and its modulation by Cai and ATP. Cai-dependent Nai/Cao and Nai/Nao exchange modes. *J Gen Physiol* 90, 505-525 (1987)

36. **Giladi, M., Hiller, R., Hirsch, J. A., and Khananshvili, D.** Population shift underlies Ca2+-induced regulatory transitions in the sodium-calcium exchanger (NCX). *The Journal of biological chemistry* 288, 23141-23149 (2013)

37. **DiPolo, R., and Beauge, L.** Ca2+ transport in nerve fibers. *Biochimica et biophysica acta* 947, 549-569 (1988)

38. **Baker, P. F., Blaustein, M. P., Keynes, R. D., Manil, J., Shaw, T. I., and Steinhardt, R. A.** The ouabain-sensitive fluxes of sodium and potassium in squid giant axons. *The Journal of physiology* 200, 459-496 (1969)

39. **Hilgemann, D. W., Matsuoka, S., Nagel, G. A., and Collins, A.** Steady-state and dynamic properties of cardiac sodium-calcium exchange. Sodium-dependent inactivation. *J Gen Physiol* 100, 905-932 (1992)

40. **Hilge, M., Aelen, J., Foarce, A., Perrakis, A., and Vuister, G. W.** Ca2+ regulation in the Na+/Ca2+ exchanger features a dual electrostatic switch mechanism. *Proceedings of the National Academy of Sciences of the United States of America* 106, 14333-14338 (2009)

41. **Quednau, B. D., Nicoll, D. A., and Philipson, K. D.** Tissue specificity and alternative splicing of the Na+/Ca2+ exchanger isoforms NCX1, NCX2, and NCX3 in rat. *The American journal of physiology* 272, C1250-1261 (1997)

42. **Nicoll, D. A., Quednau, B. D., Qui, Z., Xia, Y. R., Lusis, A. J., and Philipson, K. D.** Cloning of a third mammalian Na+-Ca2+ exchanger, NCX3. *The Journal of biological chemistry* 271, 24914-24921 (1996)

43. **Giladi, M., Sasson, Y., Fang, X., Hiller, R., Buki, T., Wang, Y. X., Hirsch, J. A., and Khananshvili, D.** A common Ca2+-driven interdomain module governs eukaryotic NCX regulation. PloS one 7, e39985 (2012)

44. **Michel, L. Y., Verkaart, S., Koopman, W. J., Willems, P. H., Hoenderop, J. G., and Bindels, R. J.** Function and regulation of the Na+-Ca2+ exchanger NCX3 splice variants in brain and skeletal muscle. *The Journal of biological chemistry* 289, 11293-11303 (2014)

45. **Breukels, V., Touw, W. G., and Vuister, G. W.** NMR structure note: solution structure of Ca(2)(+) binding domain 2B of the third isoform of the Na(+)/Ca(2)(+) exchanger. *J Biomol NMR* 54, 115-121 (2012)

46. **Besserer, G. M., Ottolia, M., Nicoll, D. A., Chaptal, V., Cascio, D., Philipson, K. D., and Abramson, J.** The second Ca2+-binding domain of the Na+ Ca2+ exchanger is essential for regulation: crystal structures and mutational analysis. *Proceedings of the National Academy of Sciences of the United States of America* 104, 18467-18472 (2007)

47. **Dyck, C., Omelchenko, A., Elias, C. L., Quednau, B. D., Philipson, K. D., Hnatowich, M., and Hryshko, L. V.** Ionic regulatory properties of brain and kidney splice variants of the NCX1 Na(+)-Ca(2+) exchanger. *J Gen Physiol* 114, 701-711 (1999)

48. **de Groot, T., Lee, K., Langeslag, M., Xi, Q., Jalink, K., Bindels, R. J., and Hoenderop, J. G.** Parathyroid hormone activates TRPV5 via PKA-dependent phosphorylation. *Journal of the American Society of Nephrology : JASN* 20, 1693-1704 (2009)

49. **Iwamoto, T., Pan, Y., Wakabayashi, S., Imagawa, T., Yamanaka, H. I., and Shigekawa, M.** Phosphorylation-dependent regulation of cardiac Na+/Ca2+ exchanger via protein kinase C. *The Journal of biological chemistry* 271, 13609-13615 (1996)

50. **Schulze, D. H., Muqhal, M., Lederer, W. J., and Ruknudin, A. M.** Sodium/calcium exchanger (NCX1) macromolecular complex. *The Journal of biological chemistry* 278, 28849-28855 (2003)

51. **Pannaccione, A., Secondo, A., Molinaro, P., D'Avanzo, C., Cantile, M., Esposito, A., Boscia, F., Scorziello, A., Sirabella, R., Di Renzo, G., and Annunziato, L.** A New Concept: Abeta1-42 Generates a Hyperfunctional Proteolytic NCX3 Fragment That Delays Caspase-12 Activation and Neuronal Death. *The Journal of neuroscience : the official journal of the Society for Neuroscience* 32, 10609-10617 (2012)

52. **Bano, D., Young, K. W., Guerin, C. J., Lefeuvre, R., Rothwell, N. J., Naldini, L., Rizzuto, R., Carafoli, E., and Nicotera, P.** Cleavage of the plasma membrane Na+/Ca2+ exchanger in excitotoxicity. *Cell* 120, 275-285 (2005)

53. **Boyman, L., Hagen, B. M., Giladi, M., Hiller, R., Lederer, W. J., and Khananshvili, D.** Proton-sensing Ca2+ binding domains regulate the cardiac Na+/Ca2+ exchanger. *The Journal of biological chemistry* 286, 28811-28820 (2011)

54. **Doering, A. E., and Lederer, W. J.** The mechanism by which cytoplasmic protons inhibit the sodium-calcium exchanger in guinea-pig heart cells. *The Journal of physiology* 466, 481-499 (1993)

55. **Doering, A. E., and Lederer, W. J.** The action of Na+ as a cofactor in the inhibition by cytoplasmic protons of the cardiac Na(+)-Ca2+ exchanger in the guinea-pig. *The Journal of physiology* 480 (Pt 1), 9-20 (1994)

56. **John, S. A., Ribalet, B., Weiss, J. N., Philipson, K. D., and Ottolia, M.** Ca2+-dependent structural rearrangements within Na+-Ca2+ exchanger dimers. *Proceedings of the National Academy of Sciences of the United States of America* 108, 1699-1704 (2011)

57. **Chen, M., and Manley, J. L.** Mechanisms of alternative splicing regulation: insights from molecular and genomics approaches. *Nature reviews. Molecular cell biology* 10, 741-754 (2009)

58. **Zhang, C., Zhang, Z., Castle, J., Sun, S., Johnson, J., Krainer, A. R., and Zhang, M. Q.** Defining the regulatory network of the tissue-specific splicing factors Fox-1 and Fox-2. *Genes & development* 22, 2550-2563 (2008)

59. **Kouadjo, K. E., Nishida, Y., Cadrin-Girard, J. F., Yoshioka, M., and St-Amand, J.** Housekeeping and tissue-specific genes in mouse tissues. *BMC genomics* 8, 127 (2007)

60. **Barber, R. D., Harmer, D. W., Coleman, R. A., and Clark, B. J.** GAPDH as a housekeeping gene: analysis of GAPDH mRNA expression in a panel of 72 human tissues. *Physiological genomics* 21, 389-395 (2005)

61. **Galpin, A. J., Raue, U., Jemiolo, B., Trappe, T. A., Harber, M. P., Minchev, K., and Trappe, S.** Human skeletal muscle fiber type specific protein content. *Analytical biochemistry* 425, 175-182 (2012)

62. **Minami, A., Xia, Y. F., and Zucker, R. S.** Increased Ca2+ influx through Na+/Ca2+ exchanger during long-term facilitation at crayfish neuromuscular junctions. *The Journal of physiology* 585, 413-427 (2007)

63. **Rebolledo, A., Speroni, F., Raingo, J., Salemme, S. V., Tanzi, F., Munin, V., Anon, M. C., and Milesi, V.** The Na+/Ca2+ exchanger is active and working in the reverse mode in human umbilical artery smooth muscle cells. *Biochemical and biophysical research communications* 339, 840-845 (2006)

64. **Viatchenko-Karpinski, S., Terentyev, D., Jenkins, L. A., Lutherer, L. O., and Gyorke, S.** Synergistic interactions between Ca2+ entries through L-type Ca2+ channels and Na+-Ca2+ exchanger in normal and failing rat heart. *The Journal of physiology* 567, 493-504 (2005)

65. **Shattock, M. J., and Bers, D. M.** Rat vs. rabbit ventricle: Ca flux and intracellular Na assessed by ion-selective microelectrodes. *The American journal of physiology* 256, C813-822 (1989)

66. **Rose, C. R., and Konnerth, A.** NMDA receptor-mediated Na+ signals in spines and dendrites. *The Journal of neuroscience : the official journal of the Society for Neuroscience* 21, 4207-4214 (2001)

67. **Juhaszova, M., and Blaustein, M. P.** Na+ pump low and high ouabain affinity alpha subunit isoforms are differently distributed in cells. *Proceedings of the National Academy of Sciences of the United States of America* 94, 1800-1805 (1997)

68. **Blaustein, M. P., Juhaszova, M., Golovina, V. A., Church, P. J., and Stanley, E. F.** Na/Ca exchanger and PMCA localization in neurons and astrocytes: functional implications. *Annals of the New York Academy of Sciences* 976, 356-366 (2002)

69. **Lencesova, L., O'Neill, A., Resneck, W. G., Bloch, R. J., and Blaustein, M. P.** Plasma membrane-cytoskeleton-endoplasmic reticulum complexes in neurons and astrocytes. *The Journal of biological chemistry* 279, 2885-2893 (2004)

70. **Moore, E. D., Etter, E. F., Philipson, K. D., Carrington, W. A., Fogarty, K. E., Lifshitz, L. M., and Fay, F. S.** Coupling of the Na+/Ca2+ exchanger, Na+/K+ pump and sarcoplasmic reticulum in smooth muscle. *Nature* 365, 657-660 (1993)

71. **Kuszczak, I., Kuner, R., Samson, S. E., and Grover, A. K.** Proximity of Na+ -Ca2+ -exchanger and sarco/endoplasmic reticulum Ca2+ pump in pig coronary artery smooth muscle: fluorescence microscopy. *Molecular and cellular biochemistry* 339, 293-300 (2010)

72. **Lemos, V. S., Poburko, D., Liao, C. H., Cole, W. C., and van Breemen, C.** Na+ entry via TRPC6 causes Ca2+ entry via NCX reversal in ATP stimulated smooth muscle cells. *Biochemical and biophysical research communications* 352, 130-134 (2007)

73. **Davis, K. A., Samson, S. E., Hammel, K. E., Kiss, L., Fulop, F., and Grover, A. K.** Functional linkage of Na+-Ca2+-exchanger to sarco/endoplasmic reticulum Ca2+ pump in coronary artery: comparison of smooth muscle and endothelial cells. *Journal of cellular and molecular medicine* 13, 1775-1783 (2009)

74. **Hirota, S., and Janssen, L. J.** Store-refilling involves both L-type calcium channels and reverse-mode sodium-calcium exchange in airway smooth muscle. *The European respiratory journal* 30, 269-278 (2007)

75. **Hove-Madsen, L., and Tort, L.** Characterization of the relationship between Na+ -Ca2+ exchange rate and cytosolic calcium in trout cardiac myocytes. *Pflugers Archiv : European journal of physiology* 441, 701-708 (2001)

76. **Huang, J., Hove-Madsen, L., and Tibbits, G. F.** SR Ca2+ refilling upon depletion and SR Ca2+ uptake rates during development in rabbit ventricular myocytes. *American journal of physiology. Cell physiology* 293, C1906-1915 (2007)

77. **Sirabella, R., Secondo, A., Pannaccione, A., Scorziello, A., Valsecchi, V., Adornetto, A., Bilo, L., Di Renzo, G., and Annunziato, L.** Anoxia-induced NF-kappaB-dependent upregulation of NCX1 contributes to Ca2+ refilling into endoplasmic reticulum in cortical neurons. *Stroke; a journal of cerebral circulation* 40, 922-929 (2009)

78. **Sisalli, M. J., Secondo, A., Esposito, A., Valsecchi, V., Savoia, C., Di Renzo, G. F., Annunziato, L., and Scorziello, A.** Endoplasmic reticulum refilling and mitochondrial calcium extrusion promoted in neurons by NCX1 and NCX3 in ischemic preconditioning are determinant for neuroprotection. *Cell death and differentiation* 21, 1142-1149 (2014)

79. **Piacentino, V., 3rd, Margulies, K. B., and Houser, S. R.** Ca influx via the Na/Ca exchanger maintains sarcoplasmic reticulum Ca content in failing human myocytes. *Annals of the New York Academy of Sciences* 976, 476-477 (2002)

80. **Larbig, R., Torres, N., Bridge, J. H., Goldhaber, J. I., and Philipson, K. D.** Activation of reverse Na+-Ca2+ exchange by the Na+ current augments the cardiac Ca2+ transient: evidence from NCX knockout mice. *The Journal of physiology* 588, 3267-3276 (2010)

81. **Endo, M.** Calcium-induced calcium release in skeletal muscle. *Physiological reviews* 89, 1153-1176 (2009)

82. **Launikonis, B. S., and Rios, E.** Store-operated Ca2+ entry during intracellular Ca2+ release in mammalian skeletal muscle. *The Journal of physiology* 583, 81-97 (2007)

83. **Majewski, L., and Kuznicki, J.** SOCE in neurons: Signaling or just refilling? *Biochimica et biophysica acta* 1853, 1940-1952 (2015)

84. **Baryshnikov, S. G., Pulina, M. V., Zulian, A., Linde, C. I., and Golovina, V. A.** Orai1, a critical component of store-operated Ca2+ entry, is functionally associated with Na+/Ca2+ exchanger and plasma membrane Ca2+ pump in proliferating human arterial myocytes. *American journal of physiology. Cell physiology* 297, C1103-1112 (2009)

85. **Germinario, E., Esposito, A., Midrio, M., Peron, S., Palade, P. T., Betto, R., and Danieli-Betto, D.** High-frequency fatigue of skeletal muscle: role of extracellular Ca(2+). *European journal of applied physiology* 104, 445-453 (2008)

86. **Jung, S. Y., Park, Y. J., Park, Y. J., Cha, S. H., Lee, M. Z., and Suh, C. K.** Na+-Ca2+ exchanger modulates Ca2+ content in intracellular Ca2+ stores in rat osteoblasts. *Experimental & molecular medicine* 39, 458-468 (2007)

87. **Uehara, A., Yasukochi, M., Imanaga, I., Nishi, M., and Takeshima, H.** Store-operated Ca2+ entry uncoupled with ryanodine receptor and junctional membrane complex in heart muscle cells. *Cell calcium* 31, 89-96 (2002)

88. **Arnon, A., Hamlyn, J. M., and Blaustein, M. P.** Na(+) entry via store-operated channels modulates Ca(2+) signaling in arterial myocytes. *American journal of physiology. Cell physiology* 278, C163-173 (2000)

89. **Lee, C. H., Poburko, D., Sahota, P., Sandhu, J., Ruehlmann, D. O., and van Breemen, C.** The mechanism of phenylephrine-mediated [Ca(2+)](i) oscillations underlying tonic contraction in the rabbit inferior vena cava. *The Journal of physiology* 534, 641-650 (2001)

90. **Liu, B., Peel, S. E., Fox, J., and Hall, I. P.** Reverse mode Na+/Ca2+ exchange mediated by STIM1 contributes to Ca2+ influx in airway smooth muscle following agonist stimulation. *Respiratory research* 11, 168 (2010)

91. **Girardin, N. C., Antigny, F., and Frieden, M.** Electrophysiological characterization of store-operated and agonist-induced Ca2+ entry pathways in endothelial cells. *Pflugers Archiv : European journal of physiology* 460, 109-120 (2010)

92. **Harper, A. G., and Sage, S. O.** A key role for reverse Na+/Ca2+ exchange influenced by the actin cytoskeleton in store-operated Ca2+ entry in human platelets: evidence against the de novo conformational coupling hypothesis. *Cell calcium* 42, 606-617 (2007)

93. **Harper, M. T., Molkentin, J. D., and Poole, A. W.** Protein kinase C alpha enhances sodium-calcium exchange during store-operated calcium entry in mouse platelets. *Cell calcium* 48, 333-340 (2010)

94. **Akolkar, G., Pande, J., Samson, S. E., and Grover, A. K.** Thapsigargin decreases the Na(+)- Ca(2+) exchanger mediated Ca(2+) entry in pig coronary artery smooth muscle. *Biochimica et biophysica acta* 1818, 730-737 (2012)

95. **Scorziello, A., Savoia, C., Sisalli, M. J., Adornetto, A., Secondo, A., Boscia, F., Esposito, A., Polishchuk, E. V., Polishchuk, R. S., Molinaro, P., Carlucci, A., Lignitto, L., Di Renzo, G., Feliciello, A., and Annunziato, L.** NCX3 regulates mitochondrial Ca(2+) handling through the AKAP121-anchored signaling complex and prevents hypoxia-induced neuronal death. *Journal of cell science* 126, 5566-5577 (2013)

96. **Wiedemann, N., Frazier, A. E., and Pfanner, N.** The protein import machinery of mitochondria. *The Journal of biological chemistry* 279, 14473-14476 (2004)

97. **Fraysse, B., Rouaud, T., Millour, M., Fontaine-Perus, J., Gardahaut, M. F., and Levitsky, D. O.** Expression of the Na(+)/Ca(2+) exchanger in skeletal muscle. *American journal of physiology. Cell physiology* 280, C146-154 (2001)

98. **Catterall, W. A., Perez-Reyes, E., Snutch, T. P., and Striessnig, J.** International Union of Pharmacology. XLVIII. Nomenclature and structure-function relationships of voltage-gated calcium channels. *Pharmacological reviews* 57, 411-425 (2005)

99. **Kallen, R. G., Sheng, Z. H., Yang, J., Chen, L. Q., Rogart, R. B., and Barchi, R. L.** Primary structure and expression of a sodium channel characteristic of denervated and immature rat skeletal muscle. *Neuron* 4, 233-242 (1990)

100. **Murphy, K. T., Nielsen, O. B., and Clausen, T.** Analysis of exercise-induced Na+-K+ exchange in rat skeletal muscle in vivo. *Experimental physiology* 93, 1249-1262 (2008)

101. **Cairns, S. P., Hing, W. A., Slack, J. R., Mills, R. G., and Loiselle, D. S.** Role of extracellular [Ca2+] in fatigue of isolated mammalian skeletal muscle. *Journal of applied physiology* 84, 1395-1406 (1998)

102. **Sokolow, S., Manto, M., Gailly, P., Molgo, J., Vandebrouck, C., Vanderwinden, J. M., Herchuelz, A., and Schurmans, S.** Impaired neuromuscular transmission and skeletal muscle fiber necrosis in mice lacking Na/Ca exchanger 3. *J Clin Invest* 113, 265-273 (2004)

103. **Ingalls, C. P., Warren, G. L., Williams, J. H., Ward, C. W., and Armstrong, R. B.** E-C coupling failure in mouse EDL muscle after in vivo eccentric contractions. *Journal of applied physiology* 85, 58-67 (1998)

104. **Lamb, G. D.** Mechanisms of excitation-contraction uncoupling relevant to activity-induced muscle fatigue. *Applied physiology, nutrition, and metabolism = Physiologie appliquee, nutrition et metabolisme* 34, 368-372 (2009)

105. **Singh, R. B., Chohan, P. K., Dhalla, N. S., and Netticadan, T.** The sarcoplasmic reticulum proteins are targets for calpain action in the ischemic-reperfused heart. *Journal of molecular and cellular cardiology* 37, 101-110 (2004)

106. **Zhao, X., Moloughney, J. G., Zhang, S., Komazaki, S., and Weisleder, N.** Orai1 mediates exacerbated Ca(2+) entry in dystrophic skeletal muscle. *PloS one* 7, e49862 (2012)

107. **Murphy, R. M., and Lamb, G. D.** Calpain-3 is activated following eccentric exercise. *Journal of applied physiology* 106, 2068; author reply 2069 (2009)

108. **Murphy, R. M., Goodman, C. A., McKenna, M. J., Bennie, J., Leikis, M., and Lamb, G. D.** Calpain-3 is autolyzed and hence activated in human skeletal muscle 24 h following a single bout of eccentric exercise. *Journal of applied physiology* 103, 926-931 (2007)

109. **Dayanithi, G., Richard, I., Viero, C., Mazuc, E., Mallie, S., Valmier, J., Bourg, N., Herasse, M., Marty, I., Lefranc, G., Mangeat, P., and Baghdiguian, S.** Alteration of sarcoplasmic reticulum ca release in skeletal muscle from calpain 3-deficient mice. *International journal of cell biology* 2009, 340346 (2009)

110. **Kramerova, I., Kudryashova, E., Wu, B., Ottenheijm, C., Granzier, H., and Spencer, M. J.** Novel role of calpain-3 in the triad-associated protein complex regulating calcium release in skeletal muscle. *Human molecular genetics* 17, 3271-3280 (2008)

111. **Johnson, B. D., Brousal, J. P., Peterson, B. Z., Gallombardo, P. A., Hockerman, G. H., Lai, Y., Scheuer, T., and Catterall, W. A.** Modulation of the cloned skeletal muscle L-type Ca2+ channel by anchored cAMP-dependent protein kinase. *The Journal of neuroscience : the official journal of the Society for Neuroscience* 17, 1243-1255 (1997)

112. **Boscia, F., D'Avanzo, C., Pannaccione, A., Secondo, A., Casamassa, A., Formisano, L., Guida, N., Sokolow, S., Herchuelz, A., and Annunziato, L.** Silencing or knocking out the Na(+)/Ca(2+) exchanger-3 (NCX3) impairs oligodendrocyte differentiation. *Cell death and differentiation* 19, 562-572 (2012)

113. **Gabellini, N.** Transcriptional regulation by cAMP and Ca2+ links the Na+/Ca2+ exchanger 3 to memory and sensory pathways. *Molecular neurobiology* 30, 91-116 (2004)

114. **Gabellini, N., Bortoluzzi, S., Danieli, G. A., and Carafoli, E.** Control of the Na+/Ca2+ exchanger 3 promoter by cyclic adenosine monophosphate and Ca2+ in differentiating neurons. *Journal of neurochemistry* 84, 282-293 (2003)

115. **Gomez-Villafuertes, R., Torres, B., Barrio, J., Savignac, M., Gabellini, N., Rizzato, F., Pintado, B., Gutierrez-Adan, A., Mellstrom, B., Carafoli, E., and Naranjo, J. R.** Downstream regulatory element antagonist modulator regulates Ca2+ homeostasis and viability in cerebellar neurons. *The Journal of neuroscience : the official journal of the Society for Neuroscience* 25, 10822-10830 (2005)

116. **Papa, M., Canitano, A., Boscia, F., Castaldo, P., Sellitti, S., Porzig, H., Taglialatela, M., and Annunziato, L.** Differential expression of the Na+-Ca2+ exchanger transcripts and proteins in rat brain regions. *The Journal of comparative neurology* 461, 31-48 (2003)

117. **Molinaro, P., Viggiano, D., Nistico, R., Sirabella, R., Secondo, A., Boscia, F., Pannaccione, A., Scorziello, A., Mehdawy, B., Sokolow, S., Herchuelz, A., Di Renzo, G. F., and Annunziato, L.** Na+ -Ca2+ exchanger (NCX3) knock-out mice display an impairment in hippocampal long-term potentiation and spatial learning and memory. *The Journal of neuroscience : the official journal of the Society for Neuroscience* 31, 7312-7321 (2011)

118. **Fontan-Lozano, A., Romero-Granados, R., del-Pozo-Martin, Y., Suarez-Pereira, I., Delgado-Garcia, J. M., Penninger, J. M., and Carrion, A. M.** Lack of DREAM protein enhances learning and memory and slows brain aging. *Current biology : CB* 19, 54-60 (2009)

119. **Jay, T. M., Gurden, H., and Yamaguchi, T.** Rapid increase in PKA activity during long-term potentiation in the hippocampal afferent fibre system to the prefrontal cortex in vivo. *The European journal of neuroscience* 10, 3302-3306 (1998)

120. **Kim, M., Huang, T., Abel, T., and Blackwell, K. T.** Temporal sensitivity of protein kinase a activation in late-phase long term potentiation. *PLoS computational biology* 6, e1000691 (2010)

121. **Bouron, A., and Reuter, H.** A role of intracellular Na+ in the regulation of synaptic transmission and turnover of the vesicular pool in cultured hippocampal cells. *Neuron* 17, 969-978 (1996)

122. **Meador, K. J.** The basic science of memory as it applies to epilepsy. *Epilepsia* 48 Suppl 9, 23-25 (2007)

123. **Yaari, Y., Konnerth, A., and Heinemann, U.** Spontaneous epileptiform activity of CA1 hippocampal neurons in low extracellular calcium solutions. *Experimental brain research* 51, 153-156 (1983)

124. **Baldy-Moulinier, M., Arias, L. P., and Passouant, P.** Hippocampal epilepsy produced by ouabain. Studies of cerebral circulation and ionic metabolism. *European neurology* 9, 333-348 (1973)

125. **Martinez, Y., and N'Gouemo, P.** Blockade of the sodium calcium exchanger exhibits anticonvulsant activity in a pilocarpine model of acute seizures in rats. *Brain research* 1366, 211-216 (2010)

126. **N'Gouemo, P.** Probing the role of the sodium/calcium exchanger in pentylenetetrazole-induced generalized seizures in rats. *Brain research bulletin* 90, 52-57 (2013)

127. **Reid, I. C., and Stewart, C. A.** Seizures, memory and synaptic plasticity. *Seizure* 6, 351-359 (1997)

128. **Zhou, J. L., Shatskikh, T. N., Liu, X., and Holmes, G. L.** Impaired single cell firing and long-term potentiation parallels memory impairment following recurrent seizures. *The European journal of neuroscience* 25, 3667-3677 (2007)

129. **Pignataro, G., Gala, R., Cuomo, O., Tortiglione, A., Giaccio, L., Castaldo, P., Sirabella, R., Matrone, C., Canitano, A., Amoroso, S., Di Renzo, G., and Annunziato, L.** Two sodium/calcium exchanger gene products, NCX1 and NCX3, play a major role in the development of permanent focal cerebral ischemia. *Stroke; a journal of cerebral circulation* 35, 2566-2570 (2004)

130. **Boscia, F., Gala, R., Pignataro, G., de Bartolomeis, A., Cicale, M., Ambesi-Impiombato, A., Di Renzo, G., and Annunziato, L.** Permanent focal brain ischemia induces isoform-dependent changes in the pattern of Na+/Ca2+ exchanger gene expression in the ischemic core, periinfarct area, and intact brain regions. *Journal of cerebral blood flow and metabolism : official journal of the International Society of Cerebral Blood Flow and Metabolism* 26, 502-517 (2006)

131. **Formisano, L., Saggese, M., Secondo, A., Sirabella, R., Vito, P., Valsecchi, V., Molinaro, P., Di Renzo, G., and Annunziato, L.** The two isoforms of the Na+/Ca2+ exchanger, NCX1 and NCX3, constitute novel additional targets for the prosurvival action of Akt/protein kinase B pathway. *Molecular pharmacology* 73, 727-737 (2008)

132. **Molinaro, P., Cuomo, O., Pignataro, G., Boscia, F., Sirabella, R., Pannaccione, A., Secondo, A., Scorziello, A., Adornetto, A., Gala, R., Viggiano, D., Sokolow, S., Herchuelz, A., Schurmans, S., Di Renzo, G., and Annunziato, L.** Targeted disruption of Na+/Ca2+ exchanger 3 (NCX3) gene leads to a worsening of ischemic brain damage. *J Neurosci* 28, 1179-1184 (2008)

133. **Martinez-Sanchez, M., Striggow, F., Schroder, U. H., Kahlert, S., Reymann, K. G., and Reiser, G.** Na(+) and Ca(2+) homeostasis pathways, cell death and protection after oxygen-glucose-deprivation in organotypic hippocampal slice cultures. *Neuroscience* 128, 729-740 (2004)

134. **Atherton, J., Kurbatskaya, K., Bondulich, M., Croft, C. L., Garwood, C. J., Chhabra, R., Wray, S., Jeromin, A., Hanger, D. P., and Noble, W.** Calpain cleavage and inactivation of the sodium calcium exchanger-3 occur downstream of Abeta in Alzheimer's disease. *Aging cell* 13, 49-59 (2014)

135. **Colvin, R. A., Bennett, J. W., Colvin, S. L., Allen, R. A., Martinez, J., and Miner, G. D.** Na+/Ca2+ exchange activity is increased in Alzheimer's disease brain tissues. *Brain research* 543, 139-147 (1991)

136. **Brisson, C. D., Lukewich, M. K., and Andrew, R. D.** A distinct boundary between the higher brain's susceptibility to ischemia and the lower brain's resistance. *PloS one* 8, e79589 (2013)

137. **Sieber, F. E., Palmon, S. C., Traystman, R. J., and Martin, L. J.** Global incomplete cerebral ischemia produces predominantly cortical neuronal injury. *Stroke* 26, 2091-2095; discussion 2096 (1995)

138. **Badawi, Y., Pal, R., Hui, D., Michaelis, E. K., and Shi, H.** Ischemic tolerance in an in vivo model of glutamate preconditioning. *Journal of neuroscience research* 93, 623-632 (2015)

139. **Inui, M., Miyado, M., Igarashi, M., Tamano, M., Kubo, A., Yamashita, S., Asahara, H., Fukami, M., and Takada, S.** Rapid generation of mouse models with defined point mutations by the CRISPR/Cas9 system. *Scientific reports* 4, 5396 (2014)

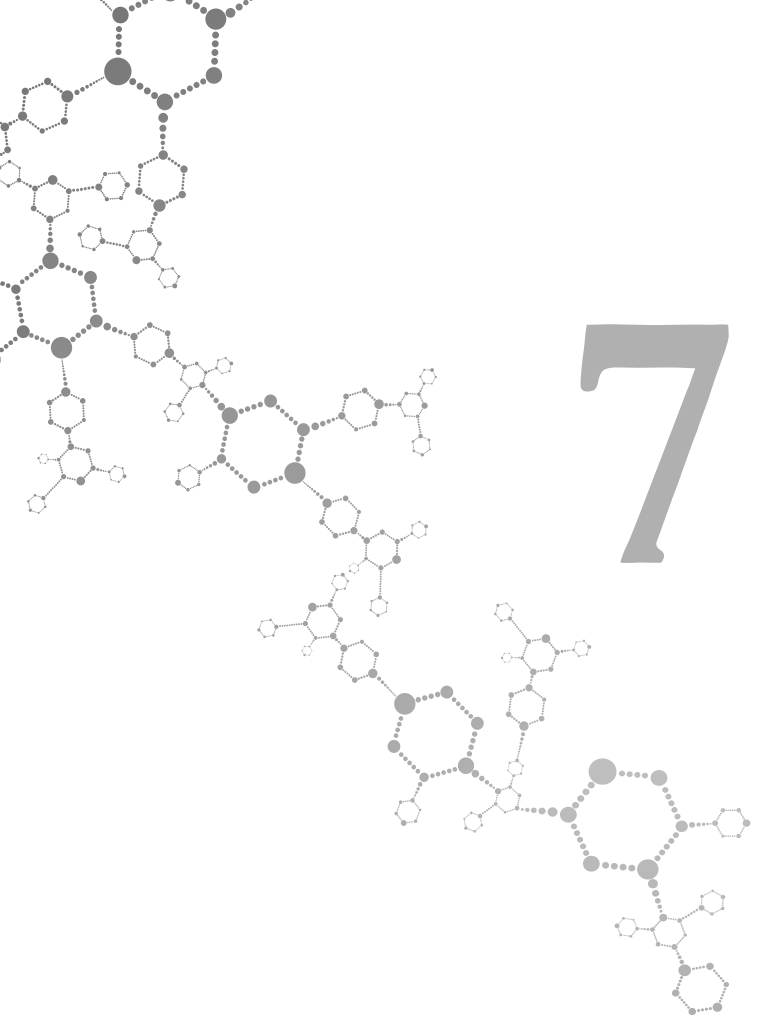

7

RIMLS Portfolio
List of abbreviations
Curriculum Vitae
List of publications
Acknowledgements

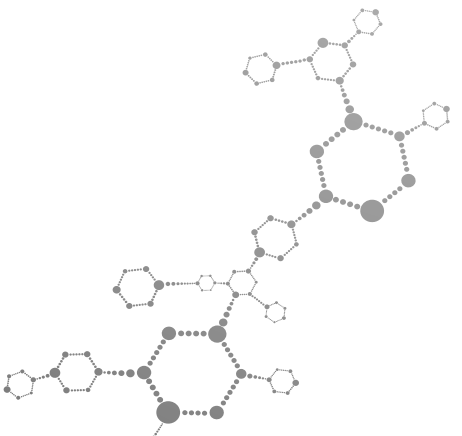

RIMLS Portfolio

Institute for Molecular Life Sciences
Radboudumc

PHD PORTFOLIO		**PhD period**	***23-05-2011 – 22-05-2015***
Name	***Lauriane Y.M. Michel***	**Promotors**	***Prof. dr. René J.M. Bindels***
Department	***Physiology***		***Prof. dr. Joost G.J. Hoenderop***
Research School	***Radboud Institute for Molecular Life Sciences***	**Co-promotor**	***Dr. Peter H.G. Willems***

	Year(s)	ECTS
TRAINING ACTIVITIES		
• Courses & Workshops		
- RIMLS Graduate course	2011	3
- RIMLS PhD retreat *	2012-2015	5
- Radiation Safety Course - Level 5B	2011	1,25
- Workshop: the art of presenting science	2014	1,5
- Pilot Workshop: Scientific Integrity	2014	1
• Seminars & lectures		
- RIMLS Technical forum	2011-2015	1,6
- RIMLS in the spotlight/ Research rounds/ Lecture Series	2011-2015	1
- RIMLS Seminars	2011-2015	3,3
• (Inter)national Symposia & congresses		
- RIMLS New frontiers 2011	2011	1
- System Biology and bioenergetics symposium 2012 *	2012	0,5
- RIMLS New frontiers 2012	2012	1
- Gordon research conference: Calcium Signaling *	2013	2
- RIMLS New frontiers 2014	2014	1
- Experimental Biology 2015 *	2015	1,75
• Other		
- Organization RIMLS technical Forum: Proteomics	2014	1
- Peer review Scientific publication	2014	0,2
TEACHING ACTIVITIES		
• Students		
- Supervision Shan Brunel	2012	1,25
- Supervision Cansu Türk	2013-2014	3
- Supervision Roderick van den Oudenalder	2014	1,25
- Supervision Mark van Eck	2014	1,25
TOTAL		**32,85**

Poster presentations and laptop-presentations are indicated with *.

List of abbreviations

$[Ca^{2+}]_{ER}$	ER Ca^{2+} concentration
$[Ca^{2+}]_{e}$	Extracellular Ca^{2+} concentration
$[Ca^{2+}]_{i}$	Intracellular Ca^{2+} concentration
$[Ca^{2+}]_{mito}$	Intramitochondrial Ca^{2+} concentration
$[Ca^{2+}]_{SR}$	SR Ca^{2+} concentration
$A\beta_{1\text{-}42}$	Amyloid peptide 1-42
AD	Alzheimer's disease
ATP	Adenosine triphosphate
a.u.	Arbitrary unit
bp	Base pair
°C	degree Celsius
Ca^{2+}	Calcium ion
$CaCl_2$	Calcium chloride
cAMP	Cyclic adenosine monophosphate
Ca_v	voltage-gated Ca^{2+} channel
CBD	Calcium-binding domain
CBP	Calcium-binding proteins
cDNA	complementary DNA
CLD	Catenin like domain
DMD	Duchenne Muscular dystrophy
DMSO	Dimethylsulphoxide
DNA	Deoxyribonucleaic acid
ECL	Enhanced chemiluminescence
ER	Endoplasmic reticulum
FDB	Flexor digitorum brevis
GAPDH	Glyceraldehyde-3-phosphate dehydrogenase
GFP	Green fluorescent protein
GPCR	G protein –coupled receptor
HEK293T	Human embryonic kidney 293T cells
HEPES	N-2-hydroxyethylpiperazine-N'-2-ethanesulfonic acid
Hr	Hour
HRP	Horseradish peroxidase
ICC	Interstitial cell of cajal
Ig	Immunoglobulin
IP_3	Inositol triphosphate
IRES	Internal ribosome entry site
K^+	Potassium ion
KCl	Potassium chloride

KDa	Kilo Dalton
KO	Knock-out
LGMD2A	Limb-girdle muscular dystrophy 2A
LTP	Long-term potentiation
Log	Logarithm
M	Molar
min	Minute
Mg^{2+}	Magnesium ion
$MgCl_2$	Magnesium chloride
mRNA	Messenger RNA
MW	Molecular weight
n	Sample size
Na^+	Sodium ion
NaCl	Sodium chloride
NaOH	Sodium hydroxide
NCX	Na^+-Ca^{2+} exchanger
NMDG	N-methyl-D-glucamine
NMJ	Neuromuscular junction
NO	Nitric oxide
nt	Nucleotide
Osm	Osmole
PAGE	Polyacrylamide gel electrophoresis
PCR	Polymerase chain reaction
PEI	Polyethylenimine
PIP_2	Phosphatidylinositol-4,5-phosphate
PKA	Protein kinase A
PKC	Protein kinase C
PMCA	Plasma membrane Ca^{2+} ATPase
RNA	Ribonucleic acid
RT	Reverse transcriptase
RT-PCR	Real-time PCR
ROS	Reactive Oxygen species
s	Second
SDS	Sodium dodecyl sulphate
SEM	Standard error of the mean
SERCA	Sarco/endoplasmic reticulum Ca^{2+} ATPase
siRNA	Small interfering RNA
SOCE	Store-operated Ca^{2+} entry
SR	Sarcoplasmic reticulum
TBS	Triethanolamine-buffered saline

Tg	Thapsigargin
TM	Transmembrane
TNFα	Tumor necrosis factor-alpha
TPA	12-O-Tetradecanoylphorbol 13-acetate
XIP	Exchanger inhibitor peptide
WT	Wild type

Curriculum Vitae

Lauriane Michel was born in Laval, France, on 28 December 1987. After graduating with honors at the Ambroise Paré Lycée, she studied Biology at the university of Rennes 1, France, where she obtained her bachelor degree with distinction in Biochemistry and Molecular Biology. She decided to further pursue her interest for Biochemistry and enrolled in the master of Biochemistry and Structural Biology at the Joseph Fourier University (UJF) in Grenoble, France. During her internship under the supervision of Prof. dr. Jesper V. Møller at the University of Århus, Denmark, she studied the mechanisms of inhibition of the sarco-endoplasmic reticulum calcium (SERCA)-ATPasis. In 2010, she investigated the regulation of mitochondrial fluxes by cytoskeletal proteins in cardiac and cancer cells at the laboratory of Bioenergetics (LBFA) of Grenoble, under the supervision of Prof. dr. Valdur Saks. The same year, she obtained her Master's degree with distinction with her thesis entitled "Study of an organized bioenergetic system: the mitochondrial interactosome". In 2011, Lauriane joined the department of Physiology and the Centre for System Biology and Bioenergetics (CSBB) of the Radboud university medical center. Under the supervision of Prof. dr. René J.M. Bindels, Prof. dr. Joost G.J. Hoenderop and Dr. Peter H.G. Willems, she investigated the alternative splicing and the post-translational regulations of the third isoform of the Na^{+}-Ca^{2+} exchanger family (NCX3) in order to better comprehend the implications of the exchanger in the brain and the skeletal muscle. During her PhD, Lauriane attended and held a poster presentation at several international conferences such as the Calcium signaling Gordon Research Conference (GRC) 2013 held in Lucca, Italy and the Experimental Biology meeting (EB) 2015 in Boston, USA. Additionally, she successfully followed the PhD training programme of the Radboud Institute for Molecular Life Sciences (RIMLS) and supervised four students from Biomedical sciences and Medicine. As of 2016, she is working as a postdoctoral researcher in the laboratory of Prof. dr. Jean-Luc Balligand in the Institute of experimental and clinical research of the University of Louvain (UCL) in Brussels, Belgium. Her new project is directed at understanding the implications of the β3-adrenergic receptor in cardiac remodeling.

List of publications

Guzun R, Karu-Varikmaa M, Gonzalez-Granillo M, Kuznetsov AV, **Michel LYM**, Cottet-Rousselle C, Saaremäe M, Kaambre T, Metsis M, Grimm M, Auffray C, Saks VA. Mitochondria-cytoskeleton interaction: distribution of β-tubulins in cardiomyocytes and HL-1 cells. *Biochim Biophys Acta* 1807, 458-469 (2011)

Michel LYM, Verkaart S, Koopman WJH, Willems PGH, Hoenderop JGJ, Bindels RJM. Function and regulation of the Na^+-Ca^{2+} exchanger NCX3 splice variants in brain and skeletal muscle. *J Biol Chem* 289, 11293-11303 (2014)

Michel LYM, Hoenderop JGJ, Bindels RJM. Towards understanding the role of the Na^+-Ca^{2+} exchanger isoform 3. *Rev Physiol Biochem Pharmacol.* 168, 31-57 (2015)

Michel LYM, Hoenderop JGJ, Bindels RJM. Calpain-3-mediated regulation of the Na^+-Ca^{2+} exchanger NCX3. *Pflügers Archiv* 468, 243-255 (2016)

Michel LYM, Michaelis EK, Pal R, Hui D, Kiliaan AJ, Hoenderop JGJ, Bindels RJM. Brain region-specific NCX1 and NCX3 expression in mice models of neuronal excitotoxicity. *Submitted for publication* (2016)

Michel LYM, Verkaart S, Hoenderop JGJ, Bindels RJM. Differential regulation of the Na^+-Ca^{2+} exchanger 3 (NCX3) by protein kinase PKC and PKA. *Submitted for publication* (2016)

Acknowledgements

This has been an incredible journey that would not have been possible if it wasn't for all the people I met on my path. To thank each one of you in detail would take an additional hundred pages which would probably imply selling one of my kidneys to pay for extra printing costs. Although I am guessing that the department of Physiology would be interested to acquire it for experiments, I think it is just best if I try to keep it relatively short!

First of all, I would like to express my sincere gratitude to my supervisors **Prof. René Bindels** and **Prof. Joost Hoenderop** for offering me this great opportunity to perform my PhD at the department of Physiology. I really enjoyed my time there. You have been with me through thick and thin. Every scientist knows that a PhD is mostly made of frustrations so I would like to thank you for your support, particularly in the bad times (when the microscope was broken, when the cells were not growing etc...) and for guiding me during these past years.

Dear **René**, I admire your drive and your proactive attitude. In the past years you advised me and pushed me to confront the challenges along the PhD road. I learned so much by working with you, scientifically but also personally as your determination and your efficiency made me a better scientist. You also gave me the freedom to shape the projects and design the studies and I really appreciated it. Thank you. Dear **Joost**, thank you for your help and support during our work discussions and your remarkable knowledge in molecular biology. I admire your voluntary mind. It always seems like nothing is impossible! It is inspiring. I would like to thank both of you for making this thesis possible.

I would like to acknowledge my co-supervisor **Dr. Willems**. Dear **Peter**, thank you for the time spent in enriching discussions and your valuable review. I greatly appreciated your constructive remarks, your suggestions and your support.

My gratitude goes to **Prof. Smeitink**, **Jan** for the unique opportunity he offered me to be part of a large system biology project such as the CSBB. It has been a wonderful and inspiring experience.

I would also like to thank our collaborators. When we first contacted **Prof. Michaelis**, he showed great interest in our study and immediately accepted to collaborate. Dear **Elias**, thank you for your collaboration and for making this project possible by providing us with samples from the *Glud1* mice. Your interest, kindness and enthusiasm have been very stimulating in this project. I would also like to thank **Dr. Amanda Kiliaan**. Dear

Amanda, thanks to our joint-effort and the samples of the mice model you kindly agreed to share with us, we extended further our knowledge of the neuronal expression of the NCX family to the alzheimer's disease mice model. This collaborative work led to a submitted manuscript and the last chapter of this thesis.

Before starting my doctoral studies, I had the opportunity to perform several internships. To **Prof. Saks** and **Dr. Guzun**, I am very thankful. Dear **Rita** and **Valdur**, during my master's internships in Grenoble I learnt so much on bioenergetics and research. Most importantly, you taught me to "enjoy science" and your passion has been very contagious! Thank you.

I have also been very lucky to be supervised by **Prof. Jesper Møller** during my first experience abroad. Dear **Jesper** thank you for welcoming me in your lab in Arhus for my first internship. Thank you for your patience while I was learning to speak a (more or less) understandable English. Thank you for this wonderful opportunity that it has been to work on the SERCA ATPase, the beginning of a great liking for Ca^{2+}.

Let's now take a drive down memory lane, in chronological order.

Silvia, **Silvietta**, you were there from the beginning, from my very first visit to Nijmegen! You are so talented, focused and energetic! I was very lucky to have you as my mentor in the lab. You have also been my first friend in the NL. From the first day you have been the bridge between me and the dutch world, in the lab and in Nijmegen. Thank you for being a true friend, for our evenings at St Anneke, our trips to Berlin, Canada and all the support you gave me. I'll always keep a bottle of Jägermeister waiting for your visit. I am looking forward to our next vacation together!

Kukiat, you immediately welcomed me in the unit we shared (unit 2 rules!) and your laugh has been very contagious! You were always calm and relaxed, even in your last months in the lab, while I was struggling in the first months of my PhD. It brought me hope and faith in the future! Thank you for that and for all the good times and the laughers inside and outside the lab. Next time I'll come to visit you in Thailand and I'll bring you foie gras!

Dear **Sjoerd**, **the "Incroyable" Sjoerd**, last year I realized that you mastered the art of throwing balls to people. The unit 2 was not a safe place anymore and I had to escape my kingdom (it will still remain mine forever!) During my PhD you have been a tremendous support. Thank you for all our scientific discussions. I admire your curiosity for any scientific topic and your generosity. Thanks to you I also progressed on my "H" pronunciation and I can finally say "Ik houd heel veel van NCX3!". These 4 years at Physiology would not have been the same if it weren't for you and your sense of humor.

Thank you for being my paranymph and for making me discover the "Rio" song!

Ganesh M, it all started with a weird lighter named "Franky"! You have been a point of reference in my Nijmegen experience. You've always been there, in the good but also the bad moments and I know that, despite the distance, I can always count on you. Thank you for your friendship and your deep generosity. I'll always bring with me the memories of our coffee breaks and all the parties including some pretty spicy Indian dinners! And I am still laughing about your suggestion to add Tabasco on the super delicate duck confit! I wish you joy and happiness in the life that awaits you. I could not be there in India but I'll surely come soon to visit you in Birmingham.

The "**derde Walstraat gang**" you have been so welcoming to me when I arrived. I had a really great time with all of you guys. Thank you so much for all these great memories and for taking me into your group right from my arrival: **Sergio**, **Eli**, **Anil**, **Asha**, **Tomacz**, **Joanna**, **Ganesh**, **Antoine**, **Angela**, **Anchel**, **Carlo**, **Cindy**, **Sip**, **Nuria** and so many more…I am confident that one day we'll find back Eli's backpack! Special thanks to **Anchel** and **Antoine** for our great "moustache evening" and for being there!

Ellen, how could I forget that you initiated me to the joy of laminating? On my side, I am very proud I introduced you to " tiny feet" in concert! You have been such a great part of my PhD experience. PhD retreats, gourmet-dinner, karaoke night and so many nice moments that we shared. Thank you for your friendship, for being my paranymph and for reaching out when I don't give news! With so much positivity and dynamism in just one person, I am confident that your future holds a lot of success.

Dear **Mark**, thanks for all our discussions and for the discovery of the toe shoes! I'll try it one day! Thank you for your support especially in the last stage of the writing of this thesis. I wish you all the best in Koln.

Liz, with Ellen you lighted up the Unit 3 with your songs! It made me happy and it annoyed Sjoerd, which made me even happier!! Thank you for showing me that Christmas songs can be sing anytime in the year!

Irene, I will remember our nice lunches and discussions. Thank you for caring and for making sure that the lab is not collapsing!

Paco, aka **Paquito**, my friend. You arrived just a few months after me. So I felt like we were "in the same boat" although in this boat you would probably be busy fishing for your experiments! You are a talented scientist and I admire your capacity to handle any situation that comes to you. Thank you for our discussions and laughers, for your empathy

and your capacity to listen. Your support has been a big help in this adventure. I hope next time we can finally go back to the Spanish cultural center to play bingo in a cozy and "frying" atmosphere!

Maxime, for a few years, you have been the other French speaker in the department. I enjoyed our discussions especially comparing the funny cultural and linguistic differences between switzerland, quebec and france. Thanks again for this beautiful visit of Montreal and for converting me to the Poutine!

Miyuki and Jonathan Thank you for the BBQs and all the board games played together. It was a lot of fun. Who knew that nuns could be on the run?

Robert, I am still not sure where you are coming from, maybe a different planet? it was great having you in the lab, with your surrealistic sense of humour! I will remember the scene of the Christmas market, seeing you and Marco napping!

Ganesh P, Thank you for all the fun times. Your good mood has lightened up the late evenings I spent in the lab! During your stay, I managed to convince you that vacation is good and you taught me that there is no bad mood that the "Sonnentanz" cannot cure. I was sad to see you leave but I am glad you have found a great place. I hope one day we'll manage to meet again for the Christmas market in Koln!

Sami, **Samoussa**, it was a great pleasure to have you as my neighbor in the lab. Your inconveniences with the NS have been such an entertainment for me (Hope it is solved though!). I really enjoyed our discussions, joyful breaks in the long days of experiments! I am glad I met you on my path, you are a great person and I wish you the very best for the future. Hope you enjoyed the mitmita and the berbere. One day I'll learn how to make injera!

Sabina, from your arrival in the lab you've been a real support. Thank you for all the crazy moments and this amazing vierdaagse 2014! Obviously, I cannot not mention the vodka lemon here so I will just say that I can't wait for our next reunion, I'm sure the next batch will be even better! You are a hardworking and talented scientist and I am confident you will be successful in your new adventure.

Marco, whenever I hear a timer ringing that no one turns off, I think of you! And in my mind I hear Sabina screaming "Marco!" haha! I wish you the best for your return in Mexico. I hope our path will cross again.

The Mallorca team, **Ellen**, **Paco**, **Marco**, **Sabina**, **Sami** and of course **Roberto**! I had a

wonderful time. Although I did not visit the "cuaves", we were quite lucky to have a "Canyon" very close to the hotel! Hope we can do that again one day. With this in mind, I'll try to continue training at footballito (pool being just hopeless!)

Roper (the microscope), our relationship has been quite a (time-)consuming passion! To share you with others was not always easy and sometimes you had a bad temper but I will take with me the great memories of those long evenings with a dimmed light looking at the fluorescence of the GFP.

In my time as a PhD student, I also got the opportunity to supervise several students. It has been a great experience from which I learnt a lot. **Shan**, I could not dream of a better first student, you were smart, passionate plus you could reach the upper shelves in the lab! **Cansu**, It was a pleasure supervising you, such an organized and focused person! **Mark and Roderick**, you came in a very hectic time in my PhD: two different characters with different properties like the two isoforms of NCX you were studying! Thanks to all of you and I wish you the best in your studies.

I would like to thank all of you who passed by the lab at one point in your career, for making the lab a nice "gezellig" environment which is so important for PhD students. I hope I won't forget anyone:
Femke, **Mark de Graaf**, **Pedro**, **Marcel**, **Dennis**, **Erik**, **Kukiat**, **Silvia**, **Mark Hess**, **Hans**, **Annemiete**, **Melissa**, **Theun**, **Maxime**, **Jitske**, **Steef**, **Sabina**, **Wilco**, **Miyuki**, **Sami**, **Sergio**, **Nase**, **Tomacz**, **Anil**, **Caro**, **Sjoerd**, **Ganesh**, **Marla**, **Joris**, **Omar**, **Claudia**, **Marco**, **Paco**, **Mohammad**, **Fareeba**, **Anke**, **Jeroen**, **Andreas**, **Robert Seng**, **Anne**, **Christiane**, **Femke v.d.H.**, **Irene**, **Eline**, **Sjoeli**, and all the students. Thank you for all these cakes (lekker!), I'd rather not count how many I had in these four years ….

Thank you also to all my Colleagues from the CSBB (**Julien**, **Dania**, **Marco**, **Ria**, **Tom**, **Herma**, **Lionel and Marco**) for the inspiring discussions and the nice atmosphere. I'd like also to thank the other departments of the 7th floor for all the good laughs and fun.

Lucia, my flatmates for half of my PhD, thank you for the good fun and the nice dinners with **Mina**. **Sarah F**, my almost flatmate (only two floors of difference) thank you for being with me the official french supporter team in the last world cup. **Chantal et Piet**, merci de m'avoir accueillie si gentiment dans votre maison. Cela a été un vrai plaisir de faire votre connaissance et de passer ces quelques mois rue Wilhelminasingel.

Finally I'd like to thank all the people who I had the chance to spend some time during dinners, parties in Nijmegen who are now spread around the world. Although I moved to a different country (not that far!). I will never forget the great people I met during my

stay. Thank you for being part of this journey.

These years have also been busy with travels from south to north: from the turtles of Mayotte to the northern lights in Lapland. Passing by the open market of Addis, the baths of Budapest and the Sugar shack of Quebec. To **Alexis**, **Raphael**, **Justine**, **Sylvain**, **Sarah**, **Silvia**, **Camille**, **Maxime**, **Julien** Thank you for hosting me and/or accompanying me in these trips. These have been wonderful interludes between my experiments and I hope for many more to come!

In few words, I would like to thank all my friends from France for our friendships that do not get weaker despite the time and the distance.

Sarah Z, merci pour ton amitié … et tes pâtisseries! C'est toujours un plaisir de vous voir Alex et toi et de voir grandir Pauline et Charlie. Dans l'attente d'une ouverture de poste de jeune fille au pair, je repasserai perdre mes cheveux chez vous!

Géraldine, aka **GG**, (Hey!) te voir est toujours une étape indispensable de mes passages à Laval. Aurais-je pu rester saine d'esprit pendant ces années de thèse sans nos balades dans le bois de l'huisserie? Pas sur! Tu es un véritable pilier dans ma vie. Merci pour ton amitié, tes visites et merci d'être toujours là malgré mes retards récurrents!

Sylvinou, tout a commencé par un covoiturage. Un million de souvenirs plus tard, rien n'a changé, ne pas t'avoir dans ma vie me parait toujours inconcevable! Merci pour tes nombreuses visites à Nijmegen! Et désolée que les retours de la famille Michel soient synonymes de changements dans ton cycle de sommeil. Je jouerai à Carcassonne pour me faire pardonner! C'est dire!

Justine, que d'aventures vécues depuis le collège! Je suis si contente que nous ayons réussi à garder contact. C'est toujours un plaisir de se voir et de reformer notre trio avec Camille. **Camille**, je ne sais pas si tu le sais, mais nos aînés se connaissent je crois! Merci pour tous ces bons souvenirs et ces quelques mois passés à Paris. Merci à vous deux de votre amitié, de nos fous rires, nos voyages et des fameux monoï à 15 euros! Vous êtes venus me voir sur chacune de mes étapes, je vous attends donc prochainement à Bruxelles! Je vais essayer de dénicher un bar à Absinthe, c'est bien connu, c'est là que le vin est le meilleur!

Alexis, **choupinou**, tu es actuellement à 7276 km de moi, environ! Et pourtant tu es proche. Si proche que tu fais véritablement partie de mon quotidien! Merci pour notre humour incompréhensible (loutchenka si tu nous entends) et nos goûts télé douteux, pour ton honnêteté et pour tous tes messages. Merci enfin pour nos voyages, formidables

excuses pour se voir, sans jamais un regret pour une destination (mis à part quelques plats macédoniens!). La prochaine étape sera probablement quelque part au sud, plus au sud encore que la d'où viens Chimène! Juste le temps de troquer mes Moon boots et j'arrive!

Anaïs, peu de gens peuvent réellement dire qu'ils se connaissent depuis toujours, c'est pourtant notre cas! Et que de bons moments depuis nos premiers mois chez tata (encore desolée pour la « bioche ») et j'espère encore bien d'autres à venir! **Elisa**, c'est toujours un plaisir de se retrouver, que ce soit pour une soirée ou pour des vacances (à la buzelière!)

A mes compagnons de "la Butte" **Sylvain**, **Simon**, **Sim's**, **Julien**, **et Clem'**, thank you for the amazing memory and all the memories! Merci d'avoir fait de mes retours en mayenne de parfaites vacances entre palet, cache-cache, uno, barbecue et tartiflette. La butte traversière résonne encore à mes oreilles!

I would like also to thank my family ever so supportive

Merci à ma marraine **Yveline**, mes oncles et tantes **Jean-Paul**, **Brigitte**, **Jean-Yves** et **Francoise** ainsi que mes cousins/cousines et leurs compagnes/compagnons pour leur soutien et leur gentillesse. A **Thomas** et **Fabien**, merci pour vos cadeaux moches difficiles à afficher et pour nos moments partagés.

Tatie, merci pour toute ton aide, je n'aurai pu gravir la montagne (avec ces bagages) sans tes précieux conseils. Merci de ton soutien indéfectible et de l'amour que tu portes à tes neveux et nièce. Nous te devons tant!

And then, there is this time of the night, after 1am, when only the Michel family is awake ….

A **Raphaël**, c'est avec une grande objectivité que j'ai posé ta candidature au «meilleur frère du monde»! Merci d'être toujours là quand j'ai besoin. Merci de tes mots d'encouragements, de tes relectures et de tous ces moments partagés depuis l'enfance. Et j'espère encore de nombreux autres à venir: voyages, discussions, chants, rires et probablement encore quelques DVD de Chuck Norris que je regarderai … un jour!

A mes parents. **Papa**, **Maman**, bien évidemment je vous dois tout depuis le départ mais si on ajoute à cela votre soutien extraordinaire durant ces années de thèse, on atteint quelque chose d'assez démentiel! Merci de m'avoir donné la liberté de poursuivre mes envies (même au-delà des frontières) et de m'avoir soutenue dans mes choix, jusqu'à me déménager à chaque nouvelle destination! Merci de m'avoir transmis vos valeurs mais

aussi votre empathie et votre curiosité pour les gens. Merci pour votre amour inconditionnel et pour nos conversations Skype tard le soir!

A mes grand-mères, dont les prénoms m'accompagnent

Lauriane

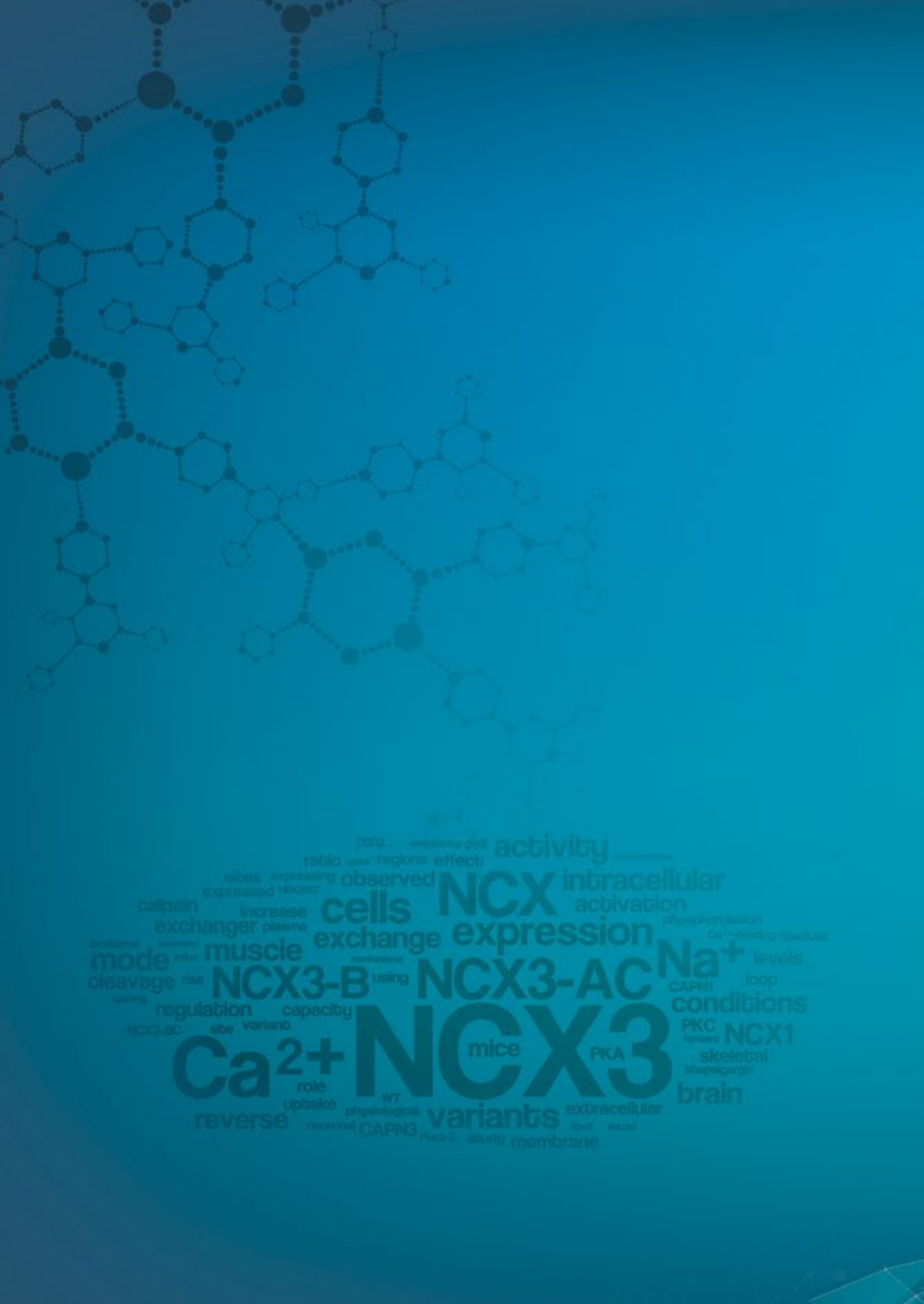
activity
observed
NCX
intracellular
cells
activation
calpain
increase
exchanger
plasma
exchange
expression
muscle
mode
cleavage
NCX3-B
using
NCX3-AC
Na+
levels
CAPN1
loop
conditions
regulation
capacity
variant
PKC
NCX1
Ca2+
NCX3
mice
PKA
skeletal
brain
role
uptake
WT
physiological
reverse
variants
extracellular
CAPN3
membrane